Bergman Cyclization of Enediyne-Based Polymers in Solution and the Solid State

Dissertation

zur Erlangung des Doktorgrades der Naturwissenschaften (Dr. rer. nat.)

der

Naturwissenschaftlichen Fakultät II Chemie, Physik und Mathematik

der Martin-Luther-Universität Halle-Wittenberg

vorgelegt

von Frau Yue Cai

Gutachter:

Prof. Dr. Wolfgang H. Binder (Martin Luther University Halle-Wittenberg)
Prof. Dr. Felix H. Schacher (University of Jena)

Defense date: 02.07.2025

Acknowledgment

First and foremost, I would like to express my deepest gratitude to Prof. Dr. Wolfgang H. Binder for offering me the opportunity to pursue my PhD and for providing such an interesting research topic. His scientific support, personal guidance, and encouragement have been instrumental throughout my doctoral journey.

I would also like to extend my sincere thanks to Ms. Anke Hassi for her attentive and considerate support in both my work and life since my first day arriving in Germany. Her assistance made my time in Halle much more convenient and warmer. I also deeply appreciate our technical assistants, Mrs. Julia Großert and Mrs. Susanne Tanner, for their meticulous support in my laboratory work. Their efficiency in providing laboratory supplies and sample testing has been invaluable. I would also like to thank my fellow group members, especially Dr. Anja Stojanovic-Marinow and those who shared the office and lab with me. Their companionship and engaging discussions have greatly enriched my PhD experience.

I am grateful to Prof. Dr. Edgar Peiter and Dr. Jie He for their significant guidance in my first project on DNA cleavage experiments, which helped solidify my commitment to this direction of research. Additionally, I want to thank Prof. Dr. Dariush Hinderberger and his group for their support with EPR experiments, which were crucial to my entire PhD project. I am also thankful to Dr. Dieder Ströhl and his team for their assistance with NMR experiments.

I would like to express my heartfelt gratitude to my family and friends. Without their unwavering support, I would not have made it this far. Without their warm companionship, it would have been difficult to get through the winters in Germany.

Lastly, I would also like to thank myself. Although the journey has been slow, it has largely been going in the right direction and aligning with my heart's desires. Embracing everything, growing personally, and looking forward to the future.

Abstract

The Bergman cyclization (BC) is a pericyclic reaction involving enediynes (EDY), characterized by two triple bonds conjugated to one centered double bond. Since the discovery of the efficient antibiotic activity of EDY and the diradical intermediates formed during cyclization, BC has garnered significant research interest. Key areas of study include factors influencing cyclization and the development of novel, site-selective EDY-based antibiotics. While previous research has largely focused on small molecules, in-depth explorations and expansions revealing the potential of EDY-based polymers have not yet been conducted.

This cumulative thesis presents the design and synthesis of three different EDY-based polymers. The first polymer is a main-chain EDY polyimine, synthesized through polycondensation of diamino-EDY ((Z)-octa-4-en-2,6-diyne-1,8-diamine) with different dialdehydes. These main-chain EDY polymers exhibit a chain-length dependent DNA cleavage activity under physiological conditions, which can be further tuned by modulating the stereoelectronic environment by modifying substitution patterns. Photochemical activation generates long-lived free radicals as verified by electron paramagnetic resonance (EPR) spectroscopy, with rates of radical formation corresponding to those observed in DNA cleavage experiments. In the second part, diamino-EDY was incorporated as a main-chain structural element in isophorone-based polyurethanes to create an EDY-based polyurethane elastomer. Upon heating, compression, or stretching, strain-induced hardening of this elastomer can be induced via BC. This cyclization serves as a crosslinking strategy triggered by heat or mechanical force in elastomeric materials. The third approach describes an initiator-free synthesis of semi-interpenetrating polymer networks (semi-IPNs) via BC. The precursor, (Z)oct-4-ene-2,6-diyne-1,8-diol (diol-EDY), was swollen into a pre-existing polyurethane network, followed by radical polymerization via an initiated BC. The so resulting semi-IPN exhibited enhanced mechanical properties and thermal stability when compared to the initial network.

In conclusion, three distinct EDY-based polymers were developed, showcasing novel functionalities driven by BC. These applications range from inducing enhanced DNA cleavage activity in solution to serving as efficient crosslinking strategies in solid films. The findings highlight the potential of molecule EDY to be embedded in polymer science with precise functional control.

Kurzdarstellung

Die Bergman-Cyclisierung (BC) ist eine pericyclische Reaktion, an der Enediyne (EDY) beteiligt sind, die durch zwei Dreifachbindungen gekennzeichnet sind, die mit einer zentralen Doppelbindung konjugiert sind. Seit der Entdeckung der effizienten antibiotischen Aktivität von EDY und der während der Cyclisierung gebildeten Diradikal-Zwischenprodukte hat die BC erhebliches Forschungsinteresse geweckt. Wichtige Forschungsbereiche umfassen Faktoren, die die Cyclisierung beeinflussen, sowie die Entwicklung neuartiger, selektiv wirkender EDY-basierter Antibiotika. Während sich die bisherige Forschung weitgehend auf kleine Moleküle konzentrierte, wurden eingehende Untersuchungen und Erweiterungen, die das Potenzial von EDY-basierten Polymeren aufzeigen, bisher noch nicht durchgeführt.

Diese kumulative Dissertation beschreibt das Design und die Synthese von drei verschiedenen EDY-basierten Polymeren. Das erste Polymer ist ein Hauptketten-EDY-Polyimin, das durch Polykondensation von Diamino-EDY ((Z)-octa-4-en-2,6-diyne-1,8-diamin) mit verschiedenen Dialdehyden synthetisiert wurde. Diese Hauptketten-EDY-Polymere zeigen eine kettenlängenabhängige DNA-Spaltungsaktivität unter physiologischen Bedingungen, die durch Modifikation des Substitutionsmusters und Beeinflussung der stereolektronischen Umgebung weiter angepasst werden kann. Photochemische Aktivierung erzeugt langlebige freie Radikale, die durch Elektronen-Paramagnetresonanz-Spektroskopie (EPR) nachgewiesen wurde, wobei die Raten der Radikalbildung denen der DNA-Spaltungsexperimenten entsprechen. Im zweiten Teil wurde Diamino-EDY als Strukturelement in Isophoron-basierten Polyurethanen eingebaut, um ein EDY-basiertes Polyurethan-Elastomer zu erzeugen. Durch Erhitzen, Kompression oder Dehnung kann eine durch Spannung induzierte Aushärtung dieses Elastomers über die BC induziert werden. Diese Cyclisierung dient als Vernetzungsstrategie, die durch Wärme oder mechanische Kraft in elastomeren Materialien ausgelöst wird. Der dritte beschreibt eine initiatorfreie semi-interpenetrierenden Ansatz Synthese von Polymernetzwerken (semi-IPNs) über BC. Der Vorläufer (Z)-oct-4-en-2,6-diyne-1,8-diol (Diol-EDY) wurde in ein vorhandenes Polyurethan-Netzwerk eingebracht, gefolgt von einer Radikalpolymerisation durch initiierte BC. Das resultierende semi-IPN zeigte verbesserte mechanische Eigenschaften und thermische Stabilität im Vergleich zum Ausgangsnetzwerk.

Abschließend wurden drei verschiedene EDY-basierte Polymere entwickelt die neuartige Funktionen durch BC aufzeigen. Diese Anwendungen reichen von der Verstärkung der DNA-Spaltungsaktivität in Lösung bis hin zur effizienten Verwendung als Vernetzungsstrategie in Feststofffilmen. Die Ergebnisse verdeutlichen das Potenzial von EDY-molekülen mit präziser Funktionskontrolle in die Polymerwissenschaft eingebunden zu werden.

Table of Contents

1.	Introduction	1
1.1.	Enediynes and the Bergman cyclization: from concepts to approaches	1
1.1.1.	Overview of enediynes and the Bergman cyclization	1
1.1.2.	Basic parameters and rate studies of the Bergman cyclization	3
1.1.3.	Catalytically induced Bergman cyclization	5
1.1.4.	Synthetic approaches of enediynes	7
1.1.5.	Characterization of the Bergman cyclization	8
1.2.	Applications of the Bergman cyclization: from single molecules to polymers	9
1.2.1.	Biological actions induced by the generated radicals via the Bergman cyclization	9
1.2.2.	Diradical-initiated polymerization via the Bergman cyclization	11
1.2.3.	Surface modification of carbon materials via the Bergman cyclization	12
1.2.4.	Synthesis of linear conjugated polymers via the Bergman cyclization	13
1.2.5.	Construction of polymeric nanoparticles via the Bergman cyclization	15
1.3.	Natural and synthetic enediynes in DNA cleavage	16
1.3.1.	Natural enediyne anticancer antibiotics	16
1.3.2.	Synthetic enediynes and enediyne-containing complexes	19
1.4.	Enediynes and the Bergman cyclization in stress-induced chemistry	20
1.4.1.	Structural investigation of stress-sensitive units	20
1.4.2.	Exploitation of enediynes as stress-sensitive units	23
1.5.	Semi-interpenetrating polymer networks	23
1.5.1.	Interpenetrating and semi-interpenetrating polymer networks	23
1.5.2.	Chemical approaches of semi-interpenetrating polymer networks	24
2.	Aim of the Thesis	26
3.	Scientific Approach	27
4.	List of Publications	30
5.	Summary and Outlook	60

6.	List of Abbreviations	65
7.	Literature	67
Curricul	um Vitae	89
Eigenstä	ndigkeitserklärung	93
Appendi	X	XXV

1. Introduction

1.1. Enediynes and the Bergman cyclization: from concepts to approaches

1.1.1. Overview of enediynes and the Bergman cyclization

In organic chemistry, pericyclic reactions represent a significant class of reactions characterized by a coordinated system surrounding a cyclic array of atoms during bond formation. In their transition states (TS), the involved bond orbitals overlap continuously and concertedly in a closed loop. Owing to the continuous flow of electrons through π -bonds and the reorganization of electron pairs in the cyclic TS, bond-breaking and bond-forming processes occur simultaneously. Therefore, they exhibit highly efficient reactivity and are recognized as an important tool in modern synthetic organic chemistry. Starting with the well-known Diels-Alder reaction first reported in 1928 as the leading example of a pericyclic reaction, the identification and formal categorization of pericyclic reactions have evolved over time through the observation and interpretation of various organic reactions. Four principle classes of pericyclic reactions have been termed as cycloadditions, electrocyclizations, sigmatropic rearrangements, and ene reactions.

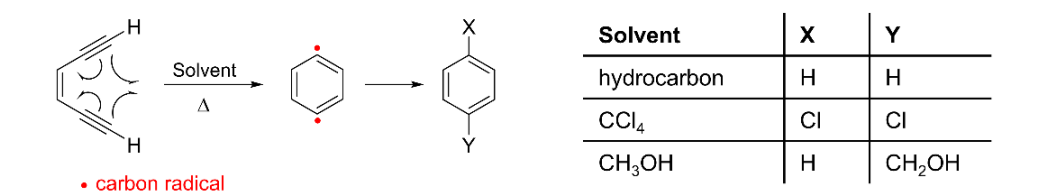


Figure 1. Bergman cyclization and its different products under various solvents.

The Bergman cyclization (BC) is one of the classical electrocyclizations, featuring a concerted cyclization by transforming one π -bond to a bond-forming σ -bond.⁸ It has a profound research background dating back to 1966 when Mayer and Sondheimer first reported the rearrangement of an enediyne that resulted in a cyclized product.^{9,10} Subsequently, in 1971, the Masamune group observed the formation of a benzenoid system during a similar conversion of the cyclic 1,5-enediyne (EDY).¹¹ In 1972, Jones and Bergman selected 3-ene-1,5-diynes as model compounds and designed a series of experiments that clearly illustrated the existence of 1,4-benzenoid diradicals during cycloaromatization as shown in **Figure 1**.¹² They also proposed that this reaction followed a mechanism similar to the cyclization previously reported by Sondheimer and Masamune. Since then, this cycloaromatization reaction of 3-ene-1,5-diynes has become widely known as Bergman cyclization. Specifically, (*Z*)-hex-3-ene-1,5-diyne was observed to undergo an exothermic rearrangement, leading to cyclization and the formation of aromatic rings. As a symmetry-allowed pericyclic reaction, BC is driven by aromaticity and characterized by the formation of a labile diradical intermediate, ¹³ which is consistent with the

1

decisive role of the solvent used in the reaction in determining the specific substitutions attached to the formed aromatic products as depicted in **Figure 1**. This typical behavior of a free-radical reaction can be explained by the presence of a symmetric 1,4-didehydrobenzene (*p*-benzyne) diradical intermediate, generated by the thermolysis of EDY. The diversity of cyclized products is largely due to the trapping of this diradical intermediate by external reagents.

However, despite the significance of BC, it received little attention in the decade following its discovery. It was only in the late 1980s, when a new class of naturally occurring antibiotics based on enediyne structures was identified, that BC and its proposed mechanism garnered significant interest from chemists and pharmacists.¹⁴ Calicheamicin (see **Figure 2**), the first representative EDY antibiotic, was initially isolated from chalky soil, or "caliche pits" in Kerrville.¹⁵ After collection and analysis by scientists from the Lederle Labs, it was accurately classified as a product of the actinomycete *Micromonospora echinospora*.¹⁶ In 1993, K. C. Nicolaou and his coworkers published the first laboratory synthesis of calicheamicin γ_II, which further inspired extensive research into bioactive small molecules containing the EDY-unit.¹⁷ Around the same time, dynemicin A, ^{18,19} kedarcidin chromophore, ^{20,21} and neocarzinostatin chromophore, ^{22,23} structurally distinct but biochemically similar, were also discovered and grouped within EDY antibiotics.

Figure 2. The first representative natural EDY anticancer antibiotic, calicheamicin γ_l^I .

The central part of the natural molecules contains the EDY unit, which accounts for their similarities in cleaving DNA in a site-specific and double-stranded manner, thereby highlighting the vital role of BC involving diradical structures. As illustrated in **Figure 3**, treatment with EDY-containing active compounds can transform original DNA by chain scission from its supercoiled Form I into different forms, specifically circular Form II (resulting from single-strand scissions), linear Form III (resulting from double-strand scissions), and small fragments.

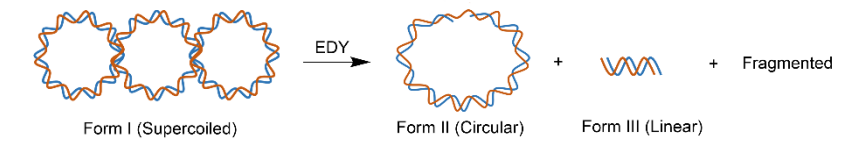


Figure 3. Schematic representation of DNA cleavage induced by EDY derivatives.

Since revealing the critical bioactivities of EDY extensive investigations have been conducted to explore BC in various fields.²⁴⁻²⁶ In chemistry, particular emphasis has been placed on factors that influence the cyclization process, such as molecular structures, substituents, and cyclic/acyclic geometries.²⁷⁻³⁵ These studies aim to better understand the parameters that affect the rate of cyclization and to develop more effective EDY substrates and catalytic approaches to facilitate BC.³⁶⁻⁵¹ Clinical applications of EDY antibiotics have also seen continuous improvement. For instance, in 2000, a derivative of the highly toxic calicheamicins, specifically a CD33 antigen-targeted immunoconjugate known as *N*-acetyl dimethyl hydrazide, was successfully marketed as a targeted therapy for acute myeloid leukemia (AML), a non-solid tumor cancer.⁵²⁻⁵⁴ In practical developments related to BC, the involvement of EDY in polymer chemistry has gained attention due to the formation of diradicals and the subsequent free radical polymerization that can be triggered.^{55,56} As a result, EDY and BC have become important due to their robust theoretical foundation, potent biological properties, and versatile applications in polymer science.

1.1.2. Basic parameters and rate studies of the Bergman cyclization

The discovery of EDY antibiotics and their site-specific DNA cleavage abilities initiated significant efforts by pharmacists and chemists to develop enediyne moieties from both naturally occurring and synthetic compounds. Due to the crucial role of the carbon diradical intermediate, the rate of double-stranded DNA cleavage is directly dependent on the rate of BC, which, in turn, affects the efficiency of related pharmaceutical activities. Therefore, understanding the kinetics of BC is fundamentally important and has always been a major focus of enediyne-centered research. The key factors influencing this process, involving species ranging from rearranged EDYs to intermediate biradicals, can be categorized into three dominant effects: (i) proximity effects;^{57,58} (ii) molecular-strain differences;⁵⁹ and (iii) electronic effects.³⁹

The proximity effects in tuning the reactivity of BC as a typical pericyclic reaction were first introduced by the Nicolaou group in 1988.⁶⁰ Specifically, this proximity is defined as the critical distance (*d*) between two carbon atoms (C1-C6) that form a new bond (see **Figure 4**). Supported by quantum chemical calculations and experimental observations, it was found that spontaneous BC can occur at body temperature if the distance ranges between 3.31 Å and

3.20 Å. From the perspective of natural bond orbital analysis, in a typical cycloaromatization reaction such as BC, a new σ -bond is typically formed at the expense of two π -orbitals. When the distance is below 3.20 Å, the two-electron stabilization interactions on the in-plane enediyne π -orbitals increase, thereby facilitating bond formation.

Figure 4. Distance (*d*) between two carbon atoms (C1-C6) that form a new bond.

Dynemicin A,^{18,61} an enediyne-core antibiotic isolated from *Micromonospora chersina sp.nov.N956-1*, serves as an example. In its inactive state, it remains dormant, activating BC only after reduction by NADPH (an electron-donating coenzyme) and the opening of the epoxide ring to release the alcohol form (quinone methide intermediate) (see **Figure 5**). Density functional theory (DFT) calculations illustrate that the untriggered epoxide-form locks the 10-membered enediyne ring in a conformation with a critical distance of 3.54 Å. After the ring opens, this critical distance decreases to 3.17 Å, and the energy barrier for BC thus is reduced from 52 to 17.9 kcal/mol, enabling dynemicin A to gain its bioactivity.

Figure 5. The process of dynemic A evoked to undergo BC.

In addition to proximity effects the differences in strain energies for the ground and transition state of EDY are also emphasized as driving forces for BC. A characteristic example from the Magnus group is illustrated in **Figure 6**. ^{59,62} The [7.3.1] bridgehead ketone, with d = 3.39 Å, undergoes BC more easily with an activation energy of 25.4 kcal/mol, while the [7.2.1] bridgehead ketone, despite displaying a slightly shorter distance of 3.36 Å, requires a higher

activation energy of 31.2 kcal/mol. This unexpected difference in reactivity arises from their respective transition states. The six-membered ring of [7.3.1] bridgehead ketone can adopt a chair conformation in its transition state, starting from an initial boat conformation, thereby reducing its strain energy by approximately 6 kcal/mol. This conversion does not occur in the five-membered ring of the [7.2.1] bridgehead ketone. As concluded by the Alabugin group based on extensive strain analysis of complex EDYs, 63,64 a strained ring incorporated into the ene part decreases cyclization activity, while strain induced at the terminal alkyne position promotes cyclization.

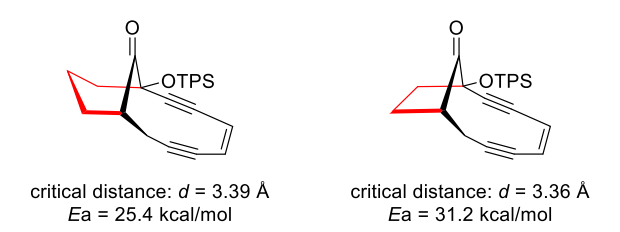


Figure 6. Comparison of [7.3.1] bridgehead ketone-EDY and [7.2.1] bridgehead ketone-EDY.

Besides the critical distances and strain influences, electronic effects play a profound role in tuning the activity of BC. Several factors contribute to electronic influence, 31,39,40,65-67 including the terminal effect, vinyl effect, benzoannelation, and ortho effect. Specifically, when the terminal position is substituted with π -donating groups such as -F, -Cl, -OH, and NH₃⁺, the electron density between carbon atoms C1 and C6 increases in the π -HOMO, thereby facilitating new bond formation. Besides, σ -withdrawing groups attached to the terminal position are expected to decrease the electron density in the σ -HOMO, in turn weakening the C1-C6 antibonding interaction and stabilizing the transition state. Regarding the vinyl effect, Jones and co-workers proposed that geometry and hybridization work synergistically to determine the repulsion between electrons in adjacent orbitals, thus modulating reactivity. 40 For example, when a halogen atom is substituted at the vinyl position, the rehybridization from a $p\pi$ -orbital to an sp2-orbital extends into space, inducing strong overlap with the in-plane lone pair orbital, which opposes cyclization. A particular form of the vinyl effect, where a benzene ring is incorporated into the double bond of enediyne, is also noteworthy. ⁶⁸ Benzo-fusion at the ene position favors cyclization by reducing the C1-C6 distance by more than 0.3 Å and stabilizing the diradical intermediate due to the conjugated system in the benzoannelated enediyne.

1.1.3. Catalytically induced Bergman cyclization

Since the first report by Jones and Bergman in 1972, BC has been primarily associated with thermal initiation. Compared to other stimuli, heat is the most straightforward method for initiating cyclization. According to the initial report, deuterated *cis*-1,5-hexadiyn-3-ene could

undergo the rearrangement at 200 °C as shown in **Figure 7A**. One example of an acyclic enediyne (EDY) is the *N*-substituted EDY with a bulky substituent at the alkyne terminus, developed by Rawat and Zaleski, which requires heating to 186 °C to undergo BC. Asymmetric deprotection of these bulky substituents can lower the required temperature to 139 °C.⁶⁹ Subsequently, Jeric and co-workers designed and synthesized a series of EDY-amino acid conjugates.^{70,71} One of these conjugates could undergo BC at relatively low temperatures (50 °C), likely due to hydrogen bonding between the terminal groups. However, the presence of a *tert*-butyloxycarbonyl (Boc) protecting group attached to EDY-based dipeptides could increase the required temperature back to 121 °C. Besides thermal initiation, UV radiation, ^{45,47,50,72-74} organometallic catalysts, ^{43,48,49} and acid induction have been widely utilized to trigger BC. Among these methods, acid induction is often observed in bioactive enediyne and DNA-related experiments, where the efficiency of cleavage is significantly enhanced when the pH < 7.⁷⁶

Figure 7. (A) Acyclic enediynes undergoing BC at different temperatures; (B) Photocycloaromatization of 3-benzo-1.5-diyne under a deuterated solvent yielding a deuterated naphthalene.

Inspired by the rich photoreactivity of double and triple bonds, significant effort has been devoted to the photochemistry of EDY. The first intramolecular rearrangement of EDY initiated by photochemistry, leading to a cyclized product, was reported accidentally in 1968.⁷⁷ Irradiation of a benzene solution of *o*-bis-iodoethynylbenzene produced *o*-bisphenylethynyl benzene as expected, whereas small quantities of substituted naphthalenes could also be detected. This unexpected discovery laid the foundation for photocatalytic BC. In 1994, Turro and Nicolaou reported a direct photocycloaromatization of 3-benzo-1.5-diyne to yield a naphthalene as shown in **Figure 7B**.⁷⁸ The photolysis was conducted in a deuterated solvent, with monitoring of GC-MS. The mass of 213 as the major product was consistent with the expected structure bearing deuterated hydrogen on the benzene ring. This result further

supported the formation of a dehydrocycloaromatic intermediate with a radical pair, followed by hydrogen abstraction from IP-Od in the reaction process.

In addition to photochemistry, metal-based initiation of EDY molecules has become pronounced. In the early stages, stoichiometric or excess amounts of metal complexes were commonly utilized for this purpose. In 1995, the Buchwald group⁷⁹ first confirmed that the addition of stoichiometric palladium(II) chloride or platinum(II) chloride could greatly accelerate the cyclization of 1,2-bis(diphenyl phosphinoethynyl)benzene. In contrast, the addition of mercury(II) chloride was found to inhibit cyclization reactivity. EDYs exhibit specific cyclization reactivities that correlate with the distance between the alkyne termini when different metal chlorides are added as shown in **Figure 8A**.

(A) Stoichiometric metal-complexes

(B) Catalytic metal-complexes

$$\begin{array}{c|c} & & \\ & & \\ & & \\ & & \\ & & \\ & & \\ & & \\ & & \\ & & \\ & & \\ & & \\ & & \\ & & \\ & & \\ & & \\ & & \\ & & \\ & & \\ & & \\ & & \\ & & \\ & & \\ & & \\ & & \\ & & \\ & & \\ & & \\ & & \\ & & \\ & & \\ & & \\ & & \\ & & \\ & & \\ & & \\ & & \\ & & \\ & & \\ & & \\ & & \\ & & \\ & & \\ & & \\ & & \\ & & \\ & & \\ & & \\ & & \\ & & \\ & & \\ & & \\ & & \\ & & \\ & & \\ & & \\ & & \\ & & \\ & & \\ & & \\ & & \\ & & \\ & & \\ & & \\ & & \\ & & \\ & & \\ & & \\ & & \\ & & \\ & & \\ & & \\ & & \\ & & \\ & & \\ & & \\ & & \\ & & \\ & & \\ & & \\ & & \\ & & \\ & & \\ & & \\ & & \\ & & \\ & & \\ & & \\ & & \\ & & \\ & & \\ & & \\ & & \\ & & \\ & & \\ & & \\ & & \\ & & \\ & & \\ & & \\ & & \\ & & \\ & & \\ & & \\ & & \\ & & \\ & & \\ & & \\ & & \\ & & \\ & & \\ & & \\ & & \\ & & \\ & & \\ & & \\ & & \\ & & \\ & & \\ & & \\ & & \\ & & \\ & & \\ & & \\ & & \\ & & \\ & & \\ & & \\ & & \\ & & \\ & & \\ & & \\ & & \\ & & \\ & & \\ & & \\ & & \\ & & \\ & & \\ & & \\ & & \\ & & \\ & & \\ & & \\ & & \\ & & \\ & & \\ & & \\ & & \\ & & \\ & & \\ & & \\ & & \\ & & \\ & & \\ & & \\ & & \\ & & \\ & & \\ & & \\ & & \\ & & \\ & & \\ & & \\ & & \\ & & \\ & & \\ & & \\ & & \\ & & \\ & & \\ & & \\ & & \\ & & \\ & & \\ & & \\ & & \\ & & \\ & & \\ & & \\ & & \\ & & \\ & & \\ & & \\ & & \\ & & \\ & & \\ & & \\ & & \\ & & \\ & & \\ & & \\ & & \\ & & \\ & & \\ & & \\ & & \\ & & \\ & & \\ & & \\ & & \\ & & \\ & & \\ & & \\ & & \\ & & \\ & & \\ & & \\ & & \\ & & \\ & & \\ & & \\ & & \\ & & \\ & & \\ & & \\ & & \\ & & \\ & & \\ & & \\ & & \\ & & \\ & & \\ & & \\ & & \\ & & \\ & & \\ & & \\ & & \\ & & \\ & & \\ & & \\ & & \\ & & \\ & & \\ & & \\ & & \\ & & \\ & & \\ & & \\ & & \\ & & \\ & & \\ & & \\ & & \\ & & \\ & & \\ & & \\ & & \\ & & \\ & & \\ & & \\ & & \\ & & \\ & & \\ & & \\ & & \\ & & \\ & & \\ & & \\ & & \\ & & \\ & & \\ & & \\ & & \\ & & \\ & & \\ & & \\ & & \\ & & \\ & & \\ & & \\ & & \\ & & \\ & & \\ & & \\ & & \\ & & \\ & & \\ & & \\ & & \\ & & \\ & & \\ & & \\ & & \\ & & \\ & & \\ & & \\ & & \\ & & \\ & & \\ & & \\ & & \\ & & \\ & & \\ & & \\ & & \\ & & \\ & & \\ & & \\ & & \\ & & \\ & & \\ & & \\ & & \\ & & \\ & & \\ & & \\ & & \\ & & \\ & & \\ & & \\ & & \\ & & \\ & & \\ & & \\ & & \\ & & \\ & & \\ & & \\ & & \\ & & \\ & & \\ & & \\ & & \\ & & \\ & & \\ & & \\ & & \\ & & \\ & & \\ & & \\ & & \\ & & \\ & & \\ & & \\ & & \\ & & \\ & & \\ & & \\ & &$$

Figure 8. (A) Metal-participated acceleration of the BC with stoichiometric amounts of metal additives; (B) Catalytic cyclization by formation of metal-complexes intermediate.

Furthermore, catalytic amounts of metal additives have been thoroughly investigated.⁸⁰ The Liu group⁸¹ reported that a catalytic dosage of PtCl₂ (5 mol%) effectively accelerated cyclization through platinum- π -alkyne intermediates as illustrated in **Figure 8B**. Through deuterium-labeling experiments, a platinum-stabilized benzene carbenoid was observed *via* C-H bond insertion of tethered alkanes, followed by the subsequent aromatization to obtain the cyclized product.

1.1.4. Synthetic approaches of enediynes

The synthesis of EDY relies on two strategies as shown in **Figure 9**. The first strategy involves using *cis*-halogenated alkenes as the starting material and attaching the alkynyl groups on both sides through Sonogashira coupling. During this process, it might become necessary to protect the terminal positions of the alkynyl moiety, making a subsequent deprotection step unavoidable. For example, a classical Pd-catalyzed Sonogashira coupling between *N*-Boc-prop-2-ynyl amine and *cis*-1,2-dichloroethylene in the presence of CuI and BuNH₂ results in an *N*-

Boc enediyne precursor with a 68% yield. Subsequent acid treatment removes the *tert*-butyloxycarbonyl group, generating the asymmetric amine EDY.⁶⁹ A similar approach is used in the synthesis of (*Z*)-octa-4-en-2,6-diyne-1,8-diol. Coupling *cis*-1,2-dichloroethylene with protected propyn-1-ol, followed by hydrolysis with Amberlyst 15H, yields the primary diol EDY.

Figure 9. Two strategies for constructing EDY molecules. (A) Sonogashira coupling between alkynes and halogenated alkenes; (B) Carbenoid coupling-elimination strategy to synthesize symmetric EDYs. LAH: lithium aluminium hydride; THF: tetrahydrofuran.

The second method to construct EDY relies on a carbenoid coupling-elimination strategy, 82 an alternative to classical Pd-mediated cross-coupling reactions. As illustrated in **Figure 9B**, optimized carbenoid coupling of lithiated propargylic halides provides efficient access to both linear and cyclic enedignes. Additionally, this approach offers a unified route to either Z or E enedignes, as the stereochemistry of the vinyl group can be adjusted by geometric constraints prior to the elimination step.

1.1.5. Characterization of the Bergman cyclization

To characterize and quantify the occurrence of BC, several measurements can be utilized, using the exothermic nature of BC, chemical structural transformations centered on EDY, and the generated diradical intermediate.

First, differential scanning calorimetry (DSC) is a powerful tool to evaluate the heat generated during the reaction, as BC is known as an exothermic reaction that releases heat during the process.⁸³ By subjecting samples to continuous heating under an inert gas flow, an exothermic peak is expected to appear, along with measurements of the onset temperature, peak temperature, and the enthalpy of the released heat.

Secondly, during the transformation of EDY to the final benzene derivatives, the most noticeable changes occur in their chemical structures, as the initial triple bonds and double bond exhibit characteristic absorption peaks in Fourier-transform infrared (FT-IR) spectroscopy. ET he strong stretching band of the alkyne (C=C) around 2340 cm⁻¹ is expected to disappear along with the consumption of the alkynyl group during the cyclization process. Meanwhile, the generated aromatic ring-bands at 800~900 cm⁻¹ can provide information about the hydrogen atoms located on the rings. For example, starting from a monosubstituted EDY (substituted at the C1 or C6 position), the generated polyphenylenes are expected to be 1,2,4-substituted. Therefore, the bending vibrations of the lone C-H at the 3-position and the two adjacent hydrogens at the 5- and 6-positions will induce specific bands in the 950-800 cm⁻¹ range.

Thirdly, the most direct evidence of the occurrence of BC comes from the detection of the generated radical moieties.¹³ Electron paramagnetic resonance (EPR) spectroscopy, which provides information on the structure and dynamics of systems with unpaired electrons, is a well-established technique for this purpose. In addition to the direct detection of the generated radicals, radical trapping agents such as 2,2,6,6-tetramethylpiperidinyloxyl (TEMPO) are also employed to monitor the growth of free radicals.⁸⁵

1.2. Applications of the Bergman cyclization: from single molecules to polymers

1.2.1. Biological actions induced by the generated radicals via the Bergman cyclization

Biological activity induced by the EDY *via* BC occurs through DNA cleavage, *via* the transient, reactive 1,4-benzenoid diradical, that acts as a nucleophile, tending to attack electrophiles to achieve a more stable form. Much research has been conducted to identify the specific mode of DNA damage induced by this diradical. In general, the diradical itself can only perform nonspecific hydrogen abstraction, leading to chemical changes at the corresponding positions. However, due to structural differences among the four types of DNA bases (adenine (A), cytosine (C), guanine (G), and thymine (T)) the mode of DNA damage varies depending on the abstraction of a hydrogen atom in different chemical environments. It is estimated that at least 80% of DNA cleavage occurs at the 5'-aldehyde of A and T moieties. ^{14,86} As illustrated in **Figure 10**, the hydrogen atom from the C(5') of deoxyribose is abstracted by the radical, followed by reaction with oxygen to form a peroxyl radical. This peroxyl radical causes strand

scission, resulting in the formation of an aldehyde and the corresponding phosphoric acid, thereby realizing DNA cleavage. Additionally, strand breaks at the C(1') and C(4') positions account for less than 20% of the total cleavage events.⁸⁷⁻⁹⁰

Figure 10. DNA cleavage induced by EDY at different positions of the ribose (C5, C1, C4).

Electrophoresis using agarose or polyacrylamide gels is widely used to detect DNA cleavage in double helices, as well as to analyze and identify DNA fragments. ⁹¹ DNA fragment mixtures are loaded into pre-cast wells in an agarose gel, followed by the application of an electric field. The negatively charged phosphate backbone of DNA migrates toward the positively charged anode. Because DNA has a uniform mass-to-charge ratio, the fragments can be separated by size: smaller molecules pass through the gel pores more easily than larger ones. Therefore, the ability of EDY to cleave DNA under irradiation can be investigated through gel electrophoresis. As illustrated in **Figure 3**, DNA in the initial supercoiled Form I can be cleaved by EDY and transformed into different forms, including circular Form II (single-strand scissions), linear Form III (double-strand scissions), and even small fragments. In 2005, the Alabugin group prepared a mixture of supercoiled plasmid and lysine-EDY conjugates and conducted irradiation for different lengths of time (ranging from 2 min to 45 min). ⁹² The conversion of the supercoiled plasmid into its respective forms can be then quantified *via*

densitometric analysis of the gel electrophoresis. As the irradiation time increased, the ratio of DNA in Form I gradually decreased, while the ratios of Form II and Form III increased, as shown in **Figure 11**.

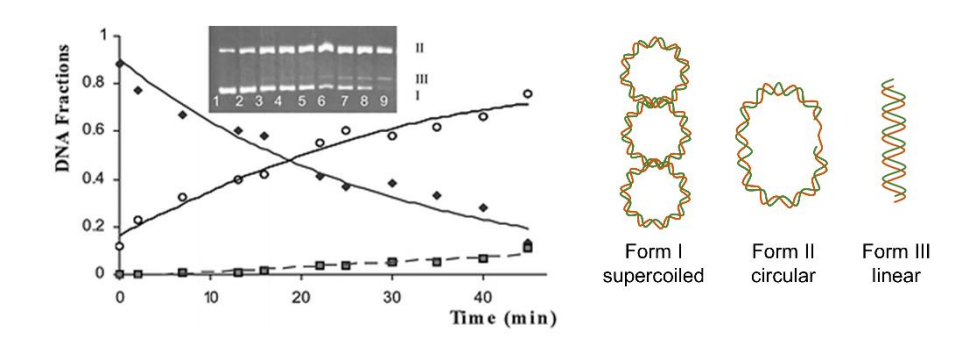


Figure 11. Cleavage of supercoiled DNA by EDY with different lengths of time. The relative amounts of the three forms are presented by diamonds (Form I), hollow circles (Form II), and squares (Form III). Figure reprinted from reference⁹² with permission from the Royal Society of Chemistry. (Copyright 2005).

1.2.2. Diradical-initiated polymerization via the Bergman cyclization

Since the 1950s, diradical-initiated polymerization has been a subject of research. 93 In principle, the combination of two polymer chains with radical centers at both ends can occur through two mechanisms: addition and disproportionation. In practical experiments, however, the cage effect is a common challenge in diradical-initiated polymerization. This effect causes the two radical centers to form a ring closure *via* intramolecular termination, resulting in circular oligomeric products. Additionally, selecting a suitable diradical precursor is essential for successful polymerization.

Given the ease of triggering EDY to form diradical moieties, diradical-initiated polymerization *via* BC has attracted the interest of polymer specialists for decades. ^{94,95} A cyclic enediyne, 3,4-benzocyclodec-3-ene-1,5-diyne, has been shown to successfully initiate radical polymerization of several monomers under heat and neat conditions. Among these monomers, methacrylates are more efficiently polymerized to high molecular weight compared to others. Research by the Rule group has revealed that the resulting polymer primarily propagates as a monoradical, highlighting that achieving high molecular weight in diradical-initiated reactions depends on chain transfer to monomers, polymeric species, or suitable chain transfer agents. Reversible addition-fragmentation chain-transfer (RAFT) polymerization, known for its rapid addition to radical centers, has emerged as an effective strategy for achieving living polymerization. In 2011, the Barner-Kowollik group published the first RAFT-mediated polymerization of methyl methacrylate with the initiation of diradical moieties derived from the EDY 3,4-benzocyclodec-3-ene-1,5-diyne *via* BC.⁹⁶ As shown in **Figure 12**, cyanoisopropyldithiobenzoate was employed as the RAFT agent, and ESI-MS measurements

gave solid evidence of the addition of the RAFT agent to both radical centers. Due to the rapid equilibrium between the propagating radicals and the dormant thiocarbonyl polymeric species, all chains could theoretically grow uniformly. This approach can effectively avoid intramolecular termination and resulting circular oligomers. After optimizing reaction conditions, including reaction time, temperature, and the concentration of EDY and RAFT agent, high molecular weight polymer products (\sim 400,000 Da) with relatively narrow polydispersities ($1.1 \le PDI \le 1.5$) could be obtained.

Figure 12. RAFT polymerization of methyl methacrylate initiated by cyclic EDY 3,4-benzocyclodec-3-ene-1,5-diyne.

1.2.3. Surface modification of carbon materials via the Bergman cyclization

Owing to the excellent thermal, mechanical, optical, electrical, and chemical properties, carbon materials have been widely applied in various fields such as nanoelectronics, biomedical delivery, and sensors. 97 However, pure carbon materials tend to form bundled structures caused by strong van der Waals forces and π - π stacking, making them insoluble in both organic and inorganic solvents. This poor solubility hinders the study of their chemical and physical properties and limits their potential applications. Therefore, surface modification is crucial in some situations. Compared to noncovalent modification, 98,99 covalent functionalization via organic reactions is more efficient and direct. Various reactions have been developed for this purpose, including cycloaddition, 100-102 electrochemical modification, 103-105 fluorination, 106 coupling reaction, ¹⁰⁷ and radical addition ¹⁰⁸⁻¹¹⁰. The Smith group achieved the first example of radical addition of a conjugated polymer to multilayer carbon material, where the conjugated polymer was derived from an EDY monomer bis-o-vinyl arene (BODA) via BC-induced radical polymerization.¹¹¹ In their previous research, BODA-derived naphthyl diradical species have shown remarkable stabilities, thus allowing the possibility of reacting with other species to propagate polymerization.¹³ As shown in **Figure 13**, thermally initiated polymerization centered on BODA monomers generates oligomers and complete polymer networks, which can be attached to the surface of carbon materials via radical addition. Some functional groups, such as fluorinated bridging group C(CF₃)₂, can be introduced first as substituents of BODA monomers to impart the resulting products with functional versatility, such as improved solubility. Through radical addition under heat, the obtained copolymers can be dissolved in chloroform and N-methyl-2-pyrrolidone. Transmission electron microscopy (TEM) and gel

permeation chromatography (GPC) can be used to investigate the degree of modification of carbon materials and the conversion ratio of BODA monomers.

Figure 13. Radical addition of a conjugated polymer derived from the EDY monomer bis-*o*-vinyl arene to multilayer carbon materials.

Furthermore, a similar strategy employing EDY and BC for the modification of carbon materials has further been developed. An EDY-containing ester is designed and grafted on the surface of multi-walled carbon nanotubes (MWNTs). After hydrolysis of the ester groups, the resulting free hydroxy groups initiate the ring-opening polymerization of caprolactone or lactide, enhancing the solubility of MWNTs in common organic solvents and polymer solutions. In another case, four enediyne-containing Fréchet-type dendrimers are synthesized and reacted with MWNTs. The dendrimer-functionalized MWNTs also demonstrate improved solubility in common solvents. These methods provide a template for utilizing conjugated radical species derived from specific EDY monomers to modify carbon materials.

1.2.4. Synthesis of linear conjugated polymers via the Bergman cyclization

Once initiated, the existence of 1,4-didehydrobenzene intermediate containing carbon centers has been a central focus of research in both biochemistry and polymer science. The first pioneering research regarding applying enediyne as the monomer to construct polyaromatic compounds *via* radical coupling was reported by John and Tour in 1994. In this fundamental study illustrated in **Figure 14**, a series of enediyne and dialkynylbenzenes with alkyl groups embedded in benzene rings were synthesized and heated in neat conditions, undergoing BC without the need for initiators or radical trapping agents. This process can result in 50-90% yields of polymerized products, including poly(*p*-phenylene)s and polynaphthalenes. Infrared analysis confirmed the formation of out-of-plane C-H bending associated with two adjacent hydrogens attached to the aromatic ring.

Figure 14. The first example regarding radical polymerization *via* BC to construct polyaromatic compounds.⁸⁴

Inspired by the pioneering work in constructing polyphenylenes and polynaphthalenes via BC, a rich series of EDYs with various substituents have been developed to establish a linear conjugated polymer library with multifunctional structures and properties. Most of the research focuses on adjusting the substituents attached to the terminal alkyne positions of EDY to introduce different properties to formed polymers. Considering that hydroxy groups are known to initiate ring-opening polymerization (ROP), the hydroxy groups can be arranged at the terminal positions of EDYs to obtain EDY-containing macromonomers after appropriate ROP. Thus, ROP and BC polymerization can be combined to produce brush polymers with polyphenylenes as the rigid backbones. 115 In a specific case, as shown in Figure 15, an ROP of caprolactone, initiated by terminal hydroxy groups of EDYs, resulted in macromonomers with polycaprolactone (PCL) acting as a chain tail. After undergoing protection (protecting ending OH-group on PCL) and deprotection (removal of trimethylsilyl group of enediyne unit), the preparative macromonomers were treated under heat to initiate BC. The resulting brush polymers exhibited excellent solubility in organic solvents. With similar strategies, various EDY-containing monomers and macromonomers have been developed, 116,117 such as chiral phthalimides-EDY for producing polynaphthalenes with pendant chiral groups, 118 EDYs terminated with naphthyl groups for obtaining one-dimensional polyphenylenes, 119 and EDYs attached to chiral amino ester groups for chiral polyphenylenes. 120

In addition to the multifunctional polyphenylenes, the use of rigid conjugated frameworks also has been explored. Ultrathin mesoporous carbon and ultrathin ordered porous carbon can be derived from self-assembled monolayers of EDY on silica and Fe₃O₄ nanoparticles. ¹²¹⁻¹²³ Due to the rigid framework, the drug delivery system has also been realized by tailing hydrophilic drugs with hydrophobic maleimide-based EDYs. ⁷³

In conclusion, by continuously modifying the functional groups attached to the EDY's olefin and terminal alkyne positions, different functional linear conjugated polymers can be achieved. This serves as a versatile template for structural modification, enabling the customization of monomers to achieve the desired polymer functions.

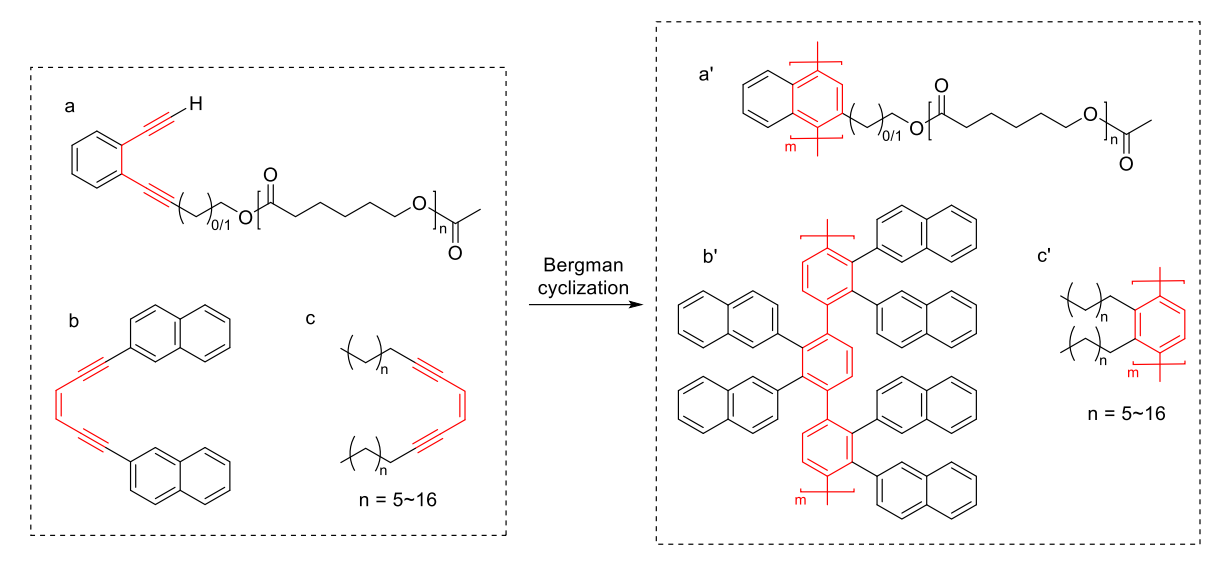


Figure 15. Representatives of constructing functional polymers with various designed EDYs.

1.2.5. Construction of polymeric nanoparticles via the Bergman cyclization

In addition to linear conjugated polyphenylenes, polymeric nanoparticles can also be reached through BC. Nanoparticles are defined as particles with diameters ranging from 1 to 100 nanometers (nm). Over the past few decades, nanoparticles have been extensively studied and applied in various fields, including drug delivery systems, ¹²⁴⁻¹²⁶ catalysis, ^{127,128} energy harvesting, ^{129,130}, and more, due to their unique morphologies and functionalities derived from their nanoscale sizes. The construction of nanoparticles typically relies on the intramolecular collapse of single polymer chains, a process usually driven by crosslinking chemistry based on pre-embedded reactive units. Various crosslinking strategies have been employed in this area, including click reactions, ¹³¹ alkyne coupling, ¹³² and self-condensation of monomers such as sulfonyl azides, ¹³³ benzocyclobutene, ¹³⁴ and benzoxazines ¹³⁵. The development of slow addition techniques under ultradilute conditions has greatly facilitated the synthesis of single-chain polymer nanoparticles (SCNPs). ¹³⁶ Given this background, BC has been developed as a crosslinking method, utilizing the diradical moieties generated during cyclization for radical coupling. This approach has been applied to the construction of polymeric nanoparticles. ^{137,138}

The key step in applying BC to the synthesis of SCNPs is embedding multiple enediyne units into precursor polymer chains. When BC is initiated, the diradical units formed from specific EDYs attached to the polymer chains randomly couple with each other, leading to the intramolecular collapse of the chains. Two main strategies have been developed for embedding EDYs into polymer chains, as shown in **Figure 16**. The first strategy involves copolymerization, where methyl methacrylate (MMA) is used as one of the monomers and copolymerized with enediyne-containing methacrylate *via* living radical polymerization. The second strategy focuses on post-polymerization modification. In this approach, functional groups that can react with each other are retained on both the small molecule EDYs and the pre-constructed polymer

chains. By adjusting the molar ratio of the two, the distribution of EDYs (whether compact or loose) along the polymer chains can be controlled. For example, trimethylsilyl-protected EDYs can be introduced as a side group into the polymer chains through either copolymerization or post-modification. After deprotecting the trimethylsilyl group, the polymer precursor is subjected to the appropriate initiation conditions to undergo BC. This process is followed by intramolecular chain collapse, typically achieved under ultradilute conditions or using a continuous addition technique, resulting in the formation of polymeric nanoparticles.

(A) Synthesis of EDY-containing copolymers

(B) Post-polymerization modifications

Figure 16. Two strategies of embedding EDYs as a side chain-element into polymers before the intramolecular collapse to obtain SCNPs.

1.3. Natural and synthetic enedignes in DNA cleavage

1.3.1. Natural enediyne anticancer antibiotics

In 1985, a touring scientist picked up a rock from the chalky soil in Waco, Texas. Out of curiosity, he brought this rock back to the laboratory. After growing a bacterial culture based on the rock, a compound named calicheamicin came to light, which was found extremely toxic to all cells. Through further research and screening, calicheamicin became known for its potent antibacterial properties and remarkable efficacy against solid tumors such as B16 melanoma

and murine cancers like L1210 leukemia, with effective doses ranging from 0.15 to 5 ug/kg.¹³⁹ Around the same time, dynemicin A was first isolated from *Micromonospora chersina*, a soil microorganism collected in the Gujarat State of India in the mid-1980s,⁶¹ followed by the isolation of kedarcidin chromophore from *Actinomycete* in 1992.¹⁴⁰ Although structurally distinct, these compounds share similar biochemical properties. **Table 1** lists these compounds, along with their dates of first isolation from nature. Most of them are classified as secondary metabolites and are primarily isolated from soil and marine microorganisms. Their structures are presented in **Figure 17**.²⁶ EDY units exist in these natural compounds with a way of incorporating them into a 9/10-membered ring. In addition to the rings containing EDY, naturally occurring EDY molecules also often have monosaccharide structures connected to the EDY-containing ring *via* an ether bond, as well as oxazoline or aziridine three-membered rings. Based on the natural enediynes' efficient and selective DNA cleavage activities, many medicinal chemists have dedicated efforts to studying the specific roles that these structures play in biological activities.

Table 1 Some representative natural enediynes

Compound	Biological Origin	First Discovery		
9-membered ring				
Neocarzinostatin	Streptomycescarzinostaticus (terrestrial)	1985		
C-1027	Streptomycesglobisporus (terrestrial)	1991		
Maduropeptin	Actinomaduramadurea (terrestrial)	1994		
Kedarcidin	ActinomyceteL585-6 (terrestrial)	1997		
N1999A2	Streptomyces sp. AJ9493 (terrestrial)	1998		
Sporolides	Salinisporatropica (marine)	1985		
Cyanosporasides	Salinisporapacifica (marine)	1985		
10-membered ring				
Esperamicin	Actinomaduraverrucosospora	1985		
Calicheamicin	Micromonospora echinospora ssp.	1985		
Dynemycin	Micromonosporachersina (terrestrial)	1985		
Namenamicin	Polysyncratonlithostrotum (marine)	1985		
Shishijimicin	Didemnumproliferum (marine)	1985		
Uncialamycin	Unknown (marine)	1985		

Reprinted with permission from ref. [26], Copyright [2013], John Wiley and Sons

Pioneered by the first synthesis of calicheamicin γ_I^{117} and the first (bio)synthesis of (+)-dynemicin A^{62,141} (see **Figure 17**) in the 1990s, an in-depth understanding of the specific roles played by various structural components of EDY molecules in site-specific, double-stranded DNA cleavage has gradually emerged. For site-specific cleavage, calicheamicin γ_I^I , a natural masterpiece, serves as an exemplary case here.¹³⁹ It consists of two vital structural regions: one

containing the critical EDY and the other an extended sugar residue. A hexasubstituted benzene ring and four monosaccharide units are linked by an unusual combination of glycosidic, thioester, and hydroxylamine groups. The carbohydrate segments play a crucial role in recognizing and specifically targeting DNA, serving as a docking unit. Strong hydrophobic interactions and van der Waals forces between the aryloligosaccharide and the DNA minor groove stabilize the complex. Localized conformational changes in the DNA enable optimal complementarity. As a result, it binds tightly to the DNA minor groove, inducing highly specific cleavage for sequences such as 5'-TCCT-3' and 5'-TTTT-3'. 144,145

In addition, nature equips these compounds with a triggering mechanism that ensures their antibacterial action is only activated when they encounter targeted bacteria or microorganisms. This triggering mechanism is crucial for activating the EDY warhead, leading to BC under appropriate conditions, such as thiol activation or ultraviolet light exposure. In the case of calicheamicin $\gamma_1{}^I$, the triggering unit is a trisulfide group, with the central sulfur atom poised to react with a nucleophile, forming a thiolate or thiol once the molecule interacts with DNA. The subsequent reactions lead to a released strain energy, which is known as facile BC. The resulting diradical intermediate abstracts a hydrogen atom from the DNA backbone, creating a carbon radical in the ribose sugar. This radical, in the presence of oxygen, initiates an oxidative process that leads to single- or double-stranded scission, ultimately causing cell death.

Overall, the three components (the enediyne warhead, docking unit, and triggering part) are combined to accomplish a naturally existing EDY antibiotic featured with site-specific cleavage, as highlighted in **Figure 17**. This has also inspired many medicinal chemists to mimic the structure of natural compounds when designing and synthesizing new EDY antibody drugs, deliberately introducing groups that can trigger the selective release of activities.

(a) Nine-membered enediynes

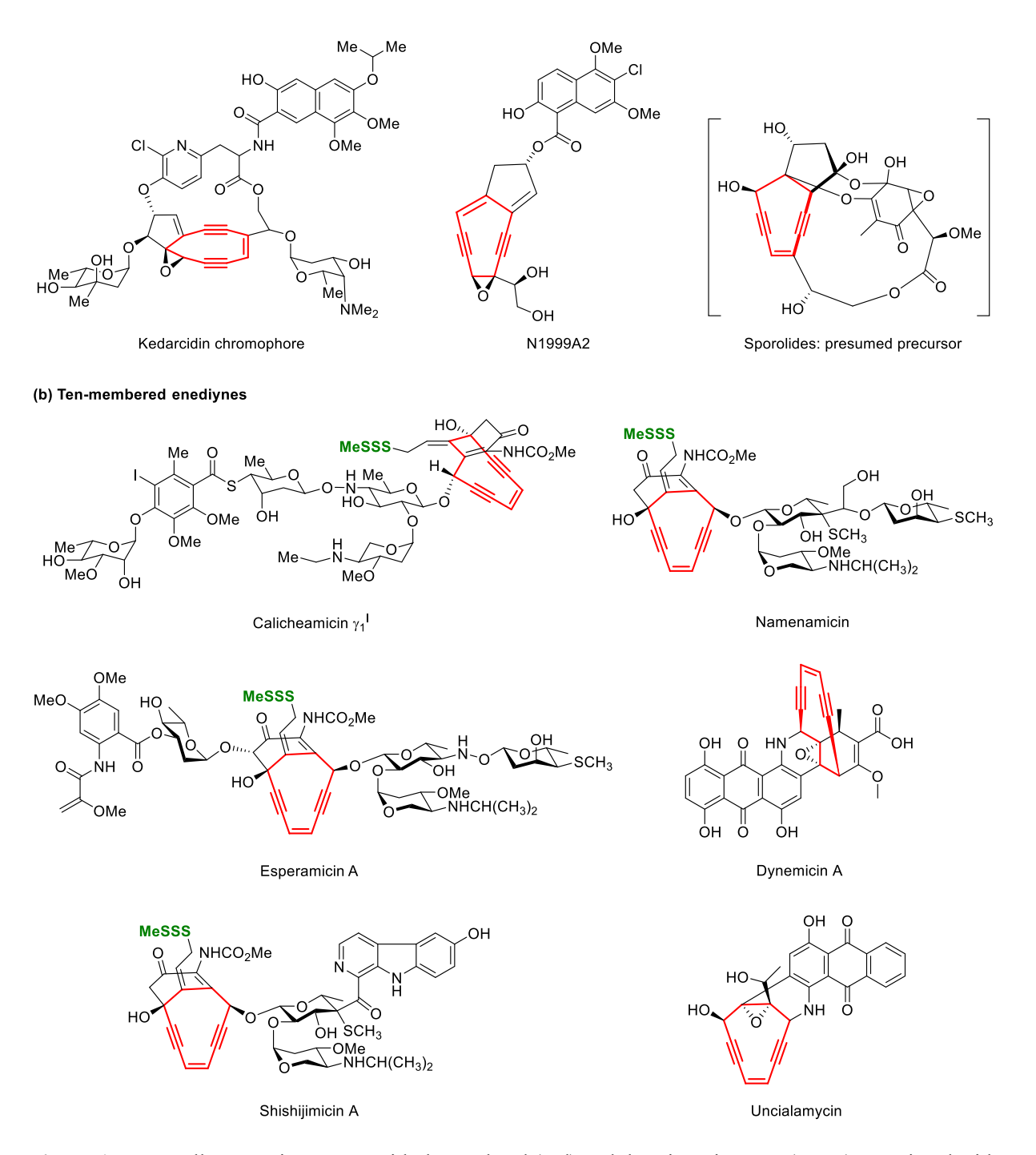


Figure 17. Naturally occurring EDYs with the warhead (red) and the triggering part (green). Reprinted with permission from ref. [26], Copyright [2013], John Wiley and Sons.

1.3.2. Synthetic enediynes and enediyne-containing complexes

Inspired by the enediyne units found in naturally occurring antibiotics, synthetic efforts have been invested in developing various EDYs and EDY-containing complexes. Meanwhile, metal complexes used in pharmaceuticals have been shown to participate in DNA-targeted processes. They are applied in medical tools such as radiation sensitization and contrast agents for enhancing visibility in high-field NMR detection. Given the growing use of metal elements in practical therapies, researchers have focused on developing not only carbon-based

EDYs but also metalloenediyne derivatives, with a focus on their radical-induced therapeutic effects. Moreover, while acyclic EDYs are generally inert in BC, ¹⁴⁷ cyclic ones, where the alkyl termini are connected to form a complete EDY-containing ring, are flexible in their size and steric patterns. The reactivities of cyclic EDYs can be fine-tuned by adjusting the inter-alkynyl distance and the degree of strain at the terminal alkyl position. As a result, metal-involved cyclic EDYs have recently garnered significant attention from chemists and pharmaceutical researchers.

Researchers such as Zaleski and coworkers have kept developing bioactive EDY compounds and their metal complexes, as illustrated in **Figure 18**. 41,43,51,72,83,148-171 In 2020, they designed and synthesized a range of metallated enediyne complexes based on the combination of (*Z*)-N,N'-bis[1-pyridin-2-yl-meth-(*E*)-ylidene]oct-4-ene-2,6-diyne-1,8-diamine (PyED) with various metal salts (Cu, Fe, and Zn) in solution. The resulting complexes, including FeCl₂-PyED, FeSO₄-PyED, CuCl₂-PyED, CuSO₄-PyED, ZnCl₂-PyED, and ZnSO₄-PyED, were tested on two different human cell lines: cultured U-1 melanoma cells and MDA-231 breast cancer cells, to assess their cytotoxicities. The study also included comparisons across different concentrations of the EDY-metal complexes and varying culture temperatures. Their findings confirmed that cytotoxicity was highly dependent on these factors, suggesting the potential for a practical therapeutic strategy involving localized heating in anticancer treatments.

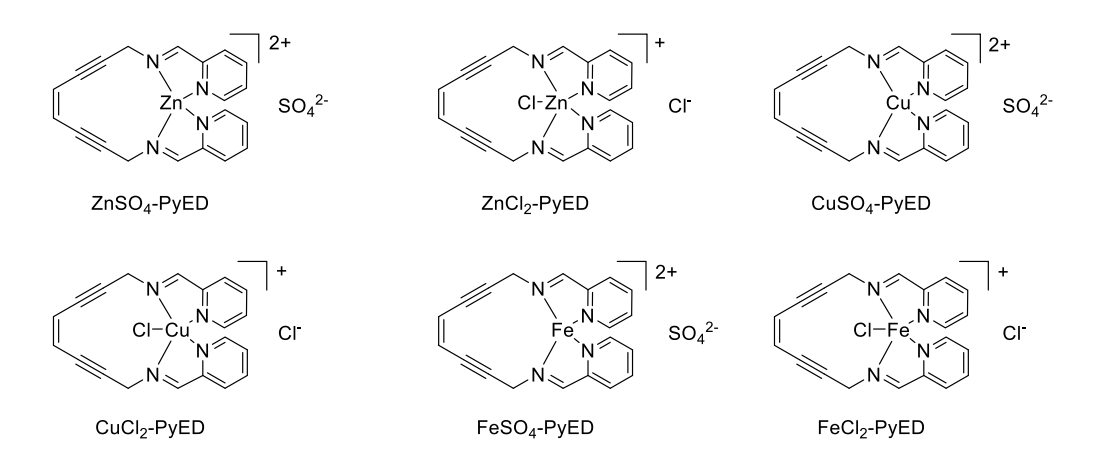


Figure 18. Metal complexes derived from EDYs.

1.4. Enediynes and the Bergman cyclization in stress-induced chemistry

1.4.1. Structural investigation of stress-sensitive units

Stress-sensitive units are distinct molecules that undergo controllable and predictable chemical transformations in response to external mechanical stress.¹⁷² The efficient energy dispersion and mass transport triggered by mechanical forces have garnered significant interest from chemists. From a macromolecular perspective, polymer chains incorporating these stress-

sensitive units tend to exhibit this practical trait. Due to the chain-like structure, the transient transfer or accumulation of mechanical energy along the polymer backbone facilitates responsive effects, ¹⁷³⁻¹⁸⁰ such as inducing color/fluorescence changes, ¹⁷⁷ or generating catalysts. ¹⁸¹ Given the wide range of polymer applications in fields like packaging, medical devices, and coatings, the development of mechanically responsive polymers has recently attracted increased attention. From the perspective of novel structure and convenient synthesis, stress-sensitive units have been a central focus of fundamental research, with significant progress made in recent years. Depending on their specific structures, these units can undergo various reactions, including bond cleavage or rearrangement, isomerization, and ring-opening reactions, as shown in **Figure 19**.

Figure 19. Examples of embedding and initiating stress-sensitive units into polymer chains to induce functionalities.

Successful design of the stress-sensitive units based on identifying key structural elements that enable mechanically initiated reactions. Most stress-sensitive units incorporate relatively weak bonds that are prone to dissociation or isomerization upon the application of mechanical force. Whether bond dissociation or scission occurs, a low bond dissociation energy (BDE) is essential. As shown in **Figure 20**, regarding the experimentally validated mechanophores, "weak bonds" ready to undergo chemical transformation are highlighted in red. Homolytic bonds, a class of bonds with relatively low dissociation energy, include examples such as the peroxide O-O bond (BDE: ~35 kcal mol⁻¹) first reported by the Encina group in 1980, ¹⁸² and the diazo group (BDE:~27 kcal mol⁻¹) developed by the Moore group in 2005 for selective scission under mechanochemical activation. For heterolytic cleavage, bonds like the C-S bond

located in arylsulfonium salt (BDE: ca. 65 kcal mol⁻¹) are commonly used.¹⁸⁴ Additionally, coordinated bonds have found mature applications in stress-sensitive units, ¹⁸⁵⁻¹⁸⁸ such as the palladium-phosphorus and ruthenium-carbene coordinative bond. For the bonds that possess relatively high BDE, such as C-O, C-C, and C-N bonds, a common strategy to reduce BDE is incorporating the bonds into cyclic moieties. Three-, ^{189,190} and four-membered rings, ^{174,176} often featuring oxacyclic rings or halogenated substituents, have attracted attention since 2009 and have been developed into several classical stress-sensitive units. Additionally, fused, bridged, and spiro rings have been extensively studied by the Moore, Craig, Sijbesma, and Boydston groups. ¹⁷² These ring systems reduce strain on the bonds, effectively lowering their high BDEs and making them more prone to mechanical activation.

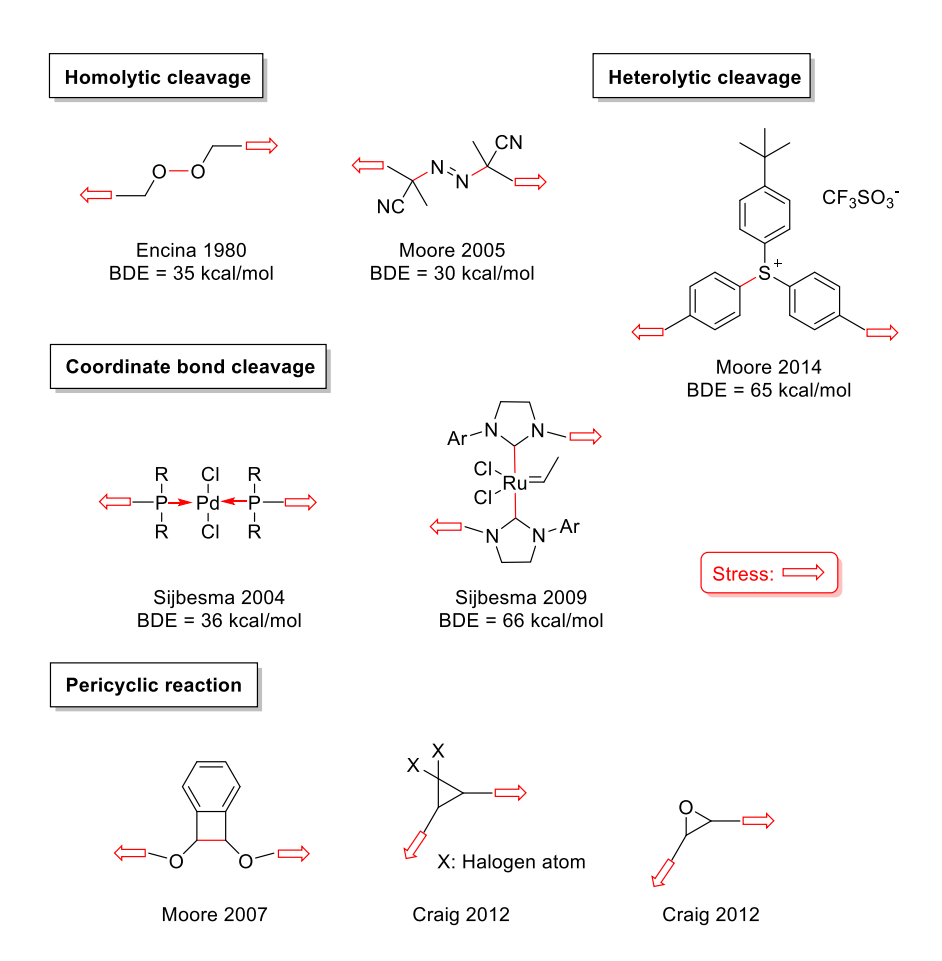


Figure 20. Developed mechanophores with their specific BDEs.

Incorporating stress-sensitive bonds into polymer chains to generate detectable responses under external forces has been widely studied.¹⁹¹ The development of such sensitive units, focusing on efficient triggering mechanisms and ease of synthesis, remains a key area of interest for chemists.

1.4.2. Exploitation of enediynes as stress-sensitive units

EDY, a small molecule prone to undergoing pericyclic reactions, has demonstrated adjustable reactivities and promising applications. Among the numerous studies focused on it, the structural factors influencing its cyclization activity have been emphasized. In addition to the molecular-strain difference^{59,192,193} and electronic effects from substituents,³¹ the proximity effect, 28,57,194 corresponding to the distance between the acetylenic carbon atoms, has been shown to play a key role in the cyclization. Consequently, the potential for enedignes to function as mechanophores was first considered in the 1990s, as noted by Moore and coworkers in a 2015 review. 172 Their initial attempt, published in 2008, explored the possibility of using specific forces induced by swelling of EDY-crosslinked networks to trigger BC. 195 Three EDY molecules with different substituents were designed and synthesized. Their thermal cyclization was investigated using DSC, and the observed thermal activities were found to align with the known effects of the substituents. These EDY triggers were then embedded into a polymer matrix as crosslinks in poly(methyl methacrylate), and the material was swollen with methyl methacrylate monomer. The swelling was expected to apply stress to the enediyne crosslinks, promoting cyclization. However, no definitive mechanical activation was detected, and insufficient force was considered the reason for the difficulty in using enediyne as mechanical triggers.

Although a computational prediction of the status of molecular stretching deformations, CoGEF, together with the convective proximity effect, theoretically supported the possibilities of force-induced cyclization, the practical results were not satisfactory. Therefore, compared to well-established triggers such as heat, ¹² photochemistry, ^{47,50,74,196} and metal catalysis, ^{48,49} force-induced acceleration of BC has been rarely studied and has not yet been successfully achieved on an experimental scale, even though some efforts have been reported. ^{34,195}

1.5. Semi-interpenetrating polymer networks

1.5.1. Interpenetrating and semi-interpenetrating polymer networks

Interpenetrated polymer networks (IPNs) are a sort of polymer consisting of two or more networks that are interpenetrated on a polymer scale but not covalently bonded to each other. These networks cannot be separated unless the interlaced chemical bonds are broken. In such systems, at least one network is synthesized and crosslinked in the presence of the other. The Aylsworth group first created a notable version of IPNs in 1914 by combining phenol-formaldehyde resin with vulcanized natural rubber. Theoretical discussion on IPNs followed in 1960 by the Millar group. Since then, IPNs have occupied a significant role in macromolecular topologies. Extensive research has been dedicated to the synthesis, physical/chemical properties, morphologies, and applications of ingeniously designed IPNs. 201-

²⁰³ Their unique swelling capacities and mechanical strengths have enabled their successful use in engineering plastics, ²⁰⁴ automotive parts, ²⁰⁵ biomedical devices, ²⁰⁶⁻²⁰⁹ damping compounds, ²¹⁰⁻²¹² and more. Represented by hydrogels, ²¹³⁻²¹⁶ a sort of classical IPNs derived from hydrophilic and bio-friendly raw materials, IPNs have been particularly applied in pharmaceutical devices ²¹⁷⁻²²⁰ and stimuli-responsive sensors ²²¹⁻²²⁴ recently.

Depending on the synthesis routes, particularly the sequence of the network formation and monomer addition, IPNs can be classified as either sequential or simultaneous IPNs. Sequential IPNs are created by swelling the monomer of the second polymer into a pre-formed network, followed by its polymerization. The second polymer is so formed in a sequential mode after the first network is already in place.²²⁵ In contrast, simultaneous IPNs are formed by mixing the monomers, crosslinkers, and initiators of both networks together, followed by simultaneous polymerizations that proceed in a noninterfering manner.²²⁶ Additionally, based on the combined patterns of the two coexisting polymers, IPNs can be classified into semi-interpenetrating polymer networks (semi-IPNs), pseudo-interpenetrating polymer networks, and fully interpenetrating polymer networks, each exhibiting distinct topologies and combinations.^{197,227} As illustrated in **Figure 21**, semi-IPNs are a type of sequential IPNs in which only one of the coexisting polymers is crosslinked while the other remains linear.²²⁸⁻²³⁰

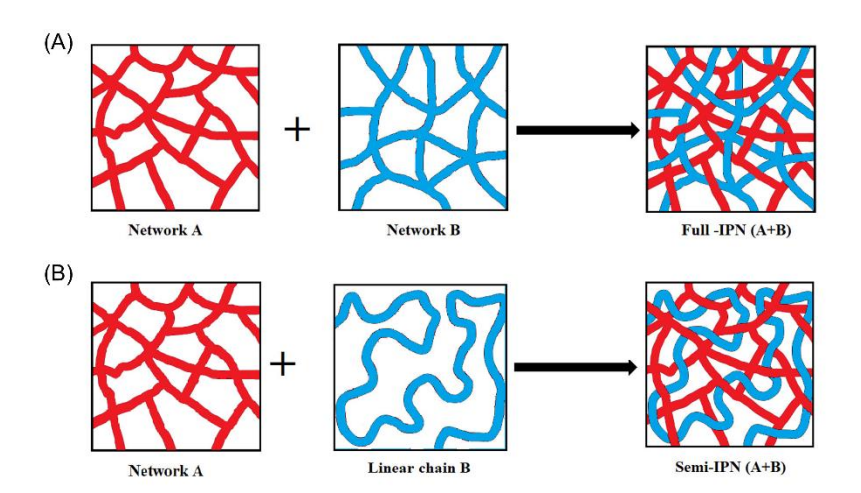


Figure 21. Definition of (A) full interpenetrating polymer network (IPN) and (B) semi-IPN structures. Reprinted with permission from ref. [229], Copyright [2018], American Chemical Society.

1.5.2. Chemical approaches of semi-interpenetrating polymer networks

Semi-IPNs combine the properties of both component polymers, offering enhanced mechanical strength, stability, and responsiveness compared to single-network systems. ²³¹⁻²³³ Several strategies have been developed to construct semi-IPNs, utilizing a variety of monomers and polymerization techniques. One common approach is sequential polymerization, where the first polymer network is synthesized and then swelled with a monomer that polymerizes to form

the second polymer, as shown in **Figure 22**. This method allows for tunability in the polymer's properties depending on the choice of monomers and conditions.

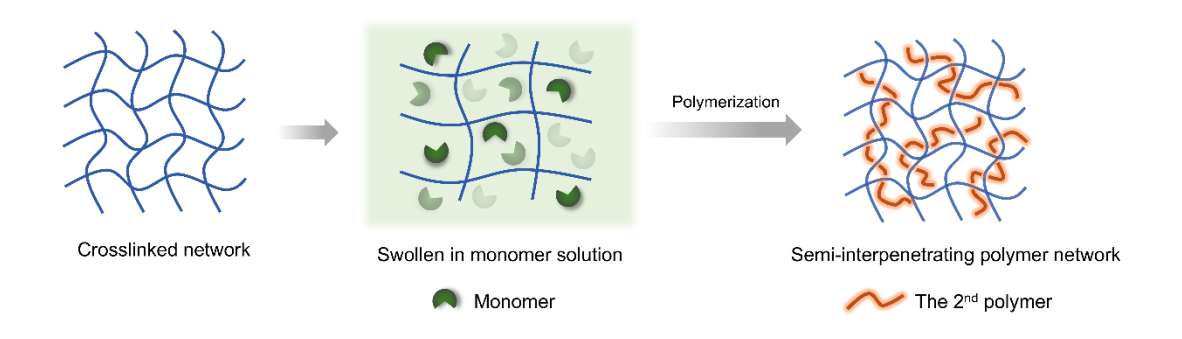


Figure 22. Schematic illustration of the preparative process of constructing semi-IPNs.

Common monomers, such as styrene,²³⁴ acrylates, acrylamide,²³⁵ are frequently utilized to form the second polymer in constructing semi-IPNs. For example, poly(methyl methacrylate) was polymerized within the polyurethane matrix to create a semi-IPN with improved thermal stability and mechanical properties.²³⁶⁻²³⁹ As for the first network matrix, epoxy resins are also commonly employed in semi-IPNs due to their robust thermal and mechanical characteristics. As example, an epoxy-based semi-IPN was reinforced with elastomers, enhancing toughness while maintaining strength.²⁴⁰ Radical polymerization is particularly common in the construction of semi-IPNs, allowing the rapid formation of the second polymer network, as seen in the synthesis of semi-IPNs consisting of polystyrene and poly(vinyl acetate).²⁴¹ These versatile methods and materials enable the customization of properties for various applications, including coatings, adhesives, and biomedical devices.

2. Aim of the Thesis

The aim of this cumulative thesis is to employ small molecule EDYs and their associated BC reaction as main-chain elements in polymers to construct EDY-based polymers, thereby expanding their potential, particularly as functional materials. As illustrated in **Figure 23**, the specific objectives of this thesis are to broaden the applications of EDY and BC in functional polymers:

- 1) Develop main-chain EDY polymers and investigate whether their DNA cleavage ability in solution can be enhanced due to the repeated embedding of EDY structures. Current EDY-related modifications in polymer chemistry mainly have linked single EDY unit as a functional side group onto a polymer backbone. However, embedding EDYs into polymer chains as repeating units has not yet been explored. A strategy to realize main-chain EDY polymers has been established in this thesis.
- 2) Trigger crosslinking of main-chain EDY polymers in the solid state using multiple stimuli, such as heat, compression, and mechanical stress, to construct novel multi-stimuli-responsive materials. EDY was considered a mechanophore in the 1990s, ¹⁷² expected to induce BC by swelling EDY-crosslinked poly(methyl methacrylate). ¹⁹⁵ Building on earlier work, we have modified the polymer matrix by directly embedding the EDY into the polymer chains.
- 3) Establish semi-interpenetrating polymer networks (semi-IPNs) by first swelling small molecule EDYs into preformed network polymers, followed by the appropriate initiation of BC. Considering the ability of small-molecule EDY to diffuse into and swell within a preformed network, this thesis is expected to propose a general framework for utilizing EDY in the post-modification of polymers beyond the specific scientific examples presented.

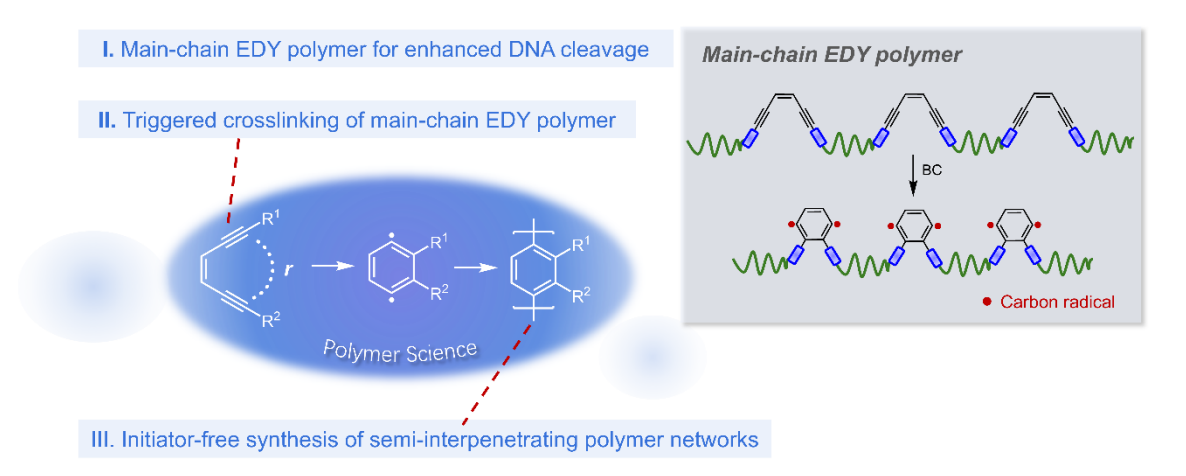


Figure 23. Aims of this thesis based on different roles of EDY in functional polymers via BC.

3. Scientific Approach

Previous work: Individual enediyne in core skeleton

A: 4,4'-oxydibenzaldehyde

Whereas EDY and BC have been extensively exploited in polymers, with most modifications linking single EDY molecules as functional side groups onto a polymer backbone, ²⁴² strategies that utilize EDYs as repeating units in main-chain polymers, along with their activation when embedded directly within the chain, have not yet been reported. In this thesis, the synthetic approaches to construct main-chain EDY polymers start by screening appropriate EDYs and polymerization methods. For the conceptualization of main-chain EDY polymers, a bifunctional EDY and a polycondensation are selected to form the desired products. Specifically, (*Z*)-octa-4-en-2,6-diyne-1,8-diamine, which was designed and synthesized by the Zaleski group in 2000, ⁶⁹ sparked interest due to its primary amine groups, exhibiting reduced steric hindrance and inducing intramolecular hydrogen bonding, which contributes to its high cyclization activity. ^{83,166,169}

This work: Main-chain enediyne polymer

NH2

OHC

CHO

Cyclization

Cyclization

Cyclization

Cyclization

Cyclization

Carbon radical

N=C

H

Figure 24. Main-chain EDY polymers derived from the diamino EDY and various dialdehydes. Reprinted from ref. [243].

C: [1,1'-biphenyl]-4,4'-dicarbaldehyde

tetrafluoroterephthalaldehyde

B: terephthalaldehyde

The first part of this thesis has been published as "Bergman Cyclization of Main-Chain Enediyne Polymers for Enhanced DNA Cleavage, Yue Cai, Florian Lehmann, Edgar Peiter, Senbin Chen, Jintao Zhu, Dariush Hinderberger, and Wolfgang H. Binder*, *Polym. Chem.*, 2022, 13, 3412." This series of main-chain EDY polymers is derived from acyclic diamino enediynes and dialdehydes as illustrated in Figure 24. The active diamino enediynes are incorporated *via* polycondensation, resulting in polyimines with controllable stability for a BC at room temperature. The presence of the enediyne units in the main-chain polymers is confirmed through FT-IR spectroscopy and two cycles of DSC analysis. The chain-length-

dependent DNA cleavage activity under physiological conditions is investigated in solution *via* gel electrophoresis alongside the stereoelectronic effects induced by the substituent patterns of the dialdehydes. EPR spectroscopy is used to observe thermal and photochemical radical formation, which is further correlated with the DNA cleavage activity of the polymers and indicates long-term stability of the formed radicals in the solid state.

The second part of this thesis has been published as "Triggered Crosslinking of Main-Chain Enediyne Polyurethanes via Bergman Cyclization, Yue Cai and Wolfgang H. Binder*, Macromol. Rapid Commun. 2023, 44, 2300440."244 Based on the potential of EDY as reactive units sensitive to mechanical force, it is of vital importance to embed EDY into a suitable polymer matrix that can effectively disperse internal energy from an applied stress. Polyurethane (PU) is selected due to its versatile properties, ranging from elastomeric to rigid polymers, and its ease of synthesis. Inspired by its unique characteristics and our previous experience, (Z)-octa-4-en-2,6-diyne-1,8-diamine is chosen to construct the second series of EDY-based polymers, as shown in Figure 25. The diamino EDY acts as a bifunctional monomer in the polycondensation with isocyanate-terminated polytetrahydrofuran, resulting in the first elastomeric main-chain EDY polymer. To explore the possibility of initiating crosslinking via BC, multiple stimuli (heating, compression, and stretching) are applied to the solid sample to induce hardening of the elastomer. Since BC is an exothermic reaction, DSC is used to monitor the exothermic values. Additionally, IR spectroscopy is employed to detect the characteristic peaks of the benzene moieties formed during BC. The mechanical properties are based on tensile tests, which can also afford controllable stretching stress during the tests.

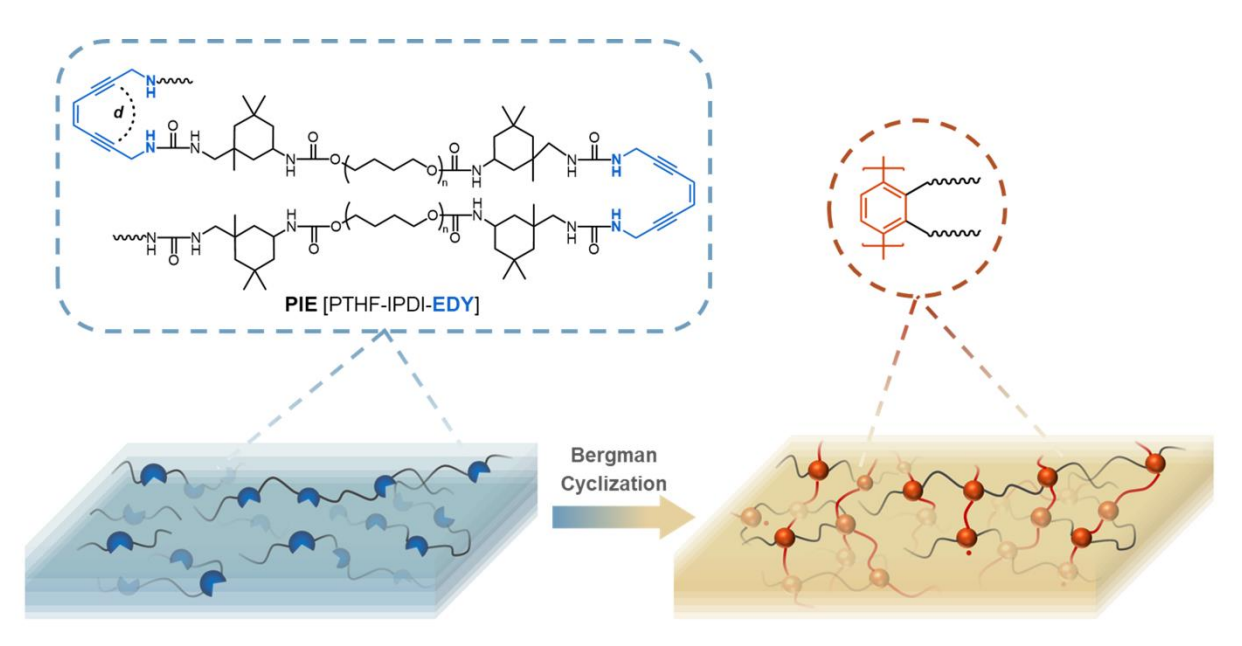


Figure 25. Schematic illustration of the designed EDY-based PU and the triggered crosslinking *via* BC. Reprinted with permission from ref. [244], Copyright [2023], John Wiley and Sons.

The third part of this thesis has been published as "Initiator-Free Synthesis of Semi-Interpenetrating Polymer Networks via Bergman Cyclization, Yue Cai, Florian Lehmann, Justus F. Thümmler, Dariush Hinderberger, and Wolfgang H. Binder*, Macromol. Chem. Phys. 2024, 2400177."245 Therein, the EDY has been applied in the formation of semi-IPNs. Semi-IPNs are practically prepared via sequential synthesis methods.²⁴¹ The semi-IPN via EDY and BC, begins with the synthesis of an appropriate EDY and a preformed crosslinked network. (Z)-oct-4-ene-2,6-diyne-1,8-diol is chosen as the precursor of the second polymer and swollen into a pre-synthesized polyurethane network, as illustrated in Figure 26. The formation of the semi-IPN is monitored via EPR spectroscopy, FT-IR spectroscopy, and thermal methods (DSC), confirming the activation of the EDY-moiety and its subsequent polymerization to form the second polymer. Stress-strain characterization and cyclic stress-strain investigations, together with thermogravimetric analysis (TGA) and differential thermogravimetric analysis (DTG), demonstrate improved mechanical properties and thermal stability of the formed semi-IPN compared to the initial network. Atomic force microscopy (AFM) analysis in the phase contrast mode and scanning electron microscopy (SEM) are performed to investigate the surface morphologies.

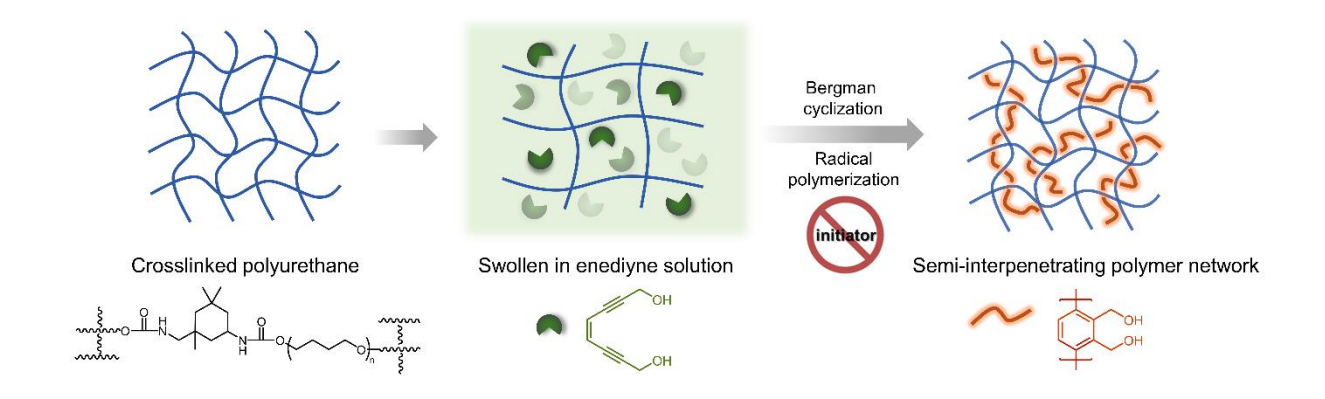


Figure 26. Schematic illustration of the construction of semi-IPNs *via* BC. Reprinted with permission from ref. [245], Copyright [2024], John Wiley and Sons.

4. List of Publications

The results of this thesis are published in the following three publications. All of the three first-author publications [P1] - [P3] are reprinted as part of this cumulative thesis with permissions from the Royal Society of Chemistry, ²⁴³ and John Wiley and Sons. ^{244,245}

[P1] Bergman Cyclization of Main-Chain Enediyne Polymers for Enhanced DNA Cleavage

Yue Cai, Florian Lehmann, Edgar Peiter, Senbin Chen, Jintao Zhu, Dariush Hinderberger, and Wolfgang H. Binder*

Polym. Chem., 2022, 13, 3412. DOI: 10.1039/D2PY00259K. Lit [243]

Conceptualization, Y.C. and W.H.B.; methodology, Y.C., F.L.; investigation, Y.C., F.L.; writing—original draft preparation, Y.C. and W.H.B.; writing—review and editing, Y.C., F.L., E.P., S.C., J.Z., D.H. and W.H.B.; supervision, W.H.B.; project administration, W.H.B.; funding acquisition, W.H.B. All authors have read and agreed to the published version of the manuscript.

[P2] Triggered Crosslinking of Main-Chain Enediyne Polyurethanes via Bergman Cyclization

Yue Cai and Wolfgang H. Binder*

Macromol. Rapid Commun. 2023, 44, 2300440. DOI: 10.1002/marc.202300440. Lit [244]

Y.C. and W.H.B.: Conceptualization, methodology, investigation, and writing; W.H.B.: Supervision, project administration, and funding acquisition. Both authors have read and agreed to the published version of the manuscript.

[P3] Initiator-Free Synthesis of Semi-Interpenetrating Polymer Networks *via* Bergman Cyclization

Yue Cai, Florian Lehmann, Justus F. Thümmler, Dariush Hinderberger, and Wolfgang H. Binder*

Macromol. Chem. Phys. 2024, 2400177. DOI: 10.1002/macp.202400177. Lit [245]

Conceptualization was performed by Y.C. and W.H.B.; methodology was performed by Y.C. and F.L.; investigation was performed by Y.C. and F.L.; writing—original draft was prepared by Y.C. and W.H.B.; writing—review and editing was performed by Y.C., F.L., J.F.T.; D.H., and W.H.B.; supervision was performed by W.H.B.; project administration was performed by W.H.B.; funding acquisition: W.H.B. All authors have read and agreed to the published version of the manuscript.

Polymer Chemistry

Volume 13 Number 23 21 June 2022 Pages 3379-3554



ISSN 1759-9962



PAPER

Polymer Chemistry



PAPER View Article Online
View Journal | View Issue



Cite this: *Polym. Chem.*, 2022, **13**, 3412

polymers for enhanced DNA cleavage†

Bergman cyclization of main-chain enediyne

Yue Cai, par Florian Lehmann, par Edgar Peiter, Senbin Chen, Jintao Zhu, par Dariush Hinderberger par and Wolfgang H. Binder sa Binder sa Albarian Senbin Chen, Jintao Zhu, par Senbin Chen, par Senbin C

Since the discovery of the role of enediynes in natural antibiotics (such as calicheamicines) via in situ diradical-induced DNA strand cleavage, Bergman cyclization has attracted fervent attention for decades. Thus, Bergman cyclization is widely used in pharmaceutics, synthesis, and polymer chemistry as a trigger for the generation of diradicals. Whereas applications of the Bergman cyclization in polymers mostly rely on side-chain linked enediynes, strategies to embed enediynes as the main repeating units into polymers are not reported yet. Here, the synthesis of main-chain enediyne polymers was accomplished, allowing to embed and control the reactivity of the diamino enediynes via polycondensation into polyimines. Such main-chain enediyne polymers in solution exert a chain-length dependent DNA cleavage activity under physiological conditions, additionally tunable by modulating the stereoelectronic environment via their substitution patterns. Photochemical activation generates long-lived free radicals as verified via electron paramagnetic resonance (EPR) spectroscopy, with rates of their formation comparable to those in DNA cleavage experiments.

Received 25th February 2022, Accepted 13th May 2022 DOI: 10.1039/d2py00259k

rsc.li/polymers

Introduction

Bergman cyclization, an intramolecular cyclization of the enediyne (EDY) motif, was first discovered in the early 1970s on *cis*-1,5-hexadiyn-3-ene, revealing an exclusive thermal rearrangement to afford the labile 1,4-didehy-drobenzene diradical. Since the discovery of the crucial role of enediynes in natural antibiotics (such as calicheamicin, esperamicin, and dynemicin A^{4,5}), wherein *in situ-*generated diradicals induce DNA strand cleavage, enediynes and the Bergman cyclization have attracted fervent attention for many years. In low molecular weight compounds the mechanism involved in the cyclization can be well tuned by molecular design, thus leading to a tremendous synthetic efforts to build up various enediyne-

influence activation of Bergman-cyclization, subsequent stabi-

containing frameworks. Together with the critical distance between the acetylenic carbon atoms, 9-11 especially the mole-

cular geometry 12-14 and substituent-induced electronic effects221 are closely related to their cyclization activity. In addition to the thermally triggered cyclization 1 UV radiation, 15-18 the induction by acids 19 and organometallic catalysts²⁰⁻²³ have been utilized widely in enediyne chemistry to access novel organic compounds, biological agents, polymers and materials. In polymers modifications mostly rely on linking single enediynes as functional side chain onto a polymeric backbone, further being responsible for the properties of the resulting polymers.24 Being a source of reactive diradicals, enediyne-containing precursor polymers can be further applied to construct linear conjugated polycyclic networks,²⁵ brush polymers²⁶ and single-chain polymer nanoparticles.²⁷ However, strategies to utilize enedignes as repeating components in main-chain polymers, together with their activation as repeating enediynes directly embedded into the chain, have not been reported up to now (Scheme 1). Considering the adjustable stability of EDY in view of modifying substituents and strain geometry, we envisioned that repeating enediynes embedded in the main polymer-chain would allow a tuning of their cyclization activities, further affecting DNA cleavage activities and the long-term stabilities of the generated radicals. We hypothesize that both, chain length of the polymers, the number of repeating enediyne-units together with potential strain imposed from the polymer chains can

^aMacromolecular Chemistry, Institute of Chemistry, Faculty of Natural Science II (Chemistry, Physics and Mathematics), Martin-Luther-University Halle-Wittenberg, von-Danckelmann-Platz 4, Halle D-06120, Germany

^bPhysical Chemistry, Institute of Chemistry, Faculty of Natural Science II (Chemistry, Physics and Mathematics), Martin-Luther-University Halle-Wittenberg, von-Danckelmann-Platz 4, Halle D-06120, Germany

^cFaculty of Natural Sciences III, Plant Nutrition Laboratory, Institute of Agricultural and Nutritional Sciences, Martin Luther University Halle-Wittenberg, Halle D-06099, Germany

^dKey Laboratory of Materials Chemistry for Energy Conversion and Storage, Ministry of Education (HUST), School of Chemistry and Chemical Engineering, Huazhong University of Science and Technology (HUST), Wuhan 430074, China

[†]Electronic supplementary information (ESI) available. See DOI: https://doi.org/ 10.1039/d2py00259k

Polymer Chemistry Paper

Previous work: Individual enedivne in core skeleton

Scheme 1 Main-chain enedigne polymers: synthesis and Bergman cyclization.

lities of the formed radicals and thus influence the DNA cleavage abilities.

context (Z)-octa-4-en-2,6-diyne-1,8-diamine,²⁸ this designed and synthesized by the Zaleski group in 2000, caught our interests, as the primary amine groups, displaying reduced steric hindrance and intramolecular hydrogen bonding, can contribute to its active cyclization performance. Since its first synthesis in 2000, the diamino enediyne has been only applied scarcely29-31 and not in polymers yet, displaying an only limited stability as such and thus being not useful for a direct use in DNA cleavage.

We here report the synthesis of main-chain enediyne polymers, derived from acyclic diamino enediyne and dialdehydes (Scheme 1). The active diamino enediynes were successfully embedded via polycondensation to afford the resulting polyimines with an excellent Bergman cyclization stability at room temperature. We propose that both, the repetitively placed enediyne components together with their increased steric hindrance via the imine bonds ultimately allow a tuning of their cyclization activities. We here investigate the stoichiometric ratio of the two starting materials for polycondensation to control the degree of polymerization. We could verify the existence of enediynes in the main chain polymers via FT-IR and two cycles of differential scanning calorimetry (DSC) analysis. Furthermore, we study the chain-length dependent DNA cleavage activity under physiological conditions, additionally modulated by the stereoelectronic environment of the substitution pattern within the polymers. Electron paramagnetic resonance (EPR) spectroscopy was used to observe thermal and photochemical radical formation, which can be correlated to the DNA cleavage activity of the polymers as well as indicate a long term stability of the formed radical in the solid state.

Results and discussion

Synthesis of diamino and diimine enediynes as building blocks for subsequent polycondensation

To firstly probe the desired polycondensation of EDY-II with aldehydes, we focused on the model reaction shown in Scheme 2 to precisely adjust the stoichiometric ratios as required according to the Carother's equation to reach adjustable chain lengths. We have used (Z)-octa-4-en-2,6-diyne-1,8diamine²⁸ for which several synthetic approaches are known^{29,31} to embed the ene-diynes into the main chain of the polymers. For initial protection, the tert-butyloxy carbonyl (Boc) group was installed within the terminal alkyne via classical Sonogashira coupling reaction between (Z)-1,2-dichloroethene and tert-butyl prop-2-yn-1-ylcarbamate, thus affording EDY-I. As during removal of the protective Boc group, the concentration of the solution of the desired diamino EDY-II was found to play a significant role as a Bergman-cyclization was already observed at room temperature, an appropriate dilution is necessary to avoid a primordial Bergman-cyclization. By adding the internal standard hexamethylbenzene, its precise concentration could be calculated from nuclear magnetic reso-

Scheme 2 Synthesis of diamino EDY-II and model reaction to obtain diimine enediyne EDY-III. i: (HCl aq., EA, rt; then 1 M NaOH aq. ii: benzaldehyde, CHCl3, rt.

nance (NMR) analysis for further polycondensation with the dialdehydes (**A**, **B**, **C**, **D**) in a ratio of NH₂/C=O equalling 1/1. When using a concentration of 0.25 mol L⁻¹, small brown particles would appear in the solution and grow quickly and spontaneously, as shown in Fig. S4† together with the evidence of radicals as confirmed by electron paramagnetic resonance (EPR) spectroscopy, indicative of a primordial Berman cyclization. Therefore, its high activity to undergo Bergman cyclization even at room temperature was verified. However, the stable di-imine compound **EDY-III** could be further generated smoothly, relying on the condensation between **EDY-II** and a

suitable equivalent of benzaldehyde, thus representing a

stable and suitable form for incorporation into the polymer chain.

Synthesis of the main-chain enediyne polymers

With the established method for *in situ* deprotection and imine-formation in hand, we shifted the synthetic target to the main-chain enediyne polymers by replacing benzaldehyde with the dialdehydes (**A**, **B**, **C**, **D**). Initial attempts with a 1/1 molar ratio of **EDY-II** and 4,4'-oxydibenzaldehyde **A** were accomplished (Fig. 1A). The resulting **Poly EDY-A** was further characterized with NMR (Fig. 1B) and MALDI-TOF (Fig. 1C), where resonances in the ¹H NMR spectrum could be assigned to the

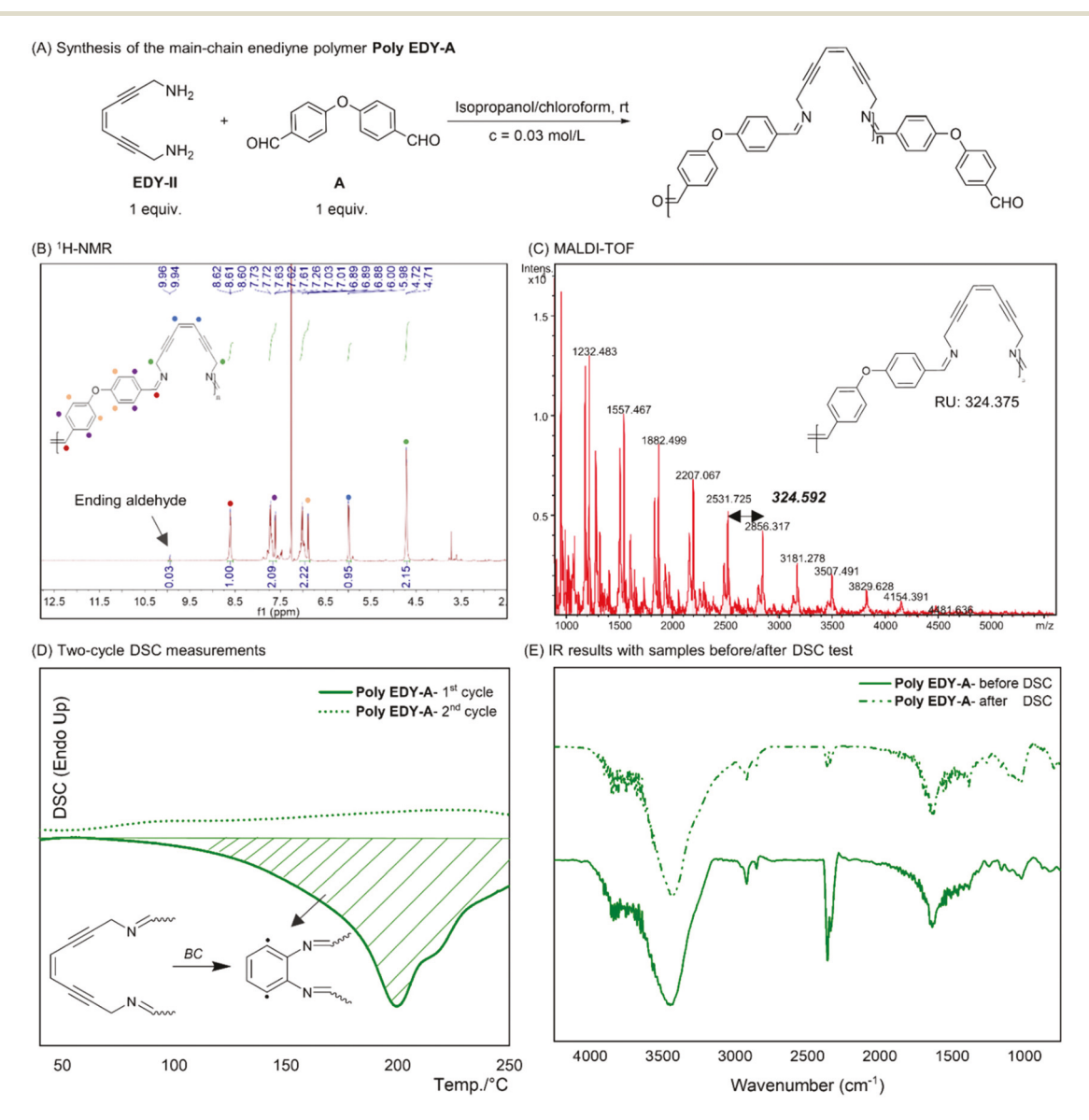
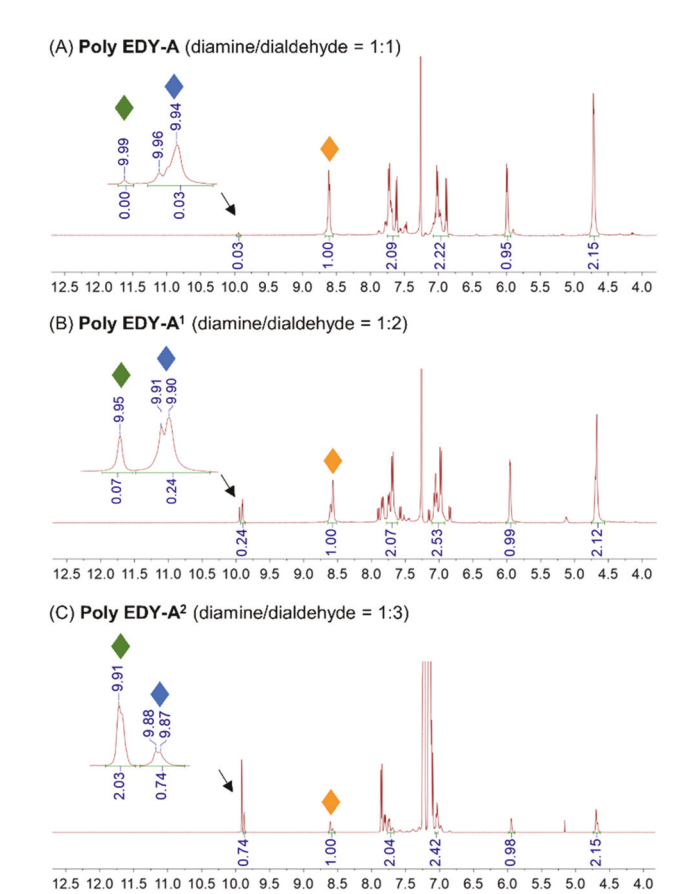


Fig. 1 Synthesis and characterization of the main-chain enediyne polymer Poly EDY-A. (A) Synthetic route, starting from a 1/1-ratio of EDY-II/4,4′-oxydibenzaldehyde (A). (B) 1 H NMR of poly EDY-A. (C) MALDI-TOF of the polymer. (D) Two-cycle DSC curves under heating conditions, N₂ atmosphere, 5 K min⁻¹: the first cycle (lower part) and the second cycle (upper part). The first cycle of Poly EDY-A shows an exothermic peak. After 250 $^{\circ}$ C and back to room temperature, only flat curves appear during the following second heating cycle. (E) FT-IR spectroscopy analysis of Poly EDY-A: the sample before the DSC (lower part) and after the DSC (upper part). Transformation is seen by the decrease of the typical stretching band of the C=C at 2340 cm⁻¹.

Polymer Chemistry Paper

corresponding positions in the structure proving a clean deprotection and the imine-formation. The weight between the peaks of one series in MALDI-TOF is also consistent with the weight of the repeating unit, which provides evidence for the formation of the polymers. Based on the fact that the enedivne-containing compounds could be sensitive to experience Bergman cyclization, the existence of enediynes in the mainchain polymers requires verification. To probe thermal Bergman cyclization,³² we utilized two cycles of differential scanning calorimetry (DSC) analysis to probe its activity. As shown in Fig. 1D, during the first cycle (lower part) exothermic peaks appear at 200 °C for Poly EDY-A, which could be attributed to a thermally triggered Bergman cyclization of the enedivne moiety. The calculated exothermic value (ΔH = 34.49 kcal mol⁻¹ EDY) is within expectations for the exothermic enediyne cyclization.33 Under an atmosphere of N2, the sample was heated until 250 °C and then cooled down to room temperature, followed by the second test cycle. As shown in the upper part, only flat curves appear in this second heating process, which is explained by the complete cyclization of enediynes in the first heating cycle. Thus, the two-cycle DSC proves the existence of the enediynes in the main-chain polymer, and the transformation of cis-l,5-hexadiyn-3-ene motifs to aromatic rings after the first heating cycle via Bergman cyclization. Moreover, Bergman cyclization basically leads to changes in FT-IR spectra (Fig. 1E) of the sample before DSC (lower part) and after DSC (upper part). The significantly decreased stretching band of the ene (C=C) at 2340 cm⁻¹, which gives solid evidence about the consumption of the alkynyl groups after heating, is also consistent with the result of DSC, thus leading to the further verification of the existence of enediynes in the main chain of the polymers.

Based on the synthesis and characterization of the mainchain EDY polymers, the stoichiometric balance of the two bifunctional monomers is further investigated in view of a typical step-growth polymerization, with the stoichiometric imbalance defined by the ratio $r = N_{\text{EDY-II, 0}}/N_{\text{dialdehyde, 0}}$. When altering the proportion of dosage of EDY-II and the dialdehyde A, the resulting polymer shows an adjustable degree of polymerization (DP), which can be observed from the ¹H NMR spectra comparing these reaction systems (Fig. 2). When r = 1, the integral ratio of the protons of the ending aldehyde group (δ = 9.96–9.94 ppm, blue rhombus) and the repeating imine bond ($\delta = \sim 8.60$ ppm, orange rhombus) is 0.03/1, corresponding to a DP of about 33.3. Signals from the remaining dialdehyde are not detected (green rhombus). With more dosage of dialdehyde (r = 0.5), a lower degree of polycondensation was reached (DP = 4.2), according to the integral ratio of the protons of the ending aldehyde group (δ = 9.91–9.90 ppm, blue rhombus) and the repeating imine bond ($\delta = \sim 8.58$ ppm, orange rhombus) (0.24/1), where almost 91% of the dialdehyde A was consumed. Under an even more imbalanced stoichiometric condition (r = 0.3), only oligomers with very low average molecular weight ($M_n = 664 \text{ g mol}^{-1}$) were observed. The influence induced by the stoichiometric balance on DP is consist-



¹H NMR spectra of reactions (A, B, C) with different ratios of the diamine EDY-II and the dialdehyde A 4,4'-oxydibenzaldehyde. Green rhombus: the protons on the aldehyde groups of the starting dialdehyde; blue rhombus: the protons on the ending aldehyde groups of the generated polymers; orange rhombus: the protons on the repeating imine bond

ent with the polycondensation-equation as calculated before.³⁴ The corresponding details are illustrated in Table 1.

With the model synthesis in hand, besides the 4,4'-oxydibenzaldehyde A, segments with different stereoelectronic surroundings were probed, including terephthalaldehyde B, [1,1'biphenyl]-4,4'-dicarbaldehyde C, and 2,3,5,6-tetrafluoroterephthalaldehyde D. The structures of the resulting enediynecontaining polymers are enumerated in Table 1, an overview of the obtained oligomers and polymers is illustrated in Table 1, reaching up to 50 incorporated, stable enediyne-units in the main chain of the respectice polymers.

DNA cleavage activities of enediyne and main-chain enediyne compounds

For molecules containing enediynes, it is attractive to explore their ability of DNA cleavage. 35 The diradicals generated in vivo via Bergman cyclization enable DNA-scissoring ability by abstracting hydrogen atoms from the sugar phosphate backbones of duplex DNA. Highly active enediynes even can cause double-stranded (ds) DNA cleavage, leading to programmed cell death in the absence of any further triggers or additives,

Table 1 Overview of synthesized main-chain enedigne oligomers and polymers based on condensation of EDY-II with various dialdehyde

Polymer	Molar ratio (diamine/di-aldehyde)	Dialdehyde Conv. b (%)	Ratio (-CHO:-CH=N-)	DP^a	$M_{\rm n}^{a}$ (NMR) [g mol ⁻¹]			
R = 4,4'-oxydibenzyl								
Poly EDY-A	1/1	>99	0.03/1	33.3	11 038			
Poly EDY-A ¹	1/2	91	0.24/1	4.2	1577			
Poly EDY-A ²	1/3	38	0.74/1	1.35	664			
R = terephthyl								
Poly EDY-B	1/1	>99	0.02/1	50.0	11 749			
R = [1,1'-biphenyl]-4,4'-dicarbyl								
Poly EDY-C	1/1	>99	0.04/1	25.0	7919			
R = 2,3,5,6-tetra	fluoroterephthyl							
Poly EDY-D	1/1	>99	0.02/1	50.0	15 419			

^a The average degree of polymerization (DP) is calculated according to the integral ratio of the protons (Fig. 2) of the ending aldehyde group (δ = 9.96–9.94 ppm for **Poly EDY-A**; δ = 9.91–9.90 ppm for **Poly EDY-A**¹; δ = 9.88–9.87 ppm for **Poly EDY-A**²) and the repeating imine bond (δ = 8.62–8.60 ppm for **Poly EDY-A**; δ = 8.61–8.56 ppm for **Poly EDY-A**; δ = 8.61–8.58 ppm for **Poly EDY-A**²). Onversion of the starting dialdehyde is calculated according to the integral ratio of the signals (Fig. 2) from remaining dialdehyde (δ = 9.99 ppm for **Poly EDY-A**; δ = 9.95 ppm for **Poly EDY-A**²) and generated ending aldehyde.

including light.³⁶⁻³⁸ As shown in Fig. 3A, under the condition in which enediynes exist, DNA in the supercoiled Form I can be transferred to other different forms, the circular Form II (single-strand scissions) and the linear Form III (double-strand scissions), and small fragments. To evaluate the performance, supercoiled pART7 plasmid (1.8 μg μL⁻¹, 8 μL) was incubated with monomeric EDY-II/III and the main-chain enediyne polymers (200 mM, 12 µL DMSO) in TE buffer (pH 7.6, 100 µL) under purely thermal conditions at 37 °C and then agarose gel electrophoresis experiments were carried out as a function of time to check the progress and to differentiate DNA in different forms. Meanwhile, two negative control experiments, Neg. 1 and Neg. 2, were set up with incubation of the sole plasmid, with or without DMSO. As depicted in lane 1, EDY-II showed the most active performance as even after only 15 minutes of incubation, the initial Form I disappeared totally and was directly converted to Form II. Further cleaved product Form III was found after 4 hours, following a gradually decreased plasmid content, which was attributed to the possibility of cleavage into smaller fragments. For EDY-III (lane 2), only Form III was generated gradually and converted to low molecular weight fragments. A more interesting finding is the trend of the activity of the three different main-chain enediyne polymers. From the 4th hour to the 24th hour, an obvious sequence appeared among the generation of Form II. When incubated with Poly EDY-A (DP = 33) (lane 5), plasmid pART7 was converted mostly to Form II within 8 hours and subsequently experienced a complete transformation during the

time between the 8th hour and the 24th hour. This similar but obviously slower cleavage happened in the plasmid incubated with Poly EDY-A¹ (DP = 4.2) (lane 4). For Poly EDY-A², nearly half of the supercoiled Form I could be found even until the 24th hour, with the transformation finished after the 48 hours (lane 3). A trend is observed intuitively from Fig. 3C after quantifying it via electrophoresis and comparing light intensity that Poly EDY-A is the most efficient polymer to cleave DNA, followed by Poly EDY-A¹ and Poly EDY-A², which matches well with the amounts of the enediynes within the main chain polymers. With more enediyne structures inside the main chain, more activity in DNA cleavage is observed, which is consistent with previous findings about the concentration-dependence of DNA cleavage.³⁹ In addition to the formation of a complex generated between the negatively charged DNA and the aminogroups on the polymer, also hydrogen bonds between the nucleotide on DNA and the imine in the polymer chains could contribute to this result.

When comparing the small, monomeric molecule **EDY-III** (one "enediyne-unit") and **Poly EDY-B** (DP = 50 units), both containing a similar stereoelectronic environment, a clearly different cleavage ability could be found with the same concentration of existing enediyne segment (200 mM). As shown in Fig. 3D the plasmid incubated with **Poly EDY-B** has been fragmented over 10 hours, whereas this happens only after 48 hours with **EDY-III**. After quantification *via* electrophoresis under comparable light intensities, the results could be directly visualized as shown in Fig. 3E.

Published on 17 May 2022. Downloaded by Martin-Luther-Universität Halle-Wittenberg on 8/19/2024 11:44:34 AM.

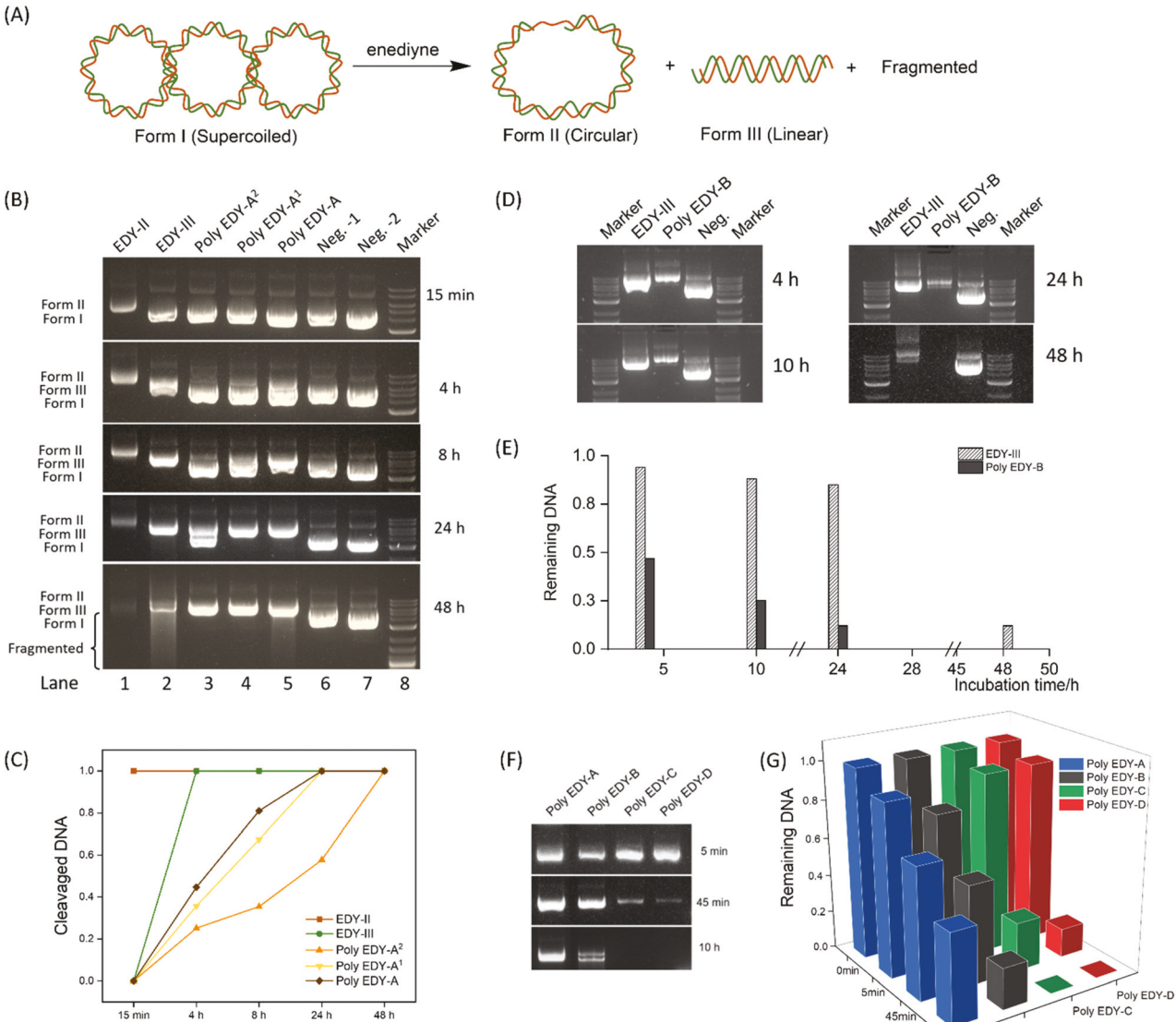


Fig. 3 (A) Schematic representation of DNA cleavage induced by the enedigne derivatives. (B) Agarose gel electrophoretic images of the DNA cleavage assays. Lane 1 to Lane 5: pART7 (1.8 μg μL⁻¹, 8 μL) incubated with EDY-II/III and Poly EDY-A/A¹/A² (200 mM, 12 μL DMSO) (lane 1-5); lane 6 (negative control 1): pART7 (1.8 μ g μ L⁻¹, 8 μ L) incubated with DMSO; lane 7 (negative control 2): pART7 (1.8 μ g μ L⁻¹, 8 μ L) incubated sole. Lane 8: 2-log DNA ladder (10 μL). In all the mixture we maintained a total volume of 120 μL in and was incubated at 37 °C. (C) After quantifying via electrophoresis and comparing their intensity, the percentage of conversion at different times of Form II cleaved from Form I of pART7 incubated with EDY-II/III and Poly EDY-A/ A^{1}/A^{2} is estimated. (D) Agarose gel electrophoretic images of DNA cleavage with EDY-III and Poly EDY-B, [EDY segment] = 200 mM, under the above-mentioned conditions. (E) After quantification via electrophoresis and comparison of intensity, quantified DNA cleavage introduced by EDY-III and Poly EDY-B, [EDY segment] = 200 mM are shown. Remaining DNA refers to the percentage of intact DNA remaining in the solution. (F) Agarose gel electrophoretic images of DNA cleavage with Poly EDY-A/B/C/D, [EDY segment] = 200 mM, under the above-mentioned conditions. (G) After quantifying via electrophoresis and comparing light intensity, quantified DNA cleavages introduced by Poly EDY-A/B/C/D, [EDY segment] = 200 m. Remaining DNA refers to the percentage of intact DNA remaining in the solution.

When equipped with various stereoelectronic environment via the substitution patterns, Poly EDY-A/B/C/D were compared respectively regarding their DNA cleavage abilities. Under identical incubation conditions and concentrations of the enediyne segments (200 mM), a clear stereoelectronic influence on DNA cleavage was observed. As illustrated in Fig. 3F, Poly EDY-D containing tetrafluoro-segments and Poly EDY-C possessing biphenyl structures, caused a fast cleavage, followed by Poly

24 h

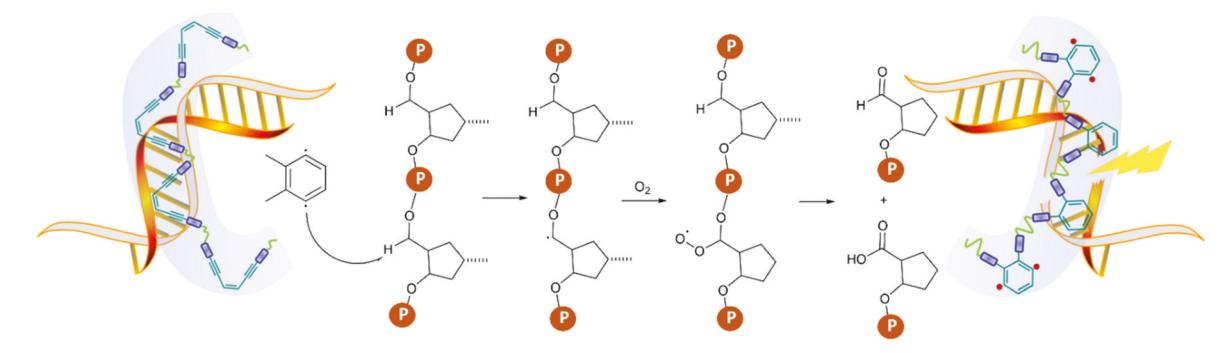
Incubation time

48 h

EDY-B substituted with terephthyl-groups and Poly EDY-A derived from 4,4'-oxydibenzaldehyde. After densiometric analysis of the stained electrophoretic images, the results could be directly compared as shown in Fig. 3G. The order of DNA-cleaving activity can be explained via the stereoelectronic influence of substituents at the terminal alkyne positions, known to affect the activity of the Bergman cyclization. Electron-withdrawing substituents decrease electron density in the σ-

Incubation time

Poly EDY-B



Scheme 3 Possible DNA cleavage mechanism by enediyne polymers. P = phosphodiester bond. A carbon-centered radical abstracts a hydrogen from the phosphate backbone of DNA, followed by attack of dioxygen to form a peroxyl radical, resulting in DNA cleavage.

HOMO-orbital, which leads to a stabilization of the transition state and in turn to a decreased barrier for the Bergman cyclization.40 Even remote substituents at the alkyne terminus can have a significant effect. 41 Poly EDY-A, derived from 4,4'-oxydibenzaldehyde, was the least efficient in DNA splitting due to conjugation between the phenyl-groups and the oxygen-atoms. Similar observations could be found in EPR experiments to observe the radical lifetime, as reported in the next section. As illustrated in Scheme 3, a possible DNA cleavage mechanism by enediyne polymers is proposed via a carbon-centered radical abstracting a hydrogen from the phosphate backbone of DNA, followed by attack of dioxygen to form a peroxyl radical, resulting in DNA cleavage.

EPR studies on the radicals generated via Bergman cyclization

In order to compare the ability to generate radicals of the main-chain enediyne polymers further and obtain a deeper insight into the radical properties of the Bergman cyclization, electron paramagnetic resonance (EPR) spectroscopy was utilized.

Conducting EPR-measurements under the same conditions of the DNA cleavage experiments at 37 °C in the dark (mainchain enediyne polymers in DMSO and plasmid in TE buffer alone), did not allow the recording of the generated radical signals. We then used 4-hydroxy-2,2,6,6-tetramethylpiperidine-1-oxyl (TEMPOL) as a radical acceptor known in EPR, able to abstract the generated radicals and give a decaying signal of its initially existing radical. Before irradiation under LED light with a peak wavelength of 419.8 nm and a FWHM of 14.74 nm for 20 min, we added TE buffer (pH 7.6, 100 μ L) with 60 μ M TEMPOL as a radical quencher solution to each Poly EDY-A/B/ C/D (200 mM, 12 µL DMSO). The volume of each sample had to be adjusted to 120 µL with a TE buffer to mirror the exact polymer concentration from DNA cleavage experiments.

As depicted in Fig. 4B-E, the integral (DI) calculated from the EPR spectra revealed that the signals from TEMPOL experienced various degrees of decrease in the presence of the irradiated main-chain enediyne polymers, indicative of the amount of the formed radicals over time. Similar to the results in DNA cleavage experiments, an influence of the steroelectro-

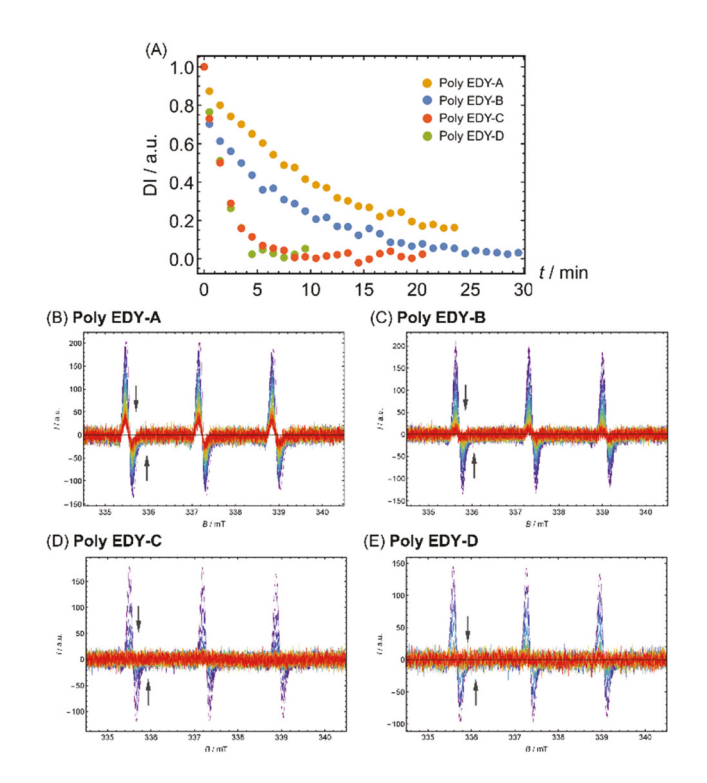


Fig. 4 (A) DI(t) calculated from EPR spectra shown in (B), (C), (D) and (E). (B-E) EPR spectra recorded during irradiation of 20 mM Poly EDY-A/B/C/D solutions with 50 μM TEMPOL in TE buffer with 6.6 vol% DMSO.

nic surroundings was observed for Poly EDY-A/B/C/D in view of its efficiency to generate radicals. The values of decreasing signals of TEMPOL were collected and analyzed in Fig. 4A. Poly EDY-A, derived from 4,4'-oxydibenzaldehyde, still occupies the position of the least efficient radical producer, whereas Poly EDY-D, containing the tetrafluoro-segments, is the most efficient, in line with expectations of the reduced steric repulsion of the incoming π -orbital in the cyclization transition

Inspired by the work of the first in situ EPR spectroscopy of a solid sample of aromatic diyne cyclopolymerization in 2004, 42 we evaporated the solvent of the solution of Poly EDY-A

Polymer Chemistry

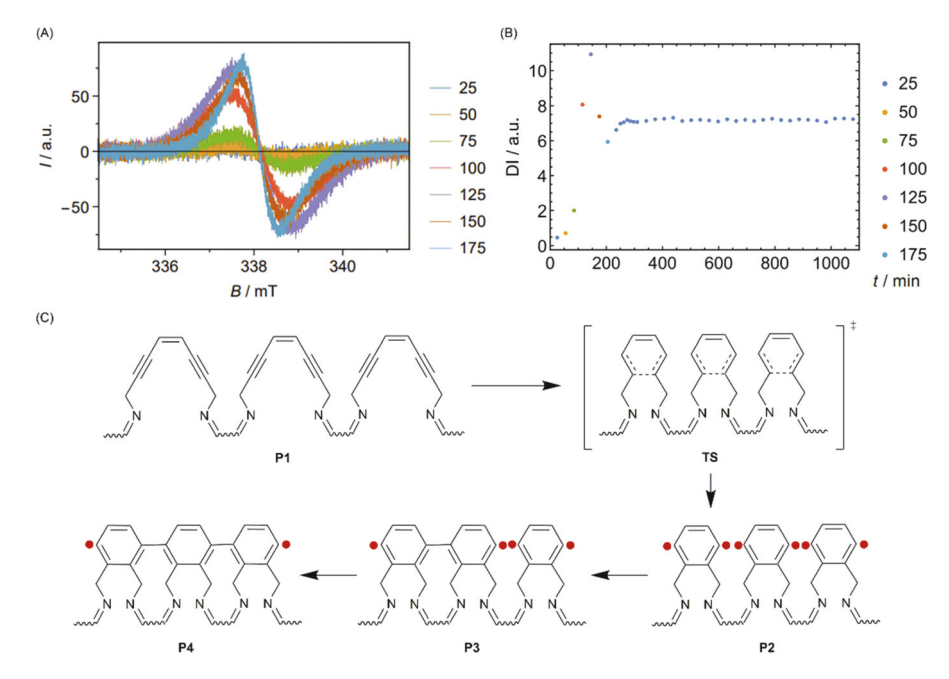


Fig. 5 (A) EPR spectra of Poly EDY-A after 20 min at each temperature (legend). (B) Double integral (DI) calculated from EPR spectra over time with t = 0 being the end of evaporating all solvent. (C) Mechanism diagram of the full Bergman cyclization of main-chain enediyne polymers (red dot: carbon radical).

to gain a solid polymer. The polymer was heated from 25 °C to 175 °C in steps of 25 °C with a setup time of 20 min before measuring an EPR spectrum. After finishing the heating process the temperature was again set to 25 °C to observe the long-term stability of the formed radicals. Raw EPR spectra of the temperature series are shown in Fig. 5A. The observed signal derived from carbon centered radicals shown in Fig. 5B displays the double integral (DI(t)) of the measured EPR spectra, which is proportional to the amount of radicals in the sample. A spark of radical formation can be noticed even at 75 °C or 50 °C. However, the most intense formation of radicals starts above 100 °C with a peak radical concentration at 125 °C. At 150 °C and 175 °C the radical concentration decreases, which is perfectly in line with the displayed mechanism in Fig. 5C. Mechanistically, as soon as the thermally triggered Bergman cyclization starts, a fusion of the in-plane acetylene bonds and a subsequent ring closure takes place from every enediyne unit in P1 to the 1,4-diyl in TS, forming the aromatic benzene rings P2 (Fig. 5C). 13 Based on previous CCSD(T) calculations, 43 TS does not possess a significant biradical character. Considering the different activation barrier between the hydrogen abstraction of p-benzyne-typed diradicals and benzyne-typed radicals,44 especially starting from ortho-substituted enediynes possessing polar and steric contributions, 45 it is reasonable that during TS transforming to P2 and P3, both, p-benzyne and biphenyl diradicals, are generated and exist concomitantly, in line with EPR results reported in previous work.42 During the following heating process, transformation from p-benzyne diradicals P2 to biphenyl- P3 and even polyphenyl-diradicals P4 via radical combination contrib-

utes to a decrease of the radical intensity in total. This matches well with an early growth of the radical intensity, whereupon a decrease took place. Nearby radicals recombine to C-C-bonds leaving some individual radicals (Fig. 5B t >250 min) highly stabilized by the obtained conjugated backbones. This observation is similar to the result of the first in situ EPR spectroscopy of aromatic diyne cyclopolymerization in 2004⁴² where an overall trend including the radical-growth under heating, followed by a slight decrease and the formation of finally long-lived radicals at room temperature was observed. With the well-delocalized spin density over the polyphenyl-like moieties,46 radicals in P4 exhibit excellent stabilities.

Conclusions

We here have realized the synthesis of main-chain enediyne polymers, derived from an acyclic diamino enediyne and various dialdehydes and demonstrated their DNA-cleaving properties. The active diamino enediynes were successfully controlled and embedded via polycondensation to afford the resulting polyimines as stable form of the enediynes, able to activated thermal/photochemical triggering. Investigation on the stoichiometric ratio of the two starting materials for polycondensation revealed its influence on the control of the degree of polymerization from \sim 3-50 units. The existence of enediynes in the main-chain polymers was verified via FT-IR and two cycles of DSC analysis. The main-chain enediyne polymers in solution show a chain-length dependent

DNA cleavage activity under physiological condition, additionally tunable by modulating the stereoelectronic environment via their substitution patterns. Thus the embedded element between the enediyne-segments influences DNA-cleavage in the order: both Poly EDY-D (tetrafluoro-segment) and Poly EDY-C (biphenyl-segment) caused a fast cleavage, followed by Poly EDY-B (terephthyl-segment) and Poly EDY-A (4,4'-oxydibenzaldehyde-segment), enabling a finetuning of kinetics of DNA cleavage. Based on EPR-measurements we propose that reactive radicals are formed initially by purely thermal activation, which then rearrange to more stable radicals persistent over longer times. We can also demonstrate that an additional photochemical activation generates free radicals under these conditions. These radicals deactivate TEMPOL with rates comparable to those in the DNA cleavage experiments. Furthermore, quite stable radicals could be detected in the solid state after evaporation of the solvent, which are potentially utilized in magnetic materials and conducting polymers. The here reported polymers are highly versatile in view of their substituent-patterns, and will be further optimized for supermolecule recognition, followed by site-selective radicalinduced cleavage. We presume this as a first step to design more, radical-generating polymers for controllable polymerization and selective DNA cleavage, in future potentially mimicking more selective cleavage methodologies.

Author contributions

Conceptualization, Y.C. and W.H.B.; methodology, Y.C., F.L.; investigation, Y.C., F.L.; writing—original draft preparation, Y.C. and W.H.B.; writing—review and editing, Y.C., F.L., E.P., S.C., J.Z., D.H. and W.H.B.; supervision, W.H.B.; project administration, W.H.B.; funding acquisition, W.H.B. All authors have read and agreed to the published version of the manuscript.

Conflicts of interest

There are no conflicts to declare.

Acknowledgements

We thank the DFG-Graduate College GRK 2670 (German research foundation – project ID 43649874, TP B2, RTG 2670); and the SFB TRR 102, TP A03 for financial support. S. C. thanks the National Natural Science Foundation of China (21801085 and 52173253) for financial support. Y. C. thanks Dr Jie He and MSc. Nico Rössner for their help in guiding experimental operation in DNA cleavage parts.

References

1 R. R. Jones and R. G. Bergman, *J. Am. Chem. Soc.*, 1972, 94, 660–661.

- 2 M. D. Lee, G. A. Ellestad and D. B. Borders, *Acc. Chem. Res.*, 1991, 24, 235–243.
- 3 J. Golik, G. Dubay, G. Groenewold, H. Kawaguchi, M. Konishi, B. Krishnan, H. Ohkuma, K. Saitoh and T. W. Doyle, *J. Am. Chem. Soc.*, 1987, **109**, 3462–3464.
- 4 M. Konishi, H. Ohkuma, K. Matsumoto, T. Tsuno, H. Kamei, T. Miyaki, T. Oki, H. Kawaguchi, G. D. Vanduyne and J. Clardy, *J. Antibiot.*, 1989, 42, 1449–1452.
- 5 R. Lindh and B. J. Persson, J. Am. Chem. Soc., 1994, 116, 4963–4969.
- 6 J. E. Garrett, E. Metzger, K. Schmitt, S. Soto, S. Northern, L. Kryah, M. Irfan, S. Rice, M. Brown, J. M. Zaleski and J. R. Dynlacht, *Radiat. Res.*, 2020, 193, 107–118.
- 7 A. R. Luxon, N. Orms, R. Kanters, A. I. Krylov and C. A. Parish, *J. Phys. Chem. A*, 2018, 122, 420–430.
- 8 K. C. Nicolaou and W. M. Dai, J. Am. Chem. Soc., 1992, 114, 8908–8921.
- 9 S. M. Gaffney, J. F. Capitani, L. Castaldo and A. Mitra, *Int. J. Quantum Chem.*, 2003, **95**, 706–712.
- 10 P. R. Schreiner, J. Am. Chem. Soc., 1998, 120, 4184-4190.
- 11 K. C. Nicolaou, G. Zuccarello, C. Riemer, V. A. Estevez and W. M. Dai, J. Am. Chem. Soc., 1992, 114, 7360-7371.
- 12 P. Magnus, S. Fortt, T. Pitterna and J. P. Snyder, *J. Am. Chem. Soc.*, 1990, **112**, 4986–4987.
- 13 J. P. Snyder, J. Am. Chem. Soc., 1989, 111, 7630-7632.
- 14 R. K. Mohamed, P. W. Peterson and I. V. Alabugin, *Chem. Rev.*, 2013, **113**, 7089–7129.
- 15 P. Bhattacharya, A. Basak, A. Campbell and I. V. Alabugin, Mol. Pharm., 2018, 15, 768–797.
- 16 D. R. Pandithavidana, A. Poloukhtine and V. V. Popik, J. Am. Chem. Soc., 2009, 131, 351–356.
- 17 G. V. Karpov and V. V. Popik, *J. Am. Chem. Soc.*, 2007, **129**, 3792–3793.
- 18 A. Evenzahav and N. J. Turro, *J. Am. Chem. Soc.*, 1998, **120**, 1835–1841.
- 19 K. Kaya, M. Johnson and I. V. Alabugin, *Photochem. Photobiol.*, 2015, **91**, 748–758.
- 20 C. Wang, S. Chen, H. Zhou, J. Gu and A. Hu, *Chin. J. Polym. Sci.*, 2017, 36, 237–243.
- 21 F. Ling, Z. Li, C. Zheng, X. Liu and C. Ma, *J. Am. Chem. Soc.*, 2014, **136**, 10914–10917.
- 22 K. Ohe, M. Kojima, K. Yonehara and S. Uemura, *Angew. Chem., Int. Ed. Engl.*, 1996, 35, 1823–1825.
- 23 Y. S. Wang and M. G. Finn, J. Am. Chem. Soc., 1995, 117, 8045–8046.
- 24 Y. F. Wang, S. D. Chen and A. G. Hu, in *Polymer Synthesis Based on Triple-Bond Building Blocks*, ed. B. Tang and R. Hu, 2018, pp. 97–126, DOI: 10.1007/s41061-017-0145-4.
- 25 C. C. Miao, J. Zhi, S. Y. Sun, X. Yang and A. G. Hu, *J. Polym. Sci., Part A: Polym. Chem.*, 2010, **48**, 2187–2193.
- 26 X. Cheng, J. G. Ma, J. Zhi, X. Yang and A. G. Hu, Macromolecules, 2010, 43, 909–913.
- 27 B. C. Zhu, S. Y. Sun, Y. F. Wang, S. Deng, G. N. Qian, M. Wang and A. G. Hu, J. Mater. Chem. C, 2013, 1, 580–586.
- 28 D. S. Rawat and J. M. Zaleski, *Chem. Commun.*, 2000, 2493–2494, DOI: 10.1039/b007360l.

- 29 K. M. Kirschner, S. C. Ratvasky, M. Pink and J. M. Zaleski, Inorg. Chem., 2019, 58, 9225-9235.
- 30 J. M. Walker and J. M. Zaleski, Chem. Mater., 2015, 27, 8448-8456.
- 31 D. S. Rawat and J. M. Zaleski, J. Am. Chem. Soc., 2001, 123, 9675-9676.
- 32 K. C. Nicolaou, A. L. Smith and E. W. Yue, Proc. Natl. Acad. Sci. U. S. A., 1993, 90, 5881-5888.
- 33 R. H. Grubbs and D. Kratz, Chem. Ber., 1993, 126, 149-157.
- 34 P. J. Flory, J. Am. Chem. Soc., 1936, 58, 1877-1885.
- 35 K. C. Nicolaou, Y. Ogawa, G. Zuccarello and H. Kataoka, I. Am. Chem. Soc., 1988, 110, 7247-7248.
- 36 M. S. Zhang, B. J. Li, H. M. Chen, H. T. Lu, H. L. Ma, X. Y. Cheng, W. B. Wang, Y. Wang, Y. Ding and A. G. Hu, J. Org. Chem., 2020, 85, 9808-9819.
- 37 H. Zhang, R. Li, S. Ba, Z. Lu, E. N. Pitsinos, T. Li and K. C. Nicolaou, J. Am. Chem. Soc., 2019, 141, 7842-7852.
- 38 D. R. Langley, T. W. Doyle and D. L. Beveridge, J. Am. Chem. Soc., 1991, 113, 4395-4403.

- 39 H. M. Chen, B. J. Li, M. S. Zhang, H. T. Lu, Y. Wang, W. B. Wang, Y. Ding and A. G. Hu, ChemistrySelect, 2020, 5, 7069-7075.
- 40 M. Prall, A. Wittkopp, A. A. Fokin and P. R. Schreiner, J. Comput. Chem., 2001, 22, 1605-1614.
- 41 A. Basak, S. S. Bag, P. A. Majumder, A. K. Das and V. Bertolasi, J. Org. Chem., 2004, 69, 6927-6930.
- 42 N. Mifsud, V. Mellon, K. P. U. Perera, D. W. S. Jr and L. Echegoyen, J. Org. Chem., 2004, 69, 6124-6127.
- 43 E. Kraka and D. Cremer, J. Am. Chem. Soc., 1994, 116, 4929-4936.
- 44 M. J. Schottelius and P. Chen, J. Am. Chem. Soc., 1996, 118, 4896-4903.
- 45 R. L. S. Pickard, A. E. Gillis, M. E. Dunn, S. Feldgus, K. N. Kirschner, G. C. Shields, M. Manoharan and I. V. Alabugin, J. Phys. Chem. A, 2006, 110, 2517-2526.
- 46 Y. Li, K.-W. Huang, Z. Sun, R. D. Webster, Z. Zeng, W. Zeng, C. Chi, K. Furukawa and J. Wu, Chem. Sci., 2014, 5, 1908-1914.



Triggered Crosslinking of Main-Chain Enediyne Polyurethanes via Bergman Cyclization

Yue Cai and Wolfgang H. Binder*

Crosslinking chemistries occupy an important position in polymer modification with a particular importance when triggered in response to external stimuli. Enediyne (EDY) moieties are used as functional entities in this work, known to undergo a pericyclic Bergman cyclization (BC) to induce a triggered crosslinking of polyurethanes (PU) via the intermediately formed diradicals. Diamino-EDYs, where the distance between the enyne-moieties is known to be critical to induce a BC, are placed repetitively as main-chain structural elements in isophorone-based PUs to induce reinforcement upon heating, compression, or stretching. A 7-day compression under room temperature results in a \approx 69% activation of the BC, together with the observation of an increase in tensile strength by 62% after 25 stretching cycles. The occurrence of BC is further proven by the decreased exothermic values in differential scanning calorimetry, together with characteristic peaks of the formed benzene moieties via IR spectroscopy. Purely heat-induced crosslinking contributes to 191% of the maximum tensile strength in comparison to the virgin PU. The BC herein forms an excellent crosslinking strategy, triggered by heat or force in PU materials.

1. Introduction

Activation of chemical bonds to induce crosslinking in polymers is a common strategy to modify and obtain polymer networks. Similar to conventional thermal, photo, and redo-x methodologies, activating chemical bonds by strain is attractive.^[1,2] Thus chemical bonds and bonding entities termed mechanophores can be activated by molecular forces, representing a promising technique for responsivity in materials by directing specific strain-dependent reaction pathways.^[2–7] Since the first observation of mechanically-induced bond-rupture by Staudinger^[8] in

Y. Cai, W. H. Binder
Macromolecular Chemistry
Institute of Chemistry
Faculty of Natural Science II
Martin Luther University Halle-Wittenberg
Von-Danckelmann-Platz 4, 06120 Halle (Saale), Germany
E-mail: wolfgang.binder@chemie.uni-halle.de

The ORCID identification number(s) for the author(s) of this article can be found under https://doi.org/10.1002/marc.202300440

© 2023 The Authors. Macromolecular Rapid Communications published by Wiley-VCH GmbH. This is an open access article under the terms of the Creative Commons Attribution-NonCommercial License, which permits use, distribution and reproduction in any medium, provided the original work is properly cited and is not used for commercial purposes.

DOI: 10.1002/marc.202300440

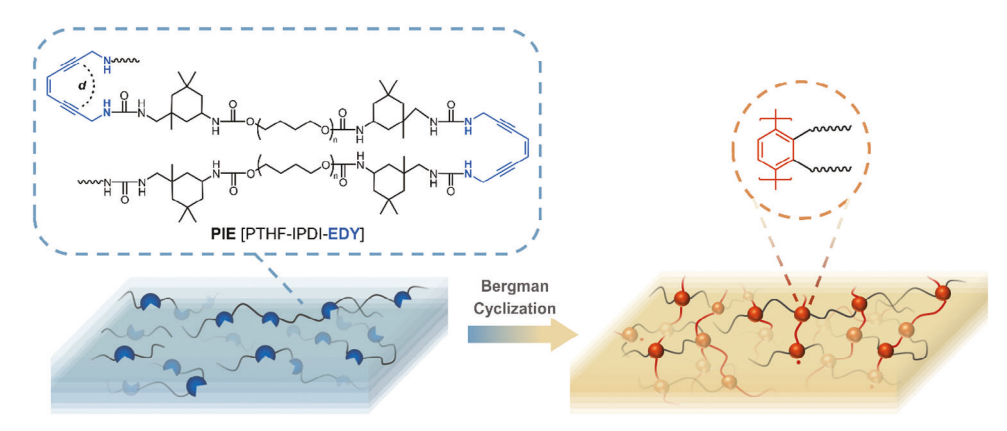
the 1930s, tremendous efforts have been accomplished in developing specific mechanophores, [9,10] wherein an applied strain is correlated to an effective geometry, chemistry, or location of a bond. Major factors to tune the efficiency of force on a chemical reaction are the position of the applied force on the specific bond^[11] in view of its regiochemistry,[12,13] the position,[14] type, [15,16] and length[17] of attached polymer chains, and also the material morphology such as in semicrystalline[18] polymers or microphase-segregated block copolymers.^[19] The use of such chemistries allows to induce chemical reactions, such as crosslinking, to form permanent networks in materials at positions where either stress or heat has been applied.

Pericyclic reactions have been investigated intensely as potential mechanophores as the geometry of bonding arrangements and the resulting molecular strain can be well predicted therein.^[3,20–29] To this end, cyclo-reversion-chemistries, such as

in 1,2,3-triazoles, $^{[30,31]}$ cyclobutanes, $^{[32-34]}$ dimeric anthracenes, $^{[35]}$ anthracene—maleimide adduct, $^{[36,37]}$ coumarin dimer, $^{[38]}$ methanone-tethered cinnamate dimer, $^{[39]}$ or dihalocyclopropanes, $^{[40]}$ can be induced mechanically, addressing even forbidden reaction pathways not accessible via purely thermal or photochemical reactions. $^{[29]}$ The activation in solution via ultrasound, in embedded materials, such as thermoplastic polymers or networks, and of single molecules (via single-force molecules spectroscopy, SFMS) have been accomplished.

In our search for stress-induced crosslinking chemistries in solid polymers we came across novel pericyclic reaction chemistries, such as the Bergman cyclization (BC), as a potential target. In Bergman cyclization, enediynes (EDYs) undergo a cycloaromatization to generate a 1,4-phenyl-diradical[41] mainly influenced by proximity effects, [42-44] namely the distance between the acetylenic carbon atoms (d) (Scheme 1). Additionally, the electronic effects brought by substituents^[45] and molecular-strain differences[46-48] allow an excellent tuning of the EDY's reactivity on a molecular basis.^[49] Conventionally, the BC is induced thermally,^[41] by photochemistry,^[50–53] or by metal catalysis.^[54,55] Inspired by these unique properties, we herein report on the crosslinking of a polyurethane (PU) polymer embedded with EDYs as the active element embedded therein. We highlight the function of EDYs as the resource of diradicals via Bergman cyclization, which undergoes coupling partially to induce covalent





Scheme 1. Schematic illustration of the designed enediyne (EDY)-embedded polyurethane (PU) and the triggered crosslinking via Bergman cyclization.

Table 1. Overview of the composition of PUs containing enediynes (EDY) (samples PIE, PME) and the PU without EDYs (PIC).

Sample	Compositions				
	Prepolymer 1 equiv.	Diisocyanate 2 equiv.	Diamine1 equiv.		
PIE	PTHF	IPDI NCO	NH ₂	10.6	
РМЕ		MDI OCN NCO	NH ₂	25.3	
PIC		OCN NCO	H_2N NH_2	8.6	

crosslinking, in turn leading to an efficient hardening of the PU material. The activation used here varied from conventional heat to force observing hardening phenomenona which leads to novel types of responsive materials.

2. Results and Discussion

We recently reported the BC of EDYs embedded into the main chain of polyimines in solution to tune a chain-length dependent Bergman cyclization with different structural elements.^[56] The potential of EDYs as latent crosslinking agents was first considered in the 1990s,^[2] expected to activate upon swelling a network equipped with embedded EDY's by triggering a BC via changing the distance of the terminal acetylen-units.^[57] Despite significant experimental and theoretical efforts^[57,58] this behavior has not been proven in materials, neither by temperature nor strain. Based on the known theoretical background^[30] we designed EDYs embedded into linear PUs, where we expected that activation of a BC would lead to a subsequent crosslinking via the intermediate biradicals. Due to the presence of hydrogen bonds at the joiningurea groups, we expected facilitation of the

BC, as BC is accelerated using metal-coordination close to the EDY-moieties, [59] and thus the chance to promote subsequent crosslinking chemistries in the PUs. EDYs embedded directly into the main chains of the linear PUs could display an enhanced activation, in turn inducing measurable and observable evidence of a BC in the formed PU network, although BC in acrylate-based networks could not be observed previously. [57]

Based on an amine-functional EDY, (*Z*)-octa-4-en-2,6-diyne-1,8-diamine (**Figure 1A**), ^[60] we were able to introduce EDY into the main chain of a PU, resulting in the polymer **PIE** containing ≈ 3 EDY-groups per chain in average (**Table 1**). We first generated an isocyanate-terminated polytetrahydrofuran (PTHF, 2.9 kDa) with isophorone diisocyanate (IPDI, molar ratio PTHF/IPDI = 1/2), followed by polyaddition with an equimolar amount of the (*Z*)-octa-4-en-2,6-diyne-1,8-diamine. The choice of IPDI was motivated by generating PUs of appropriate hardness, able for subsequent testing via the available rheology/stress-strain testing methods. Results from NMR spectroscopy (Figure 1B, assigning chemical shifts of the double bond ($\delta = 5.79$ ppm, red dot) and the methylene group ($\delta = 4.14$ ppm, purple dot)), gel permeation chromatography (Figure 1C) and



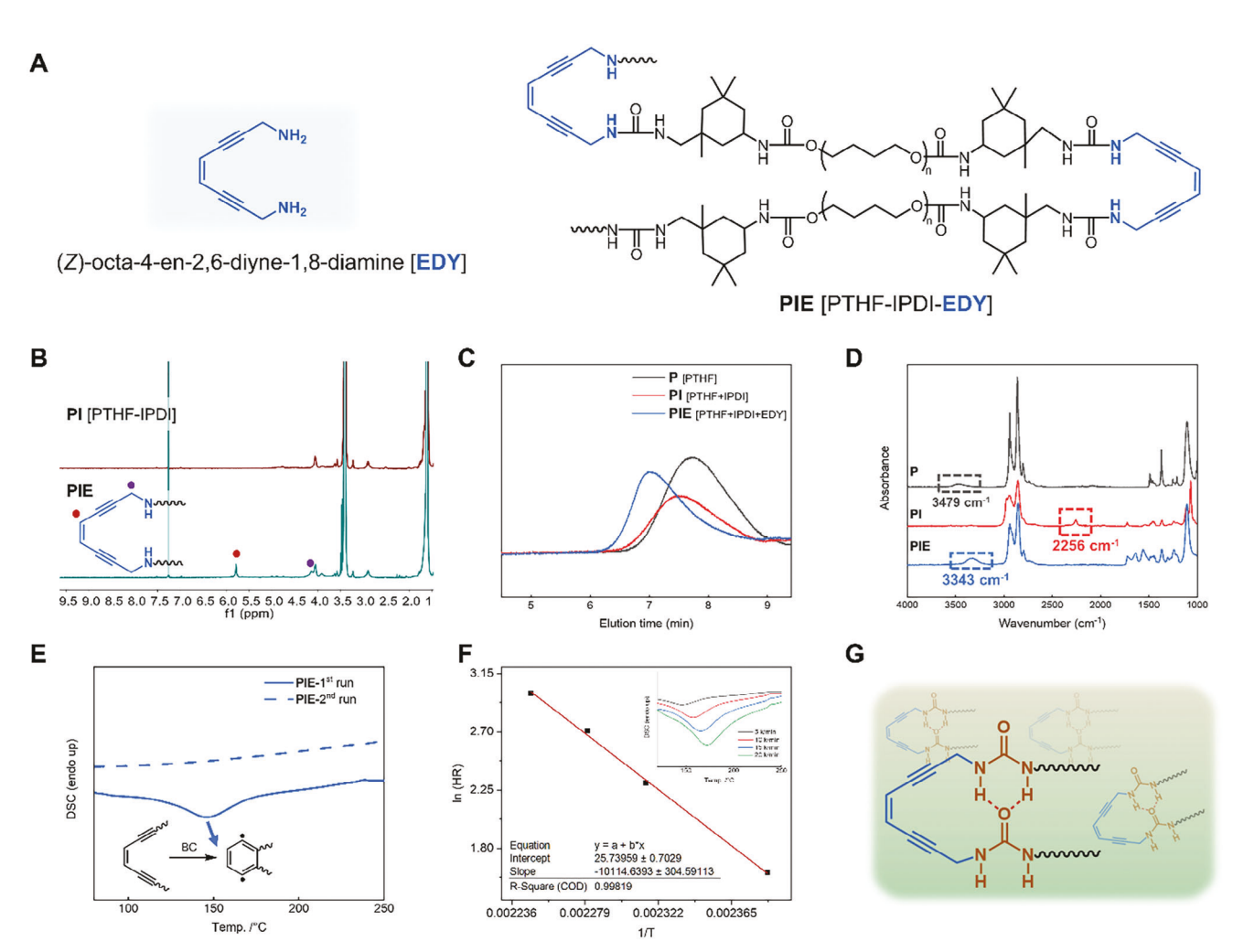


Figure 1. Synthesis and characterization of the main chain enediyne elastomeric PU polymer PIE. A) Chemical structure and compositions of PIE. B) Comparison of the ¹H NMR between the isocyanate-terminated PTHF and PIE. C) GPC of the initial PTHF, the isocyanate-terminated PTHF, and PIE. D) FT-IR. E) Two-cycle DSC curves under heating condition, N₂ atmosphere, 5 K min⁻¹: the first cycle (lower solid line) and the second cycle (upper dashed line). F) Arrhenius plot for the Bergman cyclization of PIE in neat conditions obtained by DSC measurements using ASTM E698 standard procedure. Inset: DSC thermograms at four heating rates (HR) of 5, 10, 15, and 20 K min⁻¹. G) The hydrogen bonds between the urea groups in the joint of the enediyne moieties.

FT-IR spectroscopy (Figure 1D) gave evidence of the successful synthesis of the targeted polymer PIE and the successful incorporation of the EDY-moieties with a molecular weight of ≈10.6 kDa. As depicted in Figure 1D, a full conversion of all NCO groups after the second reaction step was proven by FT-IR spectroscopy with the disappearance of the characteristic −NCO group at 2256 cm⁻¹ and the emergence of the −NH stretching band at 3343 cm⁻¹. Increasing peaks (around ≈1600 cm⁻¹) showed the appearance of the urea group (Figure S5, Supporting Information). Similar to literature, [61] the bulky chain elements between the EDYs impeded the detection of the alkynyl group in IR-spectroscopy. In a similar procedure, we also prepared PME (containing EDY, methylene diphenyl diisocyanate (MDI, instead of IPDI)), and a sample devoid of EDY as control (PIC) (Table 1).

The so-formed **PIE** was then checked for a thermally induced BC reaction: considering that BC is an exothermic reaction, the existence of the EDYs was verified with two cycles of differential scanning calorimetry (DSC) as shown in Figure 1E (and Figures

S6 and S7, Supporting Information). Under an atmosphere of N_2 , PIE was heated to 250 °C, followed by cooling to 25 °C and a second heating process. The exothermic peak ($T_{\text{peak}} = 145.96 \,^{\circ}\text{C}$) in the first cycle (solid line), which was attributed to the completion of a thermally triggered BC of the EDY moieties, did not appear in the second heating process (dashed line). The calculated exothermic value ($\Delta H = 63.9 \text{ kcal mol}^{-1} \text{ EDY}$) is within expectations for the exothermic EDY cyclization.^[62] With the method of the ASTM E698 standard procedure, [63] DSC thermograms of neat PIE at four heating rates (HR) of 5, 10, 15, and 20 K min⁻¹ yielded an Arrhenius plot for its BC with calculated activation energy as 20.1 kcal mol⁻¹ (Figure 1F and Table S2, Supporting Information). According to the literature, [65] the ASTM E698 method is reliable for comparing the reactivities of BC in structurally similar compounds, leading to verified and justifiable amounts of BC in our series of PU materials. Therefore this method was utilized specifically to compare the reactivities of PIE and PME. For a pericyclic reaction like BC, the hydrogen bonds, present not only be-

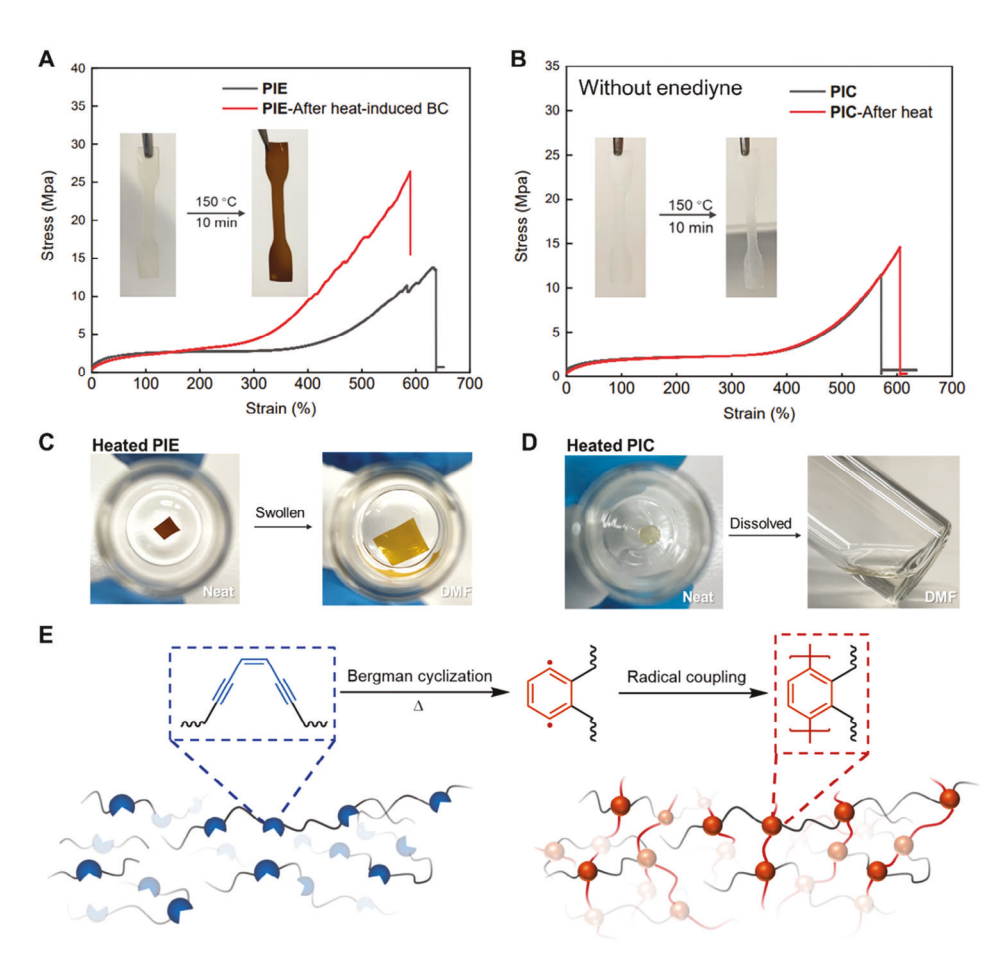


Figure 2. Changes in material properties induced by Bergman cyclization by comparing EDY-PU of PIE and the negative control PIC without EDY. A) Tensile tests of PIE before and after heat. B) Tensile tests of PIC before and after heat. C) Swelling test of heated PIE in DMF. D) Dissolution of heated PIC in DMF. E) Proposed mechanism of the generation of crosslinks induced by Bergman cyclization in the enediyne-embedded chains.

tween the PU chains but also between the urea groups in the joint of the EDY moieties as shown in Figure 1G, assist to reach this comparably low *Ea* value. Replacement of MDI by IPDI (**PME**) favoring hydrogen bonding between the PU chains^[64] gave an even lower *Ea* value of 14.1 kcal mol⁻¹ (Figures S12–S18, Supporting Information), which was considered too low, also taking into account the possibility of an underestimation in solid polymers as stated in literature^[65] (Figure S18, Supporting Information).

For comparison the polyurethane **PIC** (devoid of EDY-moieties) was synthesized as a negative control, derived from the polyaddition between the initially used isocyanate-terminated PTHF and octane-1,8-diamine, which possesses the same length of the carbon chain with EDY ($M_{\rm n,\,GPC}=8.6~{\rm kDa}$, Figures S19–S22, Supporting Information). To verify the crosslinking potential brought by the embedded EDYs, conventional heat induction with **PIE** (containing EDY) and **PIC** (devoid of EDY-unit) were first attempted, followed by stress–strain tests to prove the formation of additional covalent crosslinks during the dimerization of the diradicals formed via BC. Freshly made **PIE** and **PIC** were thus placed at 150 °C for 10 min, followed by tensile tests after cooling. As shown in **Figure 2A**, for **PIE** before and after heating, a significant improvement of the tensile strength was observed, increasing to a maximum value of 26.4 MPa (191% of the maxi-

mum tensile strength of the virgin sample), an effect which was not observed for PIC (devoid of EDYs) (Figure 2B).

Subsequently, pieces of the two heated samples (PIE, PIC) were soaked in DMF as shown in Figure 2C,D to probe the crosslinking density. The PIE-sample immediately swelled in the solvent, reaching 157% of swelling degree after swelling for 72 h (equilibrium), indicative of permanent crosslinks with a calculated density v_c as 5.50 \times 10⁻⁴ mol cm⁻³ according to the Flory-Rehner equation, [66] Table S4, Supporting Information. In comparison, PIC, which remained unchanged in its tensile strength and appearance, completely dissolved in the solvent. As illustrated in Figure 2E, triggered by heating, EDYs embedded in the PU chains underwent Bergman cyclization and were transformed into the diradical species which could recombine randomly resulting in covalent crosslinking to form a permanent network. The resulting conjugated system of benzene rings shifted the absorption to a longer wavelength in line with previous observations in literature [67] made from BCcyclization and subsequent aromatization. Monitoring with UVvis under heated conditions (Figure S8, Supporting Information) supported this assumption.

After using heat as an external trigger we then tested a pressure-induced activation of the BC as a further trigger to in-



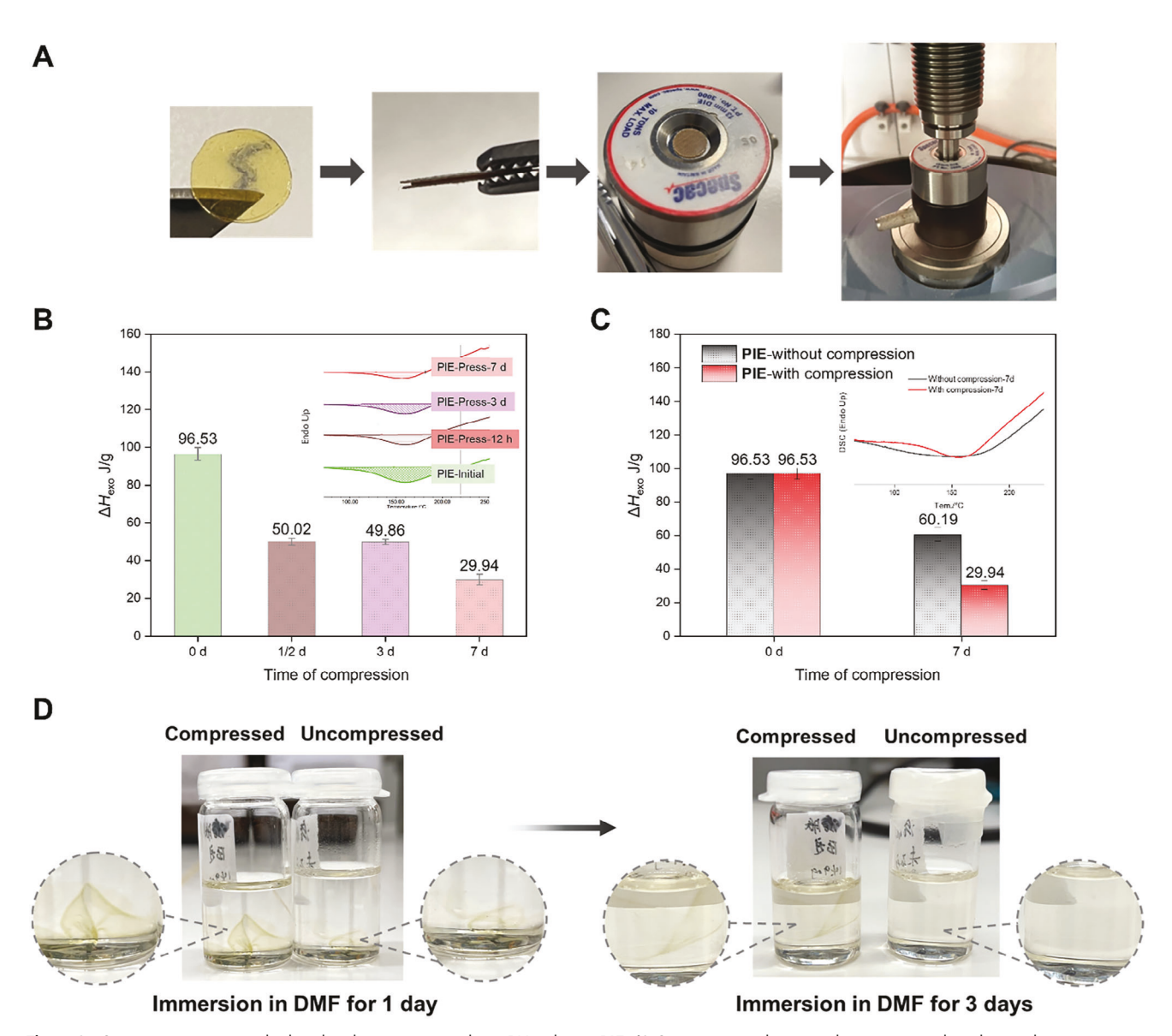


Figure 3. Compression test applied to the elastomeric enediyne PU polymer PIE. A) Compression device and operations taken during the compression. B) Monitoring with DSC during the 7-day compression of PIE. C) Comparison of ΔH calculated by DSC between PIE with or without compression for 7 days. D) Comparison of solubilities in DMF between PIE with or without compression.

duce crosslinking chemistry (**Figure 3A**). [16,20] Thus a combination of compression tests of **PIE** and DSC was utilized to monitor BC owing to its exothermal feature. With the transparent and elastomeric **PIE** in hand, the compression test proceeded by covering the well-shaped sample with two PTFE films and placing it in a press with a force of 10 tons ranging from 12 h to 7 days. As it is expected that after BC activation the materials should display a lower heat-of-conversion in an thereafter conducted DSC analysis, the decline in reaction heat can be correlated to the fraction of BC achieved during the compression cycles. As shown in Figure 3B, in neat samples that had experienced compression of various durations (up to 7 days), the exothermic values of each sample decreased gradually with time. Compared to the initial sample, 12 h of compression brought a \approx 48% decrease in the exothermic value, which dropped by \approx 69% after 7 days.

In parallel samples without compression were studied under the same conditions, but without compression and in the dark, to avoid eventual photoactivation of the BC. With an activation energy of ≈ 20.1 kcal mol⁻¹ Ea, PIE experienced a small decrease in the exothermic ($\approx 38\%$), as shown in Figure 3C. The exothermic values of PIE without compression after 12 h and 3 days are shown in Supporting Information (Figure S11, Supporting Information).

To prove that BC had formed additional crosslinks during the pressing cycles, we again conducted swelling experiments to verify the formation of a covalently linked network (Figure 3D). Two samples of PIE (one compressed for 7 days, one uncompressed) were placed in DMF. After 3 days, the uncompressed sample was dissolved completely, whereas the compressed sample was just swollen with a considerable volume expansion owing to a cova-

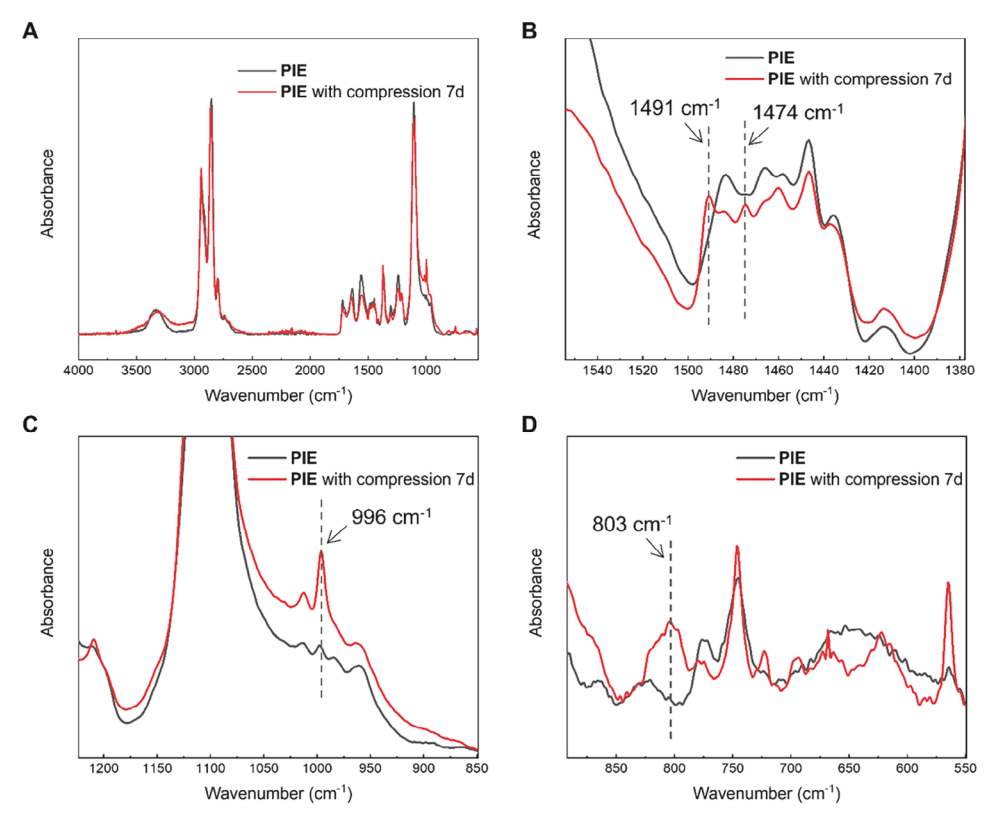


Figure 4. A) Comparison of IR spectra of fresh sample PIE and the sample after 7-days compression with 10 tons. B) Enlargement of IR spectra (wavenumber: 1600–1380 cm⁻¹). C) Enlargement of IR spectra (wavenumber: 1200–850 cm⁻¹). D) Enlargement of IR spectra (wavenumber: 900–550 cm⁻¹).

lently linked network (swelling degree 693%). By employing the equilibrium swelling method, the crosslink density (ν_c) was estimated as 9.59×10^{-5} mol cm⁻³ using the equations, introduced by Flory and Rhener^[66] (Table S4, Supporting Information). This result proves that covalent networks were formed during compressing the EDY-containing sample, **PIE**.

To further prove that radical coupling after cyclization took place in at least one of the primary reaction pathways, FT-IR spectroscopy was used focusing especially on the fingerprint region. If the diradical benzene intermediates were coupled together partially, a multi-phenylene system consisting of 1,2,3,4-substituted benzene moieties would be obtained. Correspondingly some changes in the fingerprint region could be expected and used to distinguish. As illustrated in **Figure 4**, the absorption peaks around $\approx\!1500~{\rm cm^{-1}}$ (1491 and 1474 cm $^{-1}$) are important characteristic peaks of the C=C stretching vibration of the conjugated benzene ring system. More importantly, the absorption at 996 and 803 cm $^{-1}$ can be attributed to the CH bending. Compared to the normal CH bending on the 1,2-substituted benzene, the absorption at a relatively higher wavenumber (803 cm $^{-1}$) demonstrated the existence of 1,2,3,4-substituted benzene moieties.

In addition to compression tensile stress was probed to probe crosslinking of EDY-PU polymer. With the two elastomeric materials PIE and PIC in hand and the induced crosslinking brought by heat or compression in mind, cyclic stress—strain investigations were applied to each sample under room temperature in the dark to study the possible effect induced by external stretching. Cyclic loading and unloading from 0% strain to 300% strain,

far below the strain at break, were performed continuously without rest. As depicted in **Figure 5**A, similar to Mullin's effect, ^[68,69] a notable hysteresis, together with a softening and a decreased maximum tensile stress value was detected for both samples (**PIE** and **PIC**) during the first cycles. ^[64] However, continuously enhanced toughness and growing maximum-tensile stress values (up to 4 MPa, 162.1% of the virgin maximum-tensile stress value) were observed for **PIE** as shown in Figure 5B. On the contrary, nonsignificant changes except a slight strain hardening were found for **PIC** (111.2% of the virgin maximum-tensile stress value), in line with effects known for other PU-polymers. ^[70,71] Strain-hardening of **PIE** is, therefore, a clear consequence of and at least partial crosslinking of the diradicals formed during the strain induction (Figure 5C), thus proving its potential activation by stress and its activity as a mechanophore.

3. Conclusion

We herein have accomplished a Bergman-cyclization-triggered crosslinking of polyurethane with EDYs using heat and stress, leading to an induced reinforcement in the mechanical strength of the material by generating permanent covalent crosslinks. The embedded EDY induced a Bergman cyclization as proven directly by the decreased exothermic values in DSC and the characteristic peaks of the generated benzene moieties via IR spectra, and indirectly via an increase in tensile strength and swelling of the formed network. Heat-induced crosslinking increased the tensile strength by 191% in comparison to the virgin sample. 7-

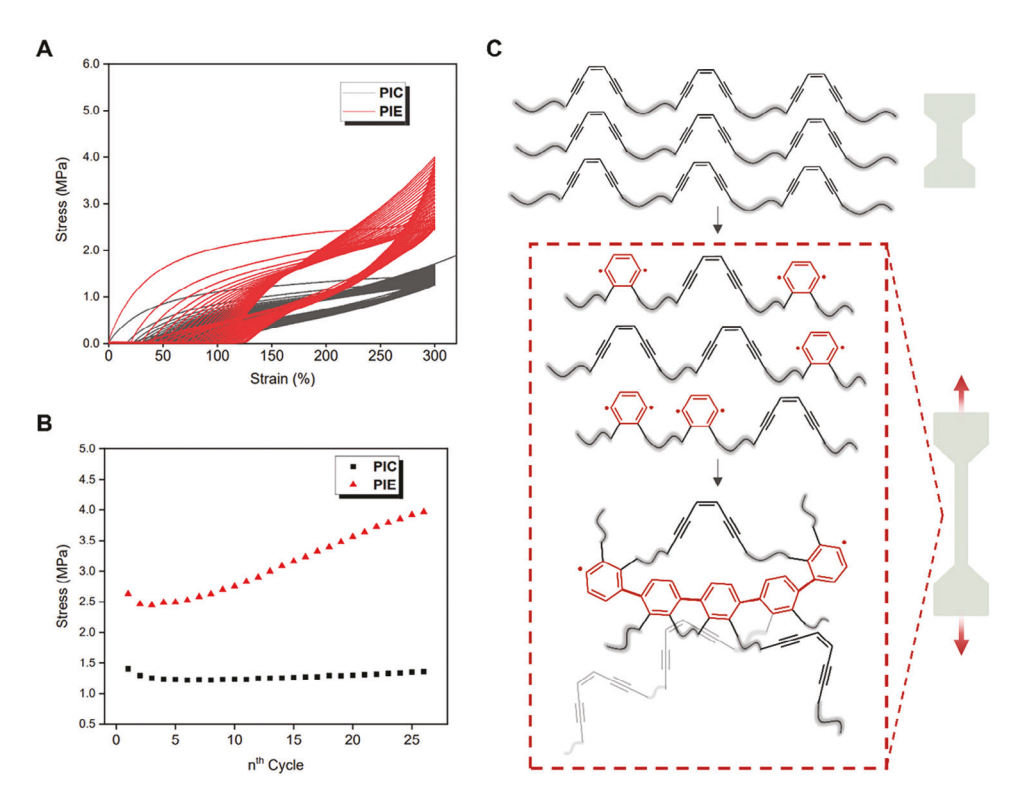


Figure 5. Stretch-induced Bergman cyclization in PIE. A) Cyclic stress—strain investigations of the enediyne PU chains PIE and the negative control PIC. B) The maximum tensile stress values of PIE and PIC during each stretch cycle. C) Proposed mechanism behind the increased toughness of PIE.

day compression resulted in a decrease of \approx 69% in BC-induced exothermic values, together with the formation of permanent (covalent) crosslinks with a density of 0.96×10^{-4} mol cm⁻³ as calculated via swelling experiments, which counts to about 25% of the heat-induced crosslinks. Stretching (25 cycles) induced a significant increase (62%) in the maximum tensile stress values of PIE. The embedding of the EDY units as latent crosslinkers into the PU polymers is simple and yields the chance to embed a subsequent reinforcement. With the well-designed structures and simple chemistry of main chain EDY PU polymers, this work demonstrated the possibility of reviving the application of EDY as a latent crosslinker, activated either thermally or via stress, to inspire a novel type of responsive materials.

4. Experimental Section

A detailed Experimental Section can be found in the Supporting Information.

Supporting Information

Supporting Information is available from the Wiley Online Library or from the author.

Acknowledgements

The authors thank the project BI DFG-Graduate College GRK 2670 (German Research Foundation-project D43649874, TP B2, RTG 2670) for financial support, as well as the DFG projects BI1337/14-1 and BI1337/15-1. Y.C. thanks MSc. Chenming Li for his help in the discussion.

Open access funding enabled and organized by Projekt DEAL.

Conflict of Interest

The authors declare no conflict of interest.

Author Contributions

Y.C. and W.H.B.: Conceptualization, methodology, investigation, and writing; W.H.B.: Supervision, project administration, and funding acquisition. Both authors have read and agreed to the published version of the manuscript.

Data Availability Statement

The data that support the findings of this study are available in the supplementary material of this article.

Keywords

Bergman cyclization, crosslinking, enediyne, polyurethane

Received: August 21, 2023 Revised: October 23, 2023 Published online: November 4, 2023 3213927, 2023, 24, Downloaded from https://onlinelibrary.wiley.com/doi/10.1002/marc.202300440, Wiley Online Library on [19/08/2024]. See the Terms and Conditions (https://onlinelibrary.wiley.com/terms-and-conditions) on Wiley Online Library for rules of use; OA articles are governed by the applicable Creative Commons License

^[1] X. G. Liu, Y. J. Li, L. Zeng, X. Li, N. Chen, S. B. Bai, H. N. He, Q. Wang, C. H. Zhang, Adv. Mater. 2022, 34, 2108327.



- [2] J. Li, C. Nagamani, J. S. Moore, Acc. Chem. Res. 2015, 48, 2181.
- [3] D. A. Davis, A. Hamilton, J. Yang, L. D. Cremar, D. Van Gough, S. L. Potisek, M. T. Ong, P. V. Braun, T. J. Martínez, S. R. White, J. S. Moore, N. R. Sottos, *Nature* 2009, 459, 68.
- [4] A. L. Black, J. A. Orlicki, S. L. Craig, J. Mater. Chem. 2011, 21, 8460
- [5] N. Willis-Fox, E. Rognin, T. A. Aljohani, R. Daly, Chem 2018, 4, 2499
- [6] M. A. Ghanem, A. Basu, R. Behrou, N. Boechler, A. J. Boydston, S. L. Craig, Y. Lin, B. E. Lynde, A. Nelson, H. Shen, D. W. Storti, Nat. Rev. Mater. 2020, 6, 84.
- [7] A. Krusenbaum, S. Grätz, G. T. Tigineh, L. Borchardt, J. G. Kim, Chem. Soc. Rev. 2022, 51, 2873.
- [8] H. Staudinger, H. F. Bondy, Ber. Dtsch. Chem. Ges. (A and B Series) 1930, 63, 734.
- [9] K. M. Wiggins, J. N. Brantley, C. W. Bielawski, Chem. Soc. Rev. 2013, 42, 7130.
- [10] Y. Chen, G. Mellot, D. Van Luijk, C. Creton, R. P. Sijbesma, Chem. Soc. Rev. 2021, 50, 4100.
- [11] G. R. Gossweiler, T. B. Kouznetsova, S. L. Craig, J. Am. Chem. Soc. 2015, 137, 6148.
- [12] Y. Lin, M. H. Barbee, C.-C. Chang, S. L. Craig, J. Am. Chem. Soc. 2018, 140, 15969.
- [13] T. A. Kim, M. J. Robb, J. S. Moore, S. R. White, N. R. Sottos, *Macro-molecules* 2018, 51, 9177.
- [14] K. L. Berkowski, S. L. Potisek, C. R. Hickenboth, J. S. Moore, Macro-molecules 2005, 38, 8975.
- [15] P. Michael, S. K. Sheidaee Mehr, W. H. Binder, J. Polym. Sci., Part A: Polym. Chem. 2017, 55, 3893.
- [16] P. Michael, W. H. Binder, Angew. Chem., Int. Ed. 2015, 54, 13918.
- [17] M. J. Kryger, A. M. Munaretto, J. S. Moore, J. Am. Chem. Soc. 2011, 133, 18992.
- [18] C. K. Lee, B. A. Beiermann, M. N. Silberstein, J. Wang, J. S. Moore, N. R. Sottos, P. V. Braun, Macromolecules 2013, 46, 3746.
- [19] A. L. Black Ramirez, J. W. Ogle, A. L. Schmitt, J. M. Lenhardt, M. P. Cashion, M. K. Mahanthappa, S. L. Craig, ACS Macro Lett. 2012, 1, 23
- [20] G. R. Gossweiler, G. B. Hewage, G. Soriano, Q. Wang, G. W. Welshofer, X. Zhao, S. L. Craig, ACS Macro Lett. 2014, 3, 216.
- [21] M. B. Larsen, A. J. Boydston, J. Am. Chem. Soc. 2013, 135, 8189.
- [22] H. M. Klukovich, Z. S. Kean, A. L. B. Ramirez, J. M. Lenhardt, J. Lin, X. Hu, S. L. Craig, J. Am. Chem. Soc. 2012, 134, 9577.
- [23] Z. S. Kean, A. L. Black Ramirez, Y. Yan, S. L. Craig, J. Am. Chem. Soc. 2012, 134, 12939.
- [24] C. E. Diesendruck, B. D. Steinberg, N. Sugai, M. N. Silberstein, N. R. Sottos, S. R. White, P. V. Braun, J. S. Moore, J. Am. Chem. Soc. 2012, 134, 12446.
- [25] Y. Chen, A. J. H. Spiering, S. Karthikeyan, G. W. M. Peters, E. W. Meijer, R. P. Sijbesma, *Nat. Chem.* **2012**, *4*, 559.
- [26] H. M. Klukovich, Z. S. Kean, S. T. Iacono, S. L. Craig, J. Am. Chem. Soc. 2011, 133, 17882.
- [27] M. J. Kryger, M. T. Ong, S. A. Odom, N. R. Sottos, S. R. White, T. J. Martinez, J. S. Moore, J. Am. Chem. Soc. 2010, 132, 4558.
- [28] J. M. Lenhardt, A. L. Black, S. L. Craig, J. Am. Chem. Soc. 2009, 131, 10818.
- [29] C. R. Hickenboth, J. S. Moore, S. R. White, N. R. Sottos, J. Baudry, S. R. Wilson, *Nature* 2007, 446, 423.
- [30] M. Krupicka, P. Dopieralski, D. Marx, Angew. Chem., Int. Ed. 2017, 56, 7745.
- [31] M. J. Jacobs, G. Schneider, K. G. Blank, Angew. Chem., Int. Ed. 2016, 55, 2899.
- [32] M. F. Pill, K. Holz, N. Preußke, F. Berger, H. Clausen-Schaumann, U. Lüning, M. K. Beyer, Chem.-Eur. J. 2016, 22, 12034.

- [33] S. Wang, H. K. Beech, B. H. Bowser, T. B. Kouznetsova, B. D. Olsen, M. Rubinstein, S. L. Craig, J. Am. Chem. Soc. 2021, 143, 3714
- [34] Y. Liu, S. Holm, J. Meisner, Y. Jia, Q. Wu, T. J. Woods, T. J. Martinez, J. S. Moore, *Science* **2021**, *373*, 208.
- [35] Y.-K. Song, K.-H. Lee, W.-S. Hong, S.-Y. Cho, H.-C. Yu, C.-M. Chung, J. Mater. Chem. 2012, 22, 1380.
- [36] D. C. Church, G. I. Peterson, A. J. Boydston, ACS Macro Lett. 2014, 3, 648.
- [37] R. Göstl, R. P. Sijbesma, Chem. Sci. 2016, 7, 370.
- [38] Z. S. Kean, G. R. Gossweiler, T. B. Kouznetsova, G. B. Hewage, S. L. Craig, Chem. Commun. 2015, 51, 9157.
- [39] M. Li, H. Zhang, F. Gao, Z. Tang, D. Zeng, Y. Pan, P. Su, Y. Ruan, Y. Xu, W. Weng, *Polym. Chem.* 2019, 10, 905.
- [40] J. Wang, T. B. Kouznetsova, Z. Niu, M. T. Ong, H. M. Klukovich, A. L. Rheingold, T. J. Martinez, S. L. Craig, Nat. Chem. 2015, 7, 323.
- [41] R. R. Jones, R. G. Bergman, J. Am. Chem. Soc. 1972, 94, 660.
- [42] K. C. Nicolaou, G. Zuccarello, C. Riemer, V. A. Estevez, W. M. Dai, J. Am. Chem. Soc. 1992, 114, 7360.
- [43] P. R. Schreiner, J. Am. Chem. Soc. 1998, 120, 4184.
- [44] S. M. Gaffney, J. F. Capitani, L. Castaldo, A. Mitra, Int. J. Quantum Chem. 2003, 95, 706.
- [45] M. Klein, T. Walenzyk, B. König, Collect. Czech. Chem. Commun. 2004, 69, 945.
- [46] J. P. Snyder, J. Am. Chem. Soc. 1989, 111, 7630.
- [47] P. Magnus, S. Fortt, T. Pitterna, J. P. Snyder, J. Am. Chem. Soc. 1990, 112, 4986.
- [48] R. K. Mohamed, P. W. Peterson, I. V. Alabugin, Chem. Rev. 2013, 113, 7089.
- [49] E. Kraka, D. Cremer, Wiley Interdiscip. Rev.: Comput. Mol. Sci. 2014, 4, 285.
- [50] A. Evenzahav, N. J. Turro, J. Am. Chem. Soc. 1998, 120, 1835.
- [51] G. V. Karpov, V. V. Popik, J. Am. Chem. Soc. 2007, 129, 3792.
- [52] D. R. Pandithavidana, A. Poloukhtine, V. V. Popik, J. Am. Chem. Soc. 2009, 131, 351.
- [53] P. Bhattacharya, A. Basak, A. Campbell, I. V. Alabugin, Mol. Pharmaceutics 2018, 15, 768.
- [54] F. Ling, Z. Li, C. Zheng, X. Liu, C. Ma, J. Am. Chem. Soc. 2014, 136, 10914.
- [55] C. Wang, S. Chen, H. Zhou, J. Gu, A. Hu, Chin. J. Polym. Sci. 2017, 36, 237.
- [56] Y. Cai, F. Lehmann, E. Peiter, S. Chen, J. Zhu, D. Hinderberger, W. H. Binder, Polym. Chem. 2022, 13, 3412.
- [57] C. R. Hickenboth, J. D. Rule, J. S. Moore, *Tetrahedron* 2008, 64, 8435.
- [58] M. Krupicka, W. Sander, D. Marx, J. Phys. Chem. Lett. 2014, 5, 905.
- [59] M. R. Porter, S. E. Lindahl, A. Lietzke, E. M. Metzger, Q. Wang, E. Henck, C. H. Chen, H. Y. Niu, J. M. Zaleski, *Proc. Natl. Acad. Sci. U. S. A.* 2017, 114, E7405.
- [60] D. S. Rawat, J. M. Zaleski, Chem. Commun. 2000, 2493.
- [61] N. K. Vishwakarma, V. K. Patel, P. Mitra, K. Ramesh, K. Mitra, S. Vishwakarma, K. Acharya, N. Misra, P. Maiti, B. Ray, J. Macromol. Sci., Part A: Pure Appl. Chem. 2021, 58, 192.
- [62] R. H. Grubbs, D. Kratz, Chem. Ber. 1993, 126, 149.
- [63] A. G. Lyapunova, N. A. Danilkina, A. M. Rumyantsev, A. F. Khlebnikov, M. V. Chislov, G. L. Starova, E. V. Sambuk, A. I. Govdi, S. Bräse, I. A. Balova, J. Org. Chem. 2018, 83, 2788.
- [64] D. Döhler, J. Kang, C. B. Cooper, J. B.-H. Tok, H. Rupp, W. H. Binder, Z. Bao, ACS Appl. Polym. Mater. 2020, 2, 4127.
- [65] T. A. Zeidan, S. V. Kovalenko, M. Manoharan, I. V. Alabugin, J. Org. Chem. 2006, 71, 962.
- [66] P. J. Flory, J. Chem. Phys. 1950, 18, 108.



- [67] B. Zhu, J. Ma, Z. Li, J. Hou, X. Cheng, G. Qian, P. Liu, A. Hu, J. Mater. Chem. 2011, 21, 2679.
- [68] L. Mullins, N. R. Tobin, Rubber Chem. Technol. 1957, 30, 555.
- [69] K. M. Schmoller, A. R. Bausch, Nat. Mater. 2013, 12, 278.
- [70] E. M. Christenson, J. M. Anderson, A. Hiltner, E. Baer, *Polymer* 2005, 46, 11744.
- [71] Y. Miao, H. He, Z. Li, Polym. Eng. Sci. 2020, 60, 1083.



Initiator-Free Synthesis of Semi-Interpenetrating Polymer Networks via Bergman Cyclization

Yue Cai, Florian Lehmann, Justus F. Thümmler, Dariush Hinderberger, and Wolfgang H. Binder*

Semi-interpenetrating polymer networks (semi-IPNs), composed of two or more polymers, forming intertwined network-architectures, represent a significant type of polymer combination in modern industry, especially in automotive and medical devices. Diverse synthesis techniques and plentiful raw materials highlight semi-IPNs in providing facile modifications of properties to meet specific needs. An initiator-free synthesis of semi-interpenetrating polymer networks via Bergman cyclization (BC) is reported here, acting as a trigger to embed a second polymer via its reactive enediyne (EDY) moiety, then embedded into the first network. (Z)-oct-4-ene-2,6-diyne-1,8-diol (diol-EDY) is targeted as the precursor of the second polymer, swollen into the first polyurethane network (PU), followed by a radical polymerization induced by the radicals formed by the BC. The formation of the semi-IPN is monitored via electron paramagnetic resonance (EPR) spectroscopy, infrared-spectroscopy (FT-IR), and thermal methods (DSC), proving the activation of the EDY-moiety and its subsequent polymerization to form the second polymer. Stress-strain characterization and cyclic stress-strain investigations, together with TGA and DTG analysis, illustrate improved mechanical properties and thermal stability of the formed semi-IPN compared to the initial PU-network. The method presented here is a novel and broadly applicable approach to generate semi-IPNs, triggered by the EDY-activation via Bergman cyclization.

Y. Cai, J. F. Thümmler, W. H. Binder Macromolecular Chemistry Institute of Chemistry Faculty of Natural Science II Martin Luther University Halle-Wittenberg von-Danckelmann-Platz 4, 06120 Halle (Saale), Germany E-mail: wolfgang.binder@chemie.uni-halle.de F. Lehmann, D. Hinderberger Physical Chemistry Institute of Chemistry Faculty of Natural Science II Martin-Luther-University Halle-Wittenberg von-Danckelmann-Platz 4, 06120 Halle (Saale), Germany

© 2024 The Author(s). Macromolecular Chemistry and Physics published by Wiley-VCH GmbH. This is an open access article under the terms of the Creative Commons Attribution-NonCommercial License, which permits use, distribution and reproduction in any medium, provided the original work is properly cited and is not used for commercial purposes.

DOI: 10.1002/macp.202400177

1. Introduction

Interpenetrating polymer networks (IPNs) are defined as the combination of two or more chemically independent polymers.[1,2] Among the coexisting networks, at least one network is synthesized and/or crosslinked in the presence of the other. Since the profound combination of phenol-formaldehyde resins with vulcanized natural rubber by Aylsworth in 1914 and the discussion from Millar[3] in 1960, IPNs have occupied a significant role in macromolecular topologies.[4] The unique properties of swelling capacity and mechanical strength of IPNs have enabled them to be widely applied in automotive parts, [5] engineering plastics, [6] damping compounds, [7–9] biomedical devices, [10–13] or as structural concepts in molding materials. Depending on the synthetic routes and the combined patterns of the two polymers, [1,14] IPNs could be classified as sequential, semi-, and simultaneous IPNs, displaying various topologies and chemical bonding.[15-19] Among them, semi interpenetrating networks (semi-IPNs) are built from of two or more polymers, one of

which is crosslinked, the other embedded into the first one, either with a linear or branched architecture, but in itself not crosslinked.[20-22] Tremendous efforts have been focused on the synthesis, morphology, physical/chemical properties, and applications of various ingeniously designed semi-IPNs. Represented by hydrogels, [23-25] which are derived from bio-friendly and hydrophilic raw materials, recently semi-IPNs have been particularly empowered in the field of stimuli-responsive sensors and pharmaceutical devices. Via sequential synthesis methods, (semi-)IPNs are prepared by firstly polymerizing monomer I with crosslinker I to produce the first network, followed by the swelling of monomer II and a subsequent polymerization to generate the second polymer.[26,27] The first generated network thus plays a fundamental role in the mechanical or thermal properties of the finally formed (semi-)IPN products. Owing to its versatile properties (elastomeric to rigid polymers) and facile synthesis, polyurethanes (PU) are identified as one of the most privileged network components. [28-30] Among the corresponding IPNs constituted from PU, various polymeric components such as epoxy resins,[31] vinyl ester resins,[7] unsaturated polyester resins,[32]



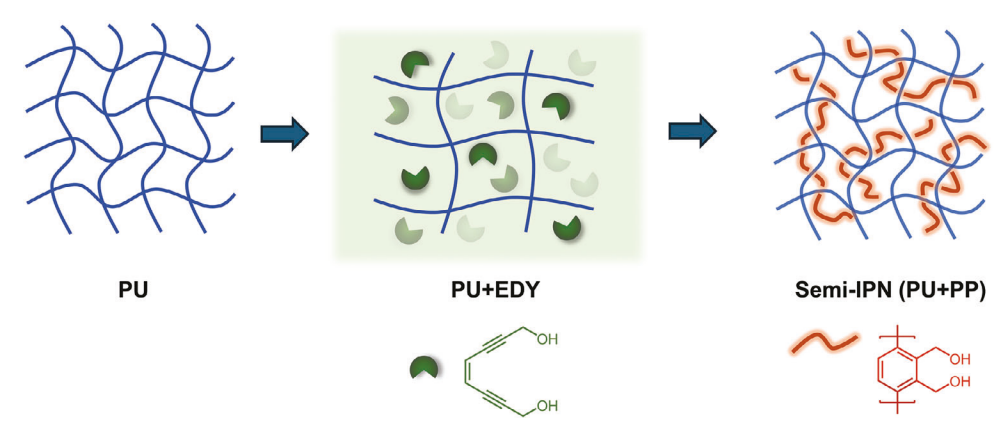


Figure 1. Schematic illustration of the designed construction of semi-interpenetrating polymer networks via a Bergman cyclization (BC).

acrylates, [33] and styrene [34] have been extensively used as the precursors of existing networks. However, for many of those networks, residues from the initiators used for the often free radical initiation processes are difficult to avoid, often hampering the broad use of those networks. Thus many reactive initiators such as peroxides, [35] azo-initiators, [36] or phosphine oxides, [37] together with the crosslinking agents or monomers^[38] as well as their residues after activation and crosslinking have been widely recognized as detrimental in the final IPNs which often prevents application due to their inherent biological toxicity. Thus there is a critical need to avoid residues of the used cross-linking (re)agents in the final IPNs.

We here report on a novel method to generate semi-IPNs, using an initiator-free approach for a radical-polymerization via a thermally triggered Bergman-cyclization (BC). In our search for initiator-free coupling chemistries, we came across a pericyclic reaction such as the Bergman cyclization (BC) as a potential target, which was first reported in 1972.[39] 3-Ene-1,5-diynes (EDYs) can undergo exothermic cycloaromatization by thermal or photochemical activation in the presence of suitable hydrogen donors to generate benzene derivatives via a diradical intermediate, generated by a pericyclic reaction in a distance-dependent (1,6)reaction. The intermediately formed 2,5-diradicals can serve as a source for a radical polymerization to form functional polymers, such as conjugated polymers, polymeric nanoparticles, or carbon nanomembranes via a direct coupling of the radicals to generate a polymer.^[40,41] Inspired by the excellent properties of the BC and our own previous work, [42,43] we herein report an initiator-free construction of a novel interpenetrating polymer network consisting of an elastic polyurethane and a rigid polyphenylene (see Figure 1). We highlight the function of EDY as one of the precursors to be swollen into the existing crosslinked polyurethane and subsequently to be initiated thermally to obtain semi-IPN. The diradicals formed via BC undergo radical-coupling to induce covalent coupling via radical polymerization, in turn leading to an efficient hardening of the original PU material. Induced changes in the physical and mechanical properties lead to a novel type of construction of semi-IPN and a promising post-modification of polyurethanes.

2. Results and Discussion

As depicted in Scheme 1, we initiated our studies by synthesizing a polyurethane (PU) network as the basis for the first network, allowing to tune its rigidity and composition. A mixture of polytetrahydrofuran (PTHF, 650 Da, 40 mmol), isophorone diisocyanate (IPDI), and glycerol (Gly) (molar ratio of PTHF/IPDI/Gly:1/2/0.67) was heated to obtain the crosslinked PU with dimethyl formamide as solvent.[44] Subsequently, the reaction mixture was cast into a mold, followed by intensive drying under vacuum and heat to remove all solvent residues. It is worth emphasizing that the synthesic procedure herein of crosslinked polyurethane is mature and the scalability is adjustable depending on practical requirements. In parallel, the precursor enediyne (EDY) of the semi-interpenetrating network was prepared, representing the basis for the second polymer. (Z)-oct-4-ene-2,6diyne-1,8-diol (diol-EDY),[45] up to now only scarcely used for BC processes,[46-51] was selected, and deemed useful due to its stability at ambient conditions, combined with its ease of preparation and the triggerable activation of the BC. For synthesis, the trimethylsilyl (TMS) group was added as a protective moiety on propargyl alcohol, followed by a classical Sonogashira coupling reaction with (Z)-1,2-dichloroethene and subsequent acidcatalyzed deprotection, in turn yielding the diol EDY (Figure \$1, Supporting Information, all data are inline with the data reported from literature). [46] It should be noted that similar to our recent results focusing on diamine EDY ((Z)-octa-4-en-2,6-diyne-1,8-diamine), the final **diol-EDY**, (*Z*)-oct-4-ene-2,6-diyne-1,8-diol, is stable in solution with the required concentration owing to its primary alcohol groups inducing intramolecular hydrogen bonding, thus allowing its integration into the first PU-network without primordial polymerized reactions.

With the original PU material and the precursor enediyne (diol-EDY) of the second polymer in hand, the preparation of various samples was conducted as shown in Figure 2A. After casting and drying as described above, a transparent and colorless film was obtained. To remove possibly unreacted monomers, the film was immersed in tetrahydrofuran for 24 h, whereafter all adsorbed initial components for the PU were removed as proven

I. Synthesis of the 1st network polyurethane (**PU**):

II. Synthesis of enediyne (**EDY**) and the 2nd polymer polyphenylene (**PP**) via BC:

Scheme 1. Synthesis of the first network polyurethane (PU), enediyne monomer (Z)-oct-4-ene-2,6-diyne-1,8-diol (diol-EDY), and the second polyphenylene (PP) via BC.

by NMR of the solvent. The so purified PU material was then soaked in the solution of the **diol-EDY** with ethyl acetate as the solvent ($c = 50 \text{ mmol L}^{-1}$). With a swelling time of 48 h, **diol-EDY** was swollen into the network of PU as expected, together with the solvent ethyl acetate without reaction with the PU-endgroups (targeted as OH), thus allowing a homogeneous distribution of the diol-EDY inside the PU-network. After probing different concentrations of the EDY-solution, the chosen concentration of 2.5 mmol mL⁻¹ was identified as the optimum to reach a successful embedding of the EDY inside the PU. Higher concentrations

or the application of neat EDY lead to primordial BC, as probed separately in solution. [43] After swelling, the film was removed from the solution and dried, the sample PU + EDY was collected and ready for characterization. During the process of drying the samples, a high vacuum with a pressure of 0.01 mbar was applied for 24 h, and a continued monitoring of the mass was conducted to ensure that the solvent, ethyl acetate, was completely removed. The gained weight of PU + EDY compared with the original PU sample was attributed to the embedded diol-EDY and showed its content as 4 wt% through calculation. After a thermally-induced

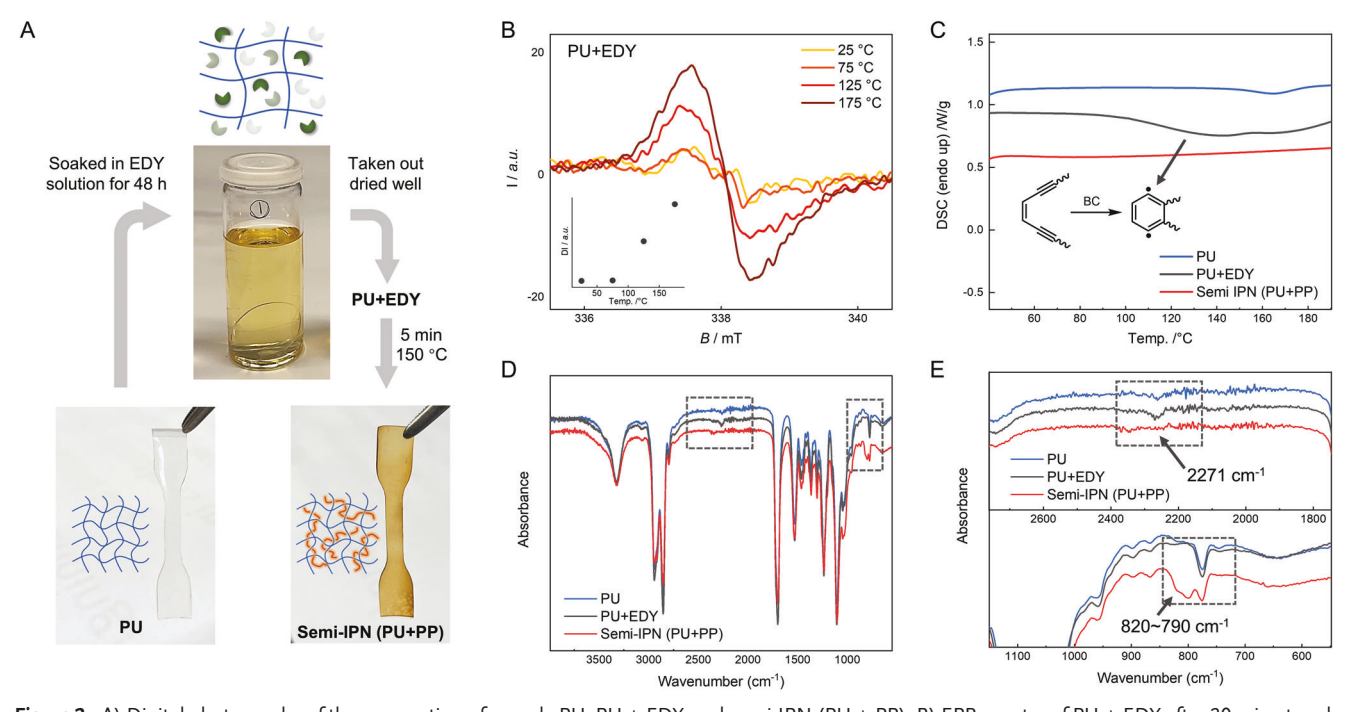


Figure 2. A) Digital photographs of the preparation of sample PU, PU + EDY, and semi-IPN (PU + PP). B) EPR spectra of PU + EDY after 20 min at each temperature (legend). C) DSC curves of PU, PU + EDY, and semi-IPN (PU + PP) under heating conditions, N_2 atmosphere, 5 K min⁻¹. D,E) Comparison and enlargement of FT-IR spectra of the samples PU, PU + EDY, and the semi-IPN (PU + PP).



Table 1. Overview of dissipated energy of sample PU and semi-IPN (PU + PP) at a maximum strain of 50%, 100%, 150%, and 200%, together with strain at break, stress at break of each sample, and swelling degree of two samples in toluene.

Sample	Dissipated energy [MJ m ⁻³]		Fracture strain [%]	Fracture stress [MPa]	Swelling [%] (toluene)		
	Strain 50%	Strain 100%	Strain 150%	Strain 200%			
PU	16.3	35.0	55.7	80.0	679 (± 58)	13.9 (± 5.1)	131
Semi-IPN (PU + PP)	27.6	53.4	77.9	102.0	672 (± 73)	15.0 (± 4.4)	119

BC (150 °C for 5 min), the semi-IPN (PU + PP) was obtained, wherein the formed 2,5-diradicals form the second polymer via radical coupling. It is worth mentioning that the temperature chosen for the thermal initiation was according to the detected peak temperature of the reaction curve in DSC, referring to previous work on the polymerization of enediynes.^[52]

To prove the successful Bergman-cyclization-chemistry and the formation of the second polymer, various analyses were conducted. First, the verification of the presence of EDY in the network was probed with electron paramagnetic resonance (EPR) spectroscopy as illustrated in Figure 2B. Thermally-induced formation of the radicals was proven by the increasing intensity of the carbon-centered radical signals when gradually heating the sample in situ from 25 to 175 °C in steps of 25 °C, revealing the progressive initiation of BC and generation of radical moieties. The double integral (DI) calculated from the EPR spectra at each temperature (25, 75, 125, and 175 °C) is directly correlated to the radical concentration in the sample. The DI was plotted against the temperature, which is shown in the inset of Figure 2B, clearly proving the formation of radicals inside the semi-IPN by thermal initiation of the embedded EDYs.

As BC is an exothermic reaction, differential scanning calorimetry (DSC) was measured with the samples PU, PU + EDY, and the semi-IPN (PU + PP) to probe the progress of the BC, indicated by a decreasing exothermic profile as the reaction proceeded. All samples were heated to 250 °C, followed by cooling to 25 °C under an atmosphere of N2. As shown in Figure 2C, for the intermediate sample PU + EDY (black line), the broad exothermic peak (≈140 °C) was attributed to a thermally triggered BC of the enediyne moiety, which did not appear for sample PU. For the formed interpenetrating sample semi-IPN (PU + PP), the flat curve (red line) during heating further proved the completion of BC of the gained enediyne inside the network. Furthermore, BC was proven by IR-spectroscopy, indicating the chemical changes occurring during BC, changing from the EDY-moieties to the poly(aromatic) polymers formed after BC (see Figure 2D/E). Comparison of the spectra of the samples PU (blue line), PU + EDY (black line), and the semi-IPN (PU + PP) (red line) showed that an increase stretching band of the ene (C≡C) at 2271 cm⁻¹ appeared first along with the embedding of the enediyne monomers, followed by a decrease at the same position during the formation of the semi-IPN, providing solid evidence about the process of incorporation first and consumption of the subsequently added enediyne monomers in the preparation of semi-IPN sample. Besides, a characteristic absorption at ≈810 cm⁻¹ in the sample semi-IPN could be attributed to the CH bending of the conjugated benzene ring system. It is worth mentioning that, compared to the CH bending on the 1,2-substituted benzene, the absorption

presented here at a higher wavenumber (810 cm⁻¹) revealed the formation of the 1,2,3,4-substituted benzene moieties as a result of free radical polymerization in the presence of diradical intermediates, which was consistent with the previous $work^{[53]}$ on the polymerization of enediynes published in 1994. In addition, as shown in **Table 1**, swelling experiments proved the formation of a second polymer by BC: the presence of the interpenetrating composition decreased the swelling degree of the network, from 131% for PU to 119% semi-IPN (PU + PP). Therefore, the presence of EDY swollen into the PU network, together with the formed skeleton of semi-IPN (PU + PP) via BC, was verified.

With the semi-IPN (PU + PP) in hand, the difference in the mechanical properties compared to the original PU was examined, as the formation of a second polymer inside the first PUnetwork was expected to yield changes in the mechanical properties. To avoid eventual errors caused by the soaking process of sample semi-IPN (PU + PP) in EDY/ethyl acetate solution, PU used in this paper was treated precisely with the same soaking process in a blank solvent (ethyl acetate) without EDY. Correspondingly, rectangular specimens with a length of 40 mm, a width of 4 mm, and a thickness between 0.2 and 0.4 mm were prepared. Three specimens for each sample were measured on average with a uniform stretching speed of 20 mm min⁻¹. As illustrated in Figure 3, the mechanical properties of both samples were studied by stress-strain characterization and cyclic stress-strain investigations. Their determined strain at break, stress at break, and dissipated energy values at each strain are depicted in Table 1. For the two elastomer samples, an increase of the tensile stress was observed from 13.9 MPa for PU to 15.0 MPa for semi-IPN (PU + PP), while the extensibility slightly decreased from 679% to 672%. The slightly improved mechanical properties could be attributed to the existence of the second polymer polyphenylene, inducing structurally physical entanglement, thus boosting its rigidity.[54,55] In the research of IPNs, higher tensile strength and lower elongation are common.^[56] Besides, cyclic stress-strain investigations of both samples were performed at room temperature to study the energy dissipation capacity related to the bonding interactions. Therefore, cyclic loading and unloading at a maximum strain of 50%, 100%, 150%, and 200%, far below the strain at break, were performed continuously without rest. The area between the load and unload stressstrain curves equals the dissipated energy. Compared to PU, the integral area of the corresponding hysteresis loop of semi-IPN (PU + PP) was increased ≈48 times on average, indicating the impact of the entanglement on the mechanical properties in its semi-interpenetrating form. Furthermore, a similar native PU* was synthesized by lowering mole ratio of the crosslinker glycerol (Gly), and corresponding semi-IPNs (PU*+ PP) were obtained. The cyclic stress-strain investigations also verified the improved

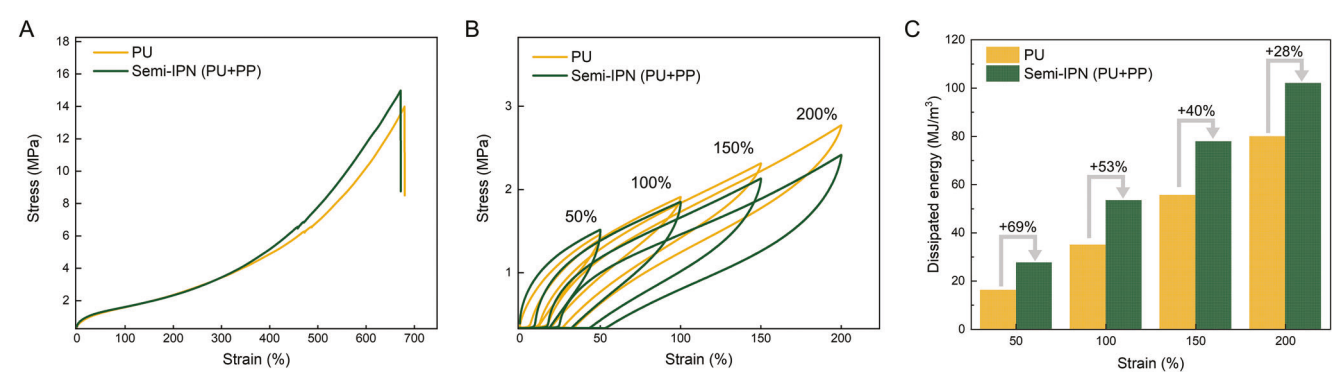


Figure 3. A) Tensile curves of PU and semi-IPN (PU + PP). B) Cyclic stress-strain curves of sample PU and semi-IPN (PU + PP). Cyclic loading and unloading were performed continuously without rest at 50%, 100%, 150%, and 200% strain. C) Dissipated energy values at each strain.

Table 2. Thermal properties of the PU and the semi-IPN (PU + PP).

Sample	T _{5wt.%} /°C	T _{15wt.%} /°C	1st decomposition		2nd decomposition		Residue (600 °C)/wt.%
			Mass loss/ wt.%	T _{max} /°C	Mass loss/ wt.%	T _{max} /°C	-
PU	281	305	62.2	338	35.9	397	0.1
Semi-IPN (PU + PP)	286	309	61.9	338	32.9	398	3.3

mechanical strength (Figure S4 and Table S2, Supporting Information). An enhancement of the mechanical properties was detected in the study, underscoring the use of the Bergman cyclization to form the semi-IPN.

As illustrated in **Figure 4**, thermogravimetric analyses (TGA) were applied further to probe the thermal stabilities of this series of samples. Along with continuous heating conditions up to 800 °C, the EDY moieties inside sample PU + EDY were supposed to undergo Bergman cyclization (according to the DSC curve in Figure 2C). Therefore, in terms of the thermal stabilities, the original PU and the obtained semi-IPN (PU + PP) were analyzed here. The determined temperature and mass loss at different stages of the decomposition, together with the residue

percentages at 600 °C are depicted in **Table 2**. The decomposition processes of both samples were quite comparable. The 5% decomposition of PU ($T_{\rm 5wt\%}$) happened at \approx 281 °C, but for the semi-IPN (PU + PP), the temperature required for the same 5% decomposition was increased to 286 °C. Additionally, two stages of degradation were recorded for both samples with similar maximum degradation temperatures (for $T_{\rm max1}$: 338 °C, for $T_{\rm max2}$: 397 °C) as shown in the corresponding DTG curves (blue line), but with respectively different proportions of mass loss in each of the two stages. During the first stage (the peak shown between 230 and 380 °C in the blue line), both samples were thermally degraded, which could be attributed to the decomposition of the urethane bonds taking place through the dissociation to

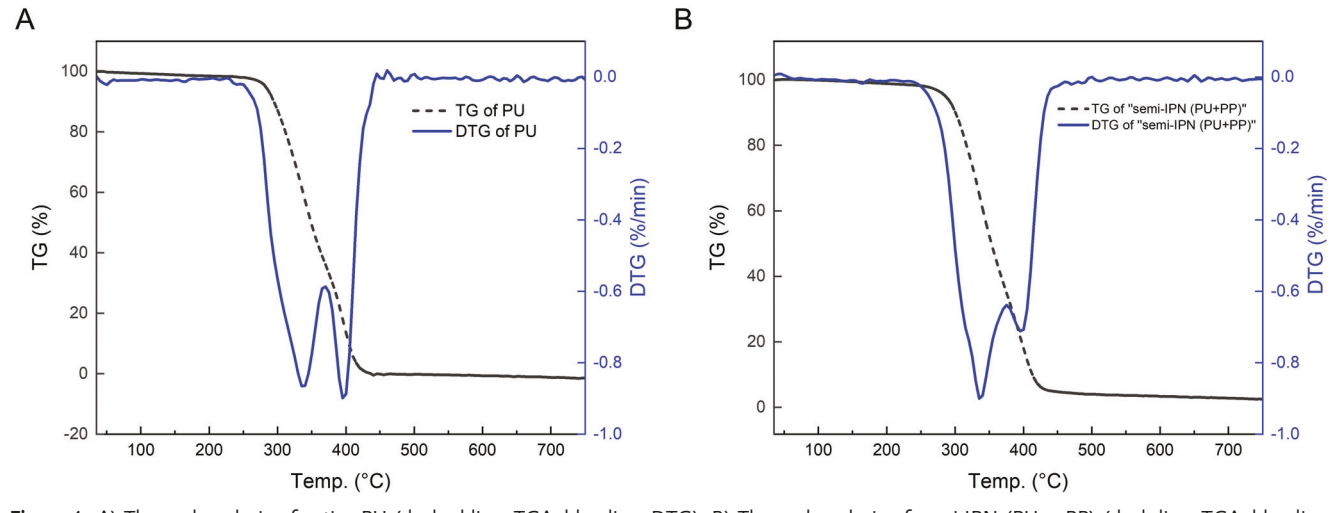


Figure 4. A) Thermal analysis of native PU (dashed line: TGA, blue line: DTG). B) Thermal analysis of semi-IPN (PU + PP) (dash line: TGA, blue line: DTG).



isocyanate and alcohol, leading to the loss of carbon dioxide from the urethane bond.^[57,58] In this stage, the semi-IPN displayed a lower mass loss compared to the native PU. A more drastic decrease in mass loss and a lower maximum weight loss rate for the semi-IPN were detected during the second stage (decomposition took place between 370 and 450 °C) involving the rupture of ester linkages and fatty acid chains of the polyurethane soft segments.^[57,58] Therefore, TGA and the corresponding DTG verified the improved thermo-stability owing to the presence of the additional PP polymer. The residual components at 600 °C for semi-IPN stemmed from the then carbonized polymers, polyphenylene, formed thermally by radical crosslinking the DEY moieties.

To investigate the surface morphologies, atomic force microscopy (AFM) analysis in the phase contrast mode was performed on three thin films prepared throughout the synthetic route: the original PU, the intermediate PU + EDY, and the final semi-IPN (PU + PP). The respective height and 3D images, together with analyzed roughness were shown in Figure 5. For PU, the surface morphology exhibited a surface with some nonnegligible gullies. After analysis (Table S3, Supporting Information); the surface possesses a roughness average of Ra = 2.3 nm, which could be attributed to the incompatibility between both rigid and flexible segments in PU. For sample PU + EDY, the height image (Figure 5B) presented local accumulation with a certain height and segregated domains, with the texture providing a height of \approx 62 nm (Figure 5E). In the meantime, a decreased roughness average (1.0 nm) was found for the surface of PU + EDY, which could be possibly attributed to the filling of EDYs in the gaps between amorphous segments of PU.[59] When

it came to the final semi-IPN (PU + PP), the roughness was significantly reduced to 0.3 nm, together with the disappearance of the segregated domains. According to the structural changes and reactions that happened inside, it was presumed that the local clusters shown in PU + EDY were due to the introduction of EDY-OH, and the intermolecular forces of EDY-OH small molecules caused molecular stacking in the PU network. With thermal initiation, molecular diffusion in the network first occurred for locally collective EDY-OHs. When the BC temperature is reached, the EDY-OHs start to form diradical species, followed by free radical polymerization to form linear polyphenylenes inline with the disappearance of the local clusters. As radical polymerization is normally associated with a decrease in volume due to entropic effects, the roughness average is reduced to 0.3 nm (Figure 5G). Scanning electron microscopy (SEM) was conducted further to obtain the surface morphologies of the three samples on a smaller scale (Figure \$5, Supporting Information) yielding results consistent with AFM.

3. Conclusion

We have accomplished a facile construction of a semi-interpenetrating polymer network via Bergman cyclization (BC) as an initiator-free process for the second polymer. The synthesis started from a preformed, first polyurethane (PU) network comprised of polytetrahydrofuran (650 Da), isophorone diisocyanate, and glycerol with a molar ratio of 1/2/0.67. (Z)-oct-4-ene-2,6-diyne-1,8-diol (diol-EDY) was targeted as the precursor of the second polymer and swollen into PU to form the interme-

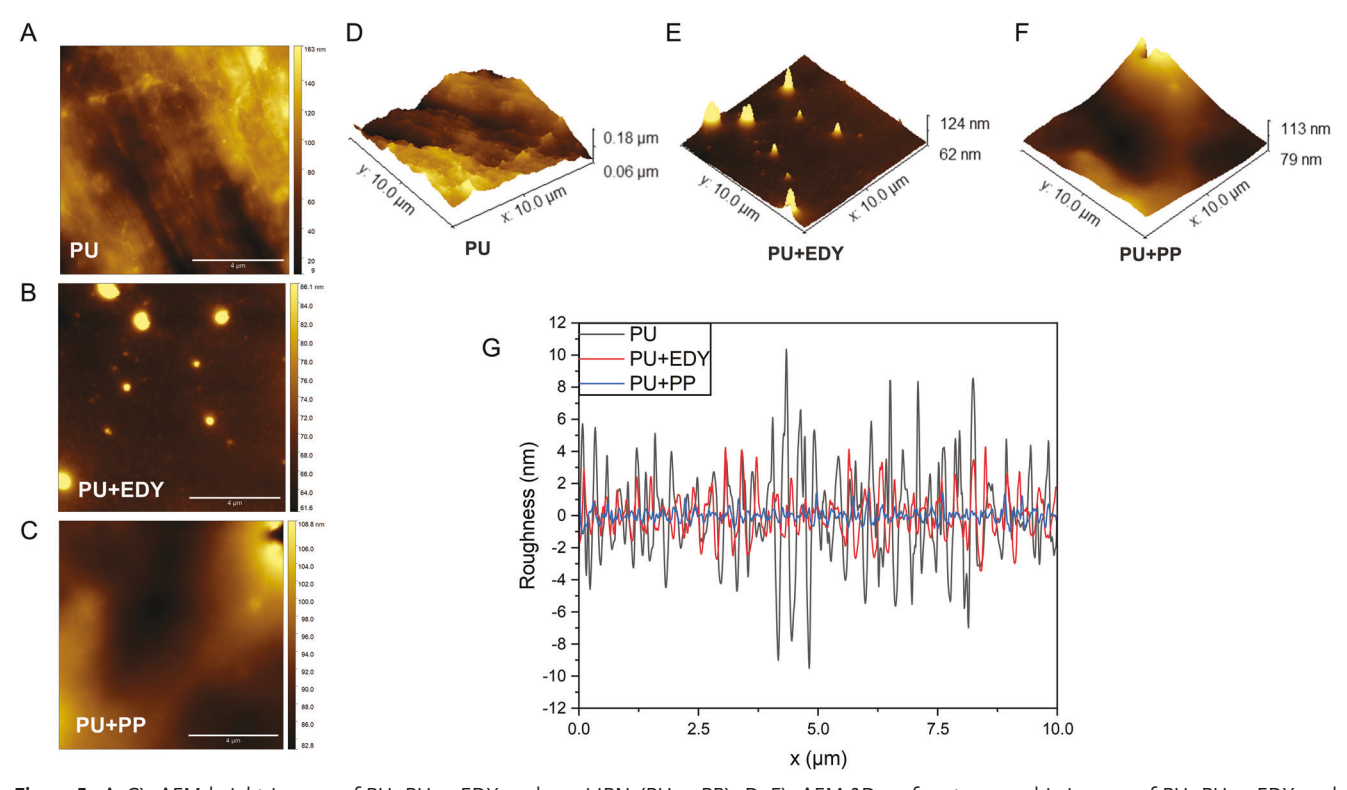


Figure 5. A-C): AFM height images of PU, PU + EDY, and semi-IPN (PU + PP). D-F): AFM 3D surface topographic images of PU, PU + EDY, and semi-IPN (PU + PP). G) Roughness analysis of three samples.



www.mcp-journal.de

diate PU + EDY. Followed by thermal initiation to undergo BC and subsequent radical polymerization, a semi-interpenetrating polymer semi-IPN (PU + PP) was established as planned. The presence of EDY in the PU network was verified by the occurrence of carbon radicals in EPR spectroscopy during the heatinitiated BC, the disappearance of absorption of the alkyne group in FT-IR spectroscopy after the consumption of EDY, and the characteristically exothermic peak in the DSC curve arising from BC verified jointly the successful insertion of EDY. Compared to the original single network PU, the obtained sample semi-IPN (PU + PP) possesses improved mechanical properties as proven by stress-strain characterization and cyclic stress-strain measurements. Furthermore, TGA and DTG indicated an improved thermal stability of the so-formed semi-IPN. The interpenetration and physical entanglement of the elastomeric PU and rigid PP resulted in a performance-enhanced polymer. The initial crosslinked polyurethane here can be replaced by any other crosslinked network, highlighting the broad approach of the here presented method to embed a second polymer into a preformed first one, using an initiator-free monomer, further allowing a simple post-modification of crosslinked polymers via enediynes and subsequent Bergman cyclization.

4. Experimental Section

A detailed Experimental Section can be found in the Supporting Informa-

Supporting Information

Supporting Information is available from the Wiley Online Library or from the author.

Acknowledgements

W.H.B. thanks the DFG project INST 271/444-1 FUGG for financial support; the DFG-Project BI1337/16-1; BI 1337/14-1 and the GRK 2670, W69000789, ProjectNr 436494874 and the DFG project BI1337/17-1 for financial support. The authors further thank the "PollFaces" initiative for financial support. Y.C. thanks MSc. Chenming Li for his fruitful help.

Open access funding enabled and organized by Projekt DEAL.

Conflict of Interest

The authors declare no conflict of interest.

Author Contributions

Conceptualization was performed by Y.C. and W.H.B.; methodology was performed Y.C. and F.L.; investigation was performed by Y.C. and F.L.; writing-original draft was prepared by Y.C. and W.H.B.; writing-review and editing was performed by Y.C., F.L., J.F.T.; D.H., and W.H.B.; supervision was performed by W.H.B.; project administration was performed by W.H.B.; funding acquisition by W.H.B. All authors have read and agreed to the published version of the manuscript.

Data Availability Statement

Macromol. Chem. Phys. 2024, 2400177

The data that support the findings of this study are available in the supplementary material of this article.

Keywords

Bergman-cyclization, interpenetrating networks, polyurethanes, radical croslsinking

> Received: June 6, 2024 Revised: June 29, 2024 Published online:

- [1] L. H. Sperling, Interpenetrating Polymer Networks, (Eds: D. Klempner; L. H. Sperling; L. A. Utracki) 1994, 239, pp 3-38.
- [2] L. H. Sperling, V. Mishra, Polym. Adv. Technol. 1996. 7. 197.
- [3] J. R. Millar, J. Chem. Soc. 1960, 1311 https://doi.org/10.1039/ JR9600001311.
- [4] L. H. Sperling, Polym. Eng. Sci. 1985, 25, 517.
- [5] S. Marinovic, I. Popovic, B. Dunjic, S. Tasic, B. Bozic, D. Jovanovic, Prog. Org. Coat. 2010, 68, 293.
- [6] C. Plesse, F. Vidal, H. Randriamahazaka, D. Teyssié, C. Chevrot, Polymer 2005, 46, 7771.
- [7] C.-L. Qin, W.-M. Cai, J. Cai, D.-Y. Tang, J.-S. Zhang, M. Qin, Mater. Chem. Phys. 2004, 85, 402.
- T. Wang, S. Chen, Q. Wang, X. Pei, Mater. Des. 2010, 31, 3810.
- [9] J. Čulin, Polimery 2021, 61, 159.
- [10] M. A. Haque, T. Kurokawa, J. P. Gong, Polymer 2012, 53, 1805.
- [11] M. S. Salehi Dashtebayaz, M. S. Nourbakhsh, Int. J. Polym. Mater. Polym. Biomater. 2019, 68, 442.
- [12] S. L. Steffensen, M. H. Vestergaard, E. H. Møller, M. Groenning, M. Alm, H. Franzyk, H. M. Nielsen, J. Biomed. Mater. Res., Part B 2016, 104, 402,
- [13] G. N. Smith, E. Brok, M. Schmiele, K. Mortensen, W. G. Bouwman, C. P. Duif, T. Hassenkam, M. Alm, P. Thomsen, L. Arleth, Polymer 2021,
- [14] I. Chikina, M. Daoud, J. Polym. Sci. Part B-Polym. Phys. 1998, 36, 1507.
- [15] M. S. Silverstein, Polymer 2020, 207, 122929.
- [16] E. S. Dragan, Chem. Eng. J. 2014, 243, 572.
- [17] L. H. Sperling, J. Polym. Sci. Macromol. Rev. 1977, 12, 141.
- [18] Y. Liu, Y. Chen, J. Zhu, M. Lu, C. Jiang, Z. Fan, T. Sun, Int. J. Smart Nano Mater. 2023, 14, 460.
- [19] Y. Liu, W. Xian, J. He, Y. Li, Int. J. Smart Nano Mater. 2023, 14, 474.
- [20] L. Chikh, V. Delhorbe, O. Fichet, J. Membr. Sci. 2011, 368, 1.
- [21] L. Xu, N. Sheybani, S. Ren, G. L. Bowlin, W. A. Yeudall, H. Yang, Pharm. Res. 2015, 32, 275.
- [22] N. Zoratto, P. Matricardi, in Polymeric Gels, (Eds: K. Pal; I. Banerjee), Woodhead Publishing, Sawston, Cambridge 2018, 91.
- [23] S. Muthyala, R. R. Bhonde, P. D. Nair, Islets 2010, 2, 357.
- [24] S. Afrin, M. Shahruzzaman, P. Haque, M. S. Islam, S. Hossain, T. U. Rashid, T. Ahmed, M. Takafuji, M. M. Rahman, Gels 2022, 8, 340.
- [25] A. Rahmatpour, P. Soleimani, A. Mirkani, React. Funct. Polym. 2022, 175, 105290.
- [26] M. Pulat, A. S. Kahraman, N. Tan, M. Gümüşderelioğlu, J. Biomater. Sci. Polym. Ed. 2013, 24, 807.
- [27] M. Retailleau, J. Pierrel, A. Ibrahim, C. Croutxé-Barghorn, X. Allonas, Polym. Adv. Technol. 2017, 28, 491.
- [28] D. Rosu, C. Ciobanu, C. N. Cascaval, Eur. Polym. J. 2001, 37, 587.
- [29] W. D. Athawale, S. L. Kolekar, S. S. Raut, J. Macromol. Sci.-Polym. Rev. 2003, 43, 1.
- [30] L. Karabanova, V. Bershtein, Y. Gomza, D. Kirilenko, S. Nesin, P. Yakushev, Polym. Compos. 2018, 39, 263.
- [31] S. Chen, Q. Wang, T. Wang, J. Reinf. Plast. Compos. 2013, 32, 1136.
- [32] S. Guhanathan, R. Hariharan, M. Sarojadevi, J. Appl. Polym. Sci. 2004, 92.817.





- [33] J. Liu, Q. Li, Y. Zhuo, W. Hong, W. Lv, G. Xing, J. Nanosci. Nanotechnol. 2014, 14, 4405.
- [34] D. S. Lee, J. H. An, S. C. Kim, in Interpenetrating Polymer Networks, American Chemical Society, Washington, D. C. 1994, 463.
- [35] M. F. Moreau, D. Chappard, M. Lesourd, J. P. Monthéard, M. F. Baslé, J. Biomed. Mater. Res. 1998, 40, 124.
- [36] T.-W. Wu, K.-P. Fung, J. Wu, C.-C. Yang, J. Lo, R. D. Weisel, Life Sci. 1995, 58, PL17,
- [37] G.-T. Kim, H.-B. Go, J.-H. Yu, S.-Y. Yang, K.-M. Kim, S.-H. Choi, J.-S. Kwon, Polymers 2022, 14, 979.
- [38] R. S. H. Wong, M. Ashton, K. Dodou, J. Pharmac. Analys. 2016, 6, 307.
- [39] R. R. Jones, R. G. Bergman, J. Am. Chem. Soc. 1972, 94, 660.
- [40] Y. L. Xiao, A. G. Hu, Macromol. Rapid Commun. 2011, 32, 1688.
- [41] S. D. Chen, A. G. Hu, Sci. China-Chem. 2015, 58, 1710.
- [42] Y. Cai, W. H. Binder, Macromol. Rapid Commun. 2023, 44, 2300440.
- [43] Y. Cai, F. Lehmann, E. Peiter, S. Chen, J. Zhu, D. Hinderberger, W. H. Binder, Polym. Chem. 2022, 13, 3412.
- [44] S. Oprea, V.-O. Potolinca, V. Oprea, Eur. Polym. J. 2016, 83, 161.
- [45] M. Mladenova, M. Alami, G. Linstrumelle, Synth. Commun. 1996, 26, 2831.
- [46] M. M. McPhee, S. M. Kerwin, J. Org. Chem. 1996, 61, 9385.
- [47] J. Suffert, S. Raeppel, F. Raeppel, B. Didier, Synlett 2000, 874, https: //doi.org/10.1055/s-2000-6703.

- [48] M. Kar, A. Basak, M. Bhattacharjee, Bioorg. Med. Chem. Lett. 2005, 15, 5392.
- [49] S. Kitagaki, K. Katoh, K. Ohdachi, Y. Takahashi, D. Shibata, C. Mukai, J. Org. Chem. 2006, 71, 6908.
- [50] S. Kitagaki, Y. Okumura, C. Mukai, Tetrahedron 2006, 62, 10311.
- M. Kadela-Tomanek, E. Bebenek, E. Chrobak, M. Latocha, S. Boryczka, Molecules 2017, 22, 447.
- [52] S. Y. Sun, C. C. Zhu, D. P. Song, F. Li, A. G. Hu, Polym. Chem. 2014, 5, 1241.
- [53] J. A. John, J. M. Tour, J. Am. Chem. Soc. 1994, 116, 5011.
- [54] J. P. Gong, Y. Katsuyama, T. Kurokawa, Y. Osada, Adv. Mater. 2003, 15, 1155
- [55] D. J. Waters, K. Engberg, R. Parke-Houben, C. N. Ta, A. J. Jackson, M. F. Toney, C. W. Frank, Macromolecules 2011, 44, 5776.
- [56] N. Alizadeh, E. Triggs, R. Farag, M. L. Auad, Eur. Polym. J. 2021, 148,
- [57] J. Oenema, H. Liu, N. D. Coensel, A. Eschenbacher, R. Van de Vijver, J. Weng, L. Li, C. Wang, K. M. Van Geem, J. Anal. Appl. Pyrolysis 2022, 168, 105723.
- [58] F. H. Yeoh, C. S. Lee, Y. B. Kang, S. F. Wong, S. F. Cheng, W. S. Ng, Polymers 2020, 12, 1842.
- [59] D. Rosu, L. Rosu, F. Mustata, C.-D. Varganici, Polym. Degrad. Stab. 2012, 97, 1261.

Macromol. Chem. Phys. 2024, 2400177

5. Summary and Outlook

In the scope of this cumulative thesis the functions of enediyne (EDY)-based polymers were expanded through three individual approaches. Each series of designed EDY-based polymers demonstrated specific functions *via* Bergman cyclization (BC), including enhancing DNA cleavage abilities through repeated EDY units in the polymer main chain, inducing hardening in elastomers where BC acts as a crosslinking strategy, and constructing semi-interpenetrating network polymers (semi-IPNs).

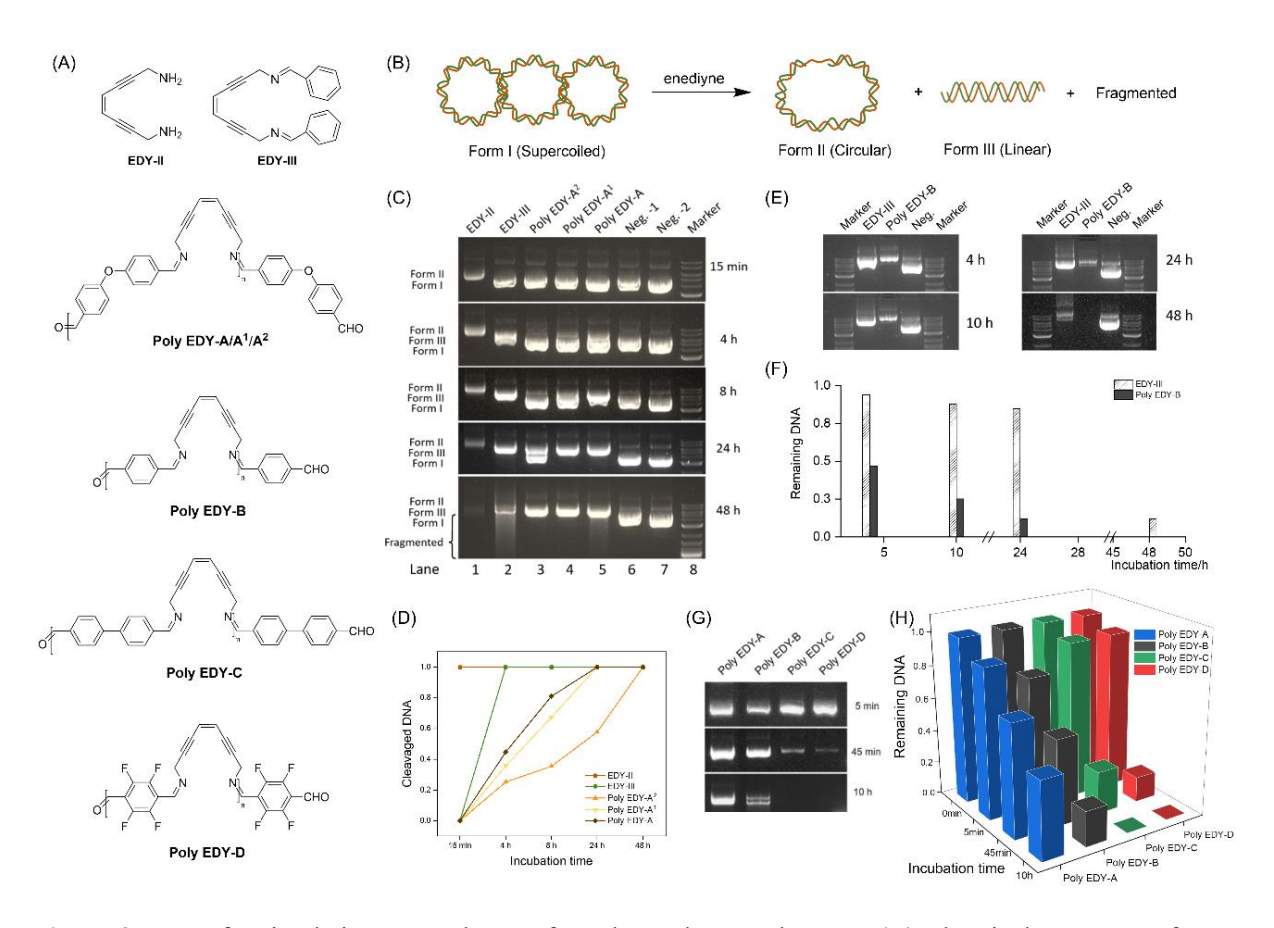


Figure 27. BC of main-chain EDY polymers for enhanced DNA cleavage. (A) Chemical structures of EDY derivatives. (B) Schematic formulation of DNA cleavage performance induced by EDY derivatives. (C) (D) Agarose gel electrophoretic images and quantified analysis of DNA cleavage assay. Lane 1 to Lane 5: pART7 incubated with **EDY-II/III** and **Poly EDY-A/A¹/A²**; Lane 6 and Lane 7: negative control. Lane 8: Marker. All the mixture maintained a total volume of 120 μL and was incubated at 37 °C. (E) (F) Agarose gel electrophoretic images and quantified analysis of DNA cleavage with **EDY-III** and **Poly EDY-B**. (G) (H) Agarose gel electrophoretic images and quantified analysis of DNA cleavage with **Poly EDY-A/B/C/D**.

First, a series of main-chain EDY polyimines (**Poly EDY-A/B/C/D**) was designed and synthesized *via* polycondensation of diamino-EDY ((*Z*)-octa-4-en-2,6-diyne-1,8-diamine) with various dialdehydes, including 4,4'-oxydibenzaldehyde, terephthalaldehyde, [1,1'-biphenyl]-4,4'-dicarbaldehyde, and 2,3,5,6-tetrafluoroterephthalaldehyde. Investigation of the stoichiometric ratio of the two starting materials for polycondensation revealed its influence on

controlling the average degree of polymerization (DP), yielding **Poly EDY-A**/**A**¹/**A**² with decreasing DP. The incorporation of EDY into the obtained polymer was verified through DSC and FT-IR spectroscopy, based on the exothermic properties of BC and the consumption of the alkynyl groups of EDY during BC. Additionally, the synthesized poly EDY was characterized by NMR and MALDI-TOF. All poly EDY samples, along with the diamino-EDY and its derived diimine-EDY (after condensation with aldehyde), were prepared in solution with a unified concentration of EDY.

These main-chain EDY polymers exhibited a chain-length dependent DNA cleavage activity under physiological conditions as shown in Figure 27C/D. With the highest DP, Poly EDY-A showed the most efficiency in cleaving DNA. Besides, polymeric EDY chains (Poly EDY-B) possessed increased activity compared to monomeric molecule EDY-III, both containing a similar stereoelectronic environment as illustrated in Figure 27E/F. The cleavage activities could be further tuned by modulating the stereoelectronic environment *via* different substitution patterns. Poly EDY-D containing tetrafluoro-segments and Poly EDY-C possessing biphenyl structures, caused a fast cleavage, followed by Poly EDY-B substituted with terephthyl-groups and Poly EDY-A derived from 4,4'-oxydibenzaldehyde as shown in Figure 27G/H. The order of DNA-cleaving activities of the different polymers can be explained *via* the stereoelectronic influence of substituents at the terminal alkyne positions, known to affect the activity of BC. Photochemical activation generates long-lived free radicals, as verified by electron paramagnetic resonance spectroscopy, with rates of radical formation corresponding to those observed in DNA cleavage experiments.

Secondly, a BC-triggered crosslinking of polyurethane with EDYs was accomplished using heat and stress, leading to an induced reinforcement in the mechanical strength of the material by generating permanent covalent crosslinks. An initial polymer matrix polytetrahydrofuran (PTHF, 2.9 kDa) was chosen to react with isophorone diisocyanate (IPDI) (mole ratio PTHF/IPDI:1/2) to generate isocyanate-terminated PTHF. Followed by polyaddition with an equimolar amount of the (*Z*)-octa-4-en-2,6-diyne-1,8-diamine, the elastomeric main-chain enediyne polymer (PIE) containing ≈3 EDY-groups per chain in average could be obtained as shown in Figure 28A. Results from GPC showed an increase in molecular weight (from 2.9 to 10.6 kDa), giving evidence of the successful accomplishment of the step-growth reaction. The existence of EDY in the chains was verified through FT-IR spectroscopy and DSC as illustrated in Figure 28D/E. With the method of the ASTM E698 standard procedure, DSC thermograms of neat PIE at four heating rates (HR) of 5, 10, 15, and 20 K min⁻¹ yielded an Arrhenius plot for its BC with calculated activation energy as 20.1 kcal mol⁻¹. The hydrogen bonds, not only between the PU chains but also between the urea groups in the joint of the EDY moieties, assisted in reaching a low *Ea* value as shown in Figure 28G.

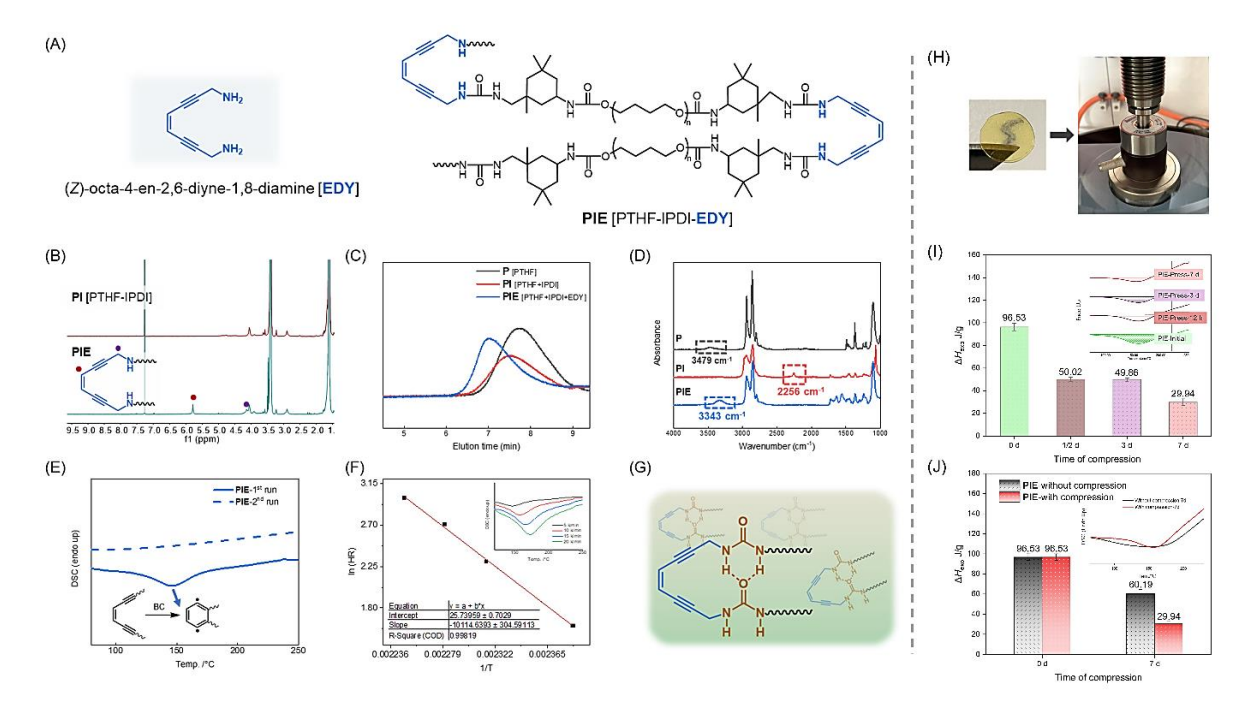


Figure 28. Triggered crosslinking of main-chain EDY polyurethanes *via* BC. (A) Chemical structure and compositions of **PIE**. (B) Comparison of the 1 H NMR between the isocyanate-terminated PTHF and **PIE**. (C) GPC of the initial PTHF, the isocyanate-terminated PTHF, and **PIE**. (D) FT-IR spectroscopy. (E) Two-cycle DSC curves under heating condition, N₂ atmosphere, 5 K min⁻¹: the first cycle (lower solid line) and the second cycle (upper dashed line). (F) Arrhenius plot for the BC of PIE in neat conditions obtained by DSC measurements using ASTM E698 standard procedure. Inset: DSC thermograms at four heating rates (HR) of 5, 10, 15, and 20 K min⁻¹. (G) The hydrogen bonds between the urea groups in the joint of the EDY moieties. (H) Compression device and operations taken during the compression. (I) Monitoring with DSC during the 7-day compression of **PIE**. (J) Comparison of Δ*H* calculated by DSC between **PIE** with or without compression for 7 days. Reprinted with permission from ref. [244], Copyright [2023], John Wiley and Sons.

PIE was subjected to multiple stimuli, such as heat, compression, and mechanical stress. Specifically, heat-induced crosslinking increased the tensile strength by 191% in comparison to the virgin sample. A 7-day compression under room temperature results in \approx 69% activation of the BC as shown in Figure 28I/J, together with the observation of an increase in tensile strength by 62% after 25 stretching cycles. The occurrence of BC is further proven by the decreased exothermic values in DSC, together with characteristic peaks of the formed benzene moieties via FT-IR spectroscopy. The BC herein forms an excellent crosslinking strategy, triggered by heat or force in polyurethane materials.

Thirdly, semi-IPNs were constructed with an initiator-free method utilizing enediyne and its BC reaction. A polyurethane (PU) network was synthesized through heating a mixture of polytetrahydrofuran (PTHF, 650 Da), isophorone diisocyanate (IPDI), and glycerol (Gly) (mole ratio of PTHF/IPDI/Gly:1/2/0.67). (*Z*)-Oct-4-ene-2,6-diyne-1,8-diol (diol-EDY) was synthesized and prepared as a solution using chloroform as the solvent. As shown in **Figure 29A**, the PU film was soaked in the EDY solution for 48 hours, allowing the diol-EDY to swell

into the network in a homogeneous manner. After drying and heating at 150 °C for 5 min, the intermediate sample PU+EDY could be transformed into the final semi-IPN (PU+PP) product, where polyphenylene (PP) was formed through radical polymerization *via* BC of EDY. The preparative process was monitored using several techniques such as DSC, EPR, and FT-IR spectroscopy. Surface morphologies of the three thin films throughout the synthetic route were analyzed by AFM.

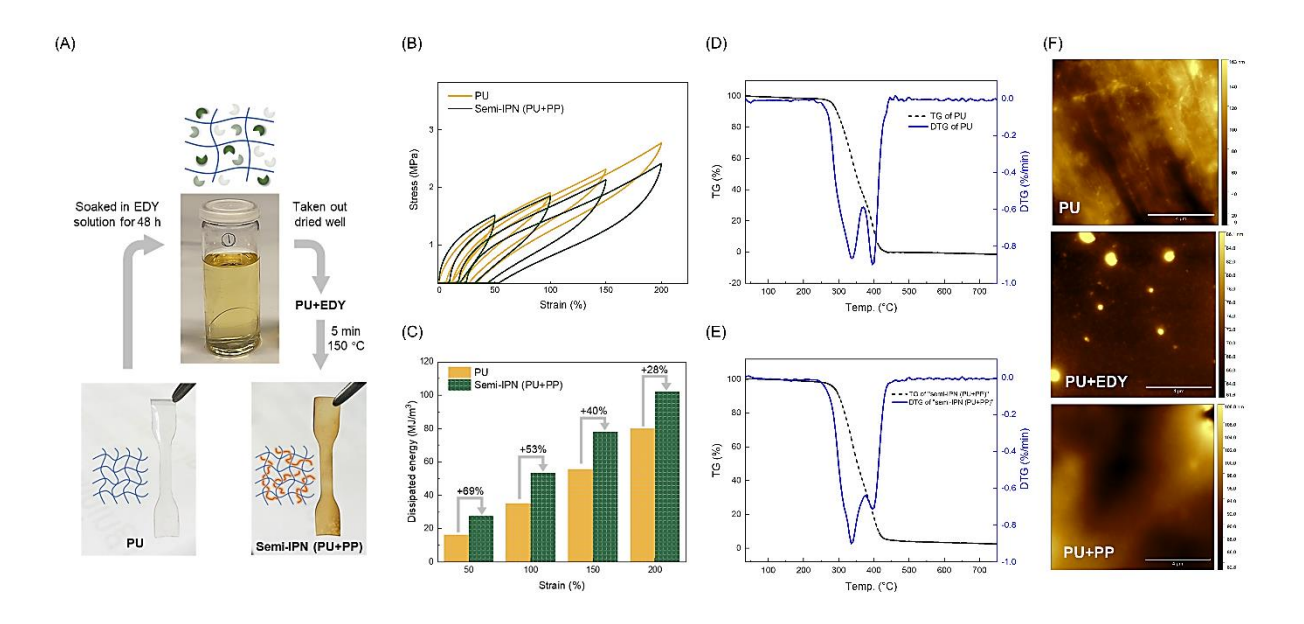


Figure 29. Initiator-free synthesis of semi-IPNs *via* BC. (A) Digital photographs of the preparation of sample PU, PU+EDY, and semi-IPN (PU+PP). (B) Cyclic stress-strain curves of sample PU and semi-IPN (PU+PP). Cyclic loading and unloading were performed continuously without rest at 50%, 100%, 150%, and 200% strain. (C) Dissipated energy values at each strain. (D) Thermal analysis of native PU (dashed line: TGA, blue line: DTG). (E) Thermal analysis of semi-IPN (PU+PP) (dash line: TGA, blue line: DTG). (F) AFM height images of PU, PU+EDY, and semi-IPN (PU+PP). Reprinted with permission from ref. [245], Copyright [2024], John Wiley and Sons.

Comparisons of the mechanical properties between the initial PU and the obtained semi-IPN (PU+PP) were first conducted through tensile tests. The tensile stress slightly increased from PU to the semi-IPN (PU+PP), while the extensibility decreased. Additionally, cyclic stress-strain investigations of both samples were performed at room temperature to study the energy dissipation capacity. Compared to the native PU, the integral area of the corresponding hysteresis loop for the semi-IPN (PU+PP) increased by approximately 48 times on average, indicating the impact of entanglement on the mechanical properties in its semi-interpenetrating form as shown in **Figure 29B/C**. TGA and the corresponding DTG analysis verified the improved thermal stability due to the presence of the PP polymer as illustrated in **Figure 29D/E**. This approach highlights a simple and convenient method to embed a second polymer into a

preformed first one using an initiator-free monomer, allowing for straightforward post-modification of crosslinked polymers *via* EDY and subsequent BC.

In conclusion, this thesis highlights the significant potential of EDY-based polymers for diverse applications, including DNA cleavage, enhanced mechanical strength, and thermal stability *via* BC. The successful design of main-chain EDY polymers, BC-triggered crosslinking, and semi-interpenetrating networks (semi-IPNs) provides a strong foundation for future developments.

Looking ahead, further exploration of stereoelectronic tuning and post-modification strategies could lead to more advanced functional materials. Expanding the scope of BC-induced crosslinking in different polymer matrices, along with scaling these methods for industrial applications, will be crucial. Investigating biocompatibility and environmental impact will also be essential for the adoption of EDY-based polymers in biomedical and sustainable material technologies.

6. List of Abbreviations

TS transition state

BC Bergman cyclization

EDY enediyne

DNA deoxyribonucleic acid
AML acute myeloid leukemia

NADPH nicotinamide adenine dinucleotide phosphate

DFT density functional theory

HOMO highest occupied molecular orbital

Boc butyloxycarbonyl

UV ultraviolet

GC-MS gas chromatography–mass spectrometry

PtCl₂ platinum(II) chloride

CuI copper(I) iodide
BuNH₂ n-butylamine

DSC differential scanning calorimetry

FT-IR Fourier-transform infrared TEMPO tetramethylpiperidinyloxyl

A adenine
T thymine
C cytosine
G guanine

RAFT reversible addition-fragmentation chain-transfer

ESI-MS electrospray ionization- mass spectrometry

PDI polydispersities

Da dalton

BODA bis-o-diynyl arene

TEM transmission electron microscopy
GPC gel permeation chromatography
MWNT multiwalled carbon nanotube
ROP ring-opening polymerization

PCL polycaprolactone

nm nanometer

SCNP single-chain polymer nanoparticle

MMA methyl methacrylate

NMR nuclear magnetic resonance

FeCl₂ iron(II) chloride FeSO₄ iron(II) sulfate

CuCl₂ copper(II) chloride CuSO₄ copper(II) sulfate

ZnCl₂ zinc chloride ZnSO₄ zinc sulfate

BDE bond dissociation energy

CoGEF constrained geometries simulate external force

IPN interpenetrated polymer network

PU polyurethane

TGA thermogravimetric analysis

DTG differential thermogravimetric analysis

AFM atomic force microscopy

SEM scanning electron microscopy

DP degree of polymerization

7. Literature

- 1. Epiotis, N. D. The Theory of Pericyclic Reactions. *Angewandte Chemie International Edition in English*, **1974**, *13*, 751-780. https://doi.org/10.1002/anie.197407511
- Houk, K. N., Li, Y. & Evanseck, J. D. Transition Structures of Hydrocarbon Pericyclic Reactions.
 Angewandte Chemie International Edition in English, 1992, 31, 682-708.
 https://doi.org/10.1002/anie.199206821
- 3. Diels, O. & Alder, K. Synthesen in der Hydroaromatischen Reihe. *Justus Liebigs Annalen der Chemie*, **1928**, *460*, 98-122. https://doi.org/10.1002/jlac.19284600106
- 4. Erden, I. & KauFmann, D. Cycloadditionsreaktionen des Heptafulvalens. *Tetrahedron Letters*, **1981**, *22*, 215-218. https://doi.org/10.1016/0040-4039(81)80058-5
- 5. Beaudry, C. M., Malerich, J. P. & Trauner, D. Biosynthetic and Biomimetic Electrocyclizations. *Chemical Reviews*, **2005**, *105*, 4757-4778. https://doi.org/10.1021/cr0406110
- 6. Miller, L. L., Greisinger, R. & Boyer, R. F. Migratory Aptitudes in a Thermal, Sigmatropic Rearrangement. *Journal of the American Chemical Society*, **1969**, *91*, 1578-1580. https://doi.org/10.1021/ja01034a076
- 7. Mikami, K. & Shimizu, M. Asymmetric Ene Reactions in Organic Synthesis. *Chemical Reviews*, **1992**, *92*, 1021-1050. https://doi.org/10.1021/cr00013a014
- 8. Morgan, K. M. 9 Reaction mechanisms. Part (ii) Pericyclic Reactions. *Annual Reports Section "B"* (Organic Chemistry), **2000**, *96*, 321-345. https://doi.org/10.1039/B0036571
- 9. Mayer, J. & Sondheimer, F. 1,5,9-Tridehydro[14]annulene and Bicyclo[9.3.0]tetradeca-1,5,7,11,13-pentaene-3,9-diyne, an Acetylenic Homolog of Azulene Containing Fused Five- and Eleven-Membered Rings¹. *Journal of the American Chemical Society*, **1966**, 88, 602-603. https://doi.org/10.1021/ja00955a037
- 10. Mayer, J. & Sondheimer, F. 5,6-Benzazulene and Derivatives from Cyclic Polyacetylenes1.

 Journal of the American Chemical Society, 1966, 88, 603-604.

 https://doi.org/10.1021/ja00955a038
- 11. Darby, N., Kim, C. U., Salaün, J. A., Shelton, K. W., Takada, S. & Masamune, S. Concerning the 1,5-Didehydro[10]annulene System. *Journal of the Chemical Society D: Chemical Communications*, **1971**, 1516-1517. https://doi.org/10.1039/C29710001516
- 12. Jones, R. R. & Bergman, R. G. *p*-Benzyne. Generation as an intermediate in a thermal isomerization reaction and trapping evidence for the 1,4-benzenediyl structure. *Journal of the American Chemical Society*, **1972**, *94*, 660-661. https://doi.org/10.1021/ja00757a071
- 13. Mifsud, N., Mellon, V., Perera, K. P. U., Smith, D. W. & Echegoyen, L. In Situ EPR Spectroscopy of Aromatic Diyne Cyclopolymerization. *The Journal of Organic Chemistry*, **2004**, *69*, 6124-6127. https://doi.org/10.1021/jo049198m

- 14. Smith, A. L. & Nicolaou, K. C. The Enediyne Antibiotics. *Journal of Medicinal Chemistry*, **1996**, 39, 2103-2117. https://doi.org/10.1021/jm9600398
- Zein, N., Sinha, A. M., McGahren, W. J. & Ellestad, G. A. Calicheamicin γ₁^I: an Antitumor Antibiotic That Cleaves Double-Stranded DNA Site Specifically. *Science*, 1988, 240, 1198-1201. https://doi.org/10.1126/science.3240341
- Lee, M. D., Dunne, T. S., Siegel, M. M., Chang, C. C., Morton, G. O. & Borders, D. B. Calichemicins, a novel family of antitumor antibiotics.
 Chemistry and partial structure of calichemicin γ₁¹. *Journal of the American Chemical Society*, 1987, 109, 3464-3466. https://doi.org/10.1021/ja00245a050
- Nicolaou, K. C., Hummel, C. W., Nakada, M., Shibayama, K., Pitsinos, E. N., Saimoto, H., Mizuno, Y., Baldenius, K. U. & Smith, A. L. Total synthesis of calicheamicin γ₁^I.
 The final stages. *Journal of the American Chemical Society*, 1993, 115, 7625-7635. https://doi.org/10.1021/ja00070a006
- 18. Konishi, M., Ohkuma, H., Matsumoto, K., Tsuno, T., Kamei, H., Miyaki, T., Oki, T., Kawaguchi, H., VanDuyne, G. D. & Clardy, J. Dynemicin A, a novel antibiotic with the anthraquinone and 1,5-diyn-3-ene subunit. *J Antibiot (Tokyo)*, **1989**, *42*, 1449-1452. https://doi.org/10.7164/antibiotics.42.1449
- Konishi, M., Ohkuma, H., Matsumoto, K., Saitoh, K., Miyaki, T., Oki, T. & Kawaguchi, H. Dynemicins, new antibiotics with the 1,5-diyn-3-ene and anthraquinone subunit. I. Production, isolation and physico-chemical properties. *J Antibiot (Tokyo)*, 1991, 44, 1300-1305. https://doi.org/10.7164/antibiotics.44.1300
- Leet, J. E., Schroeder, D. R., Hofstead, S. J., Golik, J., Colson, K. L., Huang, S., Klohr, S. E., Doyle, T. W. & Matson, J. A. Kedarcidin, a new chromoprotein antitumor antibiotic: structure elucidation of kedarcidin chromophore. *Journal of the American Chemical Society*, 1992, 114, 7946-7948. https://doi.org/10.1021/ja00046a071
- Leet, J. E., Schroeder, D. R., Langley, D. R., Colson, K. L., Huang, S., Klohr, S. E., Lee, M. S., Golik, J. & Hofstead, S. J. Chemistry and structure elucidation of the kedarcidin chromophore.
 Journal of the American Chemical Society, 1993, 115, 8432-8443.
 https://doi.org/10.1021/ja00071a062
- 22. Napier, M. A., Holmquist, B., Strydom, D. J. & Goldberg, I. H. Neocarzinostatin chromophore: purification of the major active form and characterization of its spectral and biological properties. *Biochemistry*, **1981**, *20*, 5602-5608. https://doi.org/10.1021/bi00522a038
- 23. Koide, Y., Ito, A., Edo, K. & Ishida, N. The biologically active site of neocarzinostatin-chromophore. *Chem Pharm Bull (Tokyo)*, **1986**, *34*, 4425-4428. https://doi.org/10.1248/cpb.34.4425
- 24. Nicolaou, K. C. & Dai, W. M. Molecular design and chemical synthesis of potent enediynes. 2. Dynemicin model systems equipped with C-3 triggering devices and evidence for quinone methide

- formation in the mechanism of action of dynemicin-a. *Journal of the American Chemical Society*, **1992**, *114*, 8908-8921. https://doi.org/10.1021/ja00049a023
- 25. Maretina, I. A. Design strategy of enediynes and enyne-allenes. *Russian Journal of General Chemistry*, **2011**, 78, 223-257. https://doi.org/10.1134/s1070363208020126
- 26. Kraka, E. & Cremer, D. Enediynes, enyne-allenes, their reactions, and beyond. *Wiley Interdisciplinary Reviews: Computational Molecular Science*, **2014**, *4*, 285-324. https://doi.org/10.1002/wcms.1174
- 27. Magnus, P. & Fairhurst, R. A. Relative rates of cycloaromatization of dynemicin azabicyclo 7.3.1 enediyne core structures. An unusual change in ΔS^{\ddagger} . *Journal of the Chemical Society-Chemical Communications*, **1994**, 1541-1542. https://doi.org/10.1039/c39940001541
- 28. Schreiner, P. R. Monocyclic enediynes: Relationships between ring sizes, alkyne carbon distances, cyclization barriers, and hydrogen abstraction reactions. Singlet-triplet separations of methyl-substituted p-benzynes. *Journal of the American Chemical Society*, **1998**, *120*, 4184-4190. https://doi.org/10.1021/ja973591a
- Jones, G. B., Wright, J. M., Hynd, G., Wyatt, J. K., Warner, P. M., Huber, R. S., Li, A. W., Kilgore, M. W., Sticca, R. P. & Pollenz, R. S. Oxa-enediynes: Probing the electronic and stereoelectronic contributions to the Bergman cycloaromatization. *Journal of Organic Chemistry*, 2002, 67, 5727-5732. https://doi.org/10.1021/jo0256888
- 30. Plourde, G. W., Warner, P. M., Parrish, D. A. & Jones, G. B. Halo-enediynes: Probing the electronic and stereoelectronic contributions to the Bergman cycloaromatization. *Journal of Organic Chemistry*, **2002**, *67*, 5369-5374. https://doi.org/10.1021/jo025763e
- 31. Klein, M., Walenzyk, T. & König, B. Electronic Effects on the Bergman Cyclisation of Enediynes. A Review. *Collection of Czechoslovak Chemical Communications*, **2004**, *69*, 945-965. https://doi.org/10.1135/cccc20040945
- 32. Treitel, N., Eshdat, L., Sheradsky, T., Donovan, P. M., Tykwinski, R. R., Scott, L. T., Hopf, H. & Rabinovitz, M. Reductive Bergman-type cyclizations of cross-conjugated enediynes to fulvene and fulvalene anions: The role of the substituent. *Journal of the American Chemical Society*, **2006**, *128*, 4703-4709. https://doi.org/10.1021/ja0566477
- 33. Spence, J. D., Rios, A. C., Frost, M. A., McCutcheon, C. M., Cox, C. D., Chavez, S., Fernandez, R. & Gherman, B. F. Syntheses, Thermal Reactivities, and Computational Studies of Aryl-Fused Quinoxalenediynes: Effect of Extended Benzannelation on Bergman Cyclization Energetics. *Journal of Organic Chemistry*, 2012, 77, 10329-10339. https://doi.org/10.1021/jo302009c
- 34. Krupicka, M., Sander, W. & Marx, D. Mechanical Manipulation of Chemical Reactions: Reactivity Switching of Bergman Cyclizations. *J Phys Chem Lett*, **2014**, *5*, 905-909. https://doi.org/10.1021/jz402644e

- 35. Jana, S. & Anoop, A. Effect of π - π interaction in Bergman cyclisation. *Phys Chem Chem Phys*, **2015**, *17*, 29793-29802. https://doi.org/10.1039/c5cp05395a
- 36. Magnus, P. A general strategy using η²Co₂(CO)₆ acetylene complexes for the synthesis of the enediyne antitumor agents esperamicin, calicheamicin, dynemicin and neocarzinostatin. *Tetrahedron*, **1994**, *50*, 1397-1418. https://doi.org/10.1016/s0040-4020(01)80626-8
- 37. Lhermitte, H. & Grierson, D. S. The enediyne and dienediyne based antitumour antibiotics. Methodology and strategies for total synthesis and construction of bioactive analogues. Part 1. *Contemporary Organic Synthesis*, **1996**, *3*, 41-63. https://doi.org/10.1039/co9960300041
- 38. Kim, C. S. & Russell, K. C. Rapid Bergman cyclization of 1,2-diethynylheteroarenes. *Journal of Organic Chemistry*, **1998**, *63*, 8229-8234. https://doi.org/10.1021/jo980879p
- 39. Jones, G. B. & Plourde, G. W. Electronic control of the Bergman cycloaromatization: Synthesis and chemistry of chloroenediynes. *Organic Letters*, **2000**, 2, 1757-1759. https://doi.org/10.1021/ol0059394
- 40. Jones, G. B. & Warner, P. M. Electronic control of the Bergman cyclization: The remarkable role of vinyl substitution. *Journal of the American Chemical Society*, **2001**, *123*, 2134-2145. https://doi.org/10.1021/ja0033032
- 41. Rawat, D. S., Benites, P. J., Incarvito, C. D., Rheingold, A. L. & Zaleski, J. M. The contribution of ligand flexibility to metal center geometry modulated thermal cyclization of conjugated pyridine and quinoline metalloenediynes of copper(I) and copper(II). *Inorganic Chemistry*, **2001**, *40*, 1846-1857. https://doi.org/10.1021/ic0100141
- 42. Basak, A., Bag, S. S. & Bdour, H. M. M. Synthesis and reactivity of enediynyl amino acids and peptides: a novel concept in lowering the activation energy of Bergman cyclisation by H-bonding and electrostatic interactions. *Chemical Communications*, **2003**, 2614-2615. https://doi.org/10.1039/b308976m
- 43. Bhattacharyya, S. & Zaleski, J. M. Metalloenediynes: Advances in the design of thermally and photochemically activated diradical formation for biomedical applications. *Current Topics in Medicinal Chemistry*, **2004**, *4*, 1637-1654. https://doi.org/10.2174/1568026043387403
- 44. Zhao, Z. R., Peng, Y. S., Dalley, N. K., Cannon, J. F. & Peterson, M. A. Bergman cycloaromatization of imidazole-fused enediynes: the remarkable effect of *N*-aryl substitution. *Tetrahedron Letters*, **2004**, *45*, 3621-3624. https://doi.org/10.1016/j.tetlet.2004.02.152
- 45. Zhao, Z. G., Peacock, J. G., Gubler, D. A. & Peterson, M. A. Photoinduced Bergman cycloaromatization of imidazole-fused enediynes. *Tetrahedron Letters*, **2005**, *46*, 1373-1375. https://doi.org/10.1016/j.tetlet.2004.12.136
- Kaiser, J., van Esseveldt, B. C. J., Segers, M. J. A., van Delft, F. L., Smits, J. M. M., Butterworth,
 S. & Rutjes, F. Synthesis and aromatisation of cyclic enediyne-containing amino acids. *Organic & Biomolecular Chemistry*, 2009, 7, 695-705. https://doi.org/10.1039/b815176h

- 47. Pandithavidana, D. R., Poloukhtine, A. & Popik, V. V. Photochemical Generation and Reversible Cycloaromatization of a Nine-Membered Ring Cyclic Enediyne. *Journal of the American Chemical Society*, **2009**, *131*, 351-356. https://doi.org/10.1021/ja8077076
- 48. Ling, F., Li, Z., Zheng, C., Liu, X. & Ma, C. Palladium/copper-catalyzed aerobic intermolecular cyclization of enediyne compounds and alkynes: interrupting cycloaromatization for (4 + 2) cross-benzannulation. *J Am Chem Soc*, **2014**, *136*, 10914-10917. https://doi.org/10.1021/ja506795u
- 49. Wang, C., Chen, S., Zhou, H., Gu, J. & Hu, A. Palladium-catalyzed cycloaromatization polymerization of enediynes. *Chinese Journal of Polymer Science*, **2017**, *36*, 237-243. https://doi.org/10.1007/s10118-018-2088-9
- 50. Bhattacharya, P., Basak, A., Campbell, A. & Alabugin, I. V. Photochemical Activation of Enediyne Warheads: A Potential Tool for Targeted Antitumor Therapy. *Mol Pharm*, **2018**, *15*, 768-797. https://doi.org/10.1021/acs.molpharmaceut.7b00911
- 51. Bhattacharyya, S., Dye, D. F., Pink, M. & Zaleski, J. M. A geometric switching approach toward thermal activation of metalloenediynes. *Chemical Communications*, **2005**, 5295-5297. https://doi.org/10.1039/b509125j
- 52. van Der Velden, V. H., te Marvelde, J. G., Hoogeveen, P. G., Bernstein, I. D., Houtsmuller, A. B., Berger, M. S. & van Dongen, J. J. Targeting of the CD33-calicheamicin immunoconjugate Mylotarg (CMA-676) in acute myeloid leukemia: in vivo and in vitro saturation and internalization by leukemic and normal myeloid cells. *Blood*, **2001**, *97*, 3197-3204. https://doi.org/10.1182/blood.v97.10.3197
- 53. Laszlo, G. S., Estey, E. H. & Walter, R. B. The past and future of CD33 as therapeutic target in acute myeloid leukemia. *Blood Rev*, **2014**, *28*, 143-153. https://doi.org/10.1016/j.blre.2014.04.001
- 54. Buckley, S. A. & Walter, R. B. Antigen-specific immunotherapies for acute myeloid leukemia. *Hematology*, **2015**, *2015*, *584*-595. https://doi.org/10.1182/asheducation-2015.1.584
- 55. Xiao, Y. L. & Hu, A. G. Bergman Cyclization in Polymer Chemistry and Material Science.

 *Macromolecular Rapid Communications, 2011, 32, 1688-1698.

 https://doi.org/10.1002/marc.201100378
- 56. Chen, S. D. & Hu, A. G. Recent advances of the Bergman cyclization in polymer science. *Science China-Chemistry*, **2015**, *58*, 1710-1723. https://doi.org/10.1007/s11426-015-5460-4
- 57. Gaffney, S. M., Capitani, J. F., Castaldo, L. & Mitra, A. Critical distance model for the energy of activation of the Bergman cyclization of enediynes. *International Journal of Quantum Chemistry*, **2003**, *95*, 706-712. https://doi.org/10.1002/qua.10689
- 58. Rawat, D. S. & Zaleski, J. M. Geometric and electronic control of thermal Bergman Cyclization. *Synlett,* **2004**, 393-421. https://doi.org/10.1055/s-2004-815422
- 59. Magnus, P., Fortt, S., Pitterna, T. & Snyder, J. P. Synthetic and mechanistic studies on esperamicin A_1 and calicheamicin γ_1^I . Molecular strain rather than π -bond proximity determines the

- cycloaromatization rates of bicyclo[7.3.1] enediynes. *Journal of the American Chemical Society*, **1990**, *112*, 4986-4987. https://doi.org/10.1021/ja00168a068
- 60. Nicolaou, K. C., Ogawa, Y., Zuccarello, G., Schweiger, E. J. & Kumazawa, T. Cyclic conjugated enediynes related to calicheamicins and esperamicins: calculations, synthesis, and properties.

 Journal of the American Chemical Society, 1988, 110, 4866-4868.

 https://doi.org/10.1021/ja00222a077
- 61. Best, D., Jean, M. & van de Weghe, P. in *Dynemicin A, Uncialamycin and Analogues* (eds Daniel Best, Mickael Jean, & Pierre van de Weghe) 1-70 (Elsevier, 2016). https://doi.org/10.1016/B978-1-78548-150-5.50001-1
- 62. Myers, A. G., Fraley, M. E., Tom, N. J., Cohen, S. B. & Madar, D. J. Synthesis of (+)-dynemicin A and analogs of wide structural variability: establishment of the absolute configuration of natural dynemicin A. *Chemistry & Biology*, **1995**, *2*, 33-43. https://doi.org/10.1016/1074-5521(95)90078-0
- 63. Alabugin, I. V. & Manoharan, M. Thermodynamic and strain effects in the competition between 5-exo-dig and 6-endo-dig cyclizations of vinyl and aryl radicals. *Journal of the American Chemical Society*, **2005**, *127*, 12583-12594. https://doi.org/10.1021/ja052677y
- 64. Alabugin, I., Breiner, B. & Manoharan, M. Cycloaromatization reactions: the testing ground for theory and experiment. *Advances in Physical Organic Chemistry*, **2007**, *42*, 1-33. https://doi.org/10.1016/S0065-3160(07)42001-9
- 65. Prall, M., Wittkopp, A., Fokin, A. A. & Schreiner, P. R. Substituent effects on the Bergman cyclization of (*Z*)-1,5-hexadiyne-3-enes: a systematic computational study. *Journal of Computational Chemistry*, **2001**, *22*, 1605-1614. https://doi.org/10.1002/jcc.1114
- 66. Zeidan, T. A., Kovalenko, S. V., Manoharan, M. & Alabugin, I. V. Ortho Effect in the Bergman Cyclization: Comparison of Experimental Approaches and Dissection of Cycloaromatization Kinetics. *The Journal of Organic Chemistry*, **2006**, *71*, 962-975. https://doi.org/10.1021/jo0520801
- 67. Pickard, Shepherd, R. L., Gillis, A. E., Dunn, M. E., Feldgus, S., Kirschner, K. N., Shields, G. C., Manoharan, M. & Alabugin, I. V. Ortho Effect in the Bergman Cyclization: Electronic and Steric Effects in Hydrogen Abstraction by 1-Substituted Naphthalene 5,8-Diradicals. *The Journal of Physical Chemistry A*, **2006**, *110*, 2517-2526. https://doi.org/10.1021/jp0562835
- 68. Lyapunova, A. G., Danilkina, N. A., Rumyantsev, A. M., Khlebnikov, A. F., Chislov, M. V., Starova, G. L., Sambuk, E. V., Govdi, A. I., Brase, S. & Balova, I. A. Relative Reactivity of Benzothiophene-Fused Enediynes in the Bergman Cyclization. *Journal of Organic Chemistry*, 2018, 83, 2788-2801. https://doi.org/10.1021/acs.joc.7b03258
- 69. Rawat, D. S. & Zaleski, J. M. Syntheses and thermal reactivities of symmetrically and asymmetrically substituted acyclic eneditynes: steric control of Bergman cyclization temperatures. *Chemical Communications*, **2000**, 2493-2494. https://doi.org/10.1039/b0073601

- 70. Jerić, I. & Chen, H.-M. A synthetic route to enediyne-bridged amino acids. *Tetrahedron Letters*, **2007**, *48*, 4687-4690. https://doi.org/10.1016/j.tetlet.2007.05.016
- 71. Gredičak, M., Matanović, I., Zimmermann, B. & Jerić, I. Bergman Cyclization of Acyclic Amino Acid Derived Enediynes Leads to the Formation of 2,3-Dihydrobenzo[f]isoindoles. *The Journal of Organic Chemistry*, **2010**, *75*, 6219-6228. https://doi.org/10.1021/jo101302n
- 72. Kraft, B. J., Coalter, N. L., Nath, M., Clark, A. E., Siedle, A. R., Huffman, J. C. & Zaleski, J. M. Photothermally induced Bergman cyclization of metalloenediynes via near-infrared ligand-to-metal charge-transfer excitation. *Inorganic Chemistry*, **2003**, *42*, 1663-1672. https://doi.org/10.1021/ic0207045
- 73. Li, B. J., Wu, Y. Q., Wang, Y., Zhang, M. S., Chen, H. M., Li, J., Liu, R. H., Ding, Y. & Hu, A. G. Light-Cross-linked Enediyne Small-Molecule Micelle-Based Drug-Delivery System. *Acs Applied Materials & Interfaces*, **2019**, *11*, 8896-8903. https://doi.org/10.1021/acsami.8b22516
- 74. Karpov, G. V. & Popik, V. V. Triggering of the Bergman cyclization by photochemical ring contraction. Facile cycloaromatization of benzannulated cyclodeca-3,7-diene-1,5-diynes. *Journal of the American Chemical Society*, **2007**, *129*, 3792-3793. https://doi.org/10.1021/ja064470q
- 75. Kaya, K., Johnson, M. & Alabugin, I. V. Opening Enediyne Scissors Wider: pH-Dependent DNA Photocleavage by meta-Diyne Lysine Conjugates. *Photochemistry and Photobiology*, **2015**, *91*, 748-758. https://doi.org/10.1111/php.12412
- 76. Song, D. P., Sun, S. Y., Tian, Y., Huang, S., Ding, Y., Yuan, Y. & Hu, A. G. Maleimide-based acyclic enediyne for efficient DNA-cleavage and tumor cell suppression. *Journal of Materials Chemistry B*, **2015**, *3*, 3195-3200. https://doi.org/10.1039/c4tb02018a
- 77. Cambell, I. D. & Eglinton, G. A novel photochemical cyclisation of *o*-bisiodoethynylbenzene to substituted naphthalenes. *Journal of the Chemical Society C: Organic*, **1968**, 2120-2121. https://doi.org/10.1039/J39680002120
- 78. Turro, N. J., Evenzahav, A. & Nicolaou, K. C. Photochemical analogue of the Bergman Cycloaromatization reaction. *Tetrahedron Letters*, **1994**, *35*, 8089-8092. https://doi.org/10.1016/0040-4039(94)88250-9
- 79. Warner, B. P., Millar, S. P., Broene, R. D. & Buchwald, S. L. Controlled Acceleration and Inhibition of Bergman Cyclization by Metal Chlorides. *Science*, **1995**, *269*, 814-816. https://doi.org/10.1126/science.269.5225.814
- 80. O'Connor, J. M., Friese, S. J. & Rodgers, B. L. A Transition-Metal-Catalyzed Enediyne Cycloaromatization. *Journal of the American Chemical Society*, **2005**, *127*, 16342-16343. https://doi.org/10.1021/ja050060a
- 81. Taduri, B. P., Ran, Y.-F., Huang, C.-W. & Liu, R.-S. Platinum-Catalyzed Aromatization of Enediynes via a C-H Bond Insertion of Tethered Alkanes. *Organic Letters*, **2006**, *8*, 883-886. https://doi.org/10.1021/ol052962m

- 82. Jones, G. B., Wright, J. M., Plourde, G. W., Hynd, G., Huber, R. S. & Mathews, J. E. A direct and stereocontrolled route to conjugated enediynes. *Journal of the American Chemical Society*, **2000**, *122*, 1937-1944. https://doi.org/10.1021/ja993766b
- 83. Rawat, D. S. & Zaleski, J. M. Mg²⁺-induced thermal enediyne cyclization at ambient temperature. *Journal of the American Chemical Society*, **2001**, *123*, 9675-9676. https://doi.org/10.1021/ja011215r
- 84. John, J. A. & Tour, J. M. Synthesis of Polyphenylenes and Polynaphthalenes by Thermolysis of Enediynes and Dialkynylbenzenes. *Journal of the American Chemical Society*, **1994**, *116*, 5011-5012. https://doi.org/10.1021/ja00090a066
- 85. Lu, H. T., Ma, H. L., Li, B. J., Zhang, M. S., Chen, H. M., Wang, Y., Li, X. X., Ding, Y. & Hu, A. G. Facilitating Myers-Saito cyclization through acid-triggered tautomerization for the development of maleimide-based antitumor agents. *Journal of Materials Chemistry B*, **2020**, 8, 1971-1979. https://doi.org/10.1039/c9tb02589h
- 86. Kappen, L. S. & Goldberg, I. H. Deoxyribonucleic acid damage by neocarzinostatin chromophore: strand breaks generated by selective oxidation of C-5' of deoxyribose. *Biochemistry*, **1983**, *22*, 4872-4878. https://doi.org/10.1021/bi00290a002
- 87. Saito, I., Kawabata, H., Fujiwara, T., Sugiyama, H. & Matsuura, T. A novel ribose C-4' hydroxylation pathway in neocarzinostatin-mediated degradation of oligonucleotides. *Journal of the American Chemical Society*, **1989**, *111*, 8302-8303. https://doi.org/10.1021/ja00203a054
- 88. Kappen, L. S., Goldberg, I. H., Wu, S. H., Stubbe, J., Worth, L., Jr. & Kozarich, J. W. Isotope effects on the sequence-specific cleavage of dC in d(AGC) sequences by neocarzinostatin: elucidation of chemistry of minor lesions. *Journal of the American Chemical Society*, **1990**, *112*, 2797-2798. https://doi.org/10.1021/ja00163a049
- 89. Frank, B. L., Worth, L., Jr., Christner, D. F., Kozarich, J. W., Stubbe, J., Kappen, L. S. & Goldberg, I. H. Isotope effects on the sequence-specific cleavage of DNA by neocarzinostatin: kinetic partitioning between 4'- and 5'-hydrogen abstraction at unique thymidine sites. *Journal of the American Chemical Society*, **1991**, *113*, 2271-2275. https://doi.org/10.1021/ja00006a054
- 90. Kappen, L. S., Goldberg, I. H., Frank, B. L., Worth, L., Jr., Christner, D. F., Kozarich, J. W. & Stubbe, J. Neocarzinostatin-induced hydrogen atom abstraction from C-4' and C-5' of the T residue at a d(GT) step in oligonucleotides: shuttling between deoxyribose attack sites based on isotope selection effects. *Biochemistry*, **1991**, *30*, 2034-2042. https://doi.org/10.1021/bi00222a005
- 91. Serwer, P. Agarose gels: Properties and use for electrophoresis. *Electrophoresis*, **1983**, *4*, 375-382. https://doi.org/10.1002/elps.1150040602
- 92. Kovalenko, S. V. & Alabugin, I. V. Lysine-enediyne conjugates as photochemically triggered DNA double-strand cleavage agents. *Chemical Communications*, **2005**, 1444-1446. https://doi.org/10.1039/B417012A

- 93. Haward, R. N. The termination of biradicals in a polymerizing system. *Transactions of the Faraday Society*, **1950**, *46*, 204-210. https://doi.org/10.1039/TF9504600204
- 94. Rule, J. D., Wilson, S. R. & Moore, J. S. Radical Polymerization Initiated by Bergman Cyclization. *Journal of the American Chemical Society*, **2003**, *125*, 12992-12993. https://doi.org/10.1021/ja0359198
- 95. Rule, J. D. & Moore, J. S. Polymerizations Initiated by Diradicals from Cycloaromatization Reactions. *Macromolecules*, **2005**, *38*, 7266-7273. https://doi.org/10.1021/ma050750z
- 96. Gerstel, P. & Barner-Kowollik, C. RAFT Mediated Polymerization of Methyl Methacrylate Initiated by Bergman Cyclization: Access to High Molecular Weight Narrow Polydispersity Polymers. *Macromolecular Rapid Communications*, **2011**, *32*, 444-450. https://doi.org/10.1002/marc.201000730
- 97. Egbedina, A. O., Bolade, O. P., Ewuzie, U. & Lima, E. C. Emerging trends in the application of carbon-based materials: A review. *Journal of Environmental Chemical Engineering*, **2022**, *10*, 107260. https://doi.org/10.1016/j.jece.2022.107260
- 98. Ostojic, G. N., Ireland, J. R. & Hersam, M. C. Noncovalent Functionalization of DNA-Wrapped Single-Walled Carbon Nanotubes with Platinum-Based DNA Cross-Linkers. *Langmuir*, **2008**, *24*, 9784-9789. https://doi.org/10.1021/la801311j
- 99. Isci, R., Baysak, E., Kesan, G., Minofar, B., Eroglu, M. S., Duygulu, O., Gorkem, S. F. & Ozturk, T. Non-covalent modification of single wall carbon nanotubes (SWCNTs) by thienothiophene derivatives. *Nanoscale*, **2022**, *14*, 16602-16610. https://doi.org/10.1039/D2NR04582F
- 100. Gao, C., He, H., Zhou, L., Zheng, X. & Zhang, Y. Scalable Functional Group Engineering of Carbon Nanotubes by Improved One-Step Nitrene Chemistry. *Chemistry of Materials*, **2009**, *21*, 360-370. https://doi.org/10.1021/cm802704c
- 101. Kumar, I., Rana, S. & Cho, J. W. Cycloaddition Reactions: A Controlled Approach for Carbon Nanotube Functionalization. *Chemistry-A European Journal*, 2011, 17, 11092-11101. https://doi.org/10.1002/chem.201101260
- 102. Chronopoulos, D., Karousis, N., Ichihashi, T., Yudasaka, M., Iijima, S. & Tagmatarchis, N. Benzyne cycloaddition onto carbon nanohorns. *Nanoscale*, **2013**, *5*, 6388-6394. https://doi.org/10.1039/C3NR01755A
- 103. Goldsmith, B. R., Coroneus, J. G., Khalap, V. R., Kane, A. A., Weiss, G. A. & Collins, P. G. Conductance-Controlled Point Functionalization of Single-Walled Carbon Nanotubes. *Science*, **2007**, *315*, 77-81. https://doi.org/10.1126/science.1135303
- 104. Kooi, S. E., Schlecht, U., Burghard, M. & Kern, K. Electrochemical Modification of Single Carbon Nanotubes. *Angewandte Chemie International Edition*, **2002**, *41*, 1353-1355. https://doi.org/10.1002/1521-3773(20020415)41:8<1353::AID-ANIE1353>3.0.CO;2-I

- 105. Chakrabarti, M. H., Low, C. T. J., Brandon, N. P., Yufit, V., Hashim, M. A., Irfan, M. F., Akhtar, J., Ruiz-Trejo, E. & Hussain, M. A. Progress in the electrochemical modification of graphene-based materials and their applications. *Electrochimica Acta*, 2013, 107, 425-440. https://doi.org/10.1016/j.electacta.2013.06.030
- 106. Valentini, L., Puglia, D., Armentano, I. & Kenny, J. M. Sidewall functionalization of single-walled carbon nanotubes through CF₄ plasma treatment and subsequent reaction with aliphatic amines. *Chemical Physics Letters*, **2005**, *403*, 385-389. https://doi.org/10.1016/j.cplett.2005.01.042
- 107. Shi, D., Guo, Y., Dong, Z., Lian, J., Wang, W., Liu, G., Wang, L. & Ewing, R. C. Quantum-Dot-Activated Luminescent Carbon Nanotubes via a Nano Scale Surface Functionalization for in vivo Imaging. *Advanced Materials*, **2007**, *19*, 4033-4037. https://doi.org/10.1002/adma.200700035
- 108. Chattopadhyay, J., Chakraborty, S., Mukherjee, A., Wang, R., Engel, P. S. & Billups, W. E. SET Mechanism in the Functionalization of Single-Walled Carbon Nanotubes. *The Journal of Physical Chemistry C*, **2007**, *111*, 17928-17932. https://doi.org/10.1021/jp071746n
- 109. Homenick, C. M., Lawson, G. & Adronov, A. Polymer Grafting of Carbon Nanotubes Using Living Free-Radical Polymerization. *Polymer Reviews*, **2007**, *47*, 265-290. https://doi.org/10.1080/15583720701271237
- 110. Li, Y., Wang, Y., Liu, Y. & Zhao, Y. Clean Modification of Carbon-Based Materials Using Hydroxyl Radicals and Preliminary Study on Gaseous Elemental Mercury Removal. *Energy & Fuels*, **2023**, *37*, 5953-5960. https://doi.org/10.1021/acs.energyfuels.2c04172
- 111. Rettenbacher, A. S., Perpall, M. W., Echegoyen, L., Hudson, J. & Smith, D. W. Radical Addition of a Conjugated Polymer to Multilayer Fullerenes (Carbon Nano-onions). *Chemistry of Materials*, **2007**, *19*, 1411-1417. https://doi.org/10.1021/cm0626132
- 112. Ma, J. G., Cheng, X., Ma, X. W., Deng, S. & Hu, A. G. Functionalization of Multiwalled Carbon Nanotubes with Polyesters via Bergman Cyclization and "Grafting from" Strategy. *Journal of Polymer Science Part A-Polymer Chemistry*, **2010**, 48, 5541-5548. https://doi.org/10.1002/pola.24365
- 113. Ma, J. G., Deng, S., Cheng, X., Wei, W. & Hu, A. G. Covalent Surface Functionalization of Multiwalled Carbon Nanotubes Through Bergman Cyclization of Enediyne-Containing Dendrimers. *Journal of Polymer Science Part A-Polymer Chemistry*, 2011, 49, 3951-3959. https://doi.org/10.1002/pola.24834
- 114. Ma, X. W., Li, F., Wang, Y. F. & Hu, A. G. Functionalization of Pristine Graphene with Conjugated Polymers through Diradical Addition and Propagation. *Chemistry-An Asian Journal*, **2012**, 7, 2547-2550. https://doi.org/10.1002/asia.201200520
- 115. Cheng, X., Ma, J. G., Zhi, J., Yang, X. & Hu, A. G. Synthesis of Novel "Rod-Coil" Brush Polymers with Conjugated Backbones through Bergman Cyclization. *Macromolecules*, **2010**, *43*, 909-913. https://doi.org/10.1021/ma902176j

- 116. Sun, S. Y., Zhu, C. C., Song, D. P., Li, F. & Hu, A. G. Preparation of conjugated polyphenylenes from maleimide-based enediynes through thermal-triggered Bergman cyclization polymerization. *Polymer Chemistry*, **2014**, *5*, 1241-1247. https://doi.org/10.1039/c3py00970j
- 117. Sun, S. Y., Dong, L. H., Song, D. P., Huang, B. L. & Hu, A. G. Synthesis of Polyphenylenes through Bergman Cyclization of Enediynes with Long Chain Alkyl Groups. *Chinese Journal of Polymer Science*, **2015**, *33*, 184-191. https://doi.org/10.1007/s10118-015-1566-6
- 118. Miao, C. C., Zhi, J., Sun, S. Y., Yang, X. & Hu, A. G. Formation of Conjugated Polynaphthalene via Bergman Cyclization. *Journal of Polymer Science Part a-Polymer Chemistry*, **2010**, *48*, 2187-2193. https://doi.org/10.1002/pola.23988
- 119. Sun, Q., Zhang, C., Li, Z. W., Kong, H. H., Tan, Q. G., Hu, A. G. & Xu, W. On-Surface Formation of One-Dimensional Polyphenylene through Bergman Cyclization. *Journal of the American Chemical Society*, **2013**, *135*, 8448-8451. https://doi.org/10.1021/ja404039t
- 120. Sun, S. Y., Huang, B. L., Li, F., Song, D. P. & Hu, A. G. Synthesis of Chiral Polyphenylenes through Bergman Cyclization of Enediynes with Pendant Chiral Amino Ester Groups. *Chinese Journal of Polymer Science*, **2015**, *33*, 743-753. https://doi.org/10.1007/s10118-015-1622-2
- 121. Yang, X., Li, Z. W., Zhi, J. A., Ma, J. G. & Hu, A. G. Synthesis of Ultrathin Mesoporous Carbon through Bergman Cyclization of Enediyne Self-Assembled Monolayers in SBA-15. *Langmuir*, **2010**, *26*, 11244-11248. https://doi.org/10.1021/la1005727
- 122. Li, Z. W., Song, D. P., Zhi, J. & Hu, A. G. Synthesis of Ultrathin Ordered Porous Carbon through Bergman Cyclization of Enediyne Self-Assembled Monolayers on Silica Nanoparticles. *Journal of Physical Chemistry C*, **2011**, *115*, 15829-15833. https://doi.org/10.1021/jp203393v
- 123. Li, Z. W., Zhu, X. J., Chen, S. D. & Hu, A. G. Coating Magnetite Nanoparticles with a Polyaryl Monolayer through Bergman Cyclization-Mediated Polymerization. *Chemistry-An Asian Journal*, **2013**, *8*, 560-563. https://doi.org/10.1002/asia.201201132
- 124. Singh, R. & Lillard, J. W. Nanoparticle-based targeted drug delivery. *Experimental and Molecular Pathology*, **2009**, *86*, 215-223. https://doi.org/10.1016/j.yexmp.2008.12.004
- 125. Truong, N. P., Whittaker, M. R., Mak, C. W. & Davis, T. P. The importance of nanoparticle shape in cancer drug delivery. *Expert Opinion on Drug Delivery*, **2015**, *12*, 129-142. https://doi.org/10.1517/17425247.2014.950564
- 126. Hui, Y., Yi, X., Hou, F., Wibowo, D., Zhang, F., Zhao, D., Gao, H. & Zhao, C.-X. Role of Nanoparticle Mechanical Properties in Cancer Drug Delivery. *ACS Nano*, **2019**, *13*, 7410-7424. https://doi.org/10.1021/acsnano.9b03924
- 127. Astruc, D. Introduction: Nanoparticles in Catalysis. *Chemical Reviews*, **2020**, *120*, 461-463. https://doi.org/10.1021/acs.chemrev.8b00696
- 128.Xie, C., Niu, Z., Kim, D., Li, M. & Yang, P. Surface and Interface Control in Nanoparticle Catalysis. *Chemical Reviews*, **2020**, *120*, 1184-1249. https://doi.org/10.1021/acs.chemrev.9b00220

- 129. Boghossian, A. A., Sen, F., Gibbons, B. M., Sen, S., Faltermeier, S. M., Giraldo, J. P., Zhang, C. T., Zhang, J., Heller, D. A. & Strano, M. S. Application of Nanoparticle Antioxidants to Enable Hyperstable Chloroplasts for Solar Energy Harvesting. *Advanced Energy Materials*, 2013, 3, 881-893. https://doi.org/10.1002/aenm.201201014
- 130. Yang, Y., Han, J., Huang, J., Sun, J., Wang, Z. L., Seo, S. & Sun, Q. Stretchable Energy-Harvesting Tactile Interactive Interface with Liquid-Metal-Nanoparticle-Based Electrodes. *Advanced Functional Materials*, **2020**, *30*, 1909652. https://doi.org/10.1002/adfm.201909652
- 131. Sanchez-Sanchez, A., Pérez-Baena, I. & Pomposo, J. A. Advances in Click Chemistry for Single-Chain Nanoparticle Construction. *Molecules*, **2013**, *18*, 3339-3355. https://doi.org/10.3390/molecules18033339
- 132. Perez-Baena, I., Asenjo-Sanz, I., Arbe, A., Moreno, A. J., Lo Verso, F., Colmenero, J. & Pomposo, J. A. Efficient Route to Compact Single-Chain Nanoparticles: Photoactivated Synthesis via Thiol-Yne Coupling Reaction. *Macromolecules*, 2014, 47, 8270-8280. https://doi.org/10.1021/ma5017133
- 133. Jiang, X., Pu, H. & Wang, P. Polymer nanoparticles via intramolecular crosslinking of sulfonyl azide functionalized polymers. *Polymer*, **2011**, *52*, 3597-3602. https://doi.org/10.1016/j.polymer.2011.05.054
- 134. Croce, T. A., Hamilton, S. K., Chen, M. L., Muchalski, H. & Harth, E. Alternative *o*-Quinodimethane Cross-Linking Precursors for Intramolecular Chain Collapse Nanoparticles. *Macromolecules*, **2007**, *40*, 6028-6031. https://doi.org/10.1021/ma071111m
- 135. Ergin, M., Kiskan, B., Gacal, B. & Yagci, Y. Thermally Curable Polystyrene via Click Chemistry. *Macromolecules*, **2007**, *40*, 4724-4727. https://doi.org/10.1021/ma070549j
- 136. Mecerreyes, D., Lee, V., Hawker, C. J., Hedrick, J. L., Wursch, A., Volksen, W., Magbitang, T., Huang, E. & Miller, R. D. A Novel Approach to Functionalized Nanoparticles: Self-Crosslinking of Macromolecules in Ultradilute Solution. *Advanced Materials*, **2001**, *13*, 204-208. https://doi.org/10.1002/1521-4095(200102)13:3%3C204::AID-ADMA204%3E3.0.CO;2-9
- 137. Zhu, B. C., Ma, J. G., Li, Z. W., Hou, J., Cheng, X., Qian, G. N., Liu, P. & Hu, A. G. Formation of polymeric nanoparticles via Bergman cyclization mediated intramolecular chain collapse. *Journal of Materials Chemistry*, **2011**, *21*, 2679-2683. https://doi.org/10.1039/c0jm03143g
- 138. Zhu, B. C., Qian, G. N., Xiao, Y. L., Deng, S., Wang, M. & Hu, A. G. A Convergence of Photo-Bergman Cyclization and Intramolecular Chain Collapse Towards Polymeric Nanoparticles. *Journal of Polymer Science Part A-Polymer Chemistry*, 2011, 49, 5330-5338. https://doi.org/10.1002/pola.25013
- 139. Nicolaou, K. C., Smith, A. L. & Yue, E. W. Chemistry and biology of natural and designed enediynes. *Proceedings of the National Academy of Sciences*, **1993**, *90*, 5881-5888. https://doi.org/10.1073/pnas.90.13.5881

- 140. Ren, F., Hogan, P. C., Anderson, A. J. & Myers, A. G. Kedarcidin Chromophore: Synthesis of Its Proposed Structure and Evidence for a Stereochemical Revision. *Journal of the American Chemical Society*, **2007**, *129*, 5381-5383. https://doi.org/10.1021/ja071205b
- 141. Tokiwa, Y., Miyoshi-Saitoh, M., Kobayashi, H., Sunaga, R., Konishi, M., Oki, T. & Iwasaki, S. Biosynthesis of dynemicin A, a 3-ene-1,5-diyne antitumor antibiotic. *Journal of the American Chemical Society*, **1992**, *114*, 4107-4110. https://doi.org/10.1021/ja00037a011
- 142. Zein, N., Poncin, M., Nilakantan, R. & Ellestad, G. A. Calicheamicin γ₁^I and DNA: Molecular Recognition Process Responsible for Site-Specificity. *Science*, 1989, 244, 697-699. https://doi.org/10.1126/science.2717946
- 143. Walker, S., Landovitz, R., Ding, W. D., Ellestad, G. A. & Kahne, D. Cleavage behavior of calicheamicin γ^I and calicheamicin T. *Proceedings of the National Academy of Sciences*, **1992**, 89, 4608-4612. https://doi.org/10.1073/pnas.89.10.4608
- 144. Ikemoto, N., Kumar, R. A., Ling, T. T., Ellestad, G. A., Danishefsky, S. J. & Patel, D. J. Calicheamicin-DNA complexes: warhead alignment and saccharide recognition of the minor groove. *Proceedings of the National Academy of Sciences*, **1995**, *92*, 10506-10510. https://doi.org/10.1073/pnas.92.23.10506
- 145. Nicolaou, K. C., Hale, C. R. H. & Nilewski, C. A Total Synthesis Trilogy: Calicheamicin γ_1^I , Taxol®, and Brevetoxin A. *The Chemical Record*, **2012**, *12*, 407-441. https://doi.org/10.1002/tcr.201200005
- 146. Dasari, S. & Bernard Tchounwou, P. Cisplatin in cancer therapy: Molecular mechanisms of action. *European Journal of Pharmacology*, **2014**, 740, 364-378. https://doi.org/10.1016/j.ejphar.2014.07.025
- 147. Basak, A., Mandal, S. & Bag, S. S. Chelation-Controlled Bergman Cyclization: Synthesis and Reactivity of Enediynyl Ligands. *Chemical Reviews*, **2003**, *103*, 4077-4094. https://doi.org/10.1021/cr020069k
- 148. Benites, P. J., Rawat, D. S. & Zaleski, J. M. Metalloenediynes: Ligand field control of thermal Bergman cyclization reactions. *Journal of the American Chemical Society*, **2000**, *122*, 7208-7217. https://doi.org/10.1021/ja0017918
- 149. Coalter, N. L., Concolino, T. E., Streib, W. E., Hughes, C. G., Rheingold, A. L. & Zaleski, J. M. Structure and thermal reactivity of a novel Pd(0) metalloenediyne. *Journal of the American Chemical Society*, **2000**, *122*, 3112-3117. https://doi.org/10.1021/ja9944094
- 150. Chandra, T., Pink, M. & Zaleski, J. M. Macrocyclic metalloenediynes of Cu(II) and Zn(II): A thermal reactivity comparison. *Inorganic Chemistry*, 2001, 40, 5878-5885. https://doi.org/10.1021/ic010424

- 151. Schmitt, E. W., Huffman, J. C. & Zaleski, J. M. Thermal reactivities of isostructural d¹⁰ metalloenediynes: metal-dependent Bergman cyclization. *Chemical Communications*, 2001, 167-168. https://doi.org/10.1039/b008337m
- 152. Benites, P. J., Holmberg, R. C., Rawat, D. S., Kraft, B. J., Klein, L. J., Peters, D. G., Thorp, H. H. & Zaleski, J. M. Metal-ligand charge-transfer-promoted photoelectronic Bergman cyclization of copper metalloenediynes: photochemical DNA cleavage via C-4' H-atom abstraction. *Journal of the American Chemical Society*, 2003, 125, 6434-6446. https://doi.org/10.1021/ja020939f
- 153. Bhattacharyya, S., Clark, A. E., Pink, M. & Zaleski, J. M. Isolation of electronic from geometric contributions to Bergman cyclization of metalloenediynes. *Chemical Communications*, **2003**, 1156-1157. https://doi.org/10.1039/b301690k
- 154. Chandra, T., Kraft, B. J., Huffman, J. C. & Zaleski, J. M. Synthesis and structural characterization of porphyrinic enediynes: Geometric and electronic effects on thermal and photochemical reactivity. *Inorganic Chemistry*, **2003**, *42*, 5158-5172. https://doi.org/10.1021/ic030035a
- 155. Clark, A. E., Davidson, E. R. & Zaleski, J. M. A TDDFT description of the low-energy excited states of copper and zinc metalloenediynes. *Chemical Communications*, **2003**, 2876-2877. https://doi.org/10.1039/b308633j
- 156. Nath, M., Huffman, J. C. & Zaleski, J. M. Ambient temperature activation of haloporphyrinic-enediynes: Electronic contributions to Bergman Cycloaromatization. *Journal of the American Chemical Society*, **2003**, *125*, 11484-11485. https://doi.org/10.1021/ja0302782
- 157. Nath, M., Huffman, J. C. & Zaleski, J. M. Accelerated Bergman Cyclization of Porphyrinic-enediynes. *Chemical Communications*, **2003**, 858-859. https://doi.org/10.1039/b212923j
- 158. Bhattacharyya, S., Pink, M., Huffman, J. C. & Zaleski, J. M. Thioether coordinated metalloenediynes: Syntheses, structures and thermal reactivity comparison. *Polyhedron*, **2006**, *25*, 550-558. https://doi.org/10.1016/j.poly.2005.07.032
- 159. Bhattacharyya, S., Clark, A. E., Pink, M. & Zaleski, J. M. Structure Modulated Electronic Contributions to Metalloenediyne Reactivity: Synthesis and Thermal Bergman Cyclization of MLX2 Compounds. *Inorganic Chemistry*, 2009, 48, 3916-3925. https://doi.org/10.1021/ic8011164
- 160. Clark, A. E., Bhattacharryya, S. & Zaleski, J. M. Density Functional Analysis of Ancillary Ligand Electronic Contributions to Metal-Mediated Enediyne Cyclization. *Inorganic Chemistry*, 2009, 48, 3926-3933. https://doi.org/10.1021/ic801117m
- 161. Nath, M., Pink, M. & Zaleski, J. M. PtCl₂-catalyzed benzannulation of nickel(II) 2,3-dialkynylporphyrins to form unusual phenanthroporphyrins. *Journal of Organometallic Chemistry*, **2011**, 696, 4152-4157. https://doi.org/10.1016/j.jorganchem.2011.07.008
- 162. Walker, J. M., Gou, L. F., Bhattacharyya, S., Lindahl, S. E. & Zaleski, J. M. Photothermal Plasmonic Triggering of Au Nanoparticle Surface Radical Polymerization. *Chemistry of Materials*, **2011**, *23*, 5275-5281. https://doi.org/10.1021/cm202741p

- 163. Boerner, L. J. K., Dye, D. F., Kopke, T. & Zaleski, J. M. Expansion and contraction: Shaping the porphyrin boundary via diradical reactivity. *Coordination Chemistry Reviews*, **2013**, *257*, 599-620. https://doi.org/10.1016/j.ccr.2012.07.009
- 164. Lindahl, S. E., Park, H., Pink, M. & Zaleski, J. M. Utilizing Redox-Mediated Bergman Cyclization toward the Development of Dual-Action Metalloenediyne Therapeutics. *Journal of the American Chemical Society*, 2013, 135, 3826-3833. https://doi.org/10.1021/ja308190q
- 165. Porter, M. R., Kochi, A., Karty, J. A., Lim, M. H. & Zaleski, J. M. Chelation-induced diradical formation as an approach to modulation of the amyloid-beta aggregation pathway. *Chemical Science*, **2015**, *6*, 1018-1026. https://doi.org/10.1039/c4sc01979b
- 166. Walker, J. M. & Zaleski, J. M. Magnetically Triggered Radical-Generating Fe₃O₄ Nanoparticles for Biopolymer Restructuring: Application to the Extracellular Matrix. *Chemistry of Materials*, **2015**, *27*, 8448-8456. https://doi.org/10.1021/acs.chemmater.5b04134
- 167. Porter, M. R. & Zaleski, J. M. The role of ligand covalency in the selective activation of metalloenediynes for Bergman cyclization. *Polyhedron*, 2016, 103, 187-195. https://doi.org/10.1016/j.poly.2015.10.041
- 168. Porter, M. R., Lindahl, S. E., Lietzke, A., Metzger, E. M., Wang, Q., Henck, E., Chen, C. H., Niu, H. Y. & Zaleski, J. M. Metal-mediated diradical tuning for DNA replication arrest via template strand scission. *Proceedings of the National Academy of Sciences of the United States of America*, 2017, 114, E7405-E7414. https://doi.org/10.1073/pnas.1621349114
- 169. Kirschner, K. M., Ratvasky, S. C., Pink, M. & Zaleski, J. M. Anion Control of Lanthanoenediyne Cyclization. *Inorganic Chemistry*, **2019**, *58*, 9225-9235. https://doi.org/10.1021/acs.inorgchem.9b00856
- 170. Porter, M. R., Walker, J. M. & Zaleski, J. M. The Outliers: Metal-Mediated Radical Reagents for Biological Substrate Degradation. *Accounts of Chemical Research*, **2019**, *52*, 1957-1967. https://doi.org/10.1021/acs.accounts.9b00185
- 171. Garrett, J. E., Metzger, E., Schmitt, K., Soto, S., Northern, S., Kryah, L., Irfan, M., Rice, S., Brown, M., Zaleski, J. M. & Dynlacht, J. R. Enhancement of Cytotoxicity of Enediyne Compounds by Hyperthermia: Effects of Various Metal Complexes on Tumor Cells. *Radiation Research*, 2020, 193, 107-118. https://doi.org/10.1667/rr15433.1
- 172. Li, J., Nagamani, C. & Moore, J. S. Polymer mechanochemistry: from destructive to productive. *Acc Chem Res*, **2015**, *48*, 2181-2190. https://doi.org/10.1021/acs.accounts.5b00184
- 173. Davis, D. A., Hamilton, A., Yang, J., Cremar, L. D., Van Gough, D., Potisek, S. L., Ong, M. T., Braun, P. V., Martinez, T. J., White, S. R., Moore, J. S. & Sottos, N. R. Force-induced activation of covalent bonds in mechanoresponsive polymeric materials. *Nature*, **2009**, *459*, 68-72. https://doi.org/10.1038/nature07970

- 174. Kryger, M. J., Ong, M. T., Odom, S. A., Sottos, N. R., White, S. R., Martinez, T. J. & Moore, J. S. Masked Cyanoacrylates Unveiled by Mechanical Force. *Journal of the American Chemical Society*, **2010**, *132*, 4558-4559. https://doi.org/10.1021/ja1008932
- 175. Black, A. L., Orlicki, J. A. & Craig, S. L. Mechanochemically triggered bond formation in solid-state polymers. *Journal of Materials Chemistry*, **2011**, *21*, 8460-8465. https://doi.org/10.1039/c0jm03875j
- 176. Klukovich, H. M., Kean, Z. S., Iacono, S. T. & Craig, S. L. Mechanically Induced Scission and Subsequent Thermal Remending of Perfluorocyclobutane Polymers. *Journal of the American Chemical Society*, **2011**, *133*, 17882-17888. https://doi.org/10.1021/ja2074517
- 177. Chen, Y., Spiering, A. J. H., Karthikeyan, S., Peters, G. W. M., Meijer, E. W. & Sijbesma, R. P. Mechanically induced chemiluminescence from polymers incorporating a 1,2-dioxetane unit in the main chain. *Nature Chemistry*, **2012**, *4*, 559-562. https://doi.org/10.1038/nchem.1358
- 178. Song, Y.-K., Lee, K.-H., Hong, W.-S., Cho, S.-Y., Yu, H.-C. & Chung, C.-M. Fluorescence sensing of microcracks based on cycloreversion of a dimeric anthracene moiety. *Journal of Materials Chemistry*, **2012**, *22*, 1380-1386. https://doi.org/10.1039/C1JM13709C
- 179. Larsen, M. B. & Boydston, A. J. "Flex-Activated" Mechanophores: Using Polymer Mechanochemistry to Direct Bond Bending Activation. *Journal of the American Chemical Society*, **2013**, *135*, 8189-8192. https://doi.org/10.1021/ja403757p
- 180. Lee, C. K., Beiermann, B. A., Silberstein, M. N., Wang, J., Moore, J. S., Sottos, N. R. & Braun, P. V. Exploiting Force Sensitive Spiropyrans as Molecular Level Probes. *Macromolecules*, 2013, 46, 3746-3752. https://doi.org/10.1021/ma4005428
- 181. Lenhardt, J. M., Ong, M. T., Choe, R., Evenhuis, C. R., Martinez, T. J. & Craig, S. L. Trapping a Diradical Transition State by Mechanochemical Polymer Extension. *Science*, 2010, 329, 1057-1060. https://doi.org/10.1126/science.1193412
- 182. Encina, M. V., Lissi, E., Sarasúa, M., Gargallo, L. & Radic, D. Ultrasonic degradation of polyvinylpyrrolidone: Effect of peroxide linkages. *Journal of Polymer Science: Polymer Letters Edition*, 1980, 18, 757-760. https://doi.org/10.1002/pol.1980.130181201
- 183. Berkowski, K. L., Potisek, S. L., Hickenboth, C. R. & Moore, J. S. Ultrasound-Induced Site-Specific Cleavage of Azo-Functionalized Poly(ethylene glycol). *Macromolecules*, 2005, 38, 8975-8978. https://doi.org/10.1021/ma051394n
- 184. Shiraki, T., Diesendruck, C. E. & Moore, J. S. The mechanochemical production of phenyl cations through heterolytic bond scission. *Faraday Discussions*, **2014**, *170*, 385-394. https://doi.org/10.1039/C4FD00027G
- 185. Kersey, F. R., Yount, W. C. & Craig, S. L. Single-Molecule Force Spectroscopy of Bimolecular Reactions: System Homology in the Mechanical Activation of Ligand Substitution Reactions.

- Journal of the American Chemical Society, **2006**, 128, 3886-3887. https://doi.org/10.1021/ja058516b
- 186. Karthikeyan, S., Potisek, S. L., Piermattei, A. & Sijbesma, R. P. Highly Efficient Mechanochemical Scission of Silver-Carbene Coordination Polymers. *Journal of the American Chemical Society*, **2008**, *130*, 14968-14969. https://doi.org/10.1021/ja806887k
- 187. Paulusse, J. M. J. & Sijbesma, R. P. Selectivity of mechanochemical chain scission in mixed palladium(II) and platinum(II) coordination polymers. *Chemical Communications*, **2008**, 4416-4418. https://doi.org/10.1039/B806978F
- 188. Piermattei, A., Karthikeyan, S. & Sijbesma, R. P. Activating catalysts with mechanical force. *Nature Chemistry*, **2009**, *I*, 133-137. https://doi.org/10.1038/nchem.167
- 189. Lenhardt, J. M., Black, A. L. & Craig, S. L. gem-Dichlorocyclopropanes as Abundant and Efficient Mechanophores in Polybutadiene Copolymers under Mechanical Stress. Journal of the American Chemical Society, 2009, 131, 10818-10819. https://doi.org/10.1021/ja9036548
- 190. Klukovich, H. M., Kean, Z. S., Ramirez, A. L. B., Lenhardt, J. M., Lin, J., Hu, X. & Craig, S. L. Tension Trapping of Carbonyl Ylides Facilitated by a Change in Polymer Backbone. *Journal of the American Chemical Society*, **2012**, *134*, 9577-9580. https://doi.org/10.1021/ja302996n
- 191. Ghanem, M. A., Basu, A., Behrou, R., Boechler, N., Boydston, A. J., Craig, S. L., Lin, Y., Lynde, B. E., Nelson, A., Shen, H. & Storti, D. W. The role of polymer mechanochemistry in responsive materials and additive manufacturing. *Nature Reviews Materials*, 2020, 6, 84-98. https://doi.org/10.1038/s41578-020-00249-w
- 192. Snyder, J. P. The cyclization of calicheamicin-esperamicin analogs: A predictive biradicaloid transition-state. *Journal of the American Chemical Society*, **1989**, *111*, 7630-7632. https://doi.org/10.1021/ja00201a063
- 193. Mohamed, R. K., Peterson, P. W. & Alabugin, I. V. Concerted Reactions That Produce Diradicals and Zwitterions: Electronic, Steric, Conformational, and Kinetic Control of Cycloaromatization Processes. *Chemical Reviews*, 2013, 113, 7089-7129. https://doi.org/10.1021/cr4000682
- 194. Nicolaou, K. C., Zuccarello, G., Riemer, C., Estevez, V. A. & Dai, W. M. Design, synthesis, and study of simple monocyclic conjugated enediynes. The 10-membered ring enediyne moiety of the enediyne anticancer antibiotics. *Journal of the American Chemical Society*, **1992**, *114*, 7360-7371. https://doi.org/10.1021/ja00045a005
- 195. Hickenboth, C. R., Rule, J. D. & Moore, J. S. Preparation of enediyne-crosslinked networks and their reactivity under thermal and mechanical conditions. *Tetrahedron*, **2008**, *64*, 8435-8448. https://doi.org/10.1016/j.tet.2008.04.106
- 196. Evenzahav, A. & Turro, N. J. Photochemical rearrangement of enediynes: Is a "photo-Bergman" cyclization a possibility? *Journal of the American Chemical Society*, **1998**, *120*, 1835-1841. https://doi.org/10.1021/ja9722943

- 197. Sperling, L. H. in *Interpenetrating Polymer Networks* Vol. 239 *Advances in Chemistry Series* (eds D. Klempner, L. H. Sperling, & L. A. Utracki) 3-38 (1994). https://pubs.acs.org/doi/10.1021/ba-1994-0239.ch001
- 198. Sperling, L. H. & Mishra, V. The current status of interpenetrating polymer networks. *Polymers for Advanced Technologies*, **1996**, 7, 197-208. <a href="https://doi.org/10.1002/(sici)1099-1581(199604)7:4<197::Aid-pat514>3.0.Co;2-4">https://doi.org/10.1002/(sici)1099-1581(199604)7:4<197::Aid-pat514>3.0.Co;2-4
- 199. Millar, J. R. 263. Interpenetrating polymer networks. Styrene-divinylbenzene copolymers with two and three interpenetrating networks, and their sulphonates. *Journal of the Chemical Society* (*Resumed*), **1960**, 1311-1317. https://doi.org/10.1039/JR9600001311
- 200. Sperling, L. H. Recent advances in interpenetrating polymer networks. *Polymer Engineering & Science*, **1985**, *25*, 517-520. https://doi.org/10.1002/pen.760250902
- 201. Sperling, L. H. Interpenetrating polymer networks and related materials. *Journal of Polymer Science: Macromolecular Reviews*, **1977**, *12*, 141-180. https://doi.org/10.1002/pol.1977.230120103
- 202. Dragan, E. S. Design and applications of interpenetrating polymer network hydrogels. A review. *Chemical Engineering Journal*, **2014**, *243*, 572-590. https://doi.org/10.1016/j.cej.2014.01.065
- 203. Silverstein, M. S. Interpenetrating polymer networks: So happy together? *Polymer*, **2020**, *207* https://doi.org/10.1016/j.polymer.2020.122929
- 204. Plesse, C., Vidal, F., Randriamahazaka, H., Teyssié, D. & Chevrot, C. Synthesis and characterization of conducting interpenetrating polymer networks for new actuators. *Polymer*, **2005**, 46, 7771-7778. https://doi.org/10.1016/j.polymer.2005.03.103
- 205. Marinovic, S., Popovic, I., Dunjic, B., Tasic, S., Bozic, B. & Jovanovic, D. The influence of different components on interpenetrating polymer network's (IPN's) characteristics as automotive top coats. *Progress in Organic Coatings*, 2010, 68, 293-298. https://doi.org/10.1016/j.porgcoat.2010.03.010
- 206. Haque, M. A., Kurokawa, T. & Gong, J. P. Super tough double network hydrogels and their application as biomaterials. *Polymer*, **2012**, *53*, 1805-1822. https://doi.org/10.1016/j.polymer.2012.03.013
- 207. Steffensen, S. L., Vestergaard, M. H., Møller, E. H., Groenning, M., Alm, M., Franzyk, H. & Nielsen, H. M. Soft hydrogels interpenetrating silicone—A polymer network for drug-releasing medical devices. *Journal of Biomedical Materials Research Part B: Applied Biomaterials*, **2016**, 104, 402-410. https://doi.org/10.1002/jbm.b.33371
- 208. Salehi Dashtebayaz, M. S. & Nourbakhsh, M. S. Interpenetrating networks hydrogels based on hyaluronic acid for drug delivery and tissue engineering. *International Journal of Polymeric Materials and Polymeric Biomaterials*, **2019**, *68*, 442-451. https://doi.org/10.1080/00914037.2018.1455680

- 209. Smith, G. N., Brok, E., Schmiele, M., Mortensen, K., Bouwman, W. G., Duif, C. P., Hassenkam, T., Alm, M., Thomsen, P. & Arleth, L. The microscopic distribution of hydrophilic polymers in interpenetrating polymer networks (IPNs) of medical grade silicone. *Polymer*, **2021**, *224*, 123671. https://doi.org/10.1016/j.polymer.2021.123671
- 210. Qin, C.-L., Cai, W.-M., Cai, J., Tang, D.-Y., Zhang, J.-S. & Qin, M. Damping properties and morphology of polyurethane/vinyl ester resin interpenetrating polymer network. *Materials Chemistry and Physics*, **2004**, *85*, 402-409. https://doi.org/10.1016/j.matchemphys.2004.01.019
- 211. Wang, T., Chen, S., Wang, Q. & Pei, X. Damping analysis of polyurethane/epoxy graft interpenetrating polymer network composites filled with short carbon fiber and micro hollow glass bead. *Materials & Design*, **2010**, *31*, 3810-3815. https://doi.org/10.1016/j.matdes.2010.03.029
- 212. Čulin, J. Interpenetrating polymer network composites containing polyurethanes designed for vibration damping. *Polimery*, **2021**, *61*, 159-165. https://doi.org/10.14314/polimery.2016.159
- 213. Myung, D., Waters, D., Wiseman, M., Duhamel, P. E., Noolandi, J., Ta, C. N. & Frank, C. W. Progress in the development of interpenetrating polymer network hydrogels. *Polymers for Advanced Technologies*, 2008, 19, 647-657. https://doi.org/10.1002/pat.1134
- 214. Feig, V. R., Tran, H., Lee, M. & Bao, Z. Mechanically tunable conductive interpenetrating network hydrogels that mimic the elastic moduli of biological tissue. *Nature Communications*, **2018**, *9*, 2740. https://doi.org/10.1038/s41467-018-05222-4
- 215. Latifi, N., Asgari, M., Vali, H. & Mongeau, L. A tissue-mimetic nano-fibrillar hybrid injectable hydrogel for potential soft tissue engineering applications. *Scientific Reports*, **2018**, *8*, 1047. https://doi.org/10.1038/s41598-017-18523-3
- 216. Liu, Y., Hsu, Y.-H., Huang, A. P.-H. & Hsu, S.-h. Semi-Interpenetrating Polymer Network of Hyaluronan and Chitosan Self-Healing Hydrogels for Central Nervous System Repair. *Acs Applied Materials & Interfaces*, **2020**, *12*, 40108-40120. https://doi.org/10.1021/acsami.0c11433
- 217. Fu, Y. & Kao, W. J. Drug Release Kinetics and Transport Mechanisms from Semi-interpenetrating Networks of Gelatin and Poly(ethylene glycol) diacrylate. *Pharmaceutical Research*, **2009**, *26*, 2115-2124. https://doi.org/10.1007/s11095-009-9923-1
- 218. Lohani, A., Singh, G., Bhattacharya, S. S. & Verma, A. Interpenetrating Polymer Networks as Innovative Drug Delivery Systems. *Journal of Drug Delivery*, **2014**, 2014, 583612. https://doi.org/10.1155/2014/583612
- 219. Aminabhavi, T. M., Nadagouda, M. N., More, U. A., Joshi, S. D., Kulkarni, V. H., Noolvi, M. N. & Kulkarni, P. V. Controlled release of therapeutics using interpenetrating polymeric networks. Expert Opinion on Drug Delivery, 2015, 12, 669-688. https://doi.org/10.1517/17425247.2014.974871
- 220. Xu, L., Sheybani, N., Ren, S., Bowlin, G. L., Yeudall, W. A. & Yang, H. Semi-Interpenetrating Network (sIPN) Co-Electrospun Gelatin/Insulin Fiber Formulation for Transbuccal Insulin

- Delivery. *Pharmaceutical Research*, **2015**, *32*, 275-285. https://doi.org/10.1007/s11095-014-1461-9
- 221. Kurisawa, M. & Yui, N. Dual-stimuli-responsive drug release from interpenetrating polymer network-structured hydrogels of gelatin and dextran. *Journal of Controlled Release*, **1998**, *54*, 191-200. https://doi.org/10.1016/S0168-3659(97)00247-2
- 222. Stumpel, J. E., Gil, E. R., Spoelstra, A. B., Bastiaansen, C. W. M., Broer, D. J. & Schenning, A. P. H. J. Stimuli-Responsive Materials Based on Interpenetrating Polymer Liquid Crystal Hydrogels. Advanced Functional Materials, 2015, 25, 3314-3320. https://doi.org/10.1002/adfm.201500745
- 223. Wiwatsamphan, P. & Chirachanchai, S. Persistently reversible pH-/thermo-responsive chitosan/poly (*N*-isopropyl acrylamide) hydrogel through clickable crosslinked interpenetrating network. *Polymer Degradation and Stability*, **2022**, *198*, 109874. https://doi.org/10.1016/j.polymdegradstab.2022.109874
- 224. Xiao, M., Su, X. & Xiao, C. Controllable pH- and light-responsive chitosan-based multicomponent interpenetrating networks. *Materials Chemistry and Physics*, **2024**, *312*, 128611. https://doi.org/10.1016/j.matchemphys.2023.128611
- 225. Sands, J. M., Jensen, R. E., Fink, B. K. & McKnight, S. H. Synthesis and properties of elastomer-modified epoxy–methacrylate sequential interpenetrating networks. *Journal of Applied Polymer Science*, **2001**, *81*, 530-545. https://doi.org/10.1002/app.1468
- 226. Athawale, W. D., Kolekar, S. L. & Raut, S. S. Recent developments in polyurethanes and poly(acrylates) interpenetrating polymer networks. *Journal of Macromolecular Science-Polymer Reviews*, **2003**, *C43*, 1-26. https://doi.org/10.1081/mc-120018018
- 227. Chikina, I. & Daoud, M. Structure of interpenetrating polymer networks. *Journal of Polymer Science Part B-Polymer Physics*, **1998**, *36*, 1507-1512. <a href="https://doi.org/10.1002/(sici)1099-0488(19980715)36:9<1507::Aid-polb8>3.0.Co;2-g">https://doi.org/10.1002/(sici)1099-0488(19980715)36:9<1507::Aid-polb8>3.0.Co;2-g
- 228. Farooq, U., Teuwen, J. & Dransfeld, C. Toughening of Epoxy Systems with Interpenetrating Polymer Network (IPN): A Review. *Polymers*, **2020**, *12*, 1908. https://doi.org/10.3390/polym12091908
- 229. Inamdar, A., Cherukattu, J., Anand, A. & Kandasubramanian, B. Thermoplastic-Toughened High-Temperature Cyanate Esters and Their Application in Advanced Composites. *Industrial & Engineering Chemistry Research*, **2018**, *57*, 4479-4504. https://doi.org/10.1021/acs.iecr.7b05202
- 230. Zoratto, N. & Matricardi, P. in *Polymeric Gels* (eds Kunal Pal & Indranil Banerjee) 91-124 (Woodhead Publishing, 2018). https://doi.org/10.1016/B978-0-08-102179-8.00004-1
- 231. Lee, W.-F. & Chen, Y.-J. Studies on preparation and swelling properties of the *N*-isopropylacrylamide/chitosan semi-IPN and IPN hydrogels. *Journal of Applied Polymer Science*, **2001**, *82*, 2487-2496. https://doi.org/10.1002/app.2099

- 232. Murthy, P. S. K., Murali Mohan, Y., Varaprasad, K., Sreedhar, B. & Mohana Raju, K. First successful design of semi-IPN hydrogel–silver nanocomposites: A facile approach for antibacterial application. *Journal of Colloid and Interface Science*, **2008**, *318*, 217-224. https://doi.org/10.1016/j.jcis.2007.10.014
- 233. Li, X., Xu, S., Wang, J., Chen, X. & Feng, S. Structure and characterization of amphoteric semi-IPN hydrogel based on cationic starch. *Carbohydrate Polymers*, **2009**, *75*, 688-693. https://doi.org/10.1016/j.carbpol.2008.09.009
- 234. Wang, J., He, R. & Che, Q. Anion exchange membranes based on semi-interpenetrating polymer network of quaternized chitosan and polystyrene. *Journal of Colloid and Interface Science*, **2011**, *361*, 219-225. https://doi.org/10.1016/j.jcis.2011.05.039
- 235. Merlin, D. L. & Sivasankar, B. Synthesis and characterization of semi-interpenetrating polymer networks using biocompatible polyurethane and acrylamide monomer. *European Polymer Journal*, **2009**, *45*, 165-170. https://doi.org/10.1016/j.eurpolymj.2008.10.012
- 236. Jehl, D., Widmaier, J. M. & Meyer, G. C. The transparency of polyurethane-poly(methyl methacrylate) interpenetrating and semi-interpenetrating polymer networks. *European Polymer Journal*, **1983**, *19*, 597-600. https://doi.org/10.1016/0014-3057(83)90184-2
- 237. Hermant, I. & Meyer, G. C. A comparative study of polyurethane-poly(methyl methacrylate) interpenetrating and semi-1 interpenetrating polymer networks. *European Polymer Journal*, **1984**, 20, 85-89. https://doi.org/10.1016/0014-3057(84)90229-5
- 238. Garcés-Lara, M. Á., Antonio-Cruz, R., Mendoza-Martínez, A. M., Ramírez, T. L. & Morales-Cepeda, A. B. Effect of initiator and cross-linking agent on a semi-IPN of (PU-starch)/PMMA. *Chemical Engineering Communications*, **2009**, *196*, 1227-1236. https://doi.org/10.1080/00986440902831904
- 239. Gugoasa, A. I., Racovita, S., Vasiliu, S. & Popa, M. Semi-Interpenetrating Polymer Networks Based on Hydroxy-Ethyl Methacrylate and Poly(4-vinylpyridine)/Polybetaines, as Supports for Sorption and Release of Tetracycline. *Polymers*, **2023**, *15*. https://doi.org/10.3390/polym15030490
- 240. Zolghadr, M., Shakeri, A., Zohuriaan-Mehr, M. J. & Salimi, A. Self-healing semi-IPN materials from epoxy resin by solvent-free furan—maleimide Diels-Alder polymerization. *Journal of Applied Polymer Science*, **2019**, *136*, 48015. https://doi.org/10.1002/app.48015
- 241. Shukla, P. & Srivastava, A. K. Synthesis and properties of semi-interpenetrating network based on styrene-acrylonitrile-vinyl acetate terpolymer and zinc acrylate. *Polymer Gels and Networks*, **1995**, 3, 375-386. https://doi.org/10.1016/0966-7822(95)00003-4
- 242. Wang, Y. F., Chen, S. D. & Hu, A. G. in *Polymer Synthesis Based on Triple-Bond Building Blocks Topics in Current Chemistry Collections* (eds B. Tang & R. Hu) 97-126 (2018). https://doi.org/10.1007/978-3-319-78042-9 4

- 243. Cai, Y., Lehmann, F., Peiter, E., Chen, S., Zhu, J., Hinderberger, D. & Binder, W. H. Bergman cyclization of main-chain enediyne polymers for enhanced DNA cleavage. *Polymer Chemistry*, **2022**, *13*, 3412-3421. https://doi.org/10.1039/D2PY00259K
- 244. Cai, Y. & Binder, W. H. Triggered Crosslinking of Main-Chain Enediyne Polyurethanes via Bergman Cyclization. *Macromolecular Rapid Communications*, **2023**, *44*, 2300440. https://doi.org/10.1002/marc.202300440
- 245. Cai, Y., Lehmann, F., Thümmler, J. F., Hinderberger, D. & Binder, W. H. Initiator-Free Synthesis of Semi-Interpenetrating Polymer Networks via Bergman Cyclization. *Macromolecular Chemistry and Physics*, **2024**, 2400177. https://doi.org/10.1002/macp.202400177

Curriculum Vitae

Yue Cai (M. Sc.)

Birthday:xx.xx.xxxx Birth of place: xxx Nationality: xxx

Education

➤ PhD research (Major in Macromolecular Chemistry)
 Martin Luther University Halle-Wittenberg (MLU), Halle (Saale), Germany

Supervisor: Prof. Dr. Wolfgang H. Binder

Master's Degree (Major in Pharmaceutical Engineering and Technology) 09/2015-09/2018

East China University of Science and Technology, Shanghai, P. R. China

Joint supervision in Shanghai Institute of Organic Chemistry (SIOC), Chinese Academy of Sciences

Supervisor: Prof. Dr. Shu-Li You

➤ Bachelor's Degree (Major in Pharmaceutical Engineering)

Qingdao University of Science and Technology, Shandong, P. R. China

09/2011-06/2015

Supervisor: Prof. Dr. Yamu Xia

> Senior High School

09/2008-06/2011

Taixing Senior High School, Jiangsu, P. R. China

Research

- **PhD**: Conceptualization, synthesis, characterization, and application research of novel polymers (polyimines/polyurethanes) based on bioactive monomer enediane
 - Bergman cyclization of main-chain enediyne polymers for enhanced DNA cleavage
 - Triggered crosslinking of main-chain enediyne polyurethanes via Bergman cyclization
 - Initiator-free synthesis of semi-interpenetrating polymer networks via Bergman cyclization
- ➤ **Master**: Catalytic asymmetric dearomatization reactions
 - Chiral phosphoric acid catalyzed chemoselective N-H functionalization of indole derivatives *via* Reissert-type reaction
 - Metal-catalyzed enantioselective reactions

Presentations and Conferences

- Participant as a contributed speaker at polymer conferences
 - <u>Yue Cai</u>, Florian Lehmann, Dariush Hinderberger, and Wolfgang H. Binder*: Force-induced self-strengthening of elastomer *via* Bergman cyclization; The Seventh International Symposium Frontiers in Polymer Science, May 2023, Gothenburg, Sweden.
 - Yue Cai, Florian Lehmann, Dariush Hinderberger, and Wolfgang H. Binder*: Force-induced selfstrengthening of elastomer via Bergman cyclization; The 14th Advanced Polymers *via* Macromolecular Engineering Conference, April 2023, Paris, France
 - Yue Cai, Florian Lehmann, Edgar Peiter, Senbin Chen, Jintao Zhu, Dariush Hinderberger, and Wolfgang H. Binder*: Synthesis of Enediyne-Containing Polymers and their Applications via Bergman Cyclization, SFB TRR 102 "Polymers under multiple constraints: restricted and controlled molecular order and mobility" Seminar August 2022
 - Yue Cai, Florian Lehmann, Edgar Peiter, Senbin Chen, Jintao Zhu, Dariush Hinderberger, and Wolfgang H. Binder*: Synthesis of Main-chain Enediyne Polymers and their Applications *via* Bergman Cyclization, The second edition of Bordeaux Polymer Conference, June 2022, Bordeaux, France
- Participant with posters at polymer conferences
 - Matthias Rohmer, <u>Yue Cai</u>, Özgün Ucak, and Wolfgang H. Binder*: Secondary structure, assembly
 and cooperativity in dynamic supramolecular polymers, SFB TRR 102 "Polymers under multiple
 constraints: restricted and controlled molecular order and mobility" Retreat (Final) April 2023
 - Yue Cai, Florian Lehmann, Dariush Hinderberger, and Wolfgang H. Binder*: Enediyne-main chain polymers for DNA cleavage, SFB TRR 102 "Polymers under multiple constraints: restricted and controlled molecular order and mobility" Miniworkshop, October 2022
 - Yue Cai, Florian Lehmann, Edgar Peiter, Dariush Hinderberger, and Wolfgang H. Binder*: Bergman cyclization of main-chain enediyne polymers for enhanced DNA cleavage, SFB TRR 102 "Polymers under multiple constraints: restricted and controlled molecular order and mobility" Miniworkshop, March 2022
 - Matthias Rohmer, Jan Freudenberg, Merve B. Canalp, <u>Yue Cai</u>, Özgün Ucak, and Wolfgang H. Binder*: Secondary structure, assembly and cooperativity in dynamic supramolecular polymers, SFB TRR 102 "Polymers under multiple constraints: restricted and controlled molecular order and mobility" Retreat, March 2020

Experiences

	Research Assistant A	anjing Wuhai Biotechnology Co., LTD	09/2018-09/2019				
	Synthesis of customized chemicals: chiral catalysts/bioactive molecules						
>	Clinical Research Associate Intern	Pfizer	07/2019-09/2019				
	Clinical trial project document organization, site visit plan statistics						
>	Marketing Intern	Danone Nutricia Early Life Nutrition	10/2018-01/2019				

Publication list

1. Initiator-free synthesis of semi-interpenetrating polymer networks *via* Bergman Cyclization

Cai, Y.; Lehmann, F.; Thümmler, J. F.; Chen, S.; Zhu, J.; Hinderberger, D.; Binder, W. H.* *Macromol. Chem. Phys.*, **2024**, 2400177. https://doi.org/10.1002/macp.202400177

2. Triggered Crosslinking of Main-Chain Enediyne Polyurethanes via Bergman Cyclization

Cai, Y.; Binder, W. H.*

Macromol. Rapid Commun. 2023, 44, 2300440. https://doi.org/10.1002/marc.202300440

3. Bergman Cyclization of Main-Chain Enediyne Polymers for Enhanced DNA Cleavage

Cai, Y.; Lehmann, F.; Peiter, E.; Chen, S.; Zhu, J.; Hinderberger, D.; Binder, W. H.* *Polym. Chem.*, **2022**, *13*, 3412. https://doi.org/10.1039/D2PY00259K

4. Chiral Phosphoric Acid Catalyzed Chemoselective N-H Functionalization of Indole Derivatives *via* Reissert-Type Reaction

Cai, Y.; Gu, Q.; You, S.-L.*

Org. Biomol. Chem. 2018, 16, 6146. https://doi.org/10.1039/C8OB01863D

5. Asymmetric Fluorinative Dearomatization of Tryptophol Derivatives *via* Chiral Anion Phase-Transfer Catalysis (*co-author*)

Liang, X.-W.¹; Cai, Y.¹; You, S.-L.* *Chin. J. Chem.* **2018**, *36*, 925. https://doi.org/10.1002/cjoc.201800319

6. Manipulation of Spiroindolenine Intermediates for Enantioselective Synthesis of 3-(Indol-3-yl)-Pyrrolidines (cooperation)

```
Xia, Z.-L.; Zheng, C.; Liang, X.-W.; Cai, Y.; You, S.-L.* Angew. Chem. Int. Ed. 2019, 58, 1158. <a href="https://doi.org/10.1002/anie.201812344">https://doi.org/10.1002/anie.201812344</a>
```

- 7. Metal-catalyzed enantioselective reactions (cooperation)
 - Enantioselective Synthesis of Polycyclic Pyrrole Derivatives by Iridium-Catalyzed Asymmetric Allylic Dearomatization and Ring-Expansive Migration Reactions

Huang, L.; Xie, J.-H.; Cai, Y.; Zheng, C.; Hou, X.-L.; Dai, L.-X.; You, S.-L.* *Chem. Commun.*, **2021**, *57*, 5390. https://doi.org/10.1039/D1CC01929E

■ Highly Diastereo- and Enantioselective Synthesis of Quinuclidine Derivatives by an Iridium-Catalyzed Intramolecular Allylic Dearomatization Reaction

Huang, L.; Cai, Y.; Zhang, H.-J.; Zheng, C.; Dai, L.-X.; You, S.-L.* *CCS Chem.* **2019**, *1*, 106. https://doi.org/10.31635/ccschem.019.20180006

■ Stereodivergent Synthesis of Tetrahydrofuroindoles through Pd-Catalyzed Asymmetric Dearomative Formal [3+2] Cycloaddition

Cheng, Q.; Zhang, F.; Cai, Y.; Guo, Y.-L., You, S.-L.* Angew. Chem. Int. Ed. 2018, 57, 2134. https://doi.org/10.1002/anie.201711873

Iridium-Catalyzed Enantioselective Synthesis of Pyrrole-Annulated Medium-Sized-Ring Compounds

Huang, L.; Cai, Y.; Zheng, C.; Dai, L.-X.; You, S.-L.* Angew. Chem. Int. Ed. 2017, 56, 10545. https://doi.org/10.1002/anie.201705068

Skills

- Polymer chemistry (Design, synthesis, characterization)
- Scientific writing & Publishing
- Research management & Collaboration
- DNA-related separation (Gel electrophoresis)
- Academic presentation
- Onboarding & Assisting teaching (supervising HiWi students on mini projects)

I

Languages		
Mandarin (native)	English (fluent)	German (beginning)
Halle (Saale),		
		Yue Cai

Eigenständigkeitserklärung

Ich erkläre an Eides statt, dass ich die vorliegende Dissertation mit dem Titel "Bergman Cyclization of Enediyne-Based Polymers in Solution and the Solid State" selbstständig und ohne fremde Hilfe verfasst, keine anderen als die von mir angegebenen Quellen und Hilfsmittel benutzt und die den zitierten Werken wörtlich oder inhaltlich entsnommenen Stellen als solche kenntlich gemacht habe.

Außerdem erkläre ich, dass ich die vorliegende Dissertation an keiner anderen wissenschaftlichen Einrichtung zur Erlangung eines akademischen Grades eingereicht zu haben.

Halle (Saale),		_		
			Yue	e Cai

Appendix

Supporting Information to: Bergman Cyclization of Main-Chain Enediyne Polymers for Enhanced DNA Cleavage, *Polym. Chem.*, **2022**, *13*, 3412. https://doi.org/10.1039/D2PY00259K

Supporting Information to: Triggered Crosslinking of Main-Chain Enediyne Polyurethanes *via* Bergman Cyclization, *Macromol. Rapid Commun.* **2023**, *44*, 2300440. https://doi.org/10.1002/marc.202300440

Supporting Information to: Initiator-free synthesis of semi-interpenetrating polymer networks *via* Bergman Cyclization, *Macromol. Chem. Phys.*, **2024**, 2400177. https://doi.org/10.1002/macp.202400177

Electronic Supplementary Material (ESI) for Polymer Chemistry. This journal is © The Royal Society of Chemistry 2022

Supporting Information

Bergman Cyclization of Main-Chain Enediyne Polymers

for Enhanced DNA Cleavage

Yue Cai^a, Florian Lehmann^b, Edgar Peiter^c, Senbin Chen^d, Jintao Zhu^d, Dariush Hinderberger^b, Wolfgang H. Binde**r**^{*a}

^a Macromolecular Chemistry, Institute of Chemistry, Faculty of Natural Science II (Chemistry, Physics and Mathematics), Martin-Luther-University Halle-Wittenberg, von-Danckelmann-Platz 4, Halle D-06120, Germany

^b Physical Chemistry, Institute of Chemistry, Faculty of Natural Science II (Chemistry, Physics and Mathematics), Martin-Luther-University Halle-Wittenberg, von-Danckelmann-Platz 4, Halle D-06120, Germany

^c Faculty of Natural Sciences III, Plant Nutrition Laboratory, Institute of Agricultural and Nutritional Sciences, Martin Luther University Halle-Wittenberg, Halle D-06099, Germany

^d Key Laboratory of Materials Chemistry for Energy Conversion and Storage, Ministry of Education (HUST), School of Chemistry and Chemical Engineering, Huazhong University of Science and Technology (HUST), Wuhan 430074, China

^{*} Correspondence: wolfgang.binder@chemie.uni-halle.de

1. AB		BREVIATIONS		
2.	EX	PERIMENTAL PART	3	
	2.1.	SOLVENTS AND MATERIALS	3	
	2.2.	METHODS AND INSTRUMENTATION	3	
	2.3.	SYNTHESIS	4	
	1) (Z)-a 2)	Synthesis of di-tert-butyl octa-4-en-2,6-diyne-1,8-diyl(Z)-dicarbamate (EDY-I) and octa-4-en-2,6-diyne-1,8-diamine EDY-II	5	
	(ED	Y-III) · · · · · · · · · · · · · · · · · ·		
	3)	General Synthesis of main-chain enediyne polymers ·····	7	
	2.4.	DNA-CLEAVAGE RELATED TEST	9	
	1)	DNA-cleavage test		
	2)	Hydrolysis experiment to verify the source of cleavage activity		
	2.5.	CONCENTRATION CONTROL OF EDY-II AND EPR TEST		
	1)	Concentration control of EDY-II		
	2)	EPR test of generated particles	0	
3.	IR	SPECTRA OF MAIN-CHAIN ENEDIYNE POLYMERS ·························1	1	
4.	NN	IR SPECTRA OF MODEL COMPOUNDS AND POLYMERS ·······1	3	
5.	DS	C CURVES OF MODEL COMPOUND AND POLYMERS ···················1	9	
6.	ES	I-TOF MS SPECTRA OF MODEL COMPOUNDS ······2	0	
7.	RE	FERENCE ······2	2	

1. Abbreviations

Bergman Cyclization (BC), Thin-layer Chromatography (TLC), Electrospray Ionization Time-of-Flight Mass Spectroscopy (ESI-ToF MS), Differential scanning calorimetry (DSC), Matrix-assisted Laser Desorption / Ionization Time-of-Flight Mass (MALDI-ToF MS), Nuclear magnetic resonance (NMR), Attenuated total reflection (ATR), Infrared (IR), Electrospray Ionization Time-of-Flight Mass Spectrometry (ESI-TOF MS), Fourier transformation (FT), Degree of Polymerization (DP), Tetrahydrofuran (THF), Dichloromethane (DCM), Dimethyl sulfoxide (DMSO), tert-Butyloxycarbonyl (Boc), Deoxyribonucleic acid (DNA), Electron paramagnetic resonance (EPR), **EDTA** Ethylenediaminetetraacetic acid (EDTA), Tris (TE),and 4-Hydroxy-2,2,6,6-tetramethylpiperidine-1-oxyl (TEMPOL)

2. Experimental Part

2.1. Solvents and Materials

Chloroform from VWR, ethyl acetate from Overlack, methanol from Brenntag, and toluene from Roth were purchased in technical grade and distilled at least once prior use. Deuterium chloroform (CDCl₃-d) was used as NMR deuterium solvents.

Dry solvents were prepared as follows: tetrahydrofuran (THF), from Roth, was predried over potassium hydroxide for several days and refluxed over sodium and benzophenone under inert atmosphere and distilled freshly before use; *n*-hexane, from Roth, was refluxed over concentrated sulfuric acid and oleum to remove olefins and subsequently distilled over sodium and benzophenone under an inert gas atmosphere for several hours; dichloromethane (DCM), from Overlack, was predried over calcium chloride for several days and then refluxed over calcium hydride for several hours. Moisture was removed for the following solvents: diethyl ether, from Overlack, was passed through a column filled with sodium sulfate; dimethyl sulfoxide (DMSO), from Grüssing, was stored over molecular sieves (pore diameters 4Å) for several days; N, N-dimethylformamide (DMF) from Grüssing was stored over calcium hydride for several days before use.

Prop-2-yn-1-amine, Tetrafluoroterephthalic aldehyde and 4-(4-Formylphenoxy)benzaldehyde were purchased from abcr; 4,4'-Biphenyldicarboxaldehyde was purchased from TCI; terephthalaldehyde was purchased from Fluka, *cis*-1,2-dichloroethylene, 4-Hydroxy-TEMPO and Tetrakis(triphenylphosphine)-palladium(0) was purchased from Sigma-Aldrich; All chemicals listed here were used without any purification unless otherwise stated.

2.2. Methods and Instrumentation

TLC was performed on "Merck silica gel 60" plates. Spots on TLC plate were visualized using UV light (254 or 366 nm), oxidizing agent "blue stain", or potassium permanganate solution. "Blue stain" was prepared as follow: (NH₄)₆Mo₇O₂₄·4H₂O (1 g) and Ce(SO₄)₂·4H₂O (1 g) were dissolved in a mixture of distilled water (90 mL) and concentrated sulfuric acid (6

mL). Potassium permanganate solution was prepared as follow: KMnO₄(3 g) and K₂CO₃ (10 g) were dissolved in distilled water (300 ml).

ESI-ToF MS measurements were performed using a Bruker Daltonics microTOF. 0.1 mg of samples were dissolved in HPLC grade methanol. All spectra were obtained by means of direct injection with a flow rate of 180 μ L h-1 in the negative mode with an acceleration voltage of 4.5 kV.

DSC measurements were done on a Netzsch DSC 204 F1. Samples pieces with a mass of 5 – 10 mg were placed into aluminum crucibles and were heated under nitrogen atmosphere with a heating rate of 5 K·min⁻¹ unless otherwise stated. Evaluation of the measured data was done with Netzsch Proteus Analytic software.

MALDI-ToF MS was done on a Bruker Autoflex III system in the reflection mode. Formation of ions was obtained by laser desorption (smart beam laser at 355, 532, 808, and 1064 ± 6.5 nm; 3 ns pulse width; up to 2500 Hz repetition rate). Ions were accelerated by a voltage of 20 kV, and detected as positive ions. 1,8-dihydroxy-9,10-dihydroanthracen-9-one (Dithranol, 20 mg·mL⁻¹ in THF) was used as matrix and sodium iodide (NaI, 20 mg·mL⁻¹ in THF) was used as salts for ionizing polymers functionalized with Poly EDY-A (20 mg·mL⁻¹ in THF) while applying a volume ratio of 100:20:1.

NMR-spectra were measured on a Varian Gemini 400 spectrometer at 27°C. The ¹H-NMR spectra were recorded at 400 MHz or 500 MHz and for ¹³C-NMR spectroscopy 100 MHz were used. The samples were dissolved in either CDCl₃ or DMSO. The NMR spectra were interpreted using MestReNova software (version 9.0.1-13254). Chemical shifts were given in ppm and coupling constants were given in Hz.

ATR-FTIR-spectra were measured on a Bruker Tensor VERTEX 70 spectrometer equipped with a Golden Gate Diamond ATR top-plate. For each measurement 32 background scans and 32 sample scans were averaged. The data were analyzed using Opus 6.5 software.

ESI-TOF-MS measurements were performed on a Bruker Daltonics microTOF via direct injection at a flow rate of 180 μ L h⁻¹ in positive mode with an acceleration voltage of 4.5 kV. Samples were prepared by dissolving in LC-MS grade methanol with additional sodium iodide salt in acetone. The software Data Analysis (version 4.0) was used for data evaluation

Gel electrophoresis were performed as below: after incubation for specific time, each mixture (10 μ L) of polymer containing enediyne and pART7 plasmid in TE buffer (pH = 7.6) was mixed with a 6*loading buffer (2 μ L) and subjected to 1% agarose gel electrophoresis at 90 V for 45 min, stained by SYBR® Safe DNA Gel Stain and then the gel was photographed on Intas Science Imaging instrument and analyzed by scanning densitometry.

CW EPR spectra were measured using the Miniscope MS 5000 (Magnettech GmbH, Berlin, and Freiberg Instruments, Freiberg, Germany), the MS 5000 temperature controller (Magnettech GmbH, Berlin, Germany) and Freiberg Instruments software.

Micropipettes (BLAUBRAND® intraMARK, Wertheim, Germany) were filled with about 10–15 μL of sample solution containing 50 mM TEMPOL and capped with capillary tube sealant (CRITOSEAL® Leica) and placed into the spectrometer. The temperature was fixed at 25 °C or 37 °C with an accuracy of 0.2 °C. For all X-band measurements a magnetic field sweep of 8 mT centered around 338 mT with a scan time of 60 s, modulation amplitude of 0.02 mT, modulation frequency of 100 kHz and a microwave power of 10 mW. Each spectrum is an accumulation of 10 scans.

The samples were directly exposed to light inside the EPR spectrometer using a fiber coupled multi wavelength LED light source (Prizmatix Ltd., Cholon, Israel). The LED 420Z emits light with a peak wavelength of 419.8 nm and a FWHM of 14.74 nm. A 1 m polymer optical fiber with a diameter of 1.5 mm and a NA of 0.5 was used to send the light with a maximum power of 215 mW through the hole for the Mn-standard into the resonator.

2.3. Synthesis

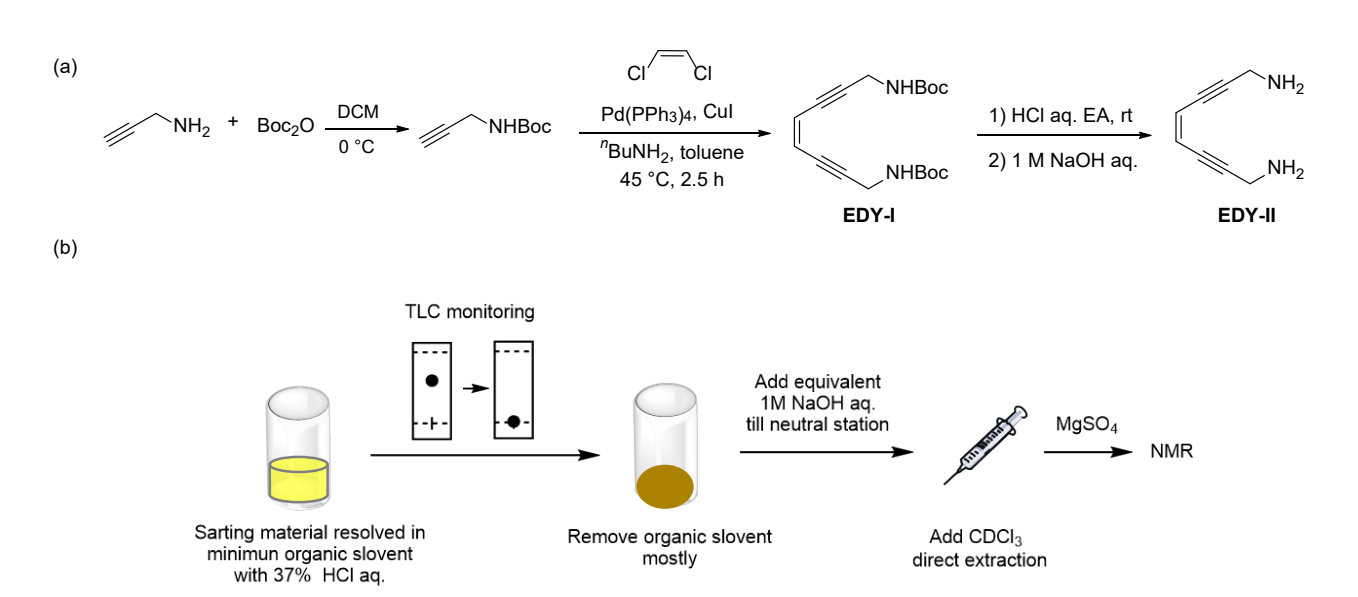


Figure S1 (a) Synthetic route of di-*tert*-butyl octa-4-en-2,6-diyne-1,8-diyl(*Z*)-dicarbamate **EDY-I** and (*Z*)-octa-4-en-2,6-diyne-1,8-diamine **EDY-II**. (b) Designed procedure of handle with **EDY-II** solution

1) Synthesis of di-tert-butyl octa-4-en-2,6-diyne-1,8-diyl(Z)-dicarbamate (EDY-I) and (Z)-octa-4-en-2,6-diyne-1,8-diamine EDY-II.

Di-*tert*-butyl dicarbonate (17.5 g, 80.0 mmol) was added dropwise at 0 °C to a solution of prop-2-yn-1-amine (5.49 mL, 80.0 mmol) in DCM (150 mL). After 1 h of stirring, the solvent was removed in vacuo and the resulting colorless oil was dried under high vacuum overnight to yield a slightly yellow solid (12.4 g, quantitative yield), which was used as such without further purification. The spectral data corresponds to that reported in the literature.¹

tert-Butyl prop-2-ynylcarbamate

¹H NMR (500 MHz, CDCl₃, δ in ppm) δ 4.79 (brs, 1H), 3.90 (s, 2H), 2.20 (t, J = 2.5 Hz, 1H),

The synthesis of **EDY-I** was realized according to reference². Alkyne (2.2 mol) was added to a mixture of *cis*-1,2-dichloroethylene (1 mol), Pd(PPh₃)₄ (0.06 mol), CuI (0.2 mol), *n*-butylamine (5 mol) in toluene at 45 °C and stirring the mixture for 4 h at that temperature. The crude product was purified by flash column chromatography (5% ethyl acetate-dichloromethane). Yield: 60%.



di-tert-butyl octa-4-en-2,6-diyne-1,8-diyl(Z)-dicarbamate

¹H NMR (400 MHz, CDCl₃, δ in ppm) δ 5.80 (s, 1H), 4.88 (br, 1H), 4.23-3.94 (m, 2H), 1.46 (s, 9H). ESI-ToF MS: $[M+Na]^+$ calculated for $C_{18}H_{26}N_2O_4$, 357.18; found, 357.20.

For **EDY-II**, 37% hydrochloric acid solution (99.7 μL, 1.20 mmol) was added to a stirring solution of **EDY-I** (20 mg, 0.06 mmol) in 0.5 mL ethyl acetate. The reaction mixture was stirred for about 30 min at room temperature till complete (monitored by TLC, PE/EA=4/1, the TLC result looks like the above graph). Following by removing the solvent via vacuum directly, equivalent 1 mol/L NaOH aqueous solution (1.2 mL) was added to the "dry" reaction mixture. The mixture was extracted with CHCl₃ (5 mL × 3). The combined organic layers were washed with brine, dried over Na₂SO4, filtrated and concentrated via vacuo. The concentration must not be over than 0.25 mol/L. **EDY-II** would stay safe and pure in this solution. Add hexamethylbenzene as reference label to obtain the concentration of enediyne for further reaction and DNA-cleavage test. Yield: 45%.



(Z)-octa-4-en-2,6-diyne-1,8-diamine

¹H-NMR (500 MHz, CDCl₃, δ in ppm): ¹H NMR (500 MHz, cdcl₃) δ 5.79 (s, 1H, CH), 3.62 (s, 2H, NCH₂), 1.50 (s, 2H, NH₂). ¹³C NMR (126 MHz, CDCl₃) δ 118.98 (CH), 97.80 (Cquart), 79.83 (Cquart), 31.14 (NCH₂). ESI-ToF MS: [M+H]⁺ calculated for C₈H₁₀N₂, 135.09; found, 135.12.

2) Synthesis of (1E,1'E)-N,N'-((Z)-octa-4-en-2,6-diyne-1,8-diyl)bis(1-phenylmethanimine) (EDY-III)

The **EDY-III** was synthesized according to reference³. (*Z*)-octa-4-en-2,6-diyne-1,8-diamine **EDY-II** (0.2 mmol) in 2 ml dichloromethane was added to a stirring solution of benzaldehyde (0.4 mmol) in 4 ml dichloromethane containing molecular sieves. After stirring under room temperature for 3 hours and monitoring the total consumption of benzaldehyde, the mixture was filtered through a celite bed and the solvent was removed under vacuum to obtain crude product **EDY-III**. Further purification was performed by recrystallization in mixture of hexane and ethyl acetate. Yield: 45%.

(1E,1'E)-N,N'-((Z)-octa-4-en-2,6-diyne-1,8-diyl)bis(1-phenylmethanimine)

¹H NMR (400 MHz, CDCl₃, δ in ppm) δ 8.63 (s, 1H, NCH), 7.81-7.63 (m, 2H), 7.46-7.33 (m, 3H), 5.97 (s, 1H, CH), 4.71 (s, 2H, NCH₂). ¹³C NMR (126 MHz, CDCl₃) δ 162.33 (NCH), 135.88 (CH), 130.88 (CH), 129.71 (CH), 128.97 (CH), 128.58 (CH), 128.23 (CH), 119.44 (CH), 92.33 (Cquart), 85.07 (Cquart), 48.01 (NCH₂). ESI-ToF MS: [M+H]⁺ calculated for C₂₂H₁₈N₂, 311.15; found, 311.16. T_{peak} for BC From DSC (heating rate: 5 K/min): 145.9 °C.

3) General Synthesis of main-chain enediyne polymers

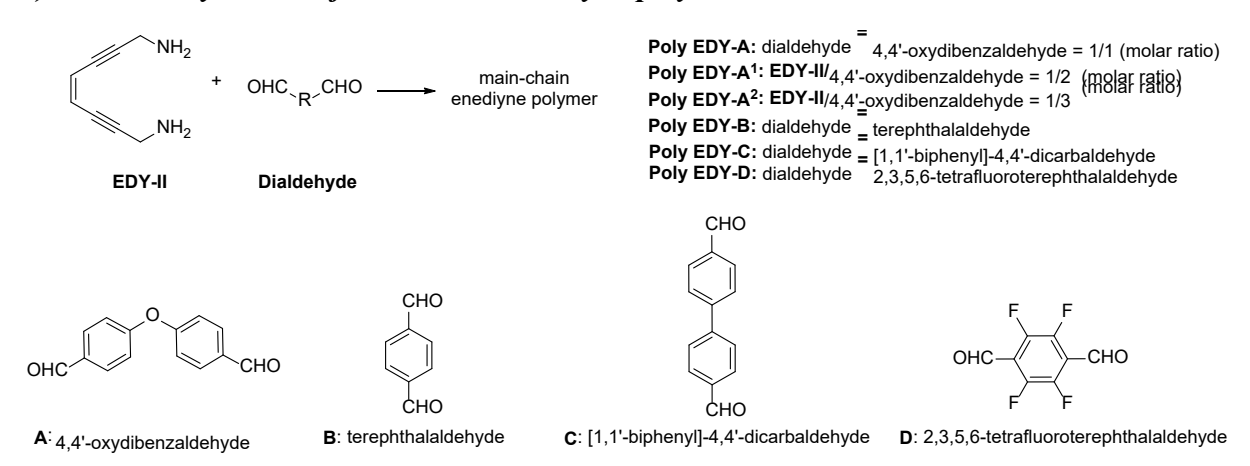


Figure S2 Synthetic route of main-chain enediyne polymers derived from different dialdehydes

To synthesize main-chain enediyne polymer, molar concentration of **EDY-II** in solution needs to be obtained based on the previous description. In a closed system, a solution of **EDY-II** (0.16 mmol) in 1.6 mL CHCl₃ was added to a stirring solution of dialdehyde (0.16 mmol) in 3.2 mL isopropanol. The reaction mixture was stirred at room temperature for 16 h (only for **Poly EDY-D**: 4 h) in dark. Following by taking 0.5 mL of reaction mixture, filtration of precipitated particles and removing the solvent via vacuum, NMR was carried out to check the reaction station, together with adding hexamethylbenzene to obtain the concentration of enediyne segment in the solution polymer for further DNA-cleavage tests and EPR measurements.

¹H NMR (500 MHz, CDCl₃) δ 9.96-9.94 (m, 0.03H, CHO), 8.62-8.60 (m, 1H, NCH), 7.73-7.72 (m, 1H, CH), 7.63-7.61 (m, 1H, CH), 7.03-7.01 (m, 1H, CH), 6.89-6.88 (m, 1H, CH), 6.00-5.98 (m, 1H, CH), 4.72-4.71 (m, 2H, NCH₂). T_{peak} for BC From DSC (heating rate: 5 K/min): 199.5 °C.

Poly EDY-A¹

¹H NMR (400 MHz, CDCl₃) δ 9.91-9.90 (m, 0.24H, CHO), 8.61-8.56 (m, 1H, NCH), 7.75-7.73 (m, 1H, CH), 7.70-7.68 (m, 1H, CH), 7.08-7.03 (m, 1H, CH), 6.99-6.97 (m, 1H, CH), 5.96-5.95 (m, 1H, CH), 4.69-4.67 (m, 2H, NCH₂). T_{peak} for BC From DSC (heating rate: 5 K/min): 197.1 °C.

¹H NMR (500 MHz, CDCl₃) δ 9.88-9.87 (m, 0.24H, CHO), 8.61-8.58 (m, 1H, NCH), 7.76-7.73 (m, 1H, CH), 7.71-7.68 (m, 1H, CH), 7.05-7.02 (m, 2H, CH), 5.95-5.94 (m, 1H, CH), 4.70-4.67 (m, 2H, NCH₂). T_{peak} for BC From DSC (heating rate: 5 K/min): 172.8 °C.

Poly EDY-B

¹H NMR (500 MHz, CDCl₃) δ 10.06-10.02 (m, 0.02H, CHO), 8.63-8.51 (m, 1H, NCH), 7.87-7.45 (m, 2H, CH), 5.97-96 (m, 1H, CH), 4.74-4.68 (m, 2H, CH). T_{peak} for BC From DSC (heating rate: 5 K/min): 152.3 °C.

Poly EDY-C

¹H NMR (500 MHz, CDCl₃) δ 10.07-10.04 (m, 0.04H, CHO), 8.72-8.58 (m, 1H, NCH), 7.82-7.30 (m, 4H, CH), 6.02-5.80 (m, 1H, CH), 4.77-4.74 (m, 2H, CH). T_{peak} for BC From DSC (heating rate: 5 K/min): 148.9 °C.

Poly EDY-D

¹H NMR (500 MHz, CDCl₃) δ 10.10-10.06 (m, 0.02H, CHO), 8.78-8.47 (m, 1H, NCH),

5.90-5.88 (m, 1H, CH), 4.77-4.64 (m, 2H, CH). T_{peak} for BC From DSC (heating rate: 5 K/min): 176.9 °C.

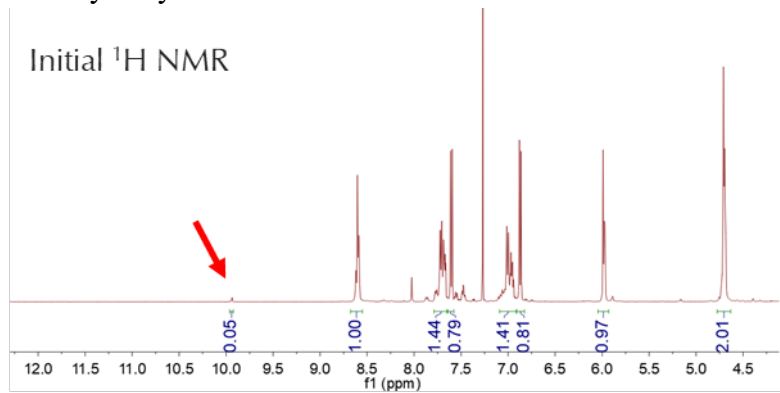
2.4. DNA-cleavage related test

1) DNA-cleavage test

Freshly prepared EDY-containing compounds were dissolved in DMSO (12 μ L) at concentrations of 200 mM. The concentration of enediyne segment is calculated by adding hexamethylbenzene as reference label. Each EDY solution was added to a solution of supercoiled plasmid pART7 (1.8 μ g μ L-1, 8 μ L) in TE buffer (pH 7.6, 100 μ L). Negative samples consisted of a solution of pART7 (1.8 μ g μ L-1, 8 μ L) in TE buffer (pH 7.6) separately incubated with or without 12 μ L DMSO. All the systems maintained in 120 μ L in total volume and were incubated at 37 °C. After incubation for specific time, each mixture (10 μ L) was mixed with a 6*loading buffer (2 μ L) and subjected to 1% agarose gel electrophoresis at 90 V for 45 min, stained by ethidium bromide and then the gel was photographed on a UV transilluminator (FR-200A) and analyzed by scanning densitometry

2) Hydrolysis experiment to verify the source of cleavage activity

Based on the condition of DNA-cleavage test, an equivalent volume of pure TE buffer except the plasmid Part7 in TE buffer was added to the DMSO solution of EDY-containing compounds. The mixture was incubated at 37 °C. After 8 h, from NMR, DP slightly decreased but no obvious diamino EDY signals appeared, which gives the conclusion of that EDY in polymer chain is responsible for DNA-cleavage performance, rather than small molecule EDY dissociated after hydrolysis.



¹H NMR after incubation with water at 37 [°]C for 8 h

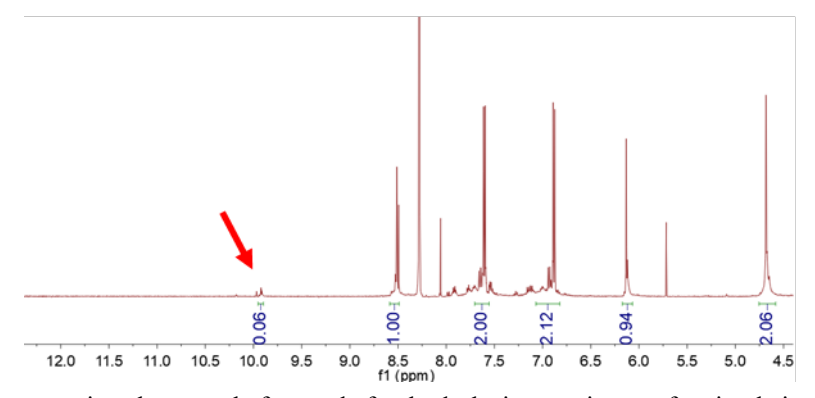


Figure S3 NMR comparison between before and after hydrolysis experiment of main-chain enediyne polymers

2.5. Concentration control of EDY-II and EPR test

1) Concentration control of EDY-II

Under >0.25 mol/L concentration, brown solids spontaneously appear in solution of diamino enediyne **EDY-II** in chloroform.



Figure S4 Brown solids spontaneously appear and grow up

2) EPR test of generated particles

Once generated, solid samples were placed in EPR tubes immediately (T=30 °C, air atmosphere). Spinning concentration was recorded every 30 min. Without heating, the radical species grew gradually and kept stable after reaching to peak.

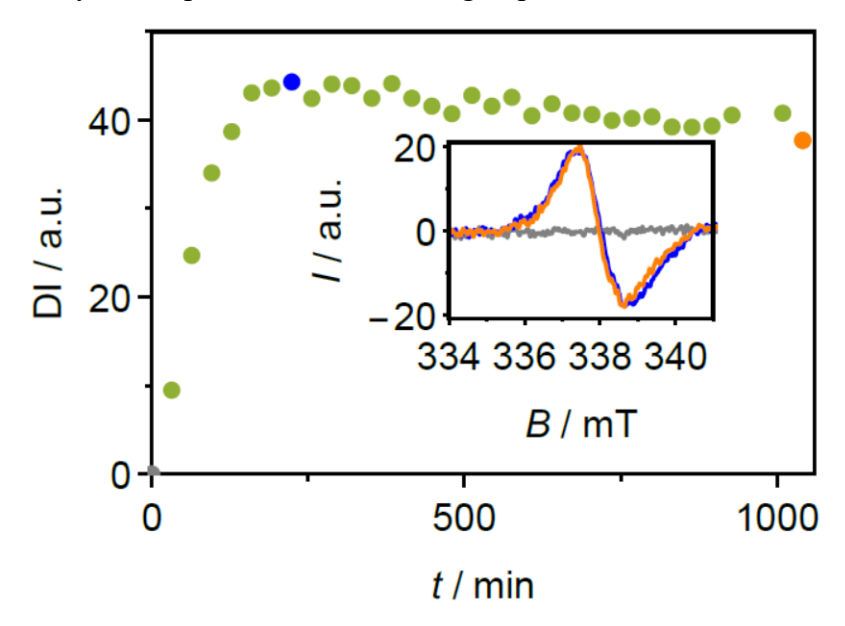
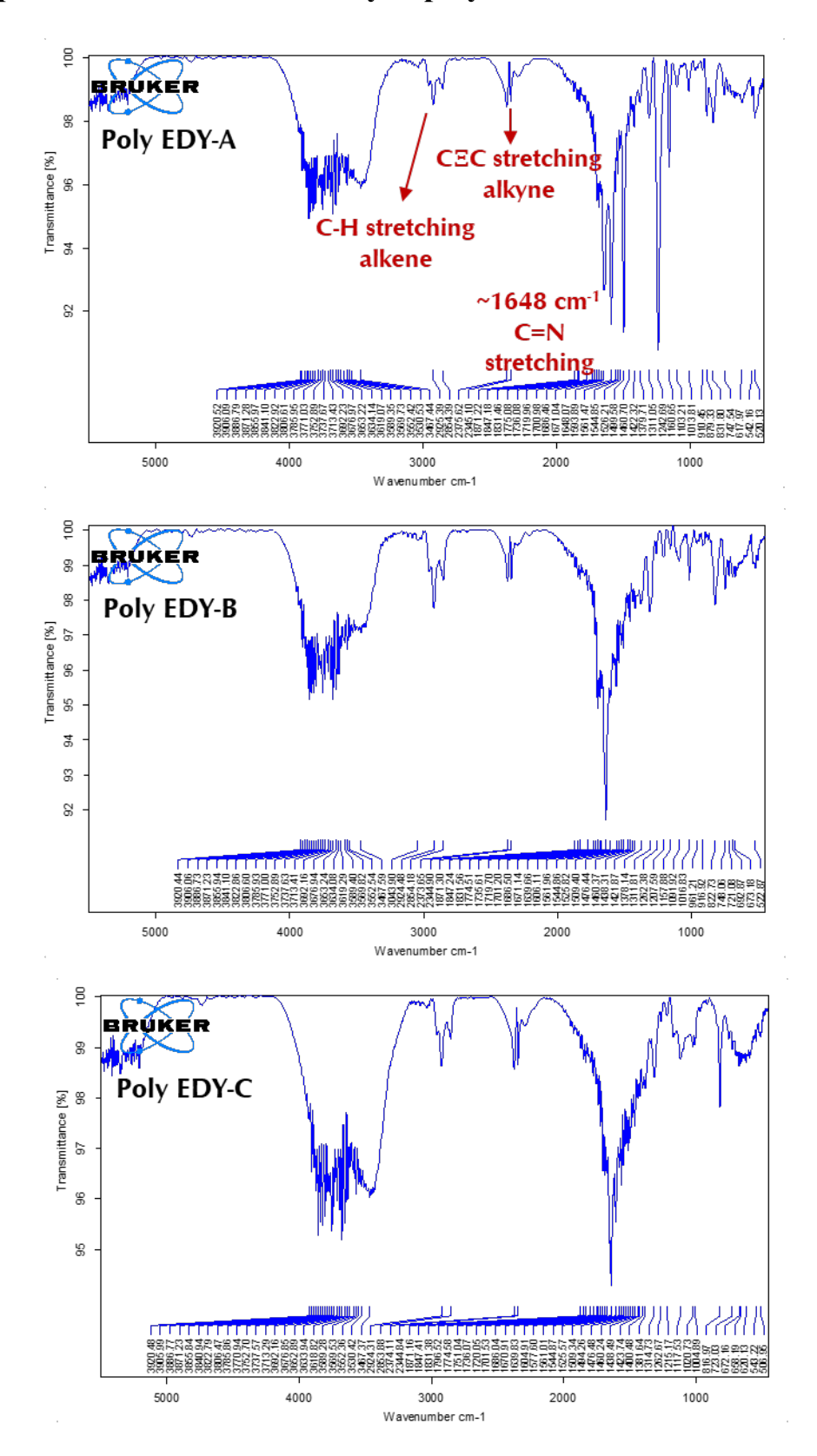


Figure S5 Records of spinning concentration of generated solid particles at room temperature

3. IR spectra of main-chain enediyne polymers



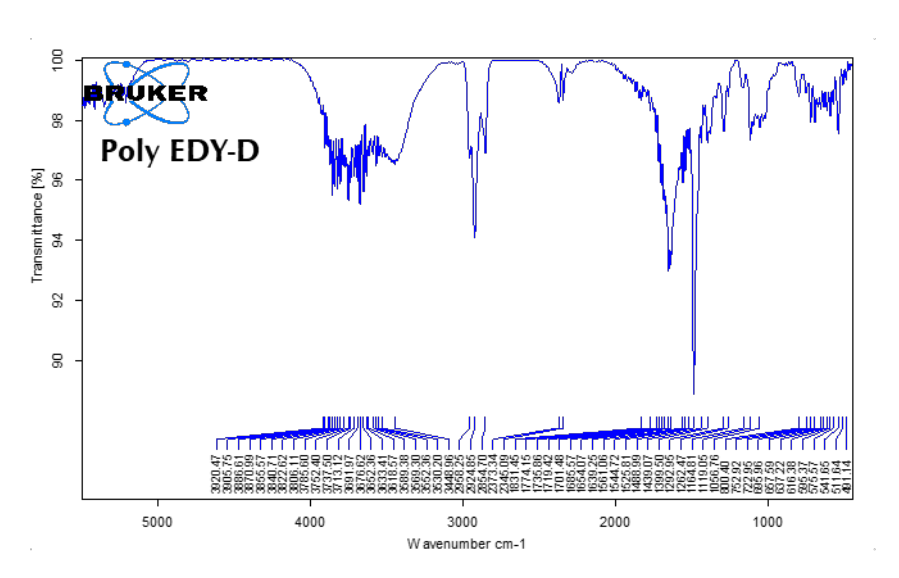


Figure S6 IR spectra of Poly EDY-A/B/C/D

4. NMR Spectra of Model Compounds and Polymers

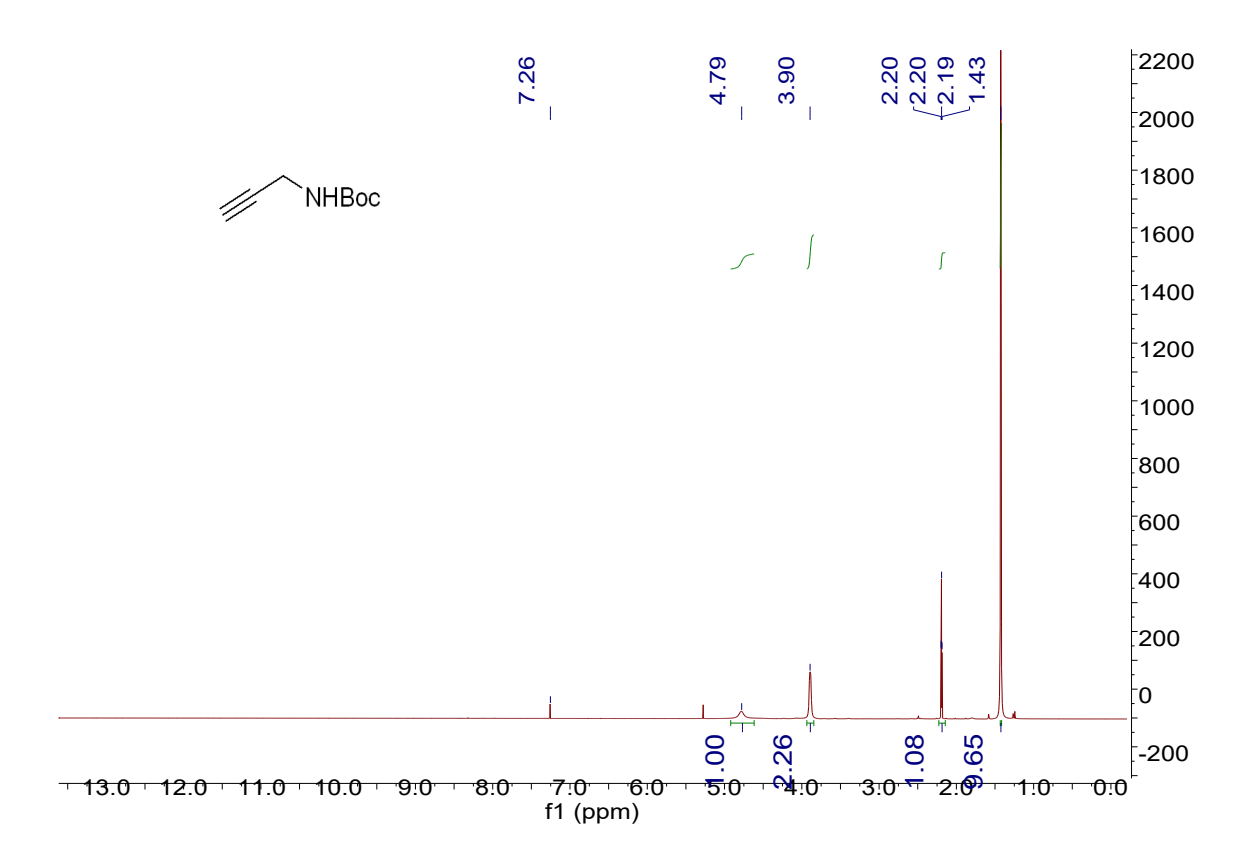


Figure S7 ¹H NMR spectrum of tert-Butyl prop-2-ynylcarbamate

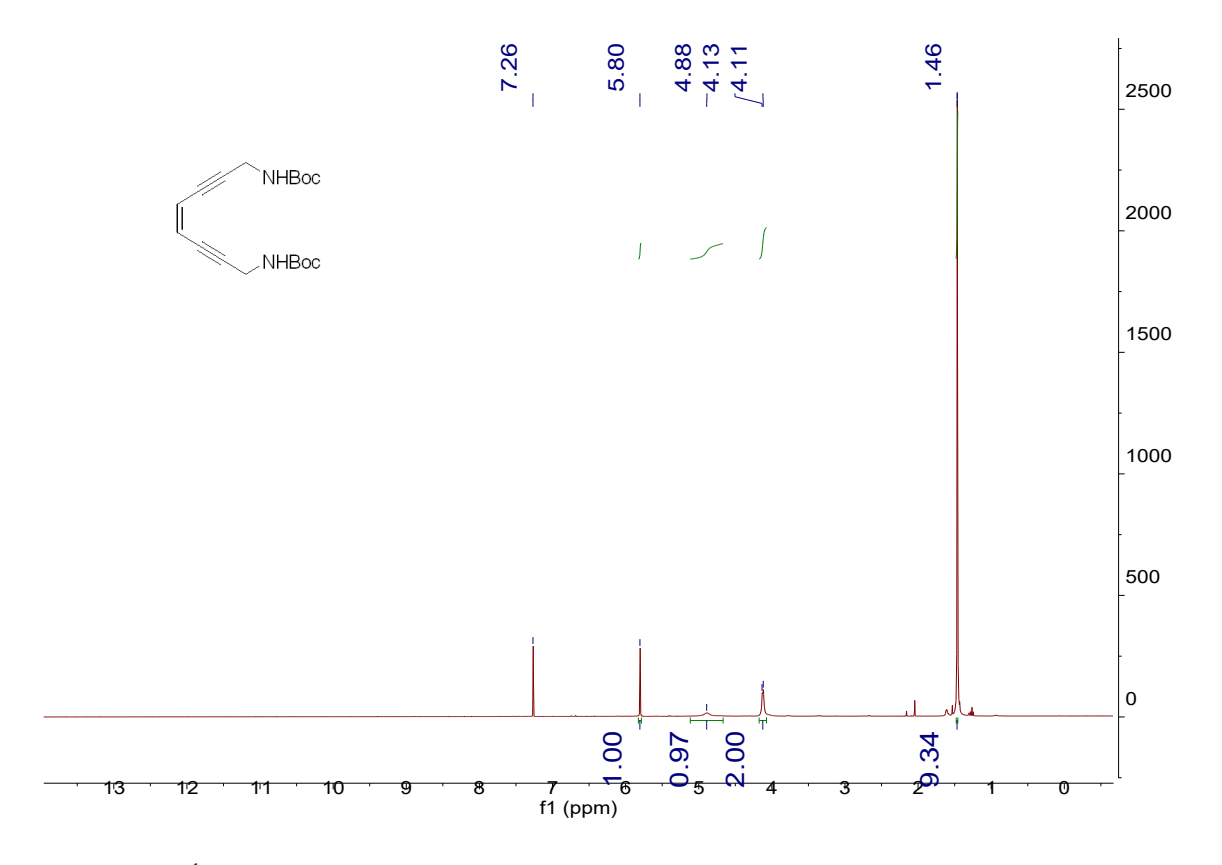


Figure S8 ¹H NMR spectrum of EDY-I: di-tert-butyl octa-4-en-2,6-diyne-1,8-diyl(Z)-dicarbamate

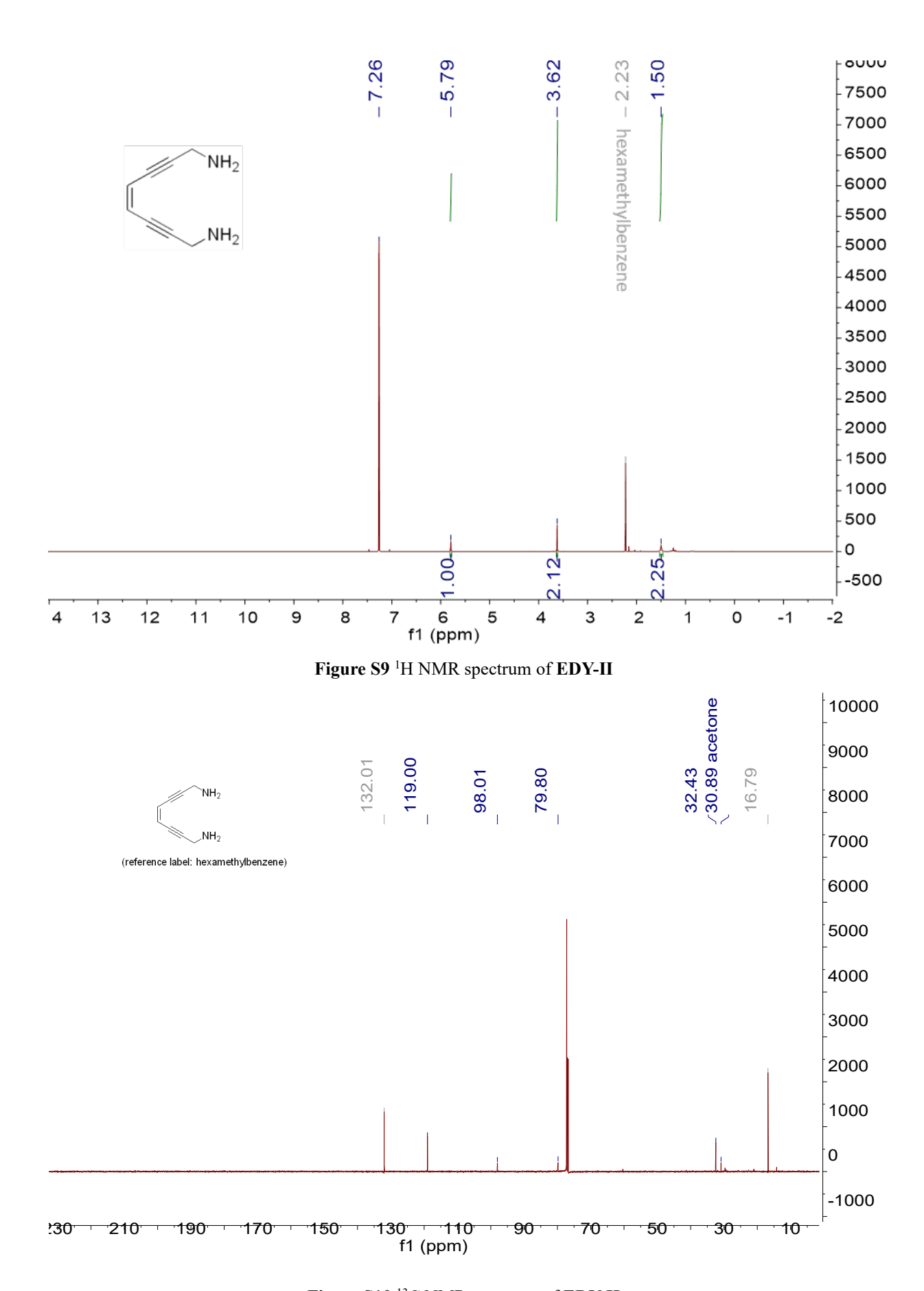


Figure S10 ¹³C NMR spectrum of EDY-II

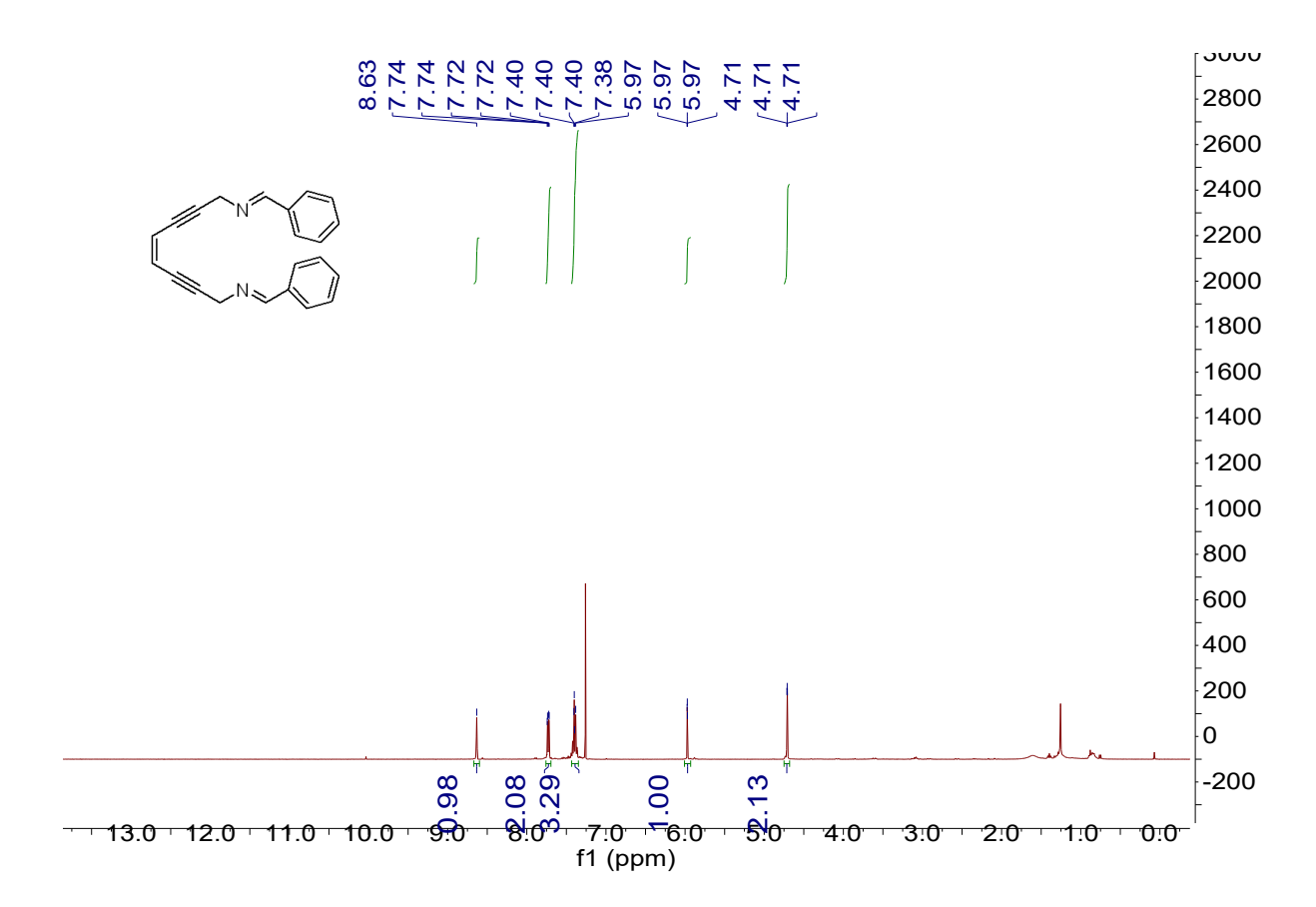


Figure S11 ¹H NMR spectrum of EDY-III

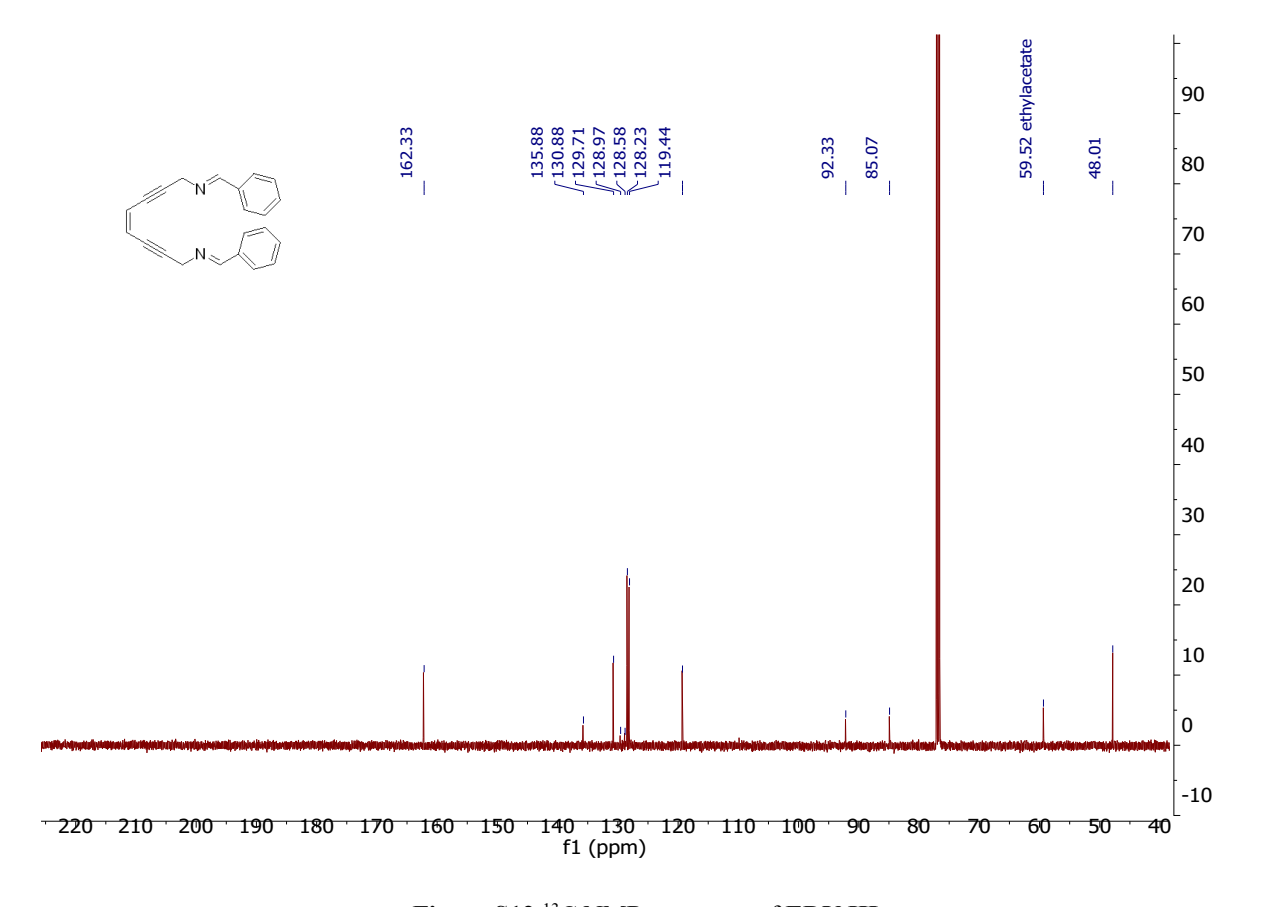


Figure S12 ¹³C NMR spectrum of EDY-III

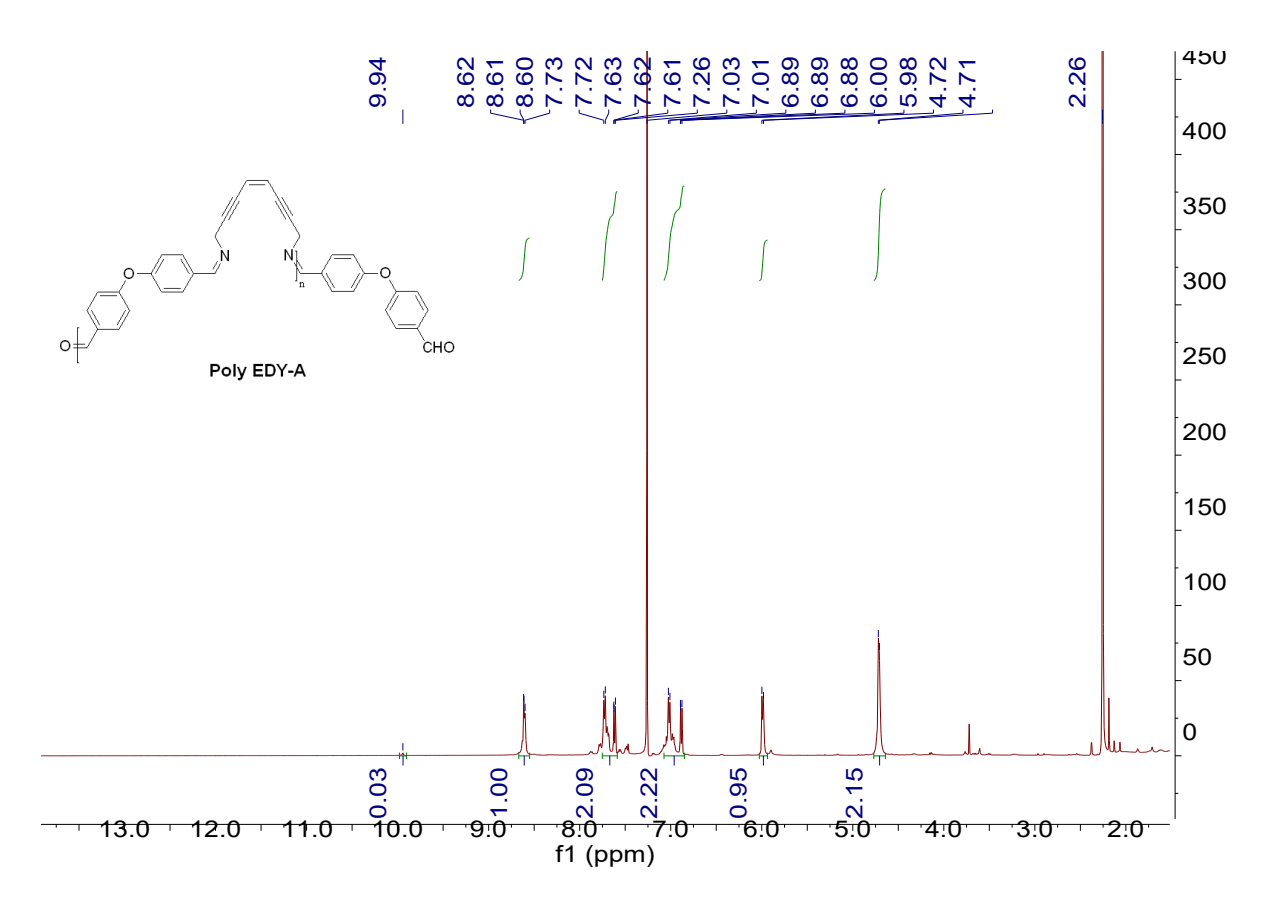


Figure S13 ¹H NMR spectrum of Poly EDY-A

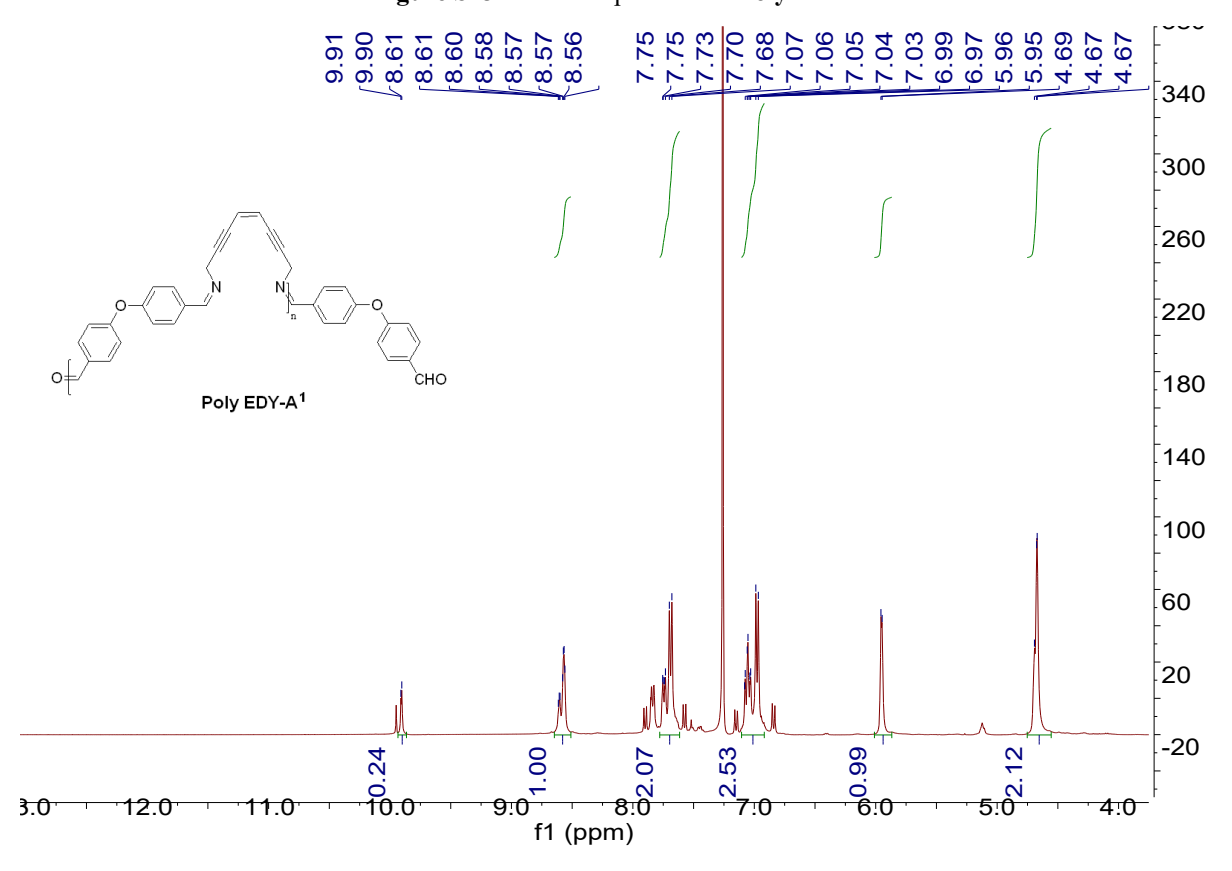


Figure S14 ¹H NMR spectrum of Poly EDY-A¹

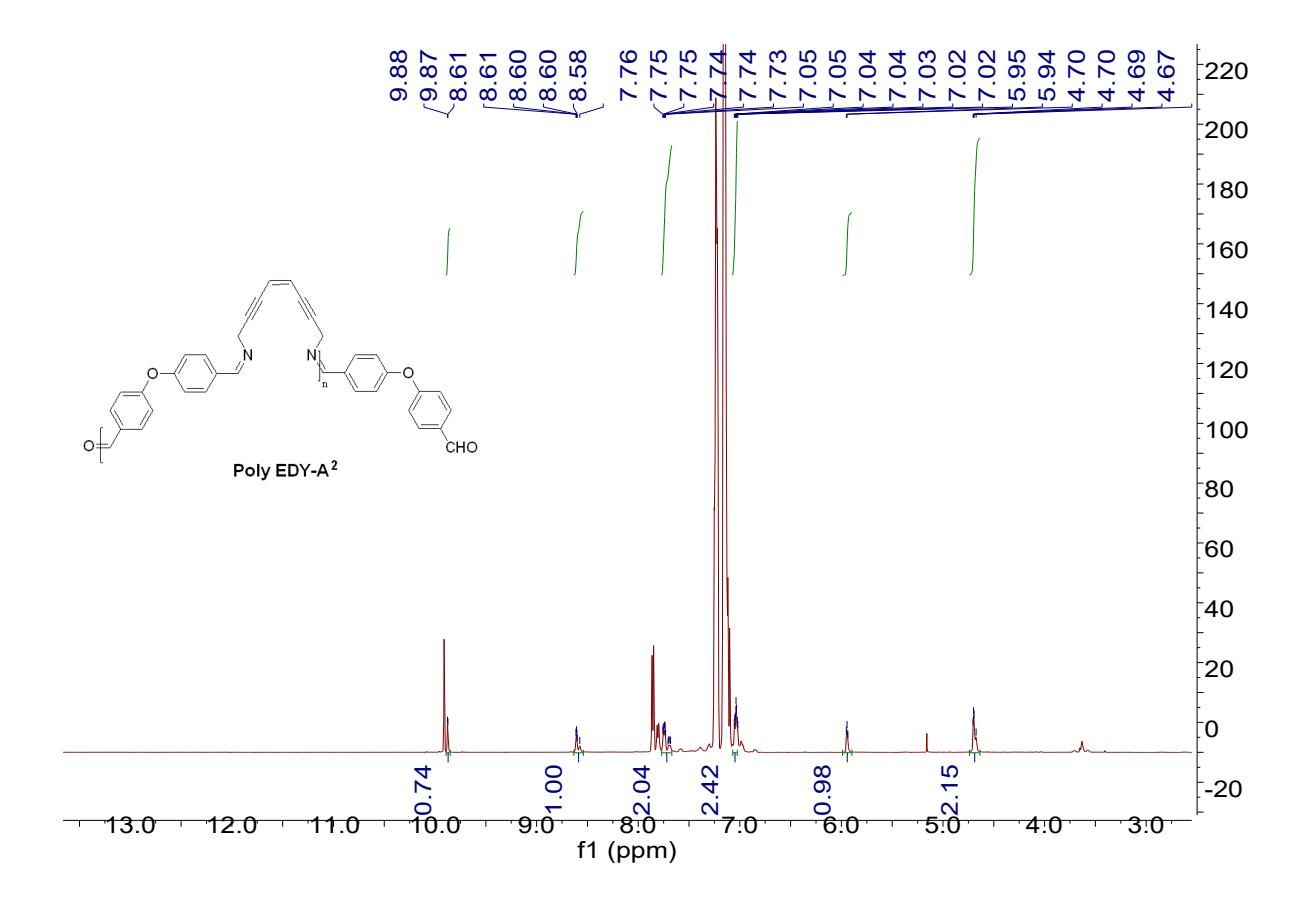


Figure S15 ¹H NMR spectrum of Poly EDY-A²

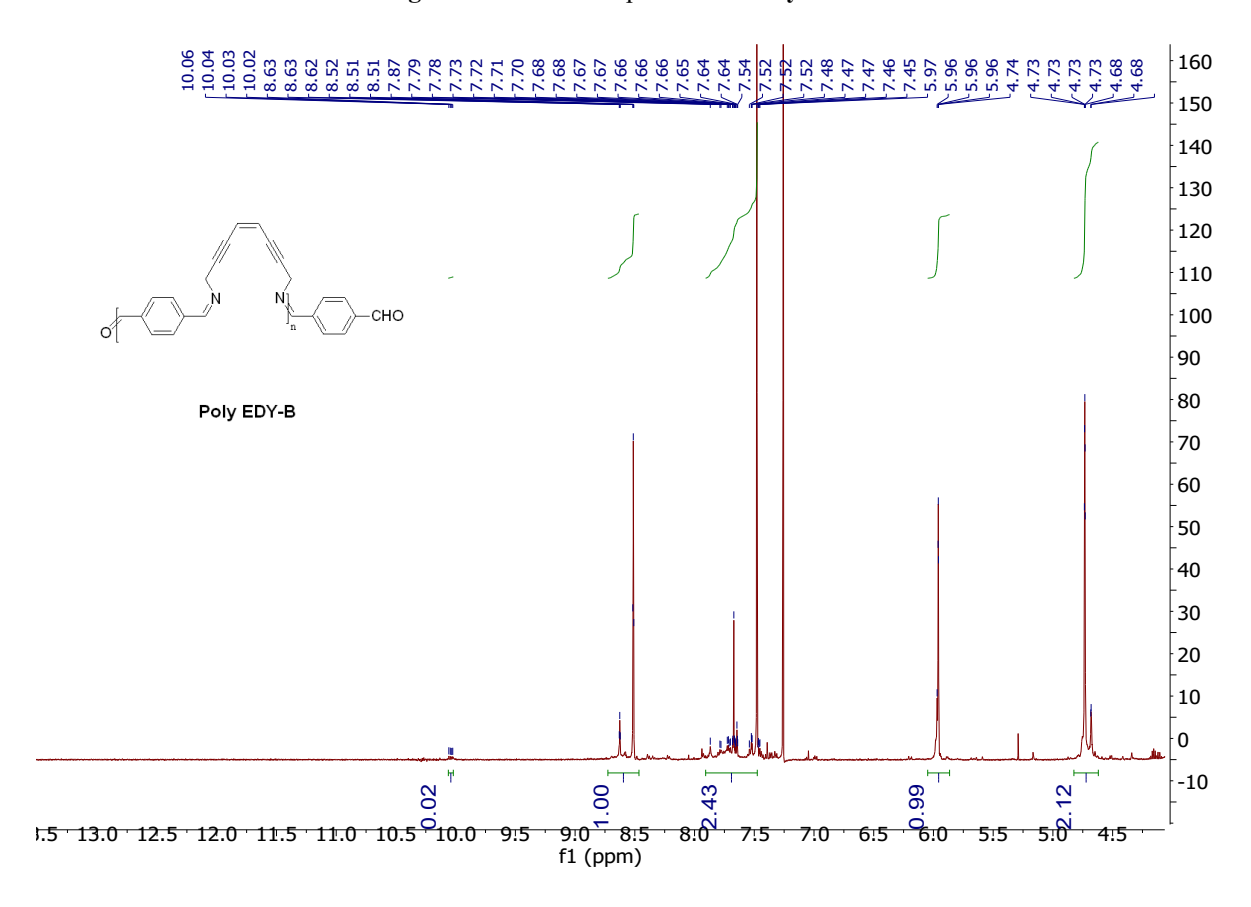


Figure S16 ¹H NMR spectrum of Poly EDY-B

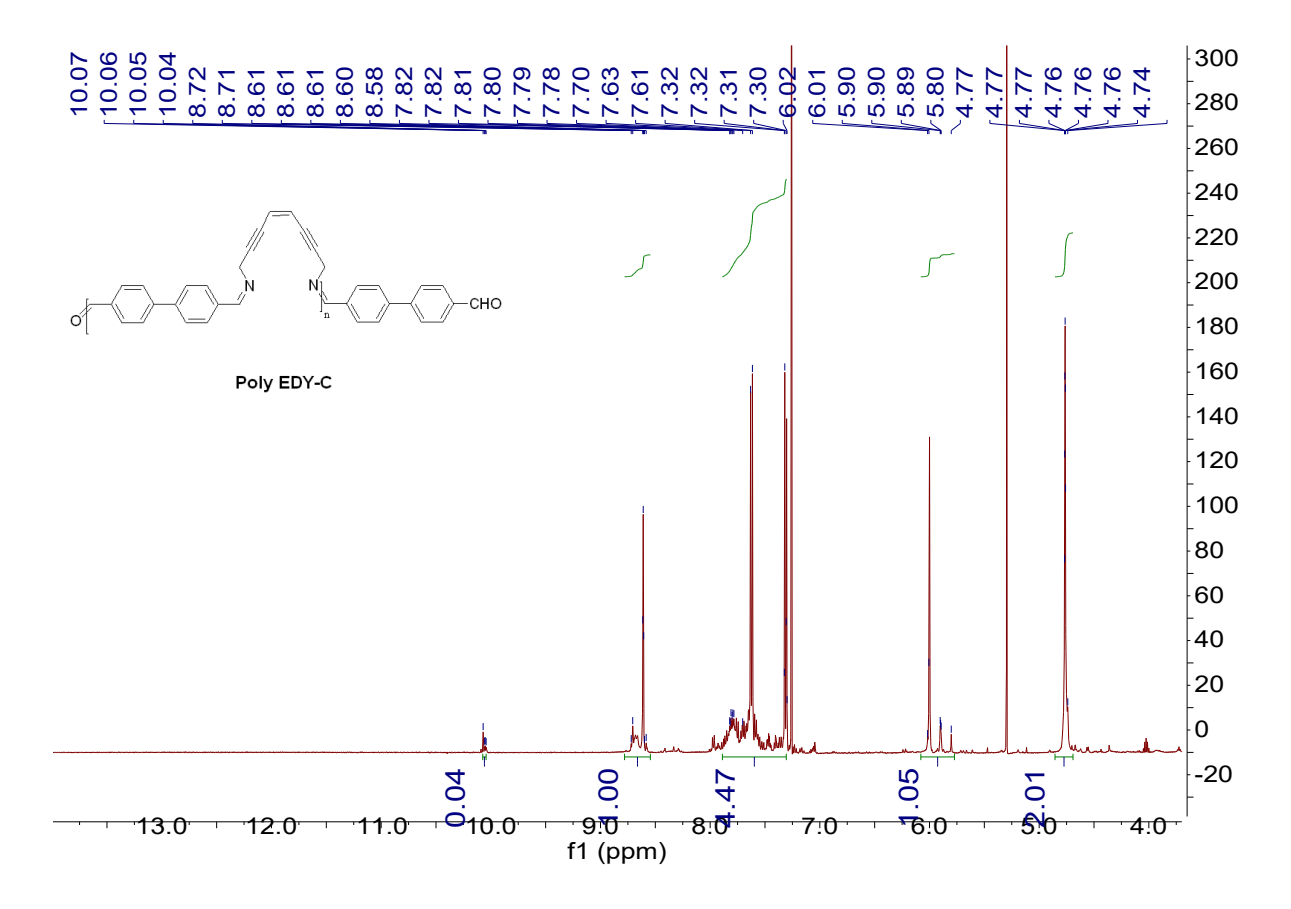


Figure S17 1 H NMR spectrum of Poly EDY-C

5. DSC Curves of Model Compound and Polymers

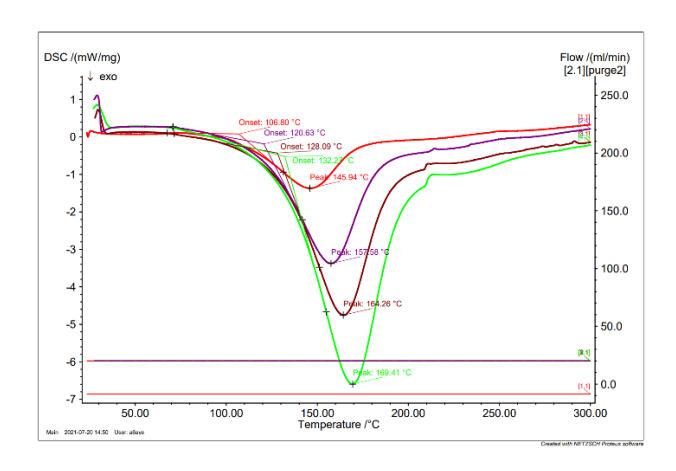


Figure S18 DSC curves of EDY-III under heating rate as 5/10/15/20 K/min

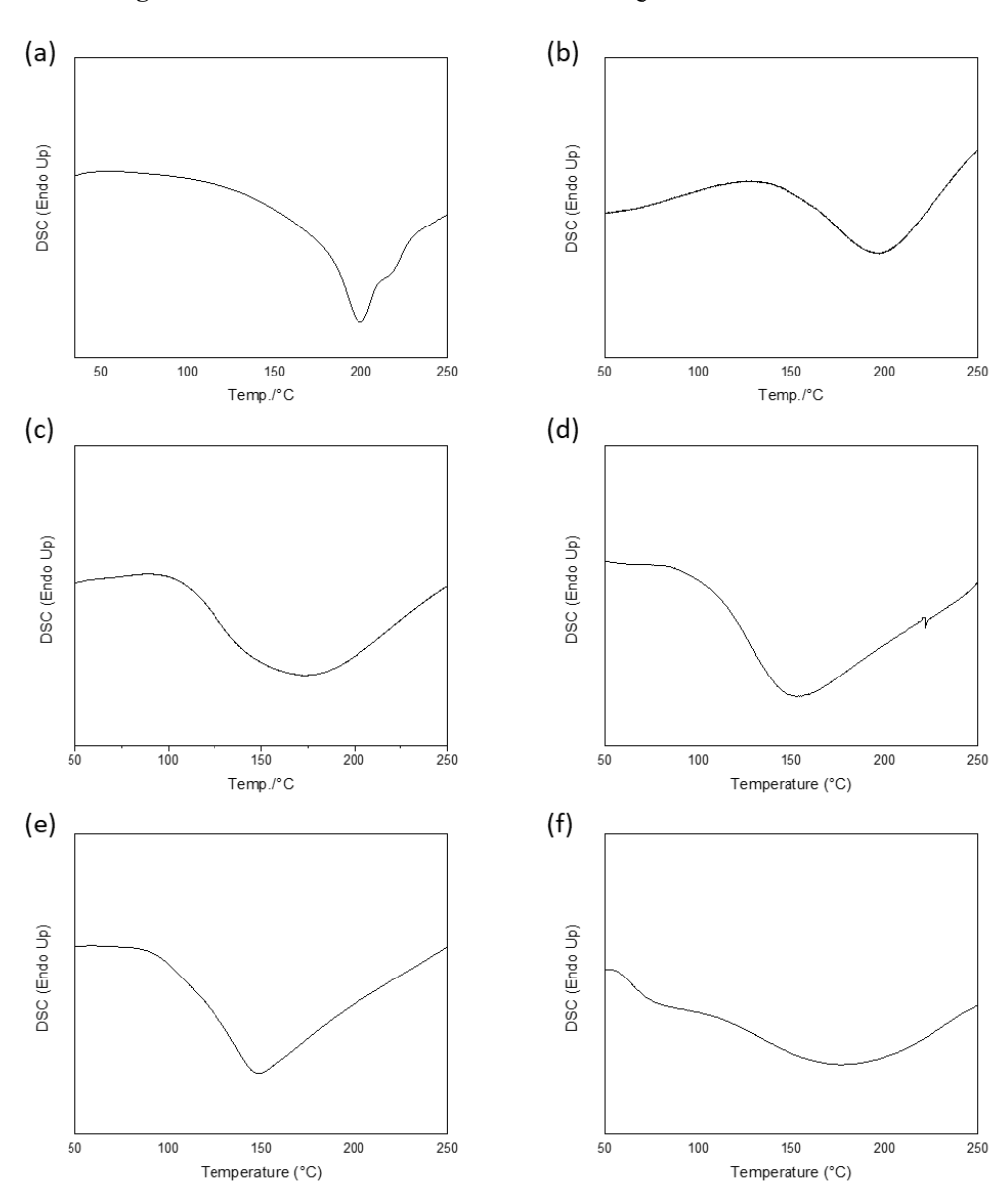
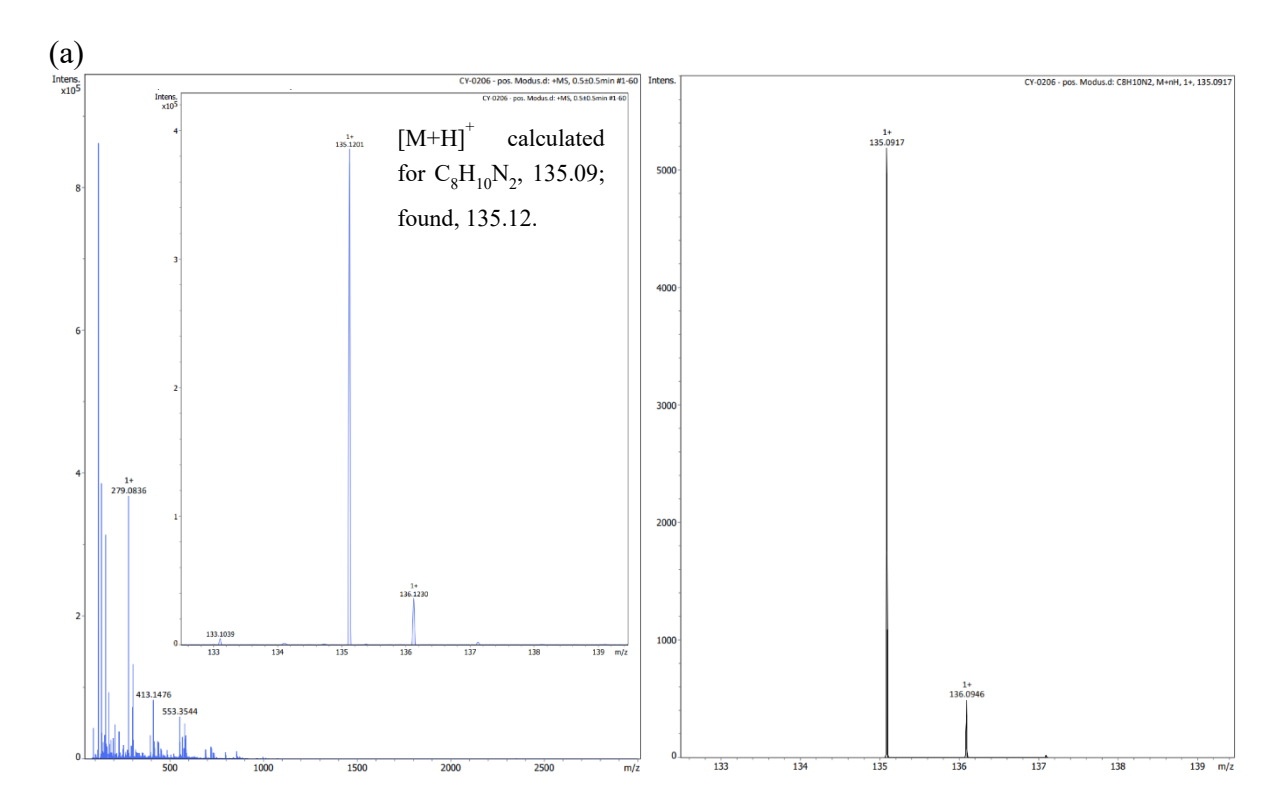
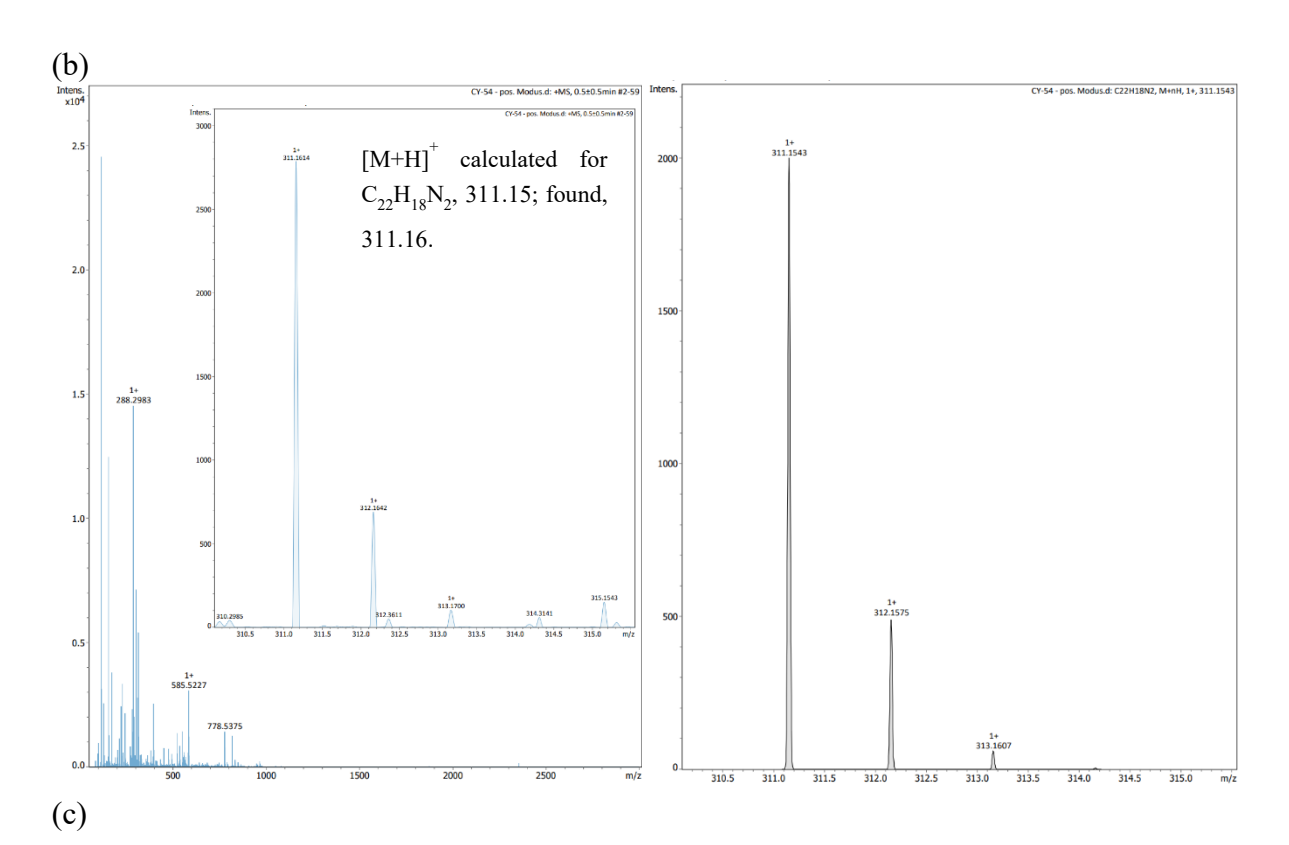


Figure S19 DSC curves of (a) Poly EDY-A; (b) Poly EDY-A¹; (c) Poly EDY-A²; (d) Poly EDY-B; (e) Poly EDY-C; (f) Poly EDY-D under heating rate as 5 K/min

6. ESI-ToF MS Spectra of Model Compounds





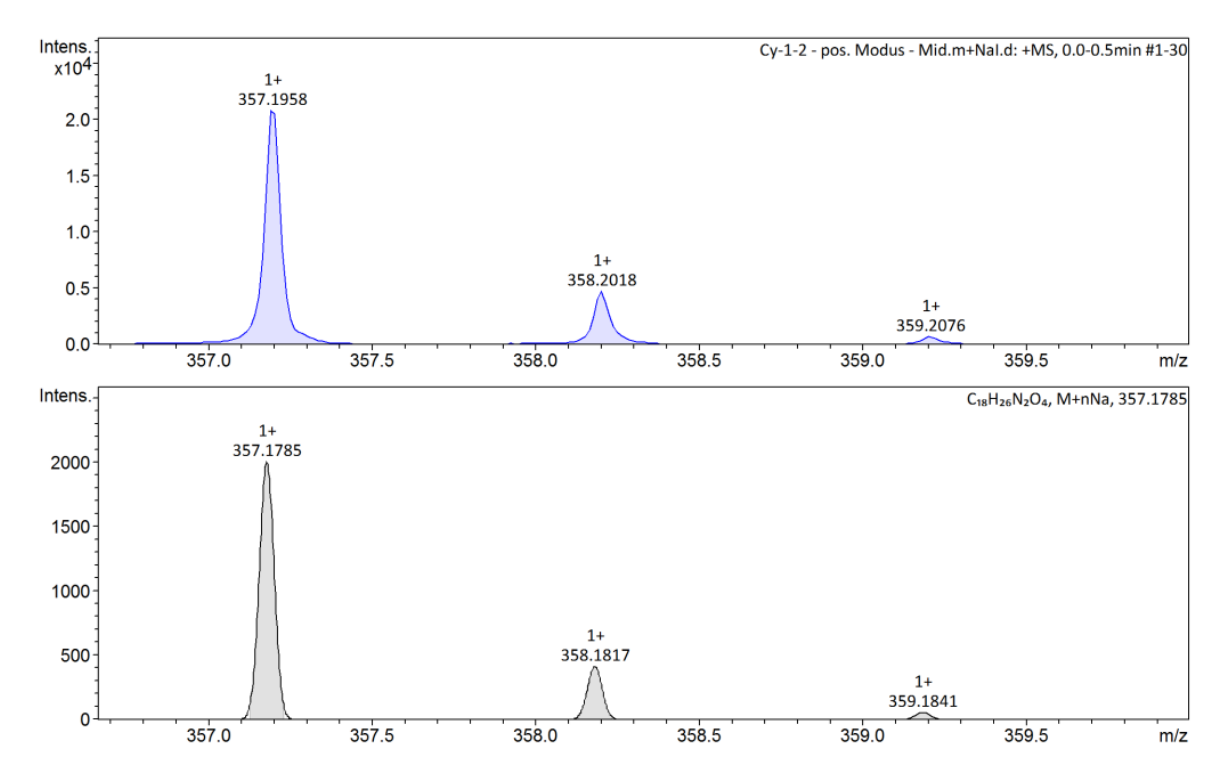


Figure S20 Left: the full experimental ESI-ToF MS spectra and insert: the compound spectra; and right: the simulated isotope pattern of compound (a) EDY II, (b) EDY III. (c) EDY-I.

7. Reference

- 1. G. A. Molander and F. Cadoret, *Tetrahedron Letters*, 2011, **52**, 2199-2202.
- 2. D. S. Rawat and J. M. Zaleski, *Chemical Communications*, 2000, DOI: 10.1039/b0073601, 2493-2494.
- 3. D. S. Rawat and J. M. Zaleski, *Journal of the American Chemical Society*, 2001, **123**, 9675-9676.



Supporting Information

for Macromol. Rapid Commun., DOI 10.1002/marc.202300440

Triggered Crosslinking of Main-Chain Enediyne Polyurethanes via Bergman Cyclization

Yue Cai and Wolfgang H. Binder*

Supporting Information

Triggered Crosslinking of Main-Chain Enediyne Polyurethanes via Bergman-Cyclization

Yue Cai, and Wolfgang H. Binder*

Y. Cai, Prof. W. H. Binder

Macromolecular Chemistry, Institute of Chemistry, Faculty of Natural Science II (Chemistry, Physics and Mathematics), Martin-Luther-University Halle-Wittenberg, von-Danckelmann-Platz 4, Halle D-06120, Germany

* Correspondence: wolfgang.binder@chemie.uni-halle.de

1.	ABB	REVIATIONS3
2.	EXP	ERIMENTAL PART ······3
	2.1.	SOLVENTS AND MATERIALS 3
	2.2.	METHODS AND INSTRUMENTATION
	2.3.	OVERVIEW OF SAMPLES (PIE, PME, PIC)4
	2.4.	SYNTHESIS AND CHARACTERIZATION OF PIE
	2.4.1	Synthesis4
	2.4.2	Copies of ¹ H NMR, GPC, IR4
	2.4.3	Kinetic studies of PIE by DSC6
	2.4.4	UV-Vis monitoring of PIE under heating7
	2.4.5	EPR studies of PIE by DSC·····8
	2.4.6	DSC monitoring of PIE without compression8
	2.5.	SYNTHESIS AND CHARACTERIZATION OF PTHF-MDI-EDY (PME)9
	2.5.1	Synthesis ————9
	2.5.2	Copies of ¹ H NMR, GPC, IR ·····9
	2.5.3	Kinetic studies of PME by DSC······11
	2.5.4	DSC curves of PME samples with or without compression12
	2.6.	SYNTHESIS AND CHARACTERIZATION OF PIC
		Synthesis13
	2.6.2	Copies of ¹ H NMR, GPC, IR ·······13
	2.7.	CALCULATION OF CROSSLINK DENSITIES OF PIE-HEATED AND PIE-COMPRESSED

1. Abbreviations

Bergman Cyclization (BC), Enediyne (EDY), Differential scanning calorimetry (DSC), Nuclear magnetic resonance (NMR), Infrared (IR), Fourier transformation (FT), Tetrahydrofuran (THF), N, N-dimethylformamide (DMF), Chloroform (CHCl₃), Deuterated chloroform (CDCl₃), Isophorone diisocyanate (IPDI), Methylene diphenyl diisocyanate (MDI), Polytetrahydrofuran (PTHF), 1,8-diazabicyclo[5.4.0]undec-7-ene (DBU), Polytetrafluoroethylene (PTFE)

2. Experimental Part

2.1. Solvents and Materials

Deuterium chloroform (CDCl₃-d) was used as NMR deuterium solvents.

Dry solvents were prepared as follows: THF, purchased from Roth, was predried over potassium hydroxide for several days and refluxed over sodium and benzophenone under inert atmosphere and distilled freshly before use; DMF, purchased from Grüssing was stored over calcium hydride for several days before use.

Isophorone diisocyanate, octane-1,8-diamine, bis(hydroxyl)-telechelic Polytetrahydrofuran (average Mn ~2,900 g/mol), 1,8-diazabicyclo[5.4.0]undec-7-ene were purchased from Sigma-Aldrich, Methylene diphenyl diisocyanate was purchased from Alfa Aesar. All chemicals listed here were used without any purification unless otherwise stated.

2.2. Methods and Instrumentation

DSC measurements were done on a Netzsch DSC 204 F1. Samples pieces with a mass of 5 − 10 mg were placed into aluminum crucibles and were heated under nitrogen atmosphere with a heating rate of 5 K·min⁻¹ unless otherwise stated. Evaluation of the measured data was done with Netzsch Proteus Analytic software.

NMR-spectra were measured on a Varian Gemini 400 spectrometer at 27°C. The ¹H-NMR spectra were recorded at 400 MHz or 500 MHz and for ¹³C-NMR spectroscopy 100 MHz were used. The samples were dissolved in CDCl₃. The NMR spectra were interpreted using MestReNova software (version 9.0.1-13254). Chemical shifts were given in ppm and coupling constants were given in Hz.

ATR-FTIR-spectra were measured on a Bruker Tensor VERTEX 70 spectrometer equipped with a Golden Gate Diamond ATR top-plate. For each measurement 32 background scans and 32 sample scans were averaged. The data were analyzed using Opus 6.5 software.

Tensile tests were performed using a universal testing machine (Z010, Zwick/Roell) at room temperature and a testing speed of 20 mm/min. Dog-bone shaped samples with a total length of 20 mm, a width of grip section of 6 mm, a thickness of 2 mm, a gage length of 12 mm and a

width of 2 mm. Each measurement was repeated at least 3 times. Engineering stress and strain values were calculated based on force and displacement as well as initial specimen dimensions:

2.3. Overview of samples (PIE, PME, PIC)

Table S1 Overview of samples

Commis	Compositions			Characterizations	
Sample	Preplolymer 1 equiv.	Diisocyanate 1 equiv.	Diamine 1 equiv.	GPC	Ea of BC
PIE	PTHF	IPDI OCN NCO	NH ₂	10.6 kDa	20.1
PME	HO(~~~o),H	MDI OCN NCO	NH ₂	25.3 kDa	14.1
PIC		IPDI OCN NCO	H ₂ N NH ₂	8.6 kDa	_

2.4. Synthesis and characterization of PIE

Figure S1 Structure of PIE

2.4.1 Synthesis

Bis(hydroxyl)-telechelic poly(tetrahydrofurane) PTHF (0.58 g, 0.2 mmol, Mn = 2900 g/mol) was weight into a 50 mL two-necked round bottom flask. Subsequently the flask was heated at 50 °C under vacuum for at least 1 hour. After drying, 0.5 mL dry, degassed THF was added to dissolve PTHF. Isophorone diisocyanate (88.9 mg, 0.4 mmol) was weight directly into one Schlenk tube, dissolved in 0.3 mL dry, degassed THF and added to the PTHF flask. Afterwards, an additional portion of 1 mL dry, degassed THF was added by rinsing on the glass wall. The reaction mixture would be stirring for 15 minutes at room temperature. Subsequently, two drops 1,8-diazabicyclo[5.4.0]undec-7-ene was added and the reaction mixture was stirred for further 15 minutes at room temperature. Parallelly, 0.2 mmol of (Z)-octa-4-en-2,6-diyne-1,8-diamine^[1, 2] in CHCl₃ (0.5 mL) was added 15 minutes after the DBU addition to the main reaction mixture. The mixture was allowed to stir for another 15 minutes before pouring into PTFE mold.

2.4.2 Copies of ¹H NMR, GPC, IR

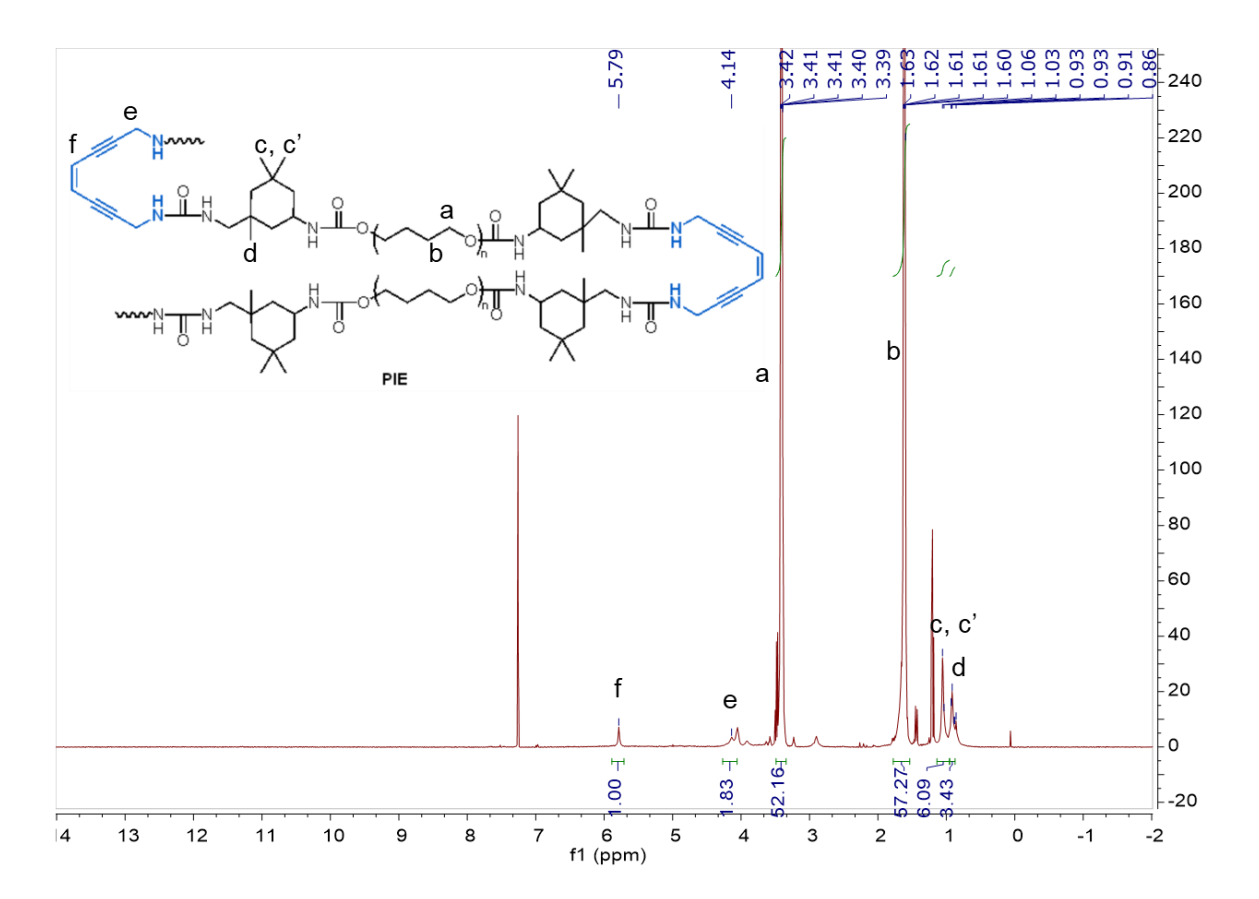


Figure S2 ¹H NMR of PIE

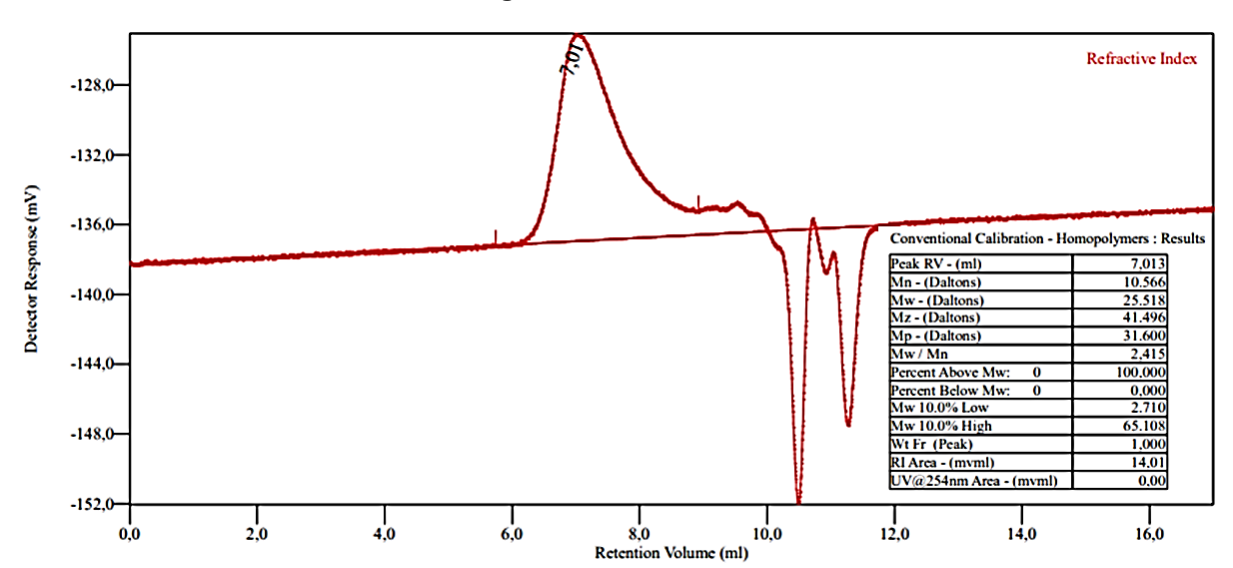


Figure S3 GPC of PIE

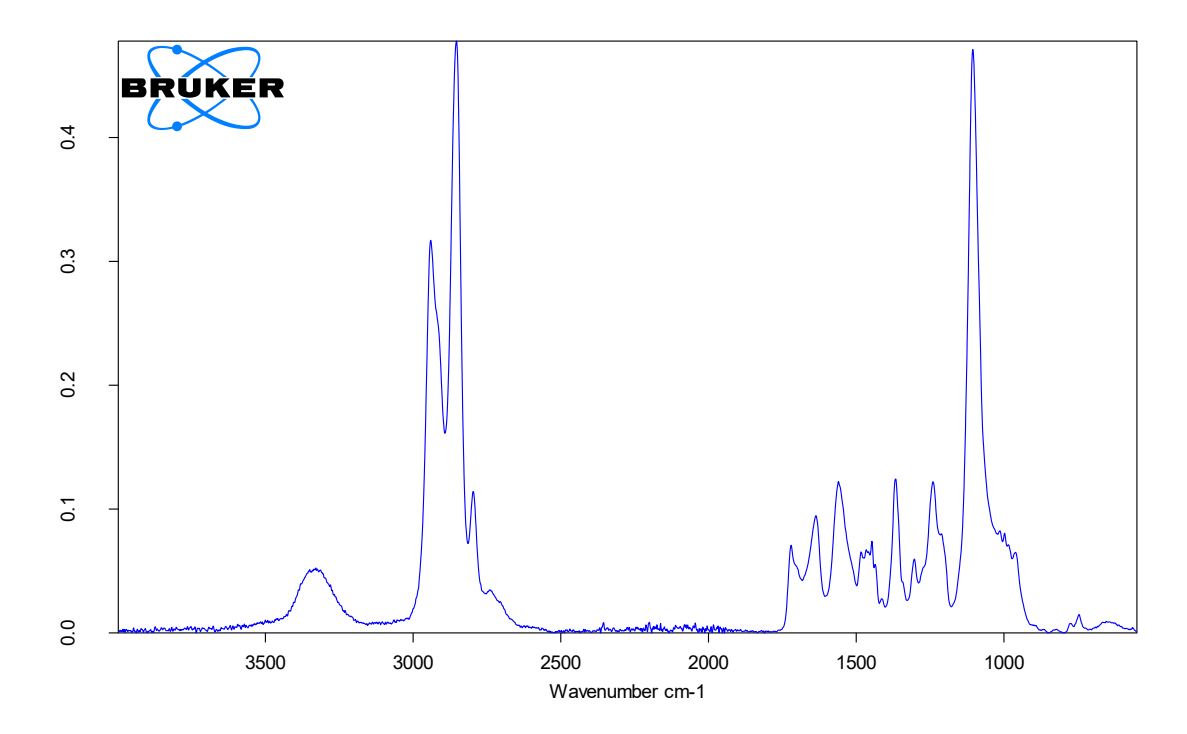


Figure S4 IR spectra of PIE

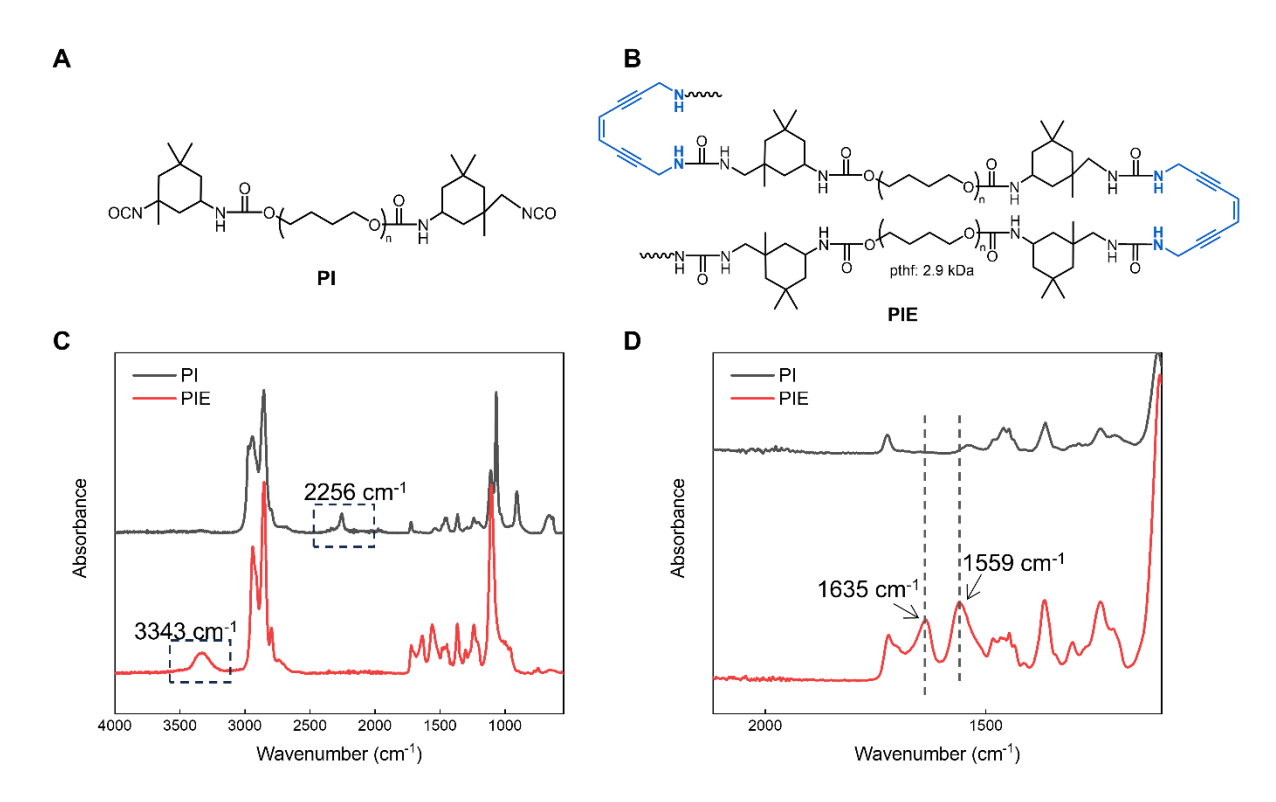


Figure S5 Comparison of IR spectra of PIE

2.4.3 Kinetic studies of PIE by DSC

Table S2 Data from DSC measurements of PIE (Run 1)

Heating Rate (K/min)	T _{peak} (°C)
5	145.96
10	158.86

15	165.36
20	171.84

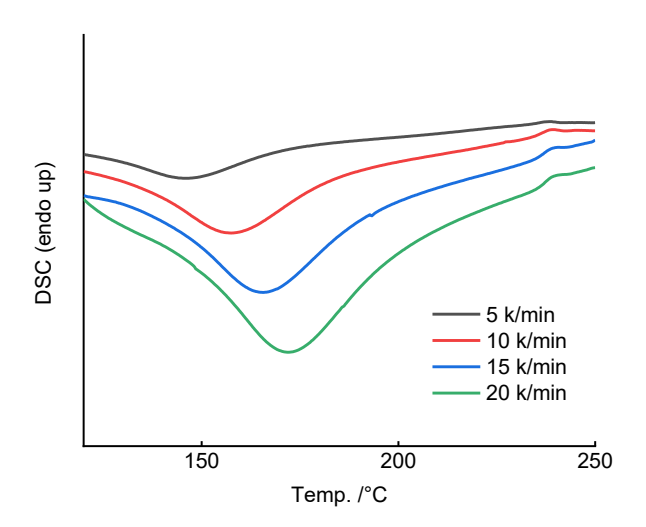


Figure S6 DSC thermograms of PIE at four heating rates (HR) of 5, 10, 15 and 20 K/min.

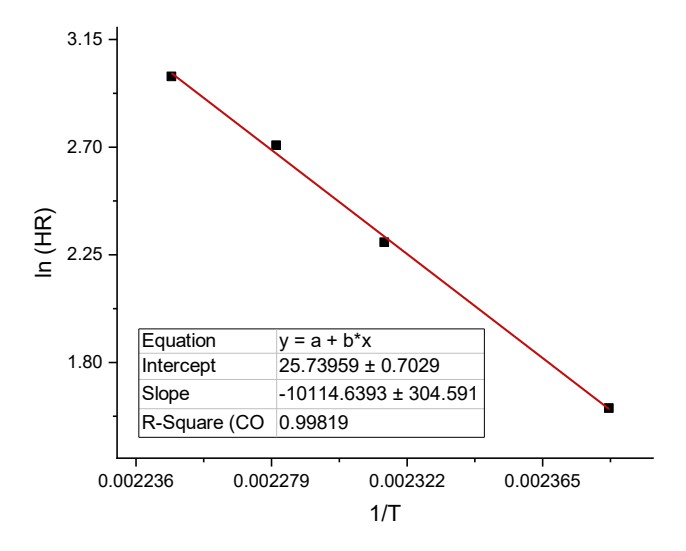


Figure S7 Arrhenius plot for the Bergman cyclization of **PIE** in neat obtained by DSC measurements using ASTM E698 standard procedure.

$$k = A \cdot e^{-Ea/RT}$$

$$\ln k = -\frac{Ea}{R} \left(\frac{1}{T}\right) + \ln A$$

$$\ln(HR) = -\frac{Ea}{R} \left(\frac{1}{T}\right) + \ln A$$

 $Ea = -slope \cdot R$, where slope is the value of slope derived from the Arrhenius plot R-gas constant, $1.9858775(34) \times 10^{-3} \text{ kcal} \times \text{K}^{-1} \times \text{mol}^{-1}$

$$Ea = 1.9859 \times 10^{-3} \times 10114.639 = 20.1 \text{ kcal/mol}$$

2.4.4 UV-Vis monitoring of PIE under heating

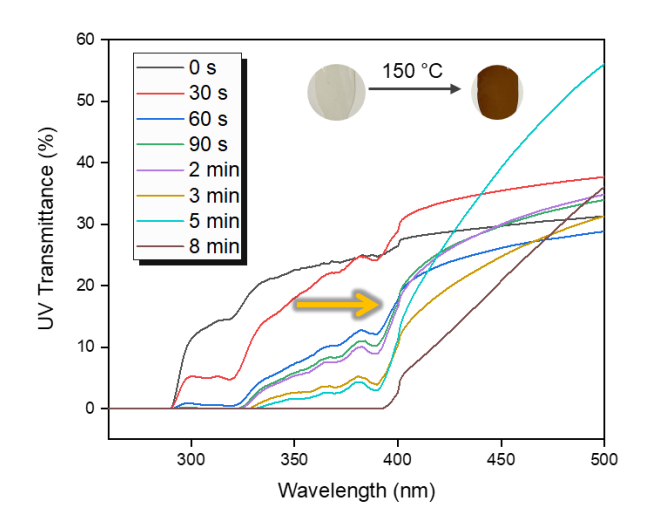


Figure S8 UV-Vis monitoring of PIE under heating

2.4.5 EPR studies of PIE by DSC

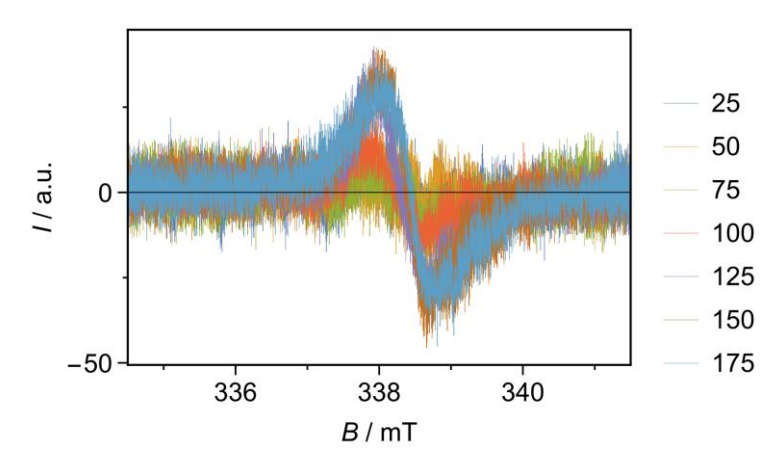


Figure S9 EPR spectra of **PIE** at each temperature (25 °C, 50 °C, 75 °C, 100 °C, 125 °C, 150 °C, 175 °C)

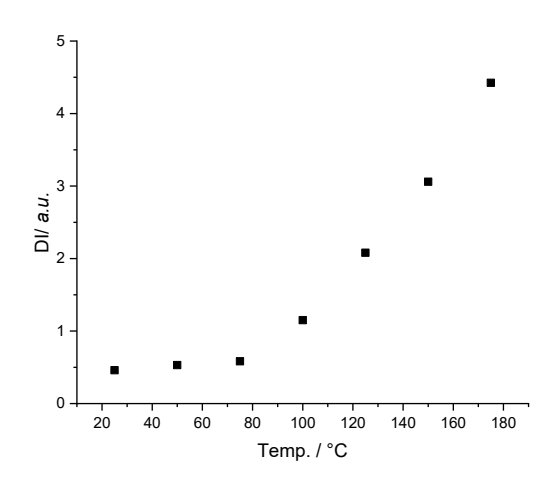


Figure S10 Double integral (DI) calculated from EPR spectra at each temperature (25 °C, 50 °C, 75 °C, 100 °C, 125 °C, 150 °C, 175 °C)

2.4.6 DSC monitoring of PIE without compression

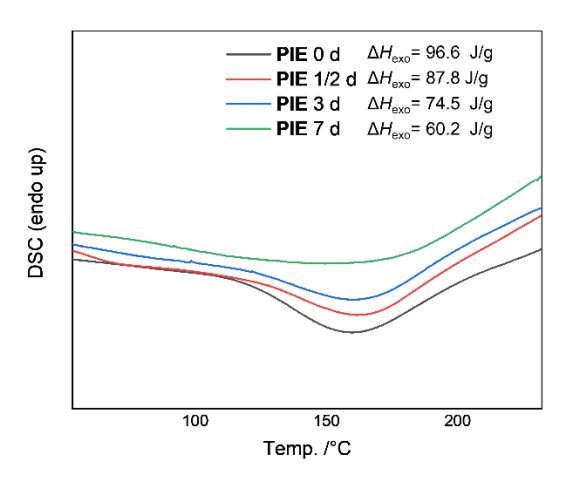


Figure S11 DSC curves of PIE without compression after 12 h, 3 d, 7 d.

2.5. Synthesis and characterization of PTHF-MDI-EDY (PME)

Figure S12 Structure of PME

2.5.1 Synthesis

Bis(hydroxyl)-telechelic poly(tetrahydrofurane) PTHF (0.58 g, 0.2 mmol, Mn = 2900 g/mol) was weight into a 50 mL two-necked round bottom flask. Subsequently the flask was heated at 50 °C under vacuum for at least 1 hour. After drying, 0.5 mL dry, degassed THF was added to dissolve PTHF. Methylene diphenyl diisocyanate (100.1 mg, 0.4 mmol) was weight directly into one Schlenk tube, dissolved in 0.3 mL dry, degassed THF and added to the PTHF flask. Afterwards, an additional portion of 1 mL dry, degassed THF was added by rinsing on the glass wall. The reaction mixture would be stirring for 15 minutes at room temperature. Subsequently, two drops 1,8-diazabicyclo[5.4.0]undec-7-ene was added and the reaction mixture was stirred for further 15 minutes at room temperature. Parallelly, 0.2 mmol of (Z)-octa-4-en-2,6-diyne-1,8-diamine^[1,2] in CHCl₃ (0.5 mL) was added 15 minutes after the DBU addition to the main reaction mixture. The mixture was allowed to stir for another 15 minutes before pouring into PTFE mold.

2.5.2 Copies of ¹H NMR, GPC, IR

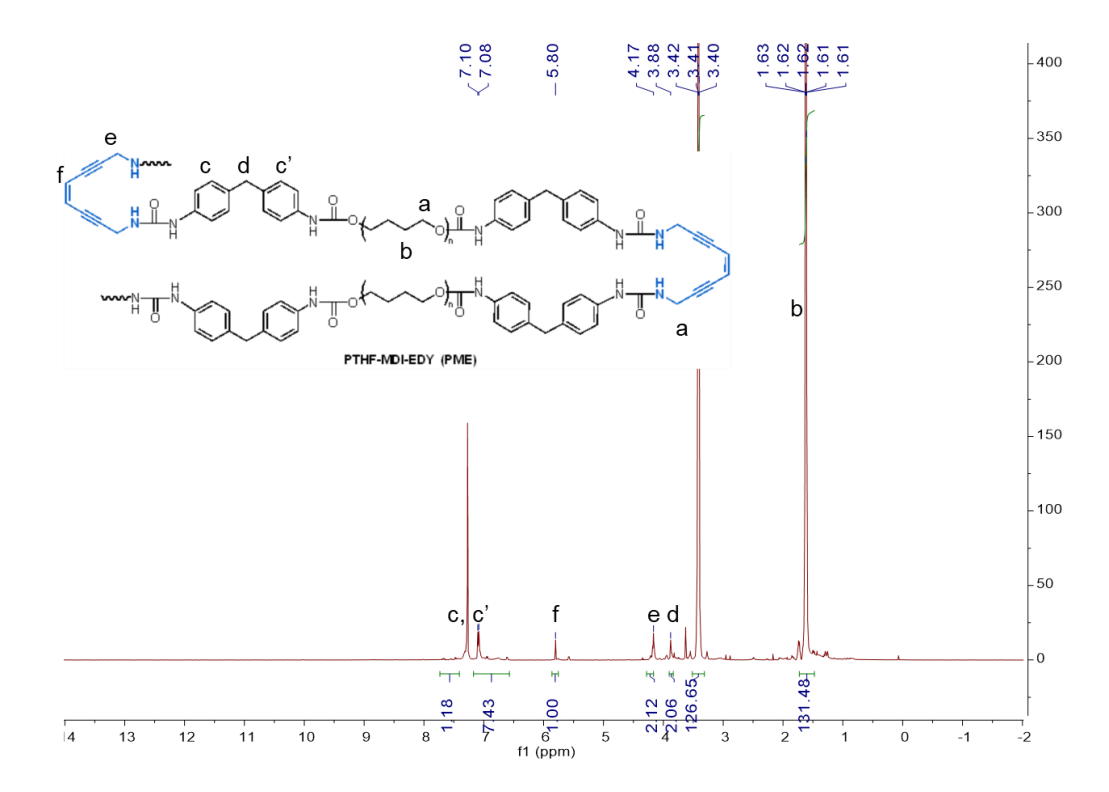


Figure S13 ¹H NMR of PME

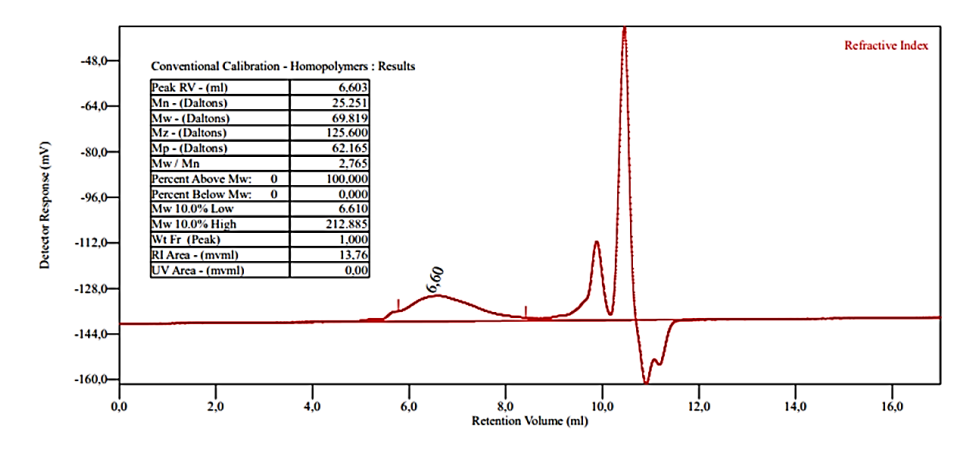


Figure S14 GPC of PME

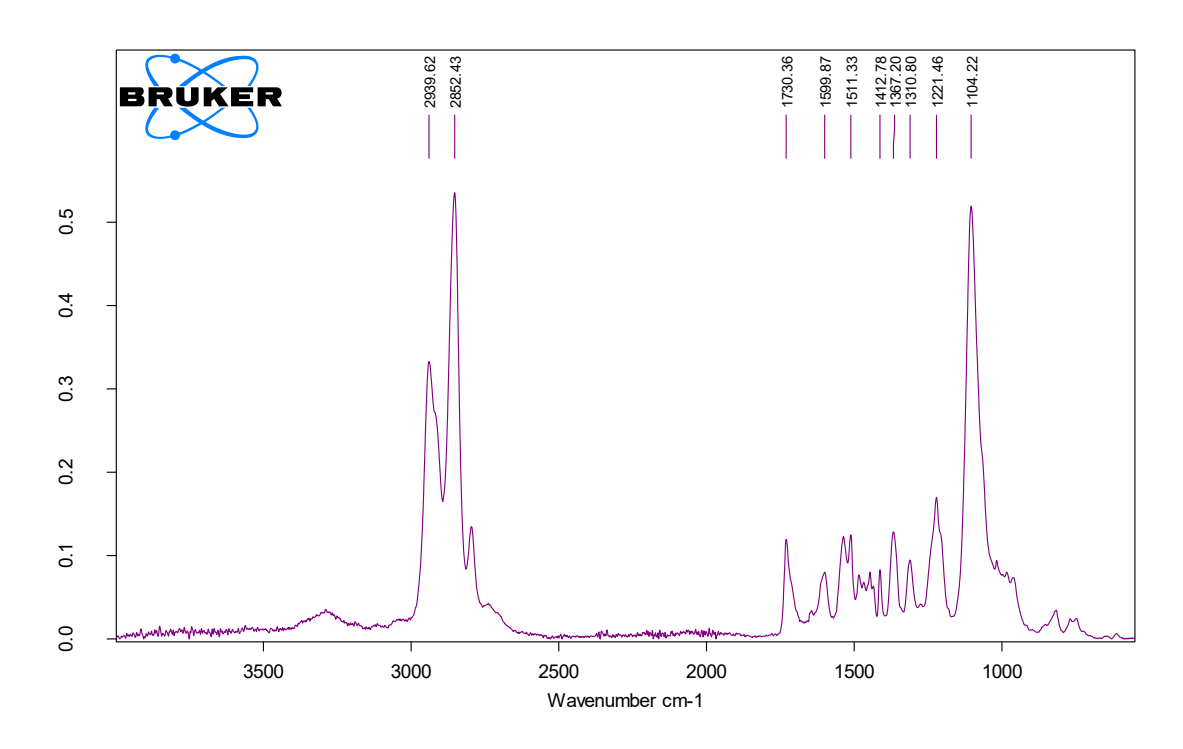


Figure S15 IR spectra of PME

2.5.3 Kinetic studies of PME by DSC

Table S3 Data from DSC measurements of PME (Run 1)

Heating Rate (K/min)	T _{peak} (°C)
5	127.53
10	142.62
15	150.06
20	162.63

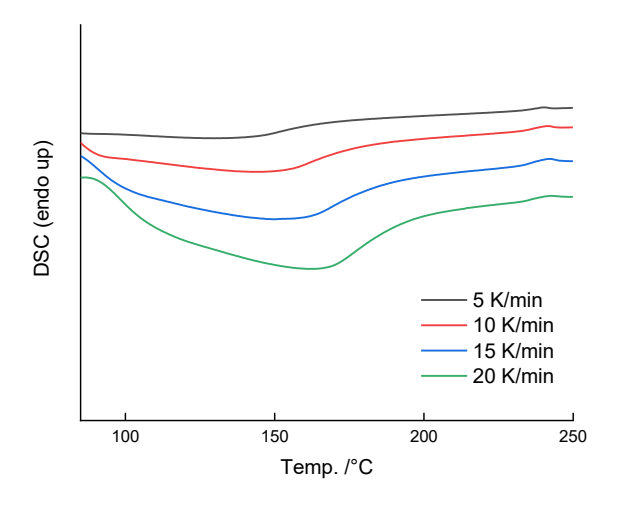


Figure S16 DSC thermograms of PME at four heating rates (HR) of 5, 10, 15 and 20 K min⁻¹

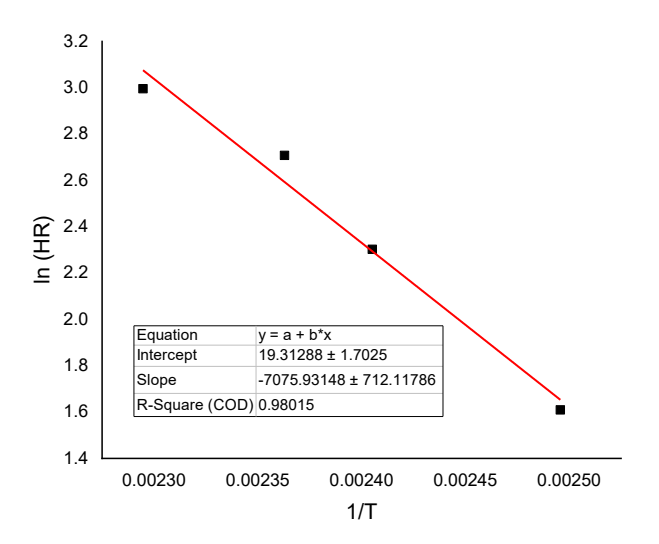


Figure S17 Arrhenius plot for the Bergman cyclization of **PME** in neat obtained by DSC measurements using ASTM E698 standard procedure.

$$k = A \cdot e^{-Ea/RT}$$

$$\ln k = -\frac{Ea}{R} \left(\frac{1}{T}\right) + \ln A$$

$$\ln(HR) = -\frac{Ea}{R} \left(\frac{1}{T}\right) + \ln A$$

 $Ea = -slope \cdot R$, where slope is the value of slope derived from the Arrhenius plot R-gas constant, $1.9858775(34) \times 10^{-3} \text{ kcal} \times \text{K}^{-1} \times \text{mol}^{-1}$

$$Ea = 1.9859 \times 10^{-3} \times 7075.931 = 14.1 \text{ kcal/mol}$$

2.5.4 DSC curves of PME samples with or without compression

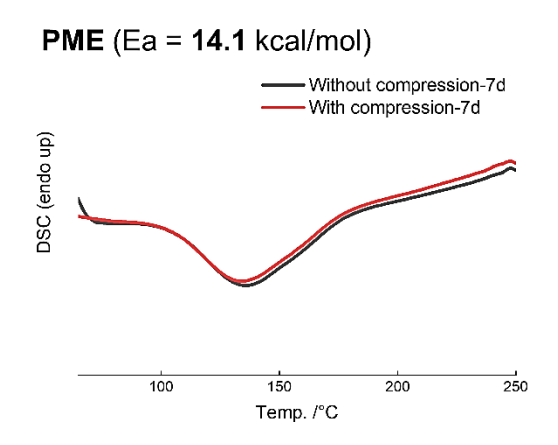


Figure S18 DSC curves of two PME samples with the treatment of compression for 7 days or without

2.6. Synthesis and characterization of PIC

Figure S19 Structure of PIC

2.6.1 Synthesis

Bis(hydroxyl)-telechelic poly(tetrahydrofurane) PTHF (0.58 g, 0.2 mmol, Mn = 2900 g/mol) was weight into a 50 mL two-necked round bottom flask. Subsequently the flask was heated at 50 °C under vacuum for at least 1 hour. After drying, 0.5 mL dry, degassed THF was added to dissolve PTHF. Isophorone diisocyanate (88.9 mg, 0.4 mmol) was weight directly into one Schlenk tube, dissolved in 0.3 mL dry, degassed THF and added to the PTHF flask. Afterwards, an additional portion of 1 mL dry, degassed THF was added by rinsing on the glass wall. The reaction mixture would be stirring for 15 minutes at room temperature. Subsequently, two drops 1,8-diazabicyclo[5.4.0]undec-7-ene was added and the reaction mixture was stirred for further 15 minutes at room temperature. Parallelly, 0.2 mmol of octane-1,8-diamine in CHCl₃ (0.5 mL) was added 15 minutes after the DBU addition to the main reaction mixture. The mixture was allowed to stir for another 15 minutes before pouring into PTFE mold.

2.6.2 Copies of ¹H NMR, GPC, IR

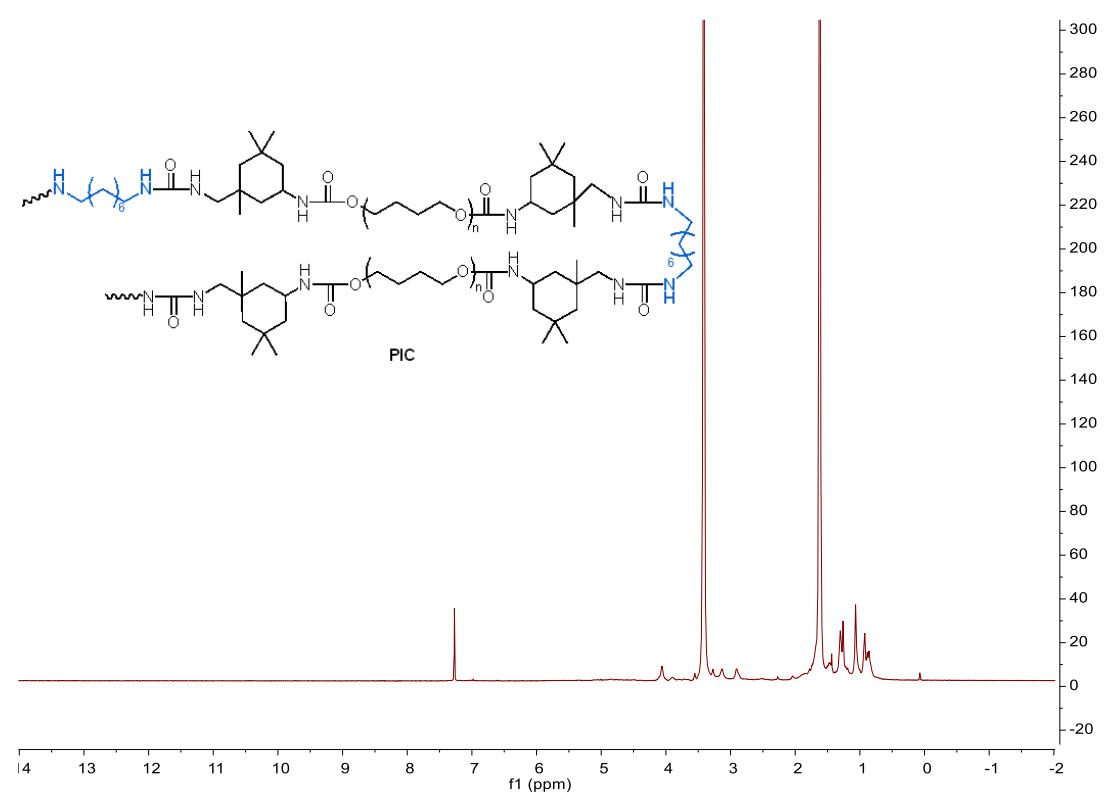


Figure S20 ¹H NMR of PIC

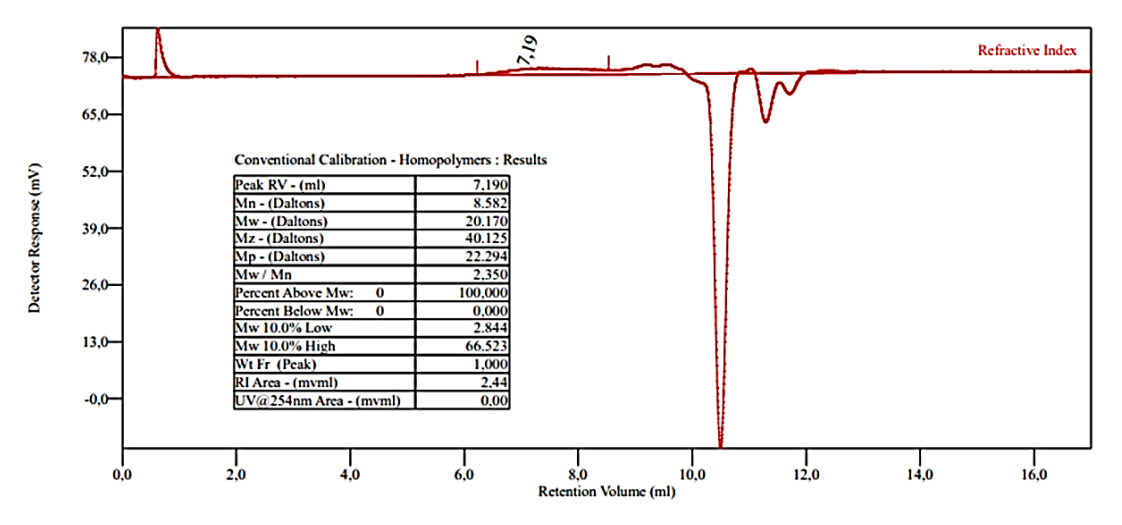


Figure S21 GPC of PIC

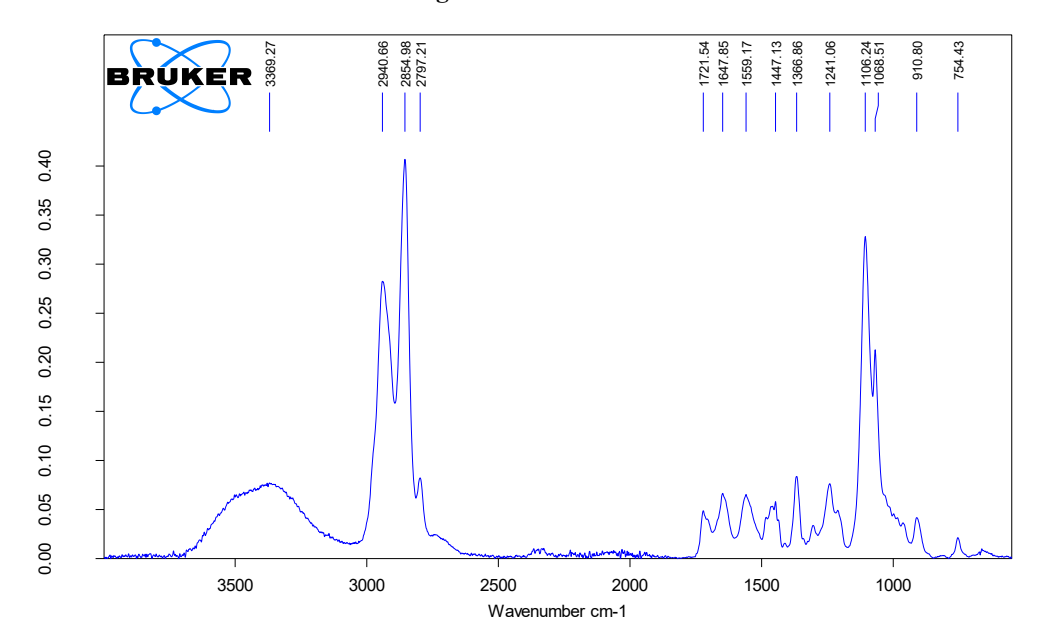


Figure S22 IR spectra of PIC

2.7. Calculation of crosslink densities of PIE-heated and PIE-compressed

$$q_v = 1 + (\omega/\omega_0 - 1) * (\rho_2/\rho_1)$$

$$v_{2m} = \frac{1}{q_v}$$

$$\chi_1 = 0.34 + \frac{V}{RT} * (\delta_p - \delta_s)^2$$

$$M_c = -V_\rho * \left(v_{2m}^{\frac{1}{3}} - \frac{v_{2m}}{2}\right) / [\ln(1 - v_{2m}) + v_{2m} + \chi_1 * v_{2m}^2]$$

$$v_c = \frac{1}{M_c}$$

where q_v is the volume swelling ratio of the elastomer, w_0 is the weight of the specimen before swelling, while w is the weight of the specimen after swelling, ρ_1 and ρ_2 are the densities of the solvent and elastomer, V is the molar volume of solvent, δ_p and δ_s are the solubility parameters of the polymer and solvent, respectively, and ρ is the density of the elastomer, while crosslink

density (v_c) (mol cm⁻³) and M_c is the apparent average molecular weight.^[3]

Table S4 Swelling properties and crosslink densities of PIE-heated and PIE-compressed.

Sample	Swelling degree	M _c (g/mol)	$v_{\rm c} \times 10^{-4} ({\rm mol/cm^3})$
PIE-heated	157.0%	1819	5.50
PIE-compressed	693.0%	10423	0.96

- [1] Y. Cai, F. Lehmann, E. Peiter, S. Chen, J. Zhu, D. Hinderberger, W. H. Binder, *Polymer Chemistry* **2022**, *13*, 3412.
- [2] D. S. Rawat, J. M. Zaleski, Chemical Communications 2000, 2493.
- [3] P. J. Flory, The Journal of Chemical Physics 1950, 18, 108.



Supporting Information

for Macromol. Chem. Phys., DOI 10.1002/macp.202400177

Initiator-Free Synthesis of Semi-Interpenetrating Polymer Networks via Bergman Cyclization

Yue Cai, Florian Lehmann, Justus F. Thümmler, Dariush Hinderberger and Wolfgang H. Binder*

Supporting Information

Initiator-free synthesis of semi-interpenetrating polymer networks *via* Bergman Cyclization

Yue Cai¹, Florian Lehmann², Justus F. Thümmler¹, Dariush Hinderberger², and Wolfgang H. Binder^{1*}

¹ Macromolecular Chemistry, Institute of Chemistry, Faculty of Natural Science II, Martin Luther University Halle-Wittenberg, Von-Danckelmann-Platz 4, 06120 Halle (Saale), Germany

² Physical Chemistry, Institute of Chemistry, Faculty of Natural Science II, Martin-Luther-University Halle-Wittenberg, Von-Danckelmann-Platz 4, 06120 Halle (Saale), Germany *Correspondence: wolfgang.binder@chemie.uni-halle.de

1. ABBREVIATIONS ···		3REVIATIONS3
2.	EXP	ERIMENTAL PART······3
	2.1.	SOLVENTS AND MATERIALS
	2.2.	METHODS AND INSTRUMENTATIONS
	2.3.	SYNTHESIS OF (Z)-OCT-4-ENE-2,6-DIYNE-1,8-DIOL AND CROSSLINKED POLYURETHANES4
	2.3.1	Synthesis procedure of (Z)-oct-4-ene-2,6-diyne-1,8-diol [1]4
		Thermal treatment of (Z)-oct-4-ene-2,6-diyne-1,8-diol
	2.3.3	Synthesis procedure of crosslinked polyurethanes6
	2.4.	CYCLIC STRESS-STRAIN CURVES OF SEMI-IPN (PU*+x%PP) 6
	2.5.	OVERVIEW OF DISSIPATED ENERGY OF PU* AND SEMI-IPN (PU*+x%PP)
	2.6.	SEM of Samples PU, PU+EDY, SEMI-IPN (PU+PP)
	2.7.	ANALYSIS OF AFM ··································
	2.8.	NMR SPECTRA ·····8
	2.8.1	Trimethyl(prop-2-yn-1-yloxy) silane: ¹ H, ¹³ C NMR ······8
	2.8.2	. (Z)-octa-4-en-2,6-diyne-1,8-diol: ¹H, ¹³C NMR······10

1. Abbreviations

Bergman Cyclization (BC), Enediyne (EDY), Electrospray Ionization Time-of-Flight (ESI-ToF MS), Differential scanning Mass Spectroscopy calorimetry Thermogravimetric analysis (TGA), Nuclear magnetic resonance (NMR), Atomic force microscopy (AFM), Infrared (IR), Fourier transformation (FT), N, N-dimethylformamide (DMF), Ethyl acetate (EA), Chloroform (CHCl₃), Deuterated chloroform (CDCl₃), Electron resonance (EPR), diisocyanate (IPDI), glycerol (Gly), paramagnetic Isophorone Polytetrahydrofuran (PTHF), Scanning electron microscope (SEM)

2. Experimental Part

2.1. Solvents and Materials

Deuterium chloroform (CDCl₃-d) was used as NMR deuterium solvents. Dry solvents were prepared as follows: DMF and toluene were treated with solvent purification systems to remove water and oxygen.

Propargyl alcohol and hexamethylbenzene were purchased from abcr; isophorone diisocyanate, bis(hydroxyl)-telechelic Polytetrahydrofuran (average Mn \sim 650 g/mol), and chlorotrimethylsilane, cis-1,2-dichloroethylene, tetrakis(triphenylphosphine)-palladium(0) was purchased from Sigma-Aldrich; cuprous iodide and n-butylamine were purchased from Alfa Aesar. All chemicals listed here were used without any purification unless otherwise stated.

2.2. Methods and Instrumentations

NMR-spectra were measured on a Varian Gemini 400 spectrometer at 27°C. The ¹H-NMR spectra were recorded at 400 MHz or 500 MHz and for ¹³C-NMR spectroscopy 100 MHz were used. The samples were dissolved in CDCl₃. The NMR spectra were interpreted using MestReNova software (version 9.0.1-13254). Chemical shifts were given in ppm and coupling constants were given in Hz.

ESI-ToF MS measurements were performed using a Bruker Daltonics microTOF. 0.1 mg of samples were dissolved in HPLC grade methanol. All spectra were obtained by means of direct injection with a flow rate of $180~\mu L~h^{-1}$ in the negative mode with an acceleration voltage of 4.5~kV.

DSC measurements were done on a Netzsch DSC 204 F1. Samples pieces with a mass of 5-10 mg were placed into aluminum crucibles and were heated under nitrogen atmosphere with a heating rate of 5 K·min⁻¹ unless otherwise stated. Evaluation of the measured data was done with Netzsch Proteus Analytic software.

TGA was performed using a TG 209 F3 Tarus by Netzsch. Samples (10 mg) were weighed in an aluminum oxide crucible and heated under nitrogen atmosphere at a heating rate of 10

K/min until a temperature of 600 °C was reached. For data analysis, the software Netzsch Proteus for Thermal Analysis (Version 5.2.1, Netzsch, Selb, Germany) was used.

ATR-FTIR-spectra were measured on a Bruker Tensor VERTEX 70 spectrometer equipped with a Golden Gate Diamond ATR top-plate. For each measurement 32 background scans and 32 sample scans were averaged. The data were analyzed using Opus 6.5 software.

CW EPR spectra were measured using the Miniscope MS 5000 (Magnettech GmbH, Berlin, and Freiberg Instruments, Freiberg, Germany), the MS 5000 temperature controller (Magnettech GmbH, Berlin, Germany) and Freiberg Instruments software. 31 mg of the sample were placed inside the sample tube. The tube was capped with capillary tube sealant (CRITOSEAL® Leica) and placed into the spectrometer. The temperature inside the spectrometer was set to 25 °C (+/- 0.2 °C) and gradually increased to 175 °C in steps of 25 °C. Before starting each measurement, the sample was equilibrated at each temperature for 20 min. A magnetic field sweep of 8 mT centered around 338 mT with a scan time of 60 s, modulation amplitude of 0.05 mT, modulation frequency of 100 kHz and a microwave power of 10 mW were set. Each spectrum is an accumulation of 10 scans and consists of 60.000 data points. The raw spectra were smoothened by applying a gaussian filter. The spectra were convolved with a Gaussian kernel of radius r=500.

Tensile tests were performed using a universal testing machine (Z010, Zwick/Roell) at room temperature and a testing speed of 20 mm/min. Rectangular specimens with a total length of 40 mm, and a width of grip section of 4 mm. Each measurement was repeated at least 3 times. Engineering stress and strain values were calculated based on force and displacement as well as initial specimen dimensions. Cyclic loading and unloading were recorded at a maximum strain of 50%, 100%, 150%, and 200%.

AFM measurements were performed using a Nanosurf CoreAFM (Nanosurf, Liestal, Switzerland) with Tap190AI-G Cantilevers in phase contrast mode. The samples (thin films) were placed in the carrier and tested at room temperature. Data analysis was accomplished using Gwyddion 2.61 (Czech Metrology Institute, Brno, Czech Republic). Roughness and waviness were analysed along a 10 μ m cross section at y = 5 μ m, without including grains on the samples surface.

SEM measurements were performed by Raith 150 system. For better SEM images, a 20-nm gold coating was deposited with an electron-beam evaporator to make the surface more conductive without affecting the morphology. After deposition, the coated samples were put in Raith to take SEM pictures. The working voltage was 5kV and the aperture was 60uA. The surface morphologies of the samples can be seen through the secondary electron signal.

2.3. Synthesis of (Z)-oct-4-ene-2,6-diyne-1,8-diol and crosslinked polyurethanes

2.3.1 Synthesis procedure of (Z)-oct-4-ene-2,6-diyne-1,8-diol [1]

Figure S1 Synthetic route of (Z)-oct-4-ene-2,6-diyne-1,8-diol

O-(trimethylsilyl)- propargyl alcohol (1.0 g, 7.8 mmol), prepared from propargyl alcohol and chlorotrimethylsilane, toluene (10 mL), tetrakis-(triphenylphosphine)palladium(0) (0.258g, 0.2 mmol), cuprous iodide (0.057 g, 0.3 mmol), and *n*-butylamine (1.1 mL, 11.1 mmol) were mixed under argon in a 100 mL round-bottomed flask. (*Z*)-1,2-Dichloroethylene (0.25 mL, 3.6 mmol) was added to the mixture. After overnight stirring, the reaction mixture was diluted with ether (50 mL) and filtered. The concentrated filtrate was dissolved then in MeOH (40 mL) containing a few drops of AcOH. Concentration and purification of the product mixture by flash chromatography on silica gel (25% EtOAc in hexanes) afforded (*Z*)-oct-4-ene-2,6-diyne-1,8-diol. (35%), which was kept in EtOAc: ¹H-NMR (500 MHz, CDCl₃, δ in ppm): ¹H NMR (500 MHz, cdcl₃) δ 5.83 (s, 1H), 4.43 (s, 4H), 1.86 (bs, 2H). ESI-ToF MS: [M+Li]⁺ calculated for C₈H₈O₂Li⁺, 143.068; found, 143.066. Copies of ¹H NMR and ¹³C NMR are listed in the individual file.

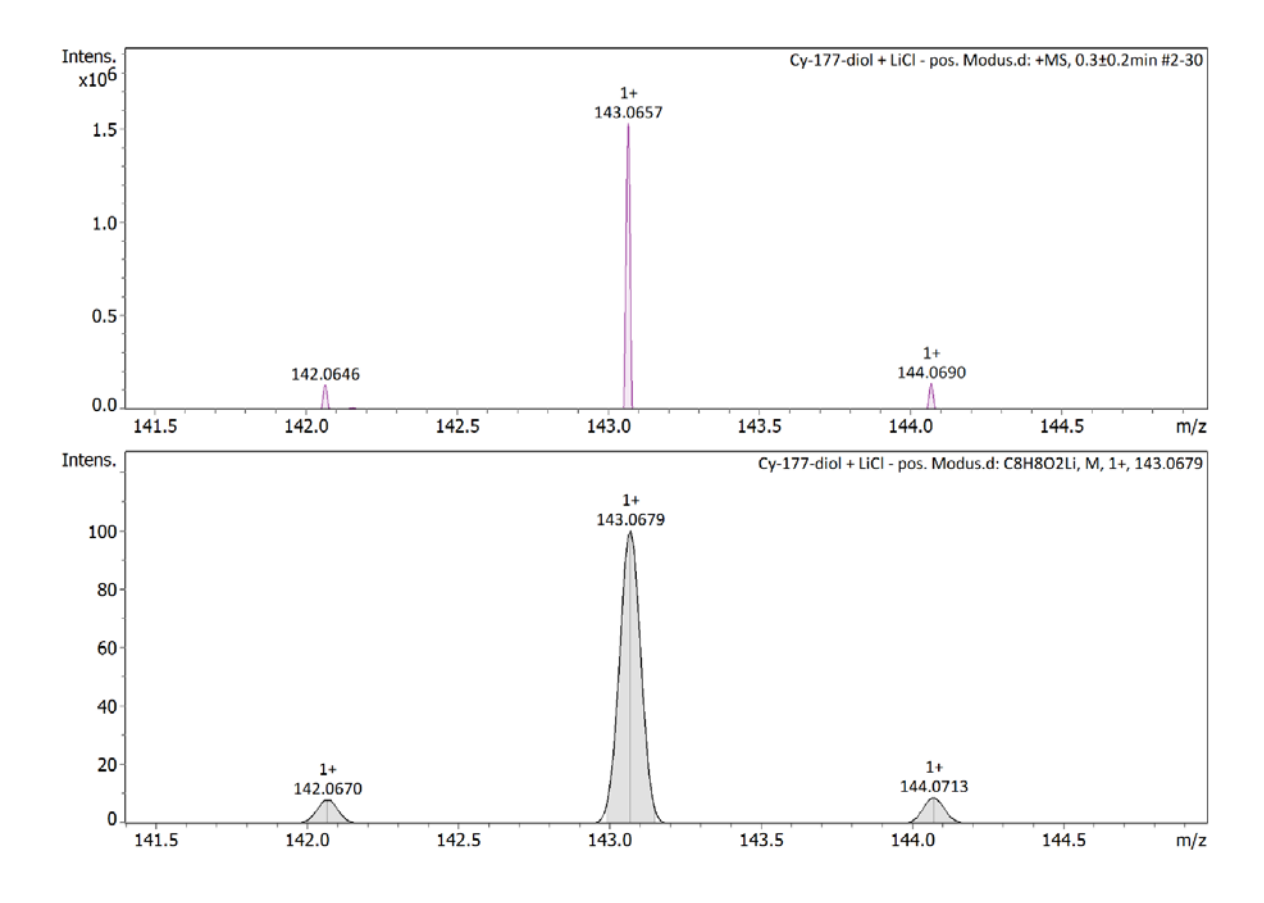


Figure S2 ESI-ToF MS Spectra of (Z)-oct-4-ene-2,6-diyne-1,8-diol

2.3.2 Thermal treatment of (Z)-oct-4-ene-2,6-diyne-1,8-diol

For a visual presentation of the occurrence of BC, an experiment where a diol-EDY solution (ethyl acetate as the solvent) was put in an oven at 150 °C for 5 min. Subsequently, the EA solvent evaporated, and only brownish solids were inside. Fresh EA was added to the vial. The solids could not be dissolved anymore.

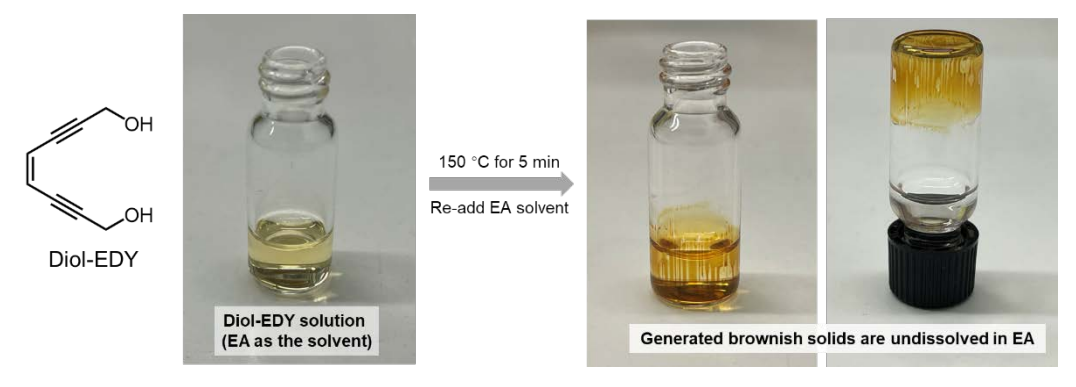


Figure S3 Thermal treatment of (Z)-oct-4-ene-2,6-diyne-1,8-diol

2.3.3 Synthesis procedure of crosslinked polyurethanes

According to the literature, [2] the synthesis of crosslinked PU is divided into two steps: first step, transforming hydroxy terminated polytetrahydrofuran (PTHF) into isocyanate-terminated PTHF with the help of isophorone diisocyanate (IPDI); second step, adding required amount of glycerol (Gly) to form the final PU. In detail, the isocyanate end-caped PTHF was prepared by reaction of the required amounts of polytetrahydrofuran (average Mn ~650 g/mol) and IPDI, in a two-neck glass reactor equipped with a mechanical stirrer at 80 °C for 2 h. The prepolymer was then crosslinked using the required amount of glycerol and small amount of DMF as solvent at 80 °C for 2 h. The polyurethane resins were then cast onto clean polytetrafluoroethylene molds and stored at 80 °C for 24 h to obtain flexible and transparent films. The detailed mole ratio of the three compositions (PTHF, IPDI, and Gly) of PU and PU* are listed below.

	1 ,	<i>y</i>
	PU	PU*
PTHF (diol)	1	1.4
IPDI	2	2
Gly	0.67	0.4

Table S1 Mole ratio of the three compositions (PTHF, IPDI, and Gly) of PU and PU*

2.4. Cyclic stress-strain curves of semi-IPN (PU*+x%PP)

With 48 h-immersion in diol-EDY solution and with different concentrations of diol-EDY solution, PU* samples were treated and converted into a series of semi-IPN* samples. The incorporated amount of diol-EDY did not get obvious improvement, with maximum arranging around 4~5%.

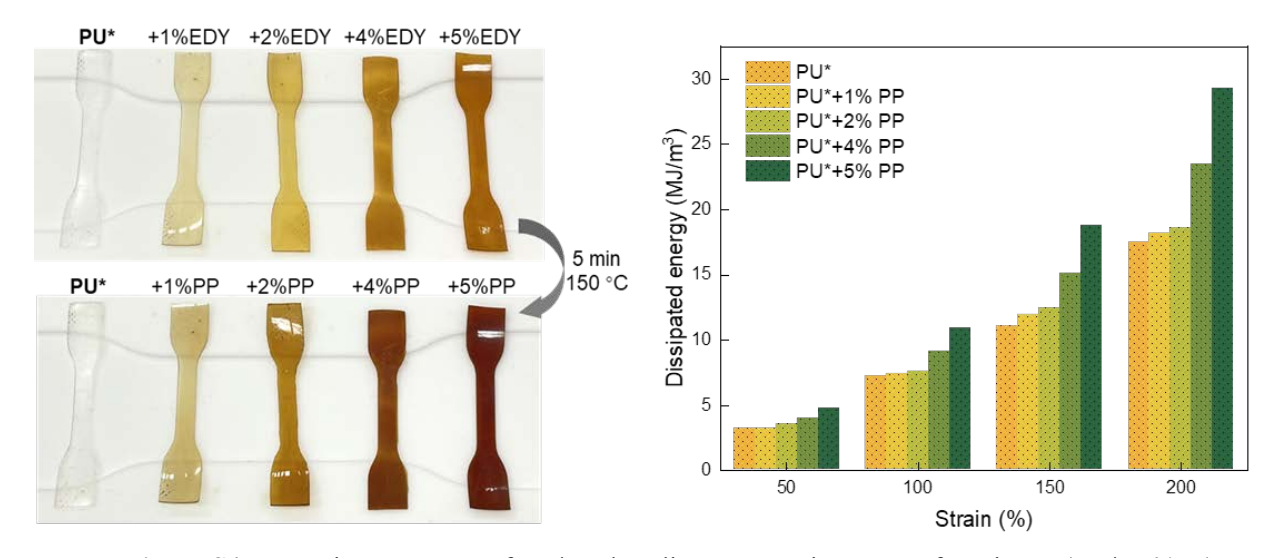


Figure S4 Immersion treatment of PU* and cyclic stress-strain curves of semi-IPN (PU*+x%PP)

2.5. Overview of dissipated energy of PU* and semi-IPN (PU*+x%PP)

Table S2 Overview of dissipated energy of PU* and semi-IPN (PU*+x%PP)

	0,		(
C 1 -	Dissipated energy (MJ/m³)			
Sample	Strain 50%	Strain 100%	Strain 150%	Strain 200%
PU*	3.2	7.2	11.1	17.5
Semi-IPN* (PU*+1% PP)	3.2	7.4	11.9	18.2
Semi-IPN* (PU*+2% PP)	3.5	7.6	12.4	18.6
Semi-IPN* (PU*+4% PP)	4.0	9.1	15.1	23.5
Semi-IPN* (PU*+5% PP)	4.7	10.9	18.8	29.3

2.6. SEM of samples PU, PU+EDY, semi-IPN (PU+PP)

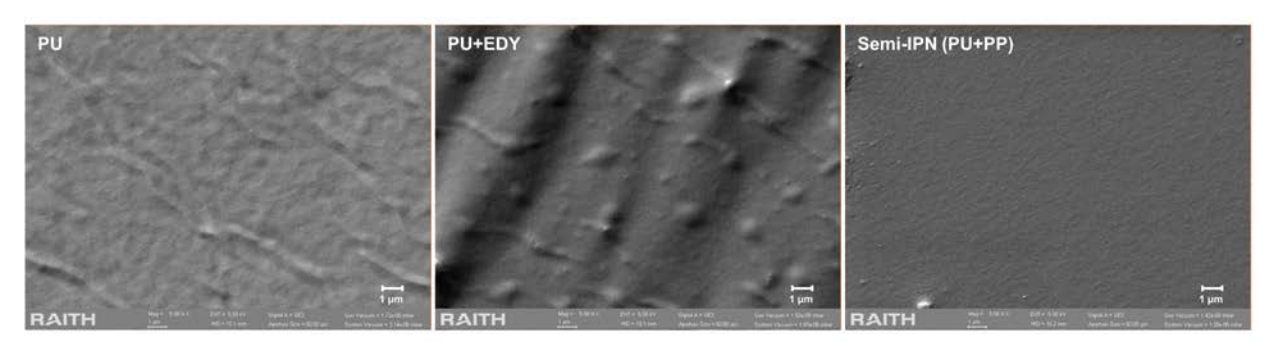


Figure S5 SEM graphs of samples PU, PU+EDY, semi-IPN (PU+PP)

2.7. Analysis of AFM

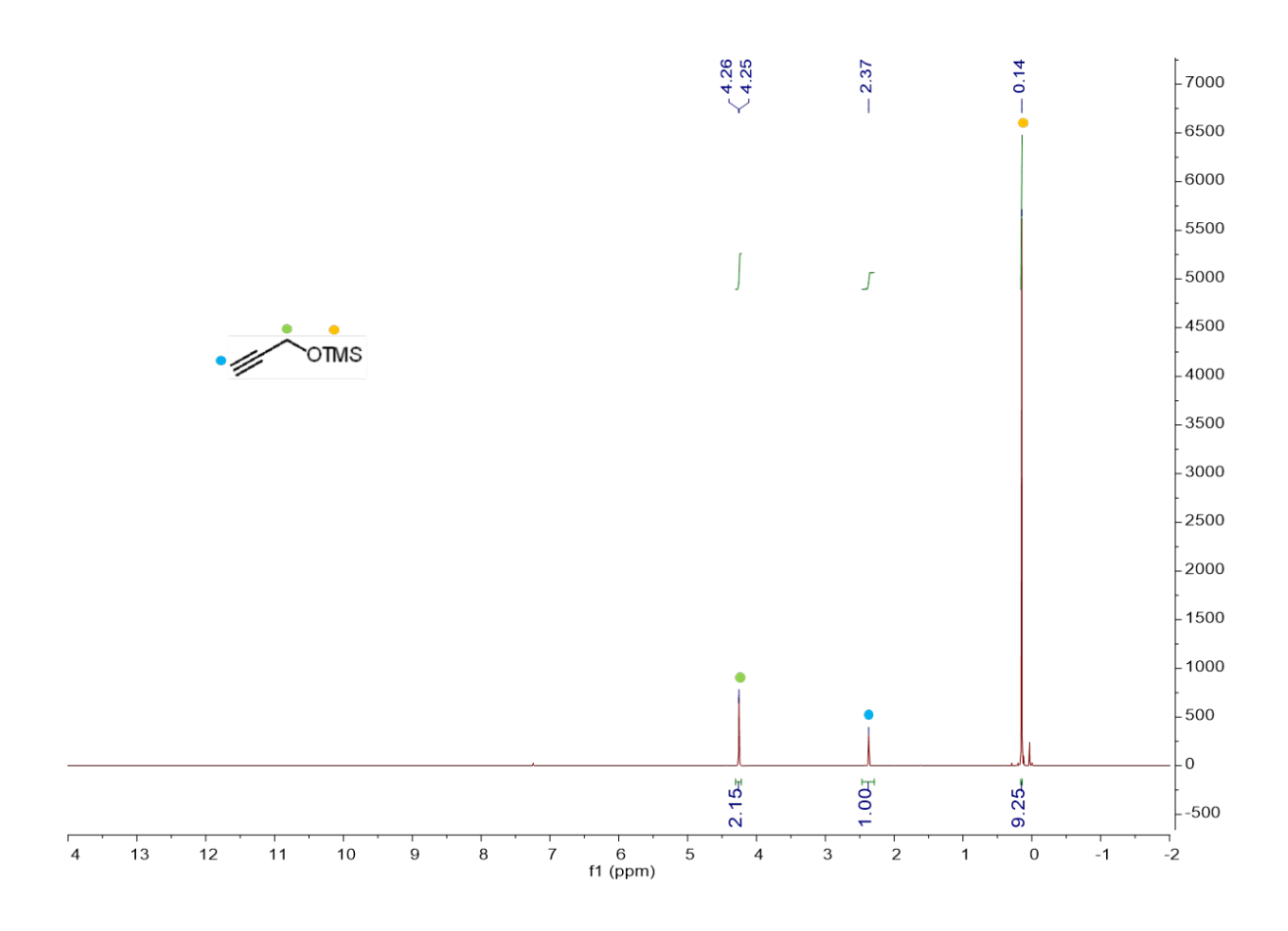
Table S3 Roughness average and root mean square roughness of three samples

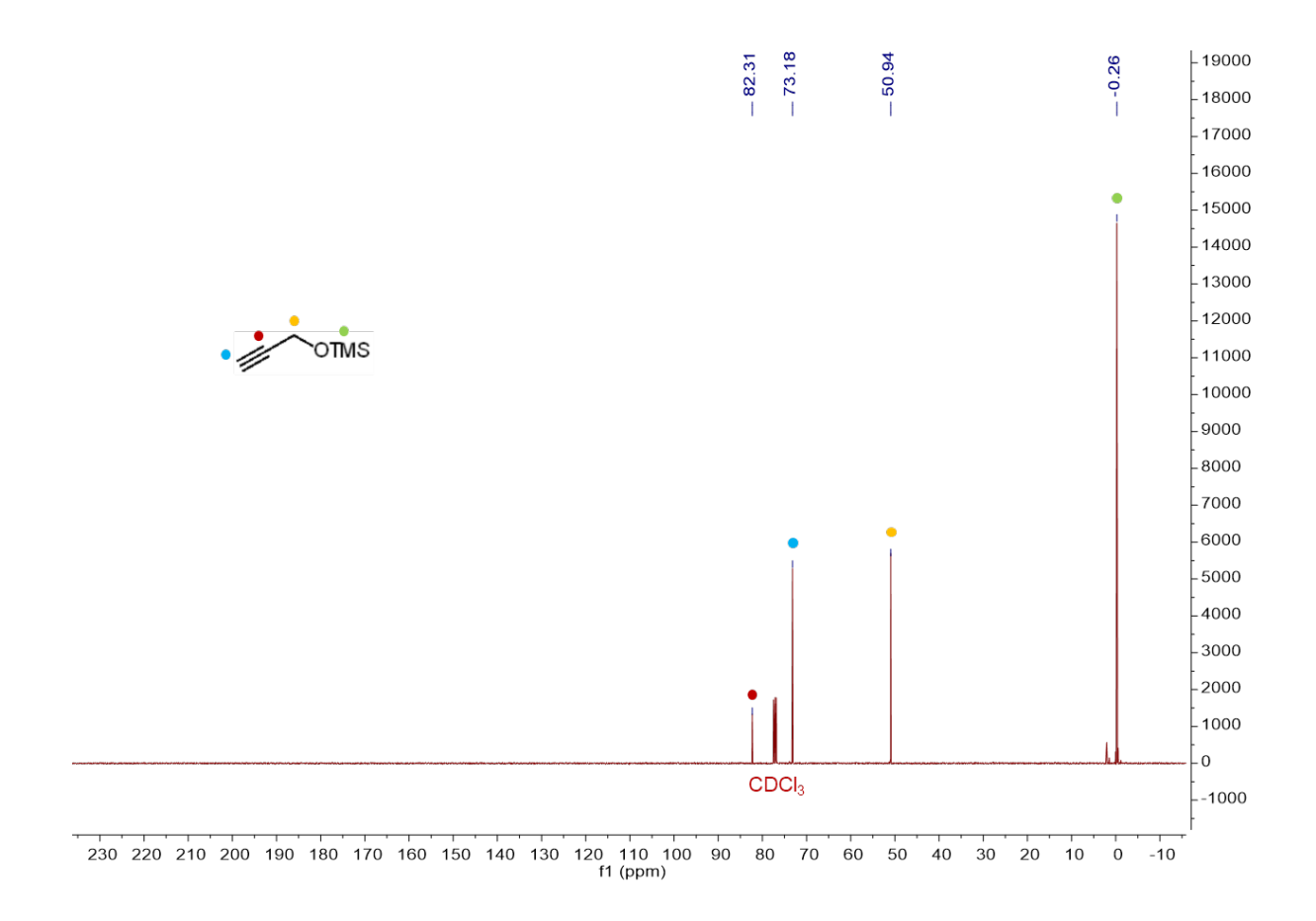
		PU	PU+EDY	PU+PP
Roughness average	R_a	2.3 nm	1.0 nm	0.3 nm
Root mean square	R_q	2.9 nm	1.3 nm	0.4 nm
roughness				

- [1] M. M. McPhee, S. M. Kerwin, J. Org. Chem. 1996, 61, 9385.
- [2] S. Oprea, V.-O. Potolinca, V. Oprea, European Polymer Journal 2016, 83, 161.

2.8. NMR spectra

2.8.1 Trimethyl(prop-2-yn-1-yloxy) silane: ¹H, ¹³C NMR





2.8.2. (Z)-octa-4-en-2,6-diyne-1,8-diol: ¹H, ¹³C NMR

